Evaluation of Historical Alluvial Channel Crossings

APRIL 2024

US Army Corps of Engineers ®

Prepared by:

US Army Corps of Engineers
Albuquerque District
Hydrology and Hydraulics Section

REPORT PREPARED BY

Jonathan AuBuchon, PE
Regional Sediment Specialist
USACE-CESPA-ECH-H

Deanna Wilson
Geospatial Unit Lead
USACE-CESPA-ECH-W

REPORT REVIEWED BY

Tamara Massong, PH
Hydrology Specialist
USACE-CESPA-ECH-H

PREPARED FOR

Middle Rio Grande Endangered Species Collaborative Program

Cover Photograph: Looking upstream on the Rio Grande in Corrales towards the Corrales Siphon

TABLE OF CONTENTS

Tables

Figures

Equations

Acknowledgements

The work documented in this report builds upon the works of others as cited throughout the document, but also utilized the expertise of Bruce Jordan within the USACE – Albuquerque District to help locate and find the locations of the historical borehole information.

List of Abbreviations/Acronyms

agg	aggradation
ABCWUA	Albuquerque Bernalillo County Water Utility Authority
AMEC	AMEC Earth and Environmental, Inc.
ASTM	American Society for Testing and Materials
BHI	Bohannan Huston, Inc.
CESPA	Albuquerque District of the USACE
cdf	cumulative distribution function
cfs	cubic feet per second
CS	coarse sand
CV	coefficient of variation
deg	degradation
E	East
ESRI	Environmental System Research Institute
Fines	clays and silts
FS	fine sand
ft	feet
GIS	Geographic Information System
GRR	General Reevaluation Report
I	Interstate
ID	identification
LiDAR	Light Detection and Ranging (remote sensing method using pulsed lasers to measure distance to the earth)
m	meters
mm	millimeters
MRG	Middle Rio Grande
MRGESCP	Middle Rio Grande Endangered Species Collaborative Program
MRGCD	Middle Rio Grande Conservancy District
MS	medium sand
MtnVw	Mountain View
NA	not applicable
NAD	North American Datum
NAVD	North American Vertical Datum
N/D	not determined
NGVD	North American Geodetic Datum

NM	New Mexico
O&M	Operation and Maintenance
pdf	probability density function
P-P	probability-probability
Q1	first quartile (lowest quarter of the sample set data)
Q2	second quartile (quarter of data below the median of the sample set data)
Q3	third quartile (quarter of data above the median of the sample set data)
Q4	fourth quartile (highest quarter of the sample set data)
Q-Q	quantile-quantile
Reclamation	Department of the Interior, Bureau of Reclamation
SP	State Plane
TM	Tukey's trimean
USACE	United States Army Corps of Engineers
USCS	Unified Soil Classification System
USGS	U.S. Geological Survey New Mexico Water Science Center
VCS	very coarse sand
VFS	very fine sands
W	West

Executive Summary

Flooding and sedimentation on the Middle Rio Grande (MRG) have created dynamic adjustments of the river channel necessitating numerous flood control projects over the last century to make the land arable and safeguard the surrounding communities. As part of the flood control effort the MRG has been laterally constrained, typically by levees or high ground, but historical documentation of the channel shows historical channels occurred outside the current levee constraints. Current active channel locations are known to consist of coarser bed materials than their correlated floodplain deposits.

The hypothesis underlying this analysis was that the historical channel locations also had coarser material deposits than their floodplains. And, when historical channels became abandoned, they were subsequently filled in, and covered with finer material, as is observed in today's floodplain system.. The crux of this hypothesis is that in certain locations, where the current river channel is in contact with coarser material from the historical channels, river water is laterally transferred through the floodplain sediments via groundwater movement.

During the 2019 spring-snow melt runoff, locations were geospatially recorded where existing levees experienced seepage and other integrity issues. These observations provide an opportunity to evaluate whether historical river planforms, compared to other conditions, such as standing water or vertical gradient change, are contributing to levee integrity issues. The historical river planforms of 1918, 1935, and 1949 are utilized for this study primarily because they are oldest planforms available on the MRG and provide a relic of where the river active channels used to be. This analysis evaluated the correlation between observed 2019 seepage issues and historical channel locations for the corridor between the Corrales siphon and the I-25 crossing south of Albuquerque, NM. To this extent the 2019 issue locations were filtered to evaluate only those locations with groundwater induced issues (e.g., seepage, sloughing in the drain, sand boils, etc.).

The conducted analyses indicates that the filtered 2019 issue locations have some correlation to the observed active channel locations in 1918, 1935, and 1949, with the earliest year having stronger visual correlations, although the active channel distance statistics favor the latter years. It was speculated that a stronger correlation may exist between the 2019 issue locations and active channel morphology that predates 1918, based on the morphological planform type changes between 1918 and 1949. The correlation between coarser sediment deposits and the 2019 issue locations is poor, however, and may be a result of correlated boreholes that were not closely associated with the 2019 issue locations.

The analysis suggested that there is a moderate correlation between the 2019 issue locations and zones identified as high to moderate risk for seepage and slope stability failures. Part of the hypothesis testing was to evaluate whether historical river planforms, compared to other conditions, such as standing water or vertical gradient change, are contributing to groundwater movement that is causing seepage and slope stability issues on the riverside drains. This analysis

was inconclusive in identifying a primary cause but suggests that historical channels and traditional seepage concerns (e.g., standing water, vertical gradient change, etc.) are likely both culprits in the observed 2019 issue locations.

While the evaluation was focused on a flood control nexus because of a dataset that provided spatially diverse and observable links to groundwater movement, it does suggest that an increased groundwater connection through coarser sediment deposits from historical active channel locations is possible. Based on the data evaluated, the relationship is moderate at best and likely more pronounced where the current active channel has incised into the stratigraphy laid down by historical active channels. Habitat restoration projects that consider the historical active channel locations may benefit from the increased groundwater connection observed in this analysis groundwater correlation to the historical active channel locations,

Additional analyses that expand on the current evaluation may provide additional insight into this relationship between groundwater movement and historical channel locations. The 2019 data collection effort included the reach of the Rio Grande around the Belen and Los Lunas, NM area. An expansion of this analysis to that area may provide insight into whether the seepage signal is stronger. Filtering the data by proximity to boreholes may also prove advantageous and minimize uncertainties introduced by correlating borehole data that is further away from identified sites of concern. A more specific elevation analysis may also be beneficial. Correlating elevations of the historical channel elevations with the current active channel location would reveal if there is an elevation connection to the observed seepage locations. If the elevation shows a seepage head towards the drain, it may suggest that direction of the historical channels may play a role in the observance of seepage concerns that is in addition to the coarser nature of the deposits.

Introduction

The Rio Grande, like many rivers is dynamic, and variations in amount of flow, depth, and velocity are present when you look at a cross-section perpendicular to the flow. Sampling of the Rio Grande bed in 2006 (Bauer 2007) showed bed material sizes for the active channel in the fine sand (FS) to greater than very coarse sand (>VCS). An assessment (Bauer 2009) of the USGS gaging station at Albuquerque (USGS site ID 08330000) showed a similar range of bed material sizes for the active channel between 1969 and 2004, while the suspended sediment sizes range from around coarse sand (CS) to silts and clays (Fines). Sediment sampling during the 2019 spring snow-melt runoff gave a similar active channel bed material and suspended size range, with a nominal bed material size in the medium sand (MS) to coarse sand (CS) size range and a nominal suspended sediment size in the FS size range (AuBuchon et al. 2023). This suggests that sand classifications [poorly graded sand (SP) or well graded sand (SW)] from the borehole stratigraphy are likely associated with historical active channel locations, especially the MS and larger grain sizes. The presence of silts [sandy silt (SM) or silt (ML) classifications] may

still indicate fluvial activity aided in the formation of that layer, but it is more likely associated with the floodplain which typically has slower moving water.

During a snow-melt runoff in 2019, AuBuchon et al. (2023) found a variation of bed material sizes across the Rio Grande in the Albuquerque area (see Figure 1). If this variation of bed material size is found within the current river channel, it is likely that a similar variation of bed material sizes can be found in historical river channel locations. The coarsening of the bed material on the Rio Grande downstream of Cochiti Dam (Bauer 2007; Bauer 2009; Lagasse 1980; Nordin and Beverage 1965; Schmidt et al. 2003) obscures this to some extent since the grain size distribution has shifted from predominantly sands to gravels and cobbles. Periodic sediment supplies from the Jemez River, the North Diversion Dam, Calabacillas Arroyo, etc. still bring in a considerable amount of sands and finer material to the Albuquerque reach of the Rio Grande that provide this observable variation of bed material across a cross-section (Makar and Aubuchon 2012). While overlays of historical channel locations can be assessed using currently available geospatial tools, like ESRI's ArcGIS Pro software, the historical channel locations are often masked in the field because of historical interventions.

Flooding and sedimentation on the Rio Grande in the first half of the 20th century created dynamic adjustments of the river channel sparking numerous flood control projects to make the land arable and safeguard the surrounding communities from flooding. As part of the flood control effort, the Rio Grande was laterally constrained typically by levees or high ground (see Figure 2). Efforts were also implemented to eliminate side channels and induce slower moving water near the levees to encourage the development of a central channel location (see Figure 3). These efforts not only cut off sections of the river, but they also created the subsequent deposition of finer sediment on top of the coarser active channel locations, masking the locations of these features in the field. This can be seen in the geotechnical borelogs that have been collected throughout the Middle Rio Grande (see Figure 4) as finer materials overlay coarser substrates.

The construction of the initial spoil levees and riverside drains was done more or less in a linear fashion, wherein portions of the active channel and floodplain were cut off from the Rio Grande (Berry and Lewis 1997). At the time of levee construction, drains, both riverside and interior, were also constructed to help drain the waterlogged soils outside of the Floodway (Berry and Lewis 1997), as illustrated in Figure 5. The excavation of the riverside drains provided the soil material from the spoil levees were constructed. As such, the existing ground elevation was lowered in the vicinity of the riverside drains, causing a positive elevation drainage for any subsurface flows from the Rio Grande. The placement of excavated soil in the spoil levee followed the alignment of the riverside drains, filling in active channels and floodplain areas. This action separated the historical floodplain and helped make the surrounding lands arable.

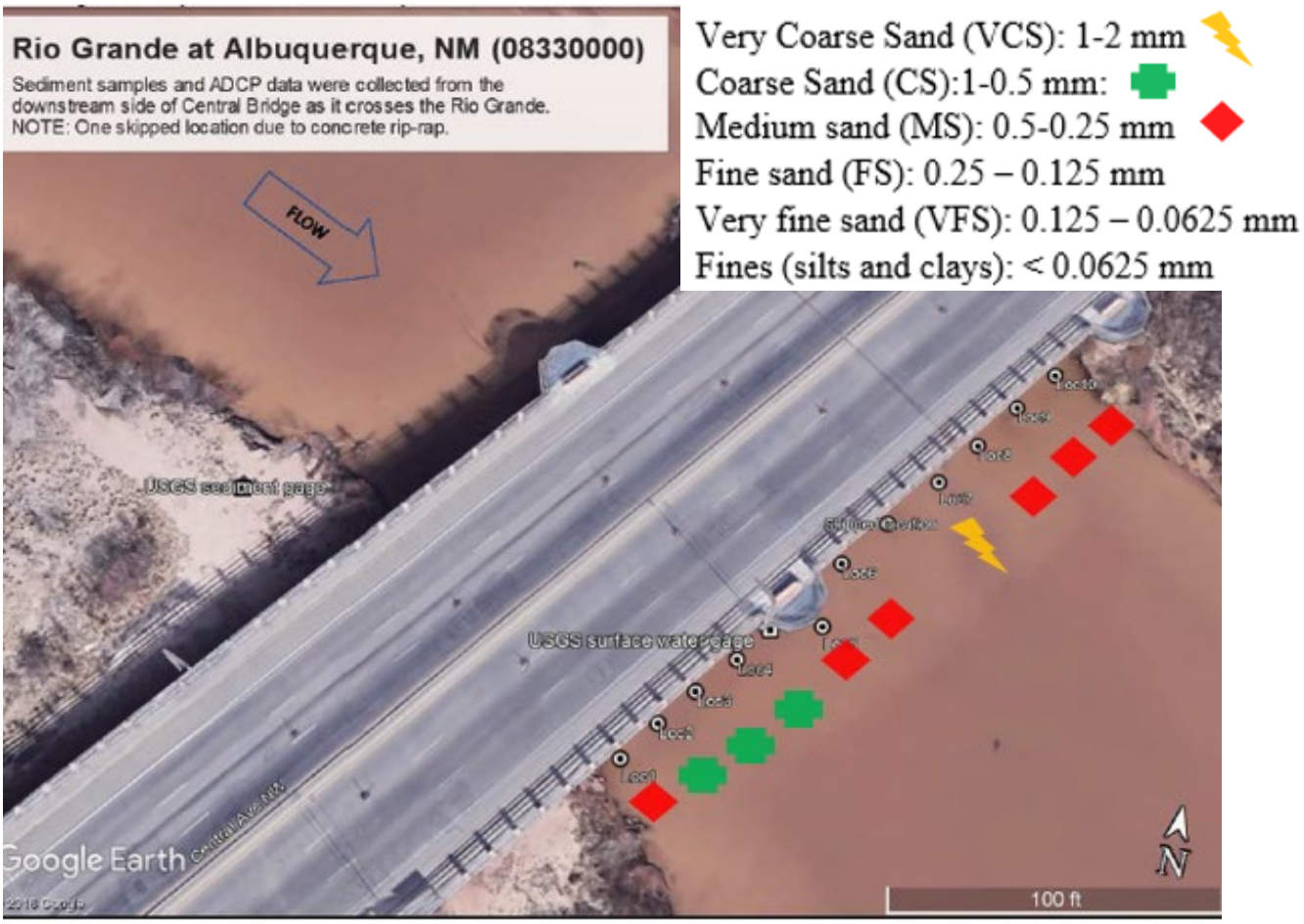

Figure 1. Sediment variation on the Rio Grande in the Albuquerque Area. Shown is a Google Earth image of the Rio Grande at the Central Avenue Bridge. Median (d50) bed material sizes are illustrated using the Wentworth (1922) scale to show bed material variation along a cross-section perpendicular to the flow.

The historical active channels likely had coarser substrates then their surrounding floodplains, so where the historical channel meandered back and forth across the floodplain, conduits facilitating greater groundwater movement were established. As time progressed and additional encumbrances, like jetty jacks, were placed between the spoil levees, an area referred to as the Floodway (see Figure 5), finer material settled on top of these historical channels. But it is possible that the historical channel locations, especially when in contact with the current active channel of the Rio Grande, still facilitated a greater groundwater movement than the floodplain deposits adjacent and now deposited above these historical channels.

As the environmental conditions changed and channelization and flood control dams did their work (Grassel 2002; Lagasse 1980), the sediment load on the Rio Grande was reduced and the active channel began to have excess energy to erode its bed substrate. This lowered the active channel and left portions of the floodplain disconnected from regular inundation. The incision also likely re-connected the current active channel elevation with some of the historical active channel deposits. This connection, coupled with the coarser material of these deposits, facilitates

the conveyance of groundwater. And where the interception happens upstream of a location where the historical channel location was cut off by the placement of the spoil levee, it is possible that certain areas of the flood control structures became more susceptible to groundwater movement. This creates conditions of seepage and sloughing when contemporary flood events create higher hydraulic head conditions within the levees.

It is therefore hypothesized that historical channel locations had coarser material deposits that were subsequently filled in, over the top, with finer material, especially in areas where the current channel location has been shifted away from the historical channel locations. When the floodplain is being flooded the finer materials likely slow the vertical movement of groundwater, aiding soil moisture and vegetation growth. It may be that in certain locations, the elevation of the current river channel is in contact with the coarser material strata from the historical channel locations, affecting the transfer of water in these lower substratum's laterally via groundwater movement, especially in areas where the historical channels more directly flow towards the levee. This in turn affects soil moisture in areas further away from the current Rio Grande channel locations, especially in lower lying floodplain zones where the groundwater fluctuates to the surface.

During the 2019 spring-snow melt runoff, locations were geospatially recorded where existing levees experienced seepage and other integrity issues. Some of these locations of concern had no apparent connection to surface water flow nor standing water adjacent to the levee. With these observations, there is an opportunity to evaluate whether historical river planforms, compared to other conditions, such as standing water or vertical gradient change, are contributing to groundwater movement that is causing seepage issues on the riverside drains. The historical river planforms of 1918, 1935, and 1949 are utilized for this study primarily because they are the oldest planforms available on the MRG and provide a relic of the active channel locations.

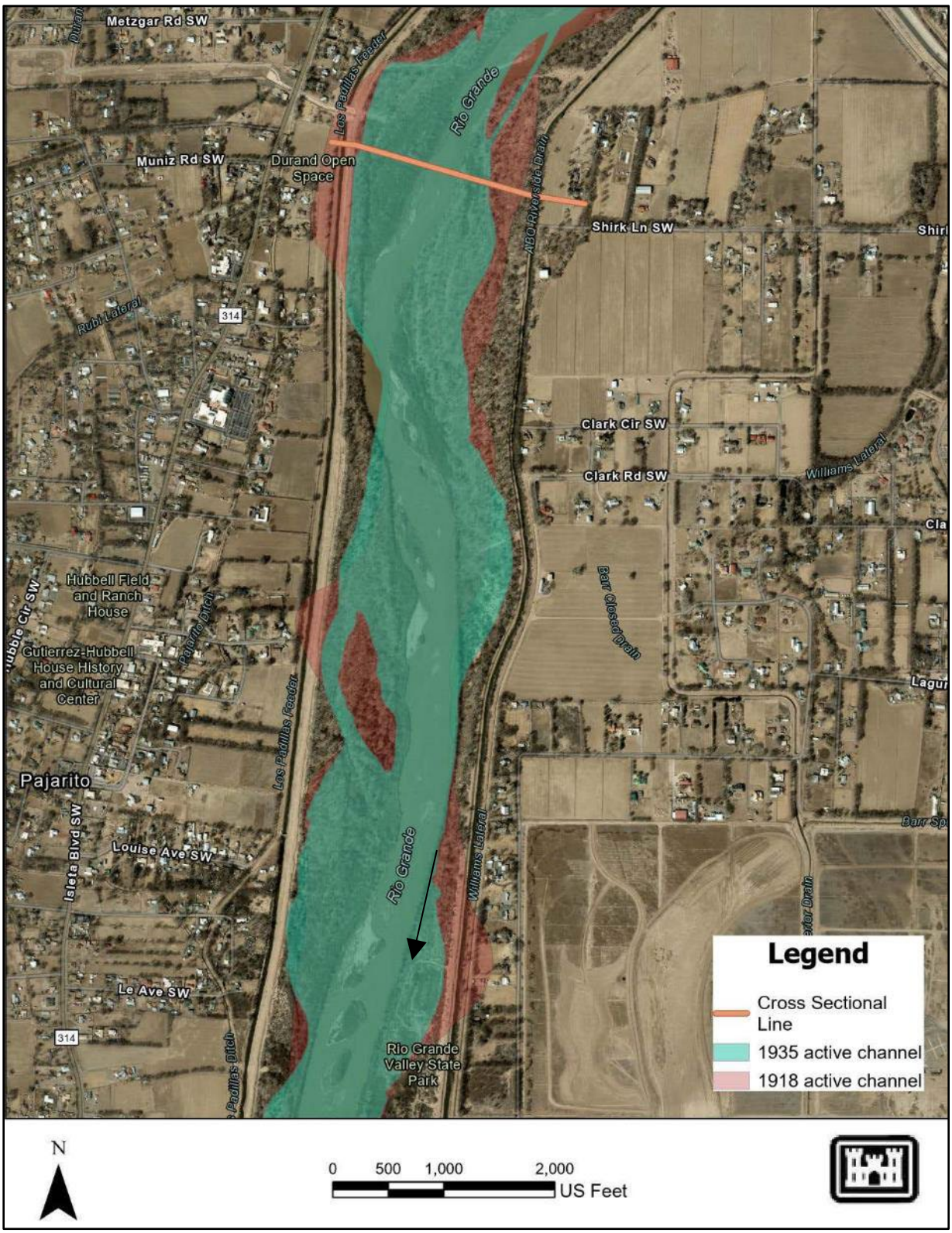

Figure 2. Active channels in 1918 and 1935 on the Rio Grande relative to current photography showing levee locations. Background aerial imagery is from the 2022 Middle Rio Grande Council of Government's aerial collection by Bohannon Huston from ESRI online imagery (accessed 14 August 2023). The levees, when constructed would have cut off sections of the active channel in 1918 at various locations.

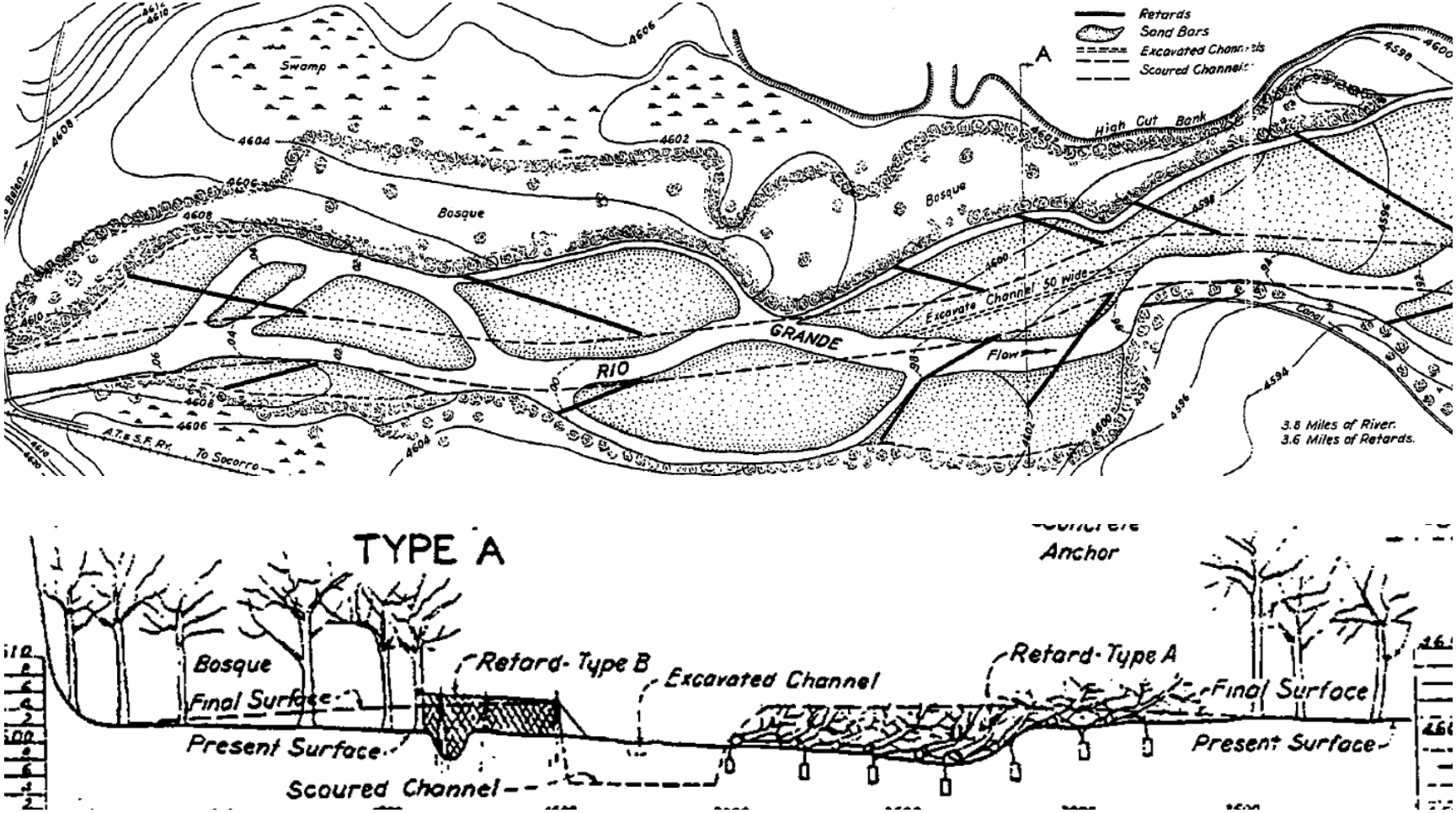

Figure 3. Typical modifications to slow the water on the Rio Grande in the 1920s and 1930s. Shown is an example of a section of the Rio Grande near Socorro, NM illustrating the types of structures and where the structures were to be placed in the channel (Berry and Lewis 1997), Retard type A structures are brush piles weighted down with concrete anchors. The brush was specified to be Cottonwood trees and willows. Retard type B structures are woven wire nets anchored with vertical pilings.

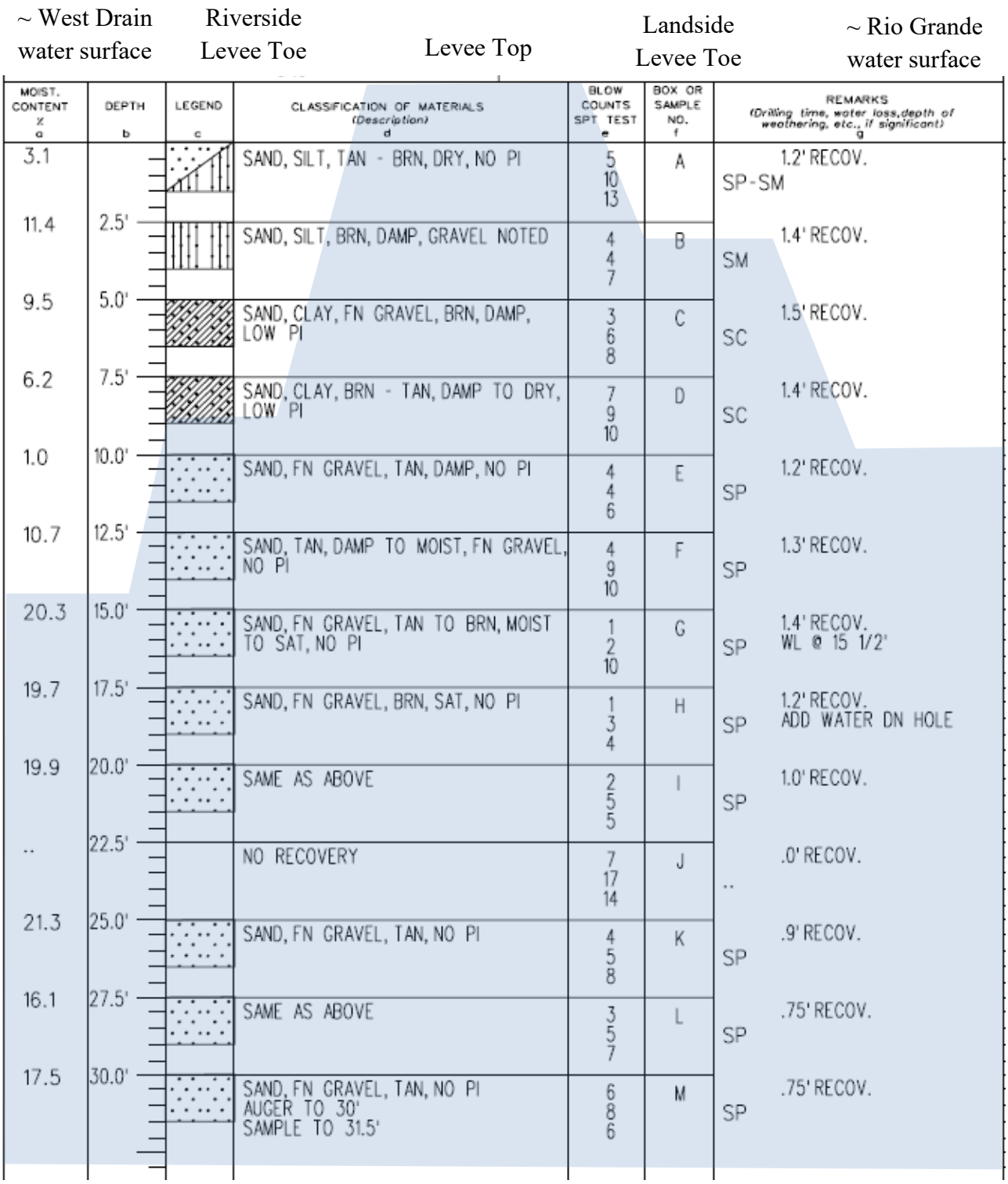

Figure 4. Typical boring log on the Middle Rio Grande overlain with a typical levee profile. Boring log shown is 8HSA-02 collected in 2006 on the spoil levee south of the Durand Open Space (Perea 2006). Outline is approximate elevations of drain-levee-Rio Grande profile, showing relative depths to features. Note layers of sandy silt and sandy clay on top of the poorly graded sand and gravel that starts about 10 feet lower than the top of the spoil levee.

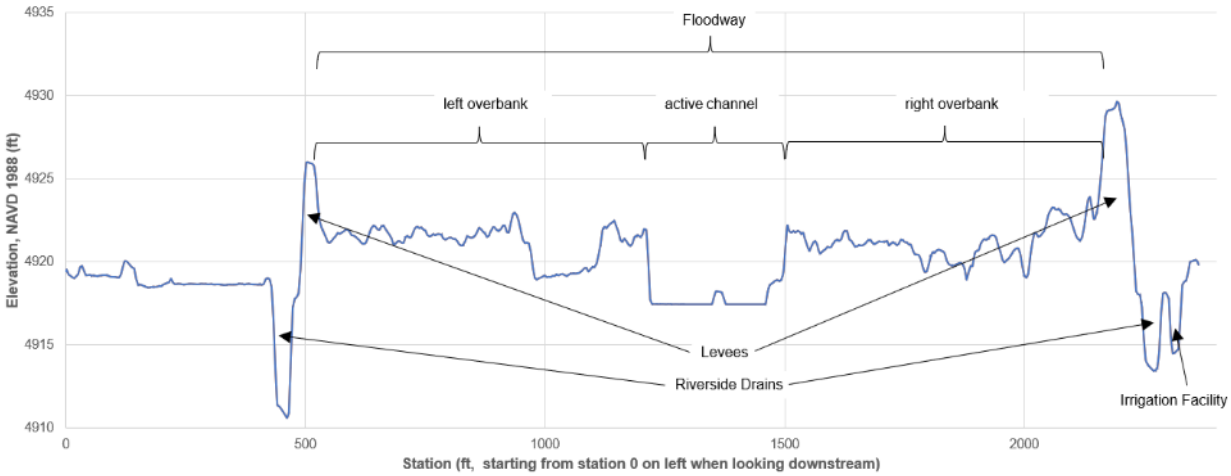

Figure 5. Typical cross-section of the Rio Grande showing nomenclature of the river and adjacent features. The cross section shown is at the Bureau of Reclamation's aggradation-degradation line # 583. Elevation data is from the 2022 LiDAR collection.

The Middle Rio Grande Conservancy District (MRGCD) was formed in 1925 after two large floods in 1874 and 1904 caused discussions to start on flood control (Berry and Lewis 1997). Deposition along the Rio Grande had reduced the acreage that could be farmed on the Middle Rio Grande from about 124,800 acres in 1880 to 45,000 in 1927. The deposition and unregulated water diversion caused waterlogged and alkali soils. The MRGCD constructed the levees and drainage systems in the 1930s to start addressing this issue. The 1918 linens provide a snapshot of the river after these two large floods at the turn of the century and reflect an actively aggrading fluvial system.

The 1935 aerial reflects the response to some of the levee and drainage improvements and another large flood in 1929 (Berry and Lewis 1997). Retards, such as are shown in Figure 3, were installed in the river at this time to induce sediment deposition on the channel edges and erosion through a central flow area to increase capacity. The retards consisted of various combinations of brush, tree plantings, and wire and cables to slow the water and drop out sediment (Berry and Lewis 1997). This essentially blocked off high flow channels and likely deposited finer sediment on top of coarser material. Drains were also constructed on either side of the fields in order to alleviate the waterlogging issue (Berry and Lewis 1997). The drain closest to the Rio Grande was called the Riverside drain, while on the other side of agricultural fields it was called the interior drain. The positive flow of groundwater towards these drains helped to make the land arable. The construction of the levees and drains however didn't always follow the existing river path and so portions of the river (both the main channel and high flow channels) were blocked off by the aforementioned retards, the riverside drain, and the levees. This blocking of flow paths is thought to have caused finer material depositing on top of coarser material creating a stratification of grain sizes in the vertical direction.

Two back-to-back large floods occurred in the MRG in 1941 and 1942. These floods were the last floods that created wide-scale flooding along this and other sections of the Rio Grande. As a consequence of this and the earlier flooding, additional flooding concerns were addressed by the MRGCD, Bureau of Reclamation, and the USACE with a massive construction flood protection project resulting in the official designation of a Rio Grande floodway (Figure 5). Of most concern for this study was the construction of Kellner jetty jack fields throughout the MRG in the early 1960s. These structures efficiently induced additional sediment deposition in what is now the overbank areas (Grassel 2002). The 1949 aerial reflects the results of a large flood and the start of the Kellner jetty jack installation.

Hypothesis

The hypothesis underlying this analysis is that the historical channel locations had coarser material deposits that were subsequently filled in, over the top, with finer material, especially in areas where the current channel location has been shifted away from the historical channel locations. Furthermore, that in certain locations, the coarser material in the current river channel is in contact with coarser material from the historical channels, facilitating the transfer of water laterally via groundwater movement into and through these old channel deposits which then intersect the levees.

Hypothesis testing

In order to test this hypothesis the levee problem areas identified in 2019 (Boberg et al. 2019) are proposed to be evaluated against the earliest channel planforms that exist on the Middle Rio Grande (1918, 1935, and 1949). This provides a specific dataset in which to evaluate these potential groundwater connections with the old channel deposits. d

Analysis Area

This analysis will focus on the area between the Corrales siphon to the I-25 crossing south of Albuquerque, NM (see Figure 6). While the evaluation is focused on a flood control nexus because these are observable links, if there is a strong correlation between flood risk issues and the historical active channels, it gives credence to the underlying supposition that there is an increased groundwater connection between the current active channel locations and the historical active channel locations.

Data Utilized

During the 2019 spring snow-melt runoff response, a multitude of levee problem areas were identified (Boberg et al. 2019). Since the stated hypothesis is to look at groundwater interactions between identified sites and the historical channel locations, the identified problem sites were screened not only by the analysis area, but also whether they were connected to groundwater related movement. This included sites that mentioned seeping, sand boils, sloughing, or tension cracks in the Operation and Maintenance (O&M) road. Within the analysis area there were 221 problem areas identified in 2019, of which only 84 are related to groundwater movement. These

84 points primarily appear in three areas: Sandia Pueblo across from the Harvey Jones channel (one point), between Alameda and Montano (10 locations on west side, two on east side – 23 points in total), and between Central and I-25 (11 locations on west side, 5 on east side – 60 points in total).

Additional data, previously collected, was also leveraged to conduct the analysis. These are briefly described below but are enumerated in more detail in Attachment 1.

- 1918, 1935, and 1949 historical planforms – These were developed by the U.S. Department of Interior, Bureau of Reclamation (Reclamation) based on the georeferenced 1918 hand-drawn linens and the 1935 and 1949 aerial photography datasets (Oliver 2012).
- 1984 Corrales and Mountain View Levee Borehole locations – Geotechnical exploration and soil analysis performed for the U.S. Army Corps of Engineers (USACE) to facilitate evaluation of flood control designs in the MRG Valley (Fox 1984; USACE 1986).
- 2002 Photogrammetry dataset – Reclamation collected aerial photography data in the January/February 2002 timeframe on the Middle Rio Grande from which a photogrammetric surface was created.
- 2006 Albuquerque Levee Borehole locations – Geotechnical exploration and soil analysis performed for the USACE to assess the Albuquerque Levee units (AMEC 2006; Perea 2006; USACE 2009). Slope and seepage stability ratings from this analysis (USACE 2009) were also utilized.
- 2007 Albuquerque West Levee Borehole locations – Geotechnical exploration and soil analysis for the USACE to prepare for the Albuquerque West Levee Construction (AMEC 2008).
- 2009 Mountain View Levee Borehole locations – Geotechnical exploration and soil analysis for the USACE in 2009 as part of the General Reevaluation Report (GRR) for the Belen to Bernalillo project (Jimenez 2009; Licon 2010; USACE 2018)
- 2022 Albuquerque Area Borehole locations – Geotechnical exploration and soil analysis for the Albuquerque Bernalillo County Water Utility Authority (Hazen 2023a; Hazen 2023b).
- 2022 LiDAR/aerial photography dataset –LiDAR and aerial photography data collected for Reclamation between 25 February 2022 and 8 March 2022 on the Middle Rio Grande (Woolpert 2022).

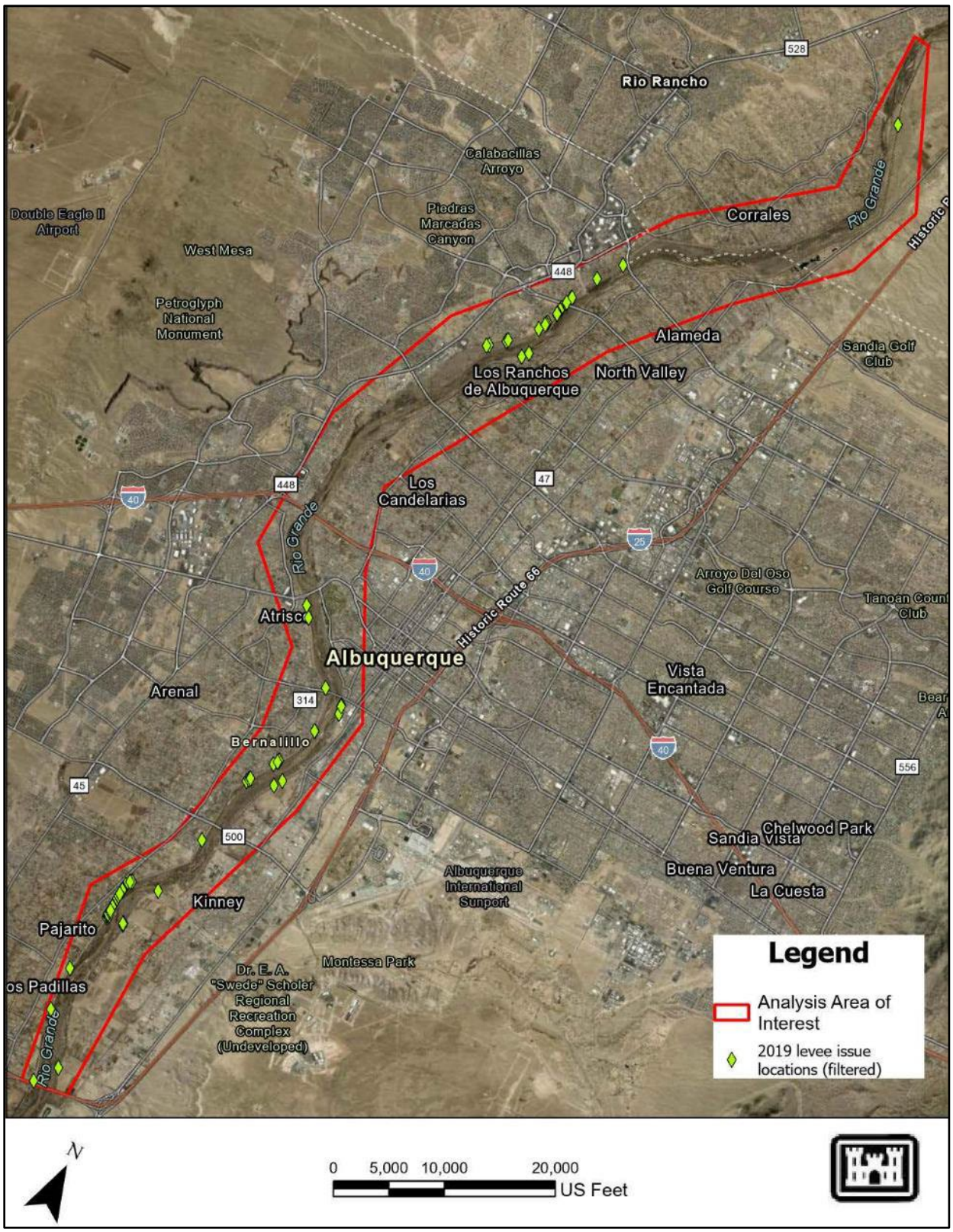

Figure 6. Analysis area of interest on the Middle Rio Grande with 2019 issue. Background aerial imagery is from the 2022 Middle Rio Grande Council of Government's aerial collection by Bohannon Huston from ESRI online imagery (accessed 18 August 2023).

Analysis Methods

Two specific questions are asked to help understand the potential link between historical channel planforms and the identified 2019 issue locations. The first question is whether the 2019 identified issue areas are correlated with historical active channel locations. This will be assessed spatially based on where the filtered 2019 issue areas are related to the (1918, 1935, and 1949 Historical planforms. The distance between the filtered 2019 issue locations to the active channel locations was assessed, along with the distance from all of the boreholes utilized in this analysis and the boreholes specifically correlated to each of the 2019 issue locations.

The second question is whether there are coarser material present at the elevation of the current active channel of the Rio Grande and the Riverside Drain than other locations, such as the Riverside and Landside Levee Toe locations. This was assessed by extracting relative depths between the levee and the riverside/landside levee toes, the water surface of the riverside drain, and the water surface of the Rio Grande, as shown in Figure 7. Locations of the Rio Grande, the riverside levee toe, the levee centerline, the landside levee toe, and the riverside drain centerline were based on digitization of these features within ArcGIS Pro at a scale of 1:2000 using the 2022 LiDAR/ aerial photography dataset.

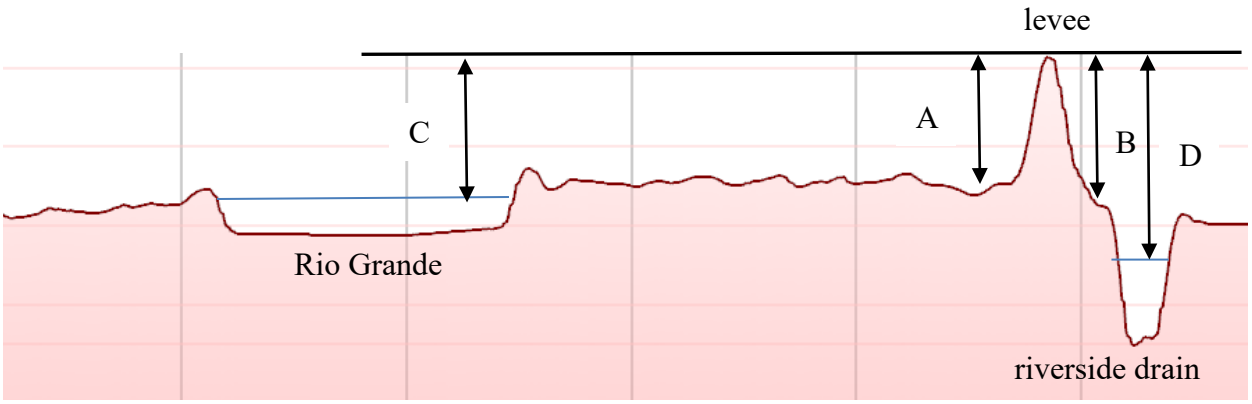

Figure 7. Typical Rio Grande cross section with evaluated relative depth areas. A is the relative depth between the top of levee to riverside toe, B is the relative depth between the top of levee and the landside toe, C is the relative depth between the top of levee and the water surface elevation of the Rio Grande at the time of the 2022 LiDAR survey, and D is the relative depth between the top of levee and the water surface elevation of the riverside drain at the time of the 2022 LiDAR survey.

The relative depths were then utilized with historical geotechnical boring (1984 Corrales and Mountain View Levee, 2006 Albuquerque Levee, 2007 Albuquerque West Levee, 2009 Mountain View Levee, and 2022 Albuquerque Area borehole locations) that occurred along the levees to extract information on the sediment size at the relative depth of the features. The historical geotechnical borings generally provide coverage for the entire analysis area. There are limited borings on the east side from the northern boundary around the Corrales siphon to around the outfall of the North Diversion Channel. Borings are spread out more within the central portion of the analysis area, especially on the east side from the North Diversion Channel outfall to the Montano Bridge and on both sides of the river from the Montano Bridge south to the South

Diversion Channel outfall to the Rio Grande. The borehole closest to the filtered 2019 area of interests was utilized to extract the required soil information.

Since it is possible that the filtered 2019 issue locations may be better correlated with more traditional geotechnical failure modes (seepage and slope stability) than the historical channel locations, an assessment was also performed to evaluate this correlation. This correlation was made based on the slope and stability analysis connected with the 2006 Albuquerque Levee Borehole locations.

The proposed analyses requires the collation of a variety of existing datasets, which are only briefly described in this section, but for which additional details are provided in Attachment 1. For example, since the borehole depths are all given relative to the ground surface sometimes elevation adjustments were required to ascertain the approximate levee elevation at the time of the actual borehole collection. The Albuquerque West levee (BHI 2009) was adjusted by taking the 2002 Photogrammetry Dataset and comparing elevation differences along the levee centerline in order to adjust the 2022 LiDAR elevations along the centerline to the conditions pre-Albuquerque West levee construction. A similar exercise was performed for the Corrales levees, since the 1984 boreholes were predominantly in this area and predated the construction of the engineered levee here. This adjustment, however, simply used the average levee change as reported by USACE (2018).

As another example, the process of extracting sediment size information at the filtered 2019 issue locations based on the borehole data required the correlation between the borehole logs and the laboratory data analyzed by collected sediment samples. While this analysis utilizes existing dataset, the correlation itself creates a new dataset. The correlated data included provided gradation data (percent mass finer passing a given sieve size), Unified Soil Classification System (USCS) designations, and general soil descriptions at each of the borehole locations. The following standard sieve sizes were employed in the analysis: #10, #16, #30, #40, #50, #100, and #200. For some of the borehole sets, a narrower set of sieves was utilized and then linear interpolation between sieve sets was utilized to fill the gap or information was extracted from the provided data to assess a d_{16}, d_{50}, and/or d_{84} size. The gradation information was also correlated to Wentworth (1922) size classifications to provide a more consistent soil taxonomy utilized in the sediment transport arena and then the percent of the sample within each of the Wentworth classifications was computed. Additional details on these developed datasets are provided in Attachment 2.

The developed datasets provided the following information that was used to feed the statistical analysis and ascertain if there was a correlation between the filtered 2019 issue locations, the historical channel locations, and the location of coarser soil materials.

- Historical planform feature type correlated to the filtered 2019 issue locations

- Distance to active channel for the filtered 2019 issue locations (1918, 1935, and 1949 planforms)
- Distance to active channel for the borehole locations utilized in this analysis (1918, 1935, and 1949 planforms) and those specifically correlated to the 2019 issue locations.
- 2019 issue locations correlated to the 1918 "vegetated island" planform
- Borehole locations utilized in this analysis correlated to the 1918 "vegetated island" planform
- The 2006 seepage rating for the filtered 2019 issue locations
- The 2006 slope stability ratings for the filtered 2019 issue locations
- Riverside drain d_{16} at the filtered 2019 issue locations
- Riverside drain d_{50} at the filtered 2019 issue locations
- Riverside drain d_{84} at the filtered 2019 issue locations
- Landside toe d_{16} at the filtered 2019 issue locations
- Landside toe d_{50} at the filtered 2019 issue locations
- Landside toe d_{84} at the filtered 2019 issue locations
- Levee centerline d_{16} at the filtered 2019 issue locations
- Levee centerline d_{50} at the filtered 2019 issue locations
- Levee centerline d_{84} at the filtered 2019 issue locations
- Riverside toe d_{16} at the filtered 2019 issue locations
- Riverside toe d_{50} at the filtered 2019 issue locations
- Riverside toe d_{84} at the filtered 2019 issue locations
- River centerline d_{16} at the filtered 2019 issue locations
- River centerline d_{50} at the filtered 2019 issue locations
- River centerline d_{84} at the filtered 2019 issue locations

Statistical Methods

The previous collated and developed datasets provide additional information at the 84 filtered issue locations identified from the 2019 spring snow-melt runoff. These 84 issue locations represent the sample field from which relations are assessed to determine if there is a correlation that can potentially explain the observed problem sites. Statistical tools are utilized to evaluate the correlation in order to assess the confidence level. The assumption is made that the 84 samples points are representative of an overall population of groundwater failure points within the Albuquerque area. Furthermore that the points and the data extracted for each of those points represent independent and discrete datasets and have similar distribution characteristics. The following statistical methods are utilized to evaluate these assumptions and the gathered dataset correlations. Additional details on the statistical methods are provided in Attachment 3.

- **Frequency distributions** – Frequency distributions are often used to gain an idea of the statistical distribution for a particular relationship (Weaver 2000). Planform type and distance to active channel were the two relationships evaluated for the 1918, 1935, and 1949 historical datasets relative to the filtered 2019 issue locations, the borehole locations, and the borehole locations correlated with the 2019 issue locations.

Distributions, whether viewed by individual units (bins) or cumulatively, provide insight into the sample's distribution. It would be expected that different types of data would show different distributions. For example, given the increased level of anthropogenic activity in the Rio Grande and its floodplain between 1918 and 1949, the planform type and distribution of the distance to the active channel at the 2019 areas of interest would be expected to differ. Conversely, the distance to the active channels for a given year at the 2019 areas of interest would be expected to have a similar distribution as the boreholes correlated to those areas of interest, which would be different than all of the boreholes together.

- **Summary statistics** – These are numerical values determined from the sample sets to evaluate planform type, bed material at various locations, and the distance to the active channel for the 1918, 1935, and 1949 historical datasets relative to the filtered 2019 issue locations, the borehole locations, and the borehole locations correlated with the 2019 issue locations. These relationships help to quantify the central tendency, dispersion, and skewness of the datasets. The central tendency provides insight into where most of the data is located, while the dispersion states if the data is strongly or weakly clustered around this value. If the 2019 issue locations are strongly correlated to the historical active channels, it would be expected that the distance to the active channel location would have a lower central tendency value with a strong clustering around the value. If the hypothesis is true, it would also be expected to find larger particle sizes associated with the riverside drain and current active channel elevations. Finally, data skews help assess underlying distributions of data. Low skew and kurtosis values for the distance to active channel or a coarse particle size argue for a strongly correlated dataset with fewer outliers, while the opposite suggests there is significant variability, and any correlation is much weaker.
- **Independence checks** – One of the underlying assumptions is that the datasets being assessed are independent and discrete sample points. This was only evaluated for the distance to the active channel for the 1918, 1935, and 1949 historical datasets relative to the filtered 2019 issue locations, the borehole locations, and the borehole locations correlated with the 2019 issue locations. Both run-sequence and lag plots were utilized to assess this independence. Run-sequence plots view the sample set either chronologically or spatially, while the lag plots compare consecutive sample values against each other. A truly independent and discrete sample would show no visual pattern, while a visual observation of a pattern suggests a degree of correlation in the sample set. For example, a plot of the distance to the active channel at each of the 2019 areas of interest, would be expected to show a scattershot of data if the values are truly independent. This would suggest a poor correlation between the 2019 areas of interest and the historical channel locations. Conversely, the identification of a pattern would suggest some level of correlation.

- **Regression relationships** – Regression lines were evaluated between data sets to determine the degree of correlation between the distance from the active channel for the 1918, 1935, and 1949 historical datasets to the filtered 2019 issue locations and the median sediment size, seepage rating, and slope stability rating. Data relationships between two sample sets, for example distance to active channel and bed material size, can help determine if observed trends are strong or weak between the two plotted variables. Only linear regressions were evaluated as part of this analysis.

Results

Overall, the statistical analysis showed that there is some linkage between the historical channel and the filtered 2019 issue locations. The connection to the 1918 active channel is stronger than found for either 1935 or 1949. The presence of coarse material based on the borelogs at the elevation of the riverside drain, or the current Rio Grande active channel shows only a slight correlation, with some of the 2019 issue locations showing a strong correlation and others no correlation. The same was true when looking at the 2019 issue locations and locations where seepage and slope stability rating were considered high. Four statistical evaluation techniques were utilized in this analysis: frequency distributions, summary statistics, independence checks, and linear regressions. The results from each of these analyses are summarized in the sections that follow.

Frequency Distributions

Both planform type and distance to active channel frequency distributions were evaluated. The evaluation of the planform types showed a change in the distribution pattern between 1918, 1935, and 1949. About 19% of the identified 2019 issue locations are within the active channel and none in 1935 and 1949. A summary of the results is provided in Table 1.

Underlying data associated with this analysis is found in Attachment 2, with graphical representations available in Attachment 3.

The distribution of the distances to the active channel and the filtered 2019 issue locations also seems to be different between 1918 and 1935/1949. In 1918 there is a cluster of 2019 issue locations that are very close or in the active channel and then a distribution of points further away. The best fitting distribution is a gamma distribution (p-value of 0.56), but both the gamma and lognormal distributions have trouble fitting the distribution centers for the 1918 sample set. The 1935 and 1949 active channel distances have a more singular clustering, with reasonable fits to both the gamma and lognormal distributions. The 1935 active channel distance is best fit by the gamma distribution (p-value of 0.56), while the 1949 active channel distance is best fit by a lognormal distribution (p-value of 0.60).

The boreholes correlated to the 2019 issue locations have a similar distribution of active channel distances as described for the 2019 issue locations. The 1918 distances are best described by a normal distribution, while a gamma distribution best describes that for 1935 and 1949. The

distribution of all the borehole locations has a cluster of data less than 250 feet with a long, positively skewed tail that doesn't fit a normal, lognormal, or gamma distribution. This suggests that the distribution of active channel distances to drilled boreholes from 1984 through 2022 is distinct from the distributions of the active channel distances to the 2019 issue locations and the boreholes correlated to those issue locations. There are some dissimilarities between the 2019 issue locations and the correlated boreholes as well, which may suggest that the assessed stratigraphy (which comes from the correlated boreholes) may not be as representative of all the 2019 issue locations.

Table 1. Summary of planform type found for the filtered 2019 areas of interest and the borehole locations.

Planform Type	Bin #	% of points found in the historical datasets					
		1918		1935		1949	
		2019 issue locations	Borehole Locations	2019 issue locations	Borehole Locations	2019 issue locations	Borehole Locations
active channel	2	19	24		14		5
vegetated island	13	11	3				1
historic channel	5				25		48
recent channel change					4		
flood prone	4			95	54	6	
upland use	12					94	43
out of study area	8			5	3		3
no data	7	70	73				

Summary Statistics

Summary statistics were used to primarily evaluate distance to active channel, seepage ratings, slope stability ratings, and particle sizes at various stratigraphy elevations that correlate with cross-section features on the Rio Grande. Underlying data is shown in more detail in Attachment 3. Assuming the sample sets are normally distributed, the estimated minimum required sample numbers are met or are greatly exceeded by the actual sample set counts. This implies that the tested sample sets provide a reasonable approximation of the data population.

The mode, mean, median, and Tukey's Trimean all suggest a strong to moderate correlation (central tendency of less than 100 ft) between the 2019 issue locations and the 1918, 1935, and 1949 planform locations. The 1935 and 1949 planforms have a shorter distance than the 1918 planform. The borehole locations and the boreholes correlated to the 2019 issue locations have a central tendency that is significantly greater, with the correlated boreholes often being worse than all the boreholes together. This is somewhat expected since the borehole locations were assigned to provide general representation along the levee systems instead of targeting specific issue locations. The other sample set moments (dispersion, skew, and kurtosis) show a stronger correlation with the active channel distances being strongly clustered. This suggests that there is

a correlation to the active channel locations but that the boreholes may have a different sample distribution and so extrapolation of borehole stratigraphy to the 2019 issue locations may not be representative.

The 2019 issue locations are generally not associated with a vegetated island in the 1918 planform, which would have suggested finer particle distributions would have been possible. The 2019 issue locations do have a have a Tukey's trimean seepage rating of three (high risk) and a slope stability rating of two (moderate risk). A little over half (43) of the 2019 issue locations are located in reaches with high seepage risk. None of the 2019 issue locations were located in areas of high slope stability risk, although more than half (55) were in areas of moderate risk. This suggests that there is some correlation of seepage and slope stability risk that is also associated with the 2019 issue locations. These risk factors evaluated current soil conditions at the levees and potential surface to groundwater gradient factors, suggesting that some of the 2019 issue locations are driven by traditional geotechnical concerns, as opposed to, or in addition to a connection to historical channel locations.

Statistics related to grain sizes for the 2019 issue locations based on elevation at various cross-sectional features (e.g., riverside drain, landside levee toe, levee centerline, riverside levee toe, and river centerline) showed little variability. The riverside drain shows a coarser grain size that is statistically different than the other cross section locations for the d_{16} grain size. The interquartile range (Q_1 through Q_3) is generally larger at the Riverside Drain for the d_{16} and d_{50} grain sizes than the other locations, except for the river centerline location. The interquartile range for the d_{84} grain size at the Riverside Drain is about the same as other locations, although the landside toe is finer. Of one interesting note is the error estimate, assuming a normal distribution, which is significantly less than a grain classification, suggesting the differences in the central tendency may be significant.

The borehole stratigraphy evaluated as part of this project generally had finer material at the surface that coarsened with depth (SM/ML to SM/SP layers). Often there is a lens of clay material in the stratigraphy as well, but generally this is in the upper ten feet. Most of the observed 2019 issue locations had correlated borehole stratigraphy that is in the Wentworth categories of FS or smaller, suggesting deposits are more likely correlated to a floodplain fluvial setting than the coarser material of the active channel. The range of the nominal particle size (d_{50}) did have some larger particles (MS or larger) within the third quartile for the riverside drain (31 out of the 82 issue locations identified) and current river channel locations (24 out of the 82 issue locations identified), suggesting that some of the issue locations likely are influenced by historical active channel locations.

Figures of the 2019 issue locations, boreholes which were evaluated in this analysis, active channel locations from 1918, 1935, and 1949, and issue locations with median grain size material of around the MS or larger are shown in the figures that follow. Evaluation of these figures reveals that some of the issue locations are in a different planform location than the

borehole from which the grain size was extracted. For example, an issue location was noted on Sandia Pueblo on the east side in a section of the river where the current and historical channels of the Rio Grande are primarily straight. The borehole correlated to this site is downstream of this site along the outside bank of a river bend. This area of the river likely had higher energy and thus any deposited material would likely be larger in size than material deposited in a straighter section, which may be why this particular site shows the presence of coarser material at the current drain elevation. There are other areas, shown in these figures, where the correlated boreholes are within the same general planform feature and likely are better representations of historical conditions. These areas include an outside bend in the Los Ranchos area and a series of bends from Bridge Blvd to around the Pajarito area. The 2019 issue locations in these areas that are correlated with coarser material tend to be on the outside of active historical river bends.

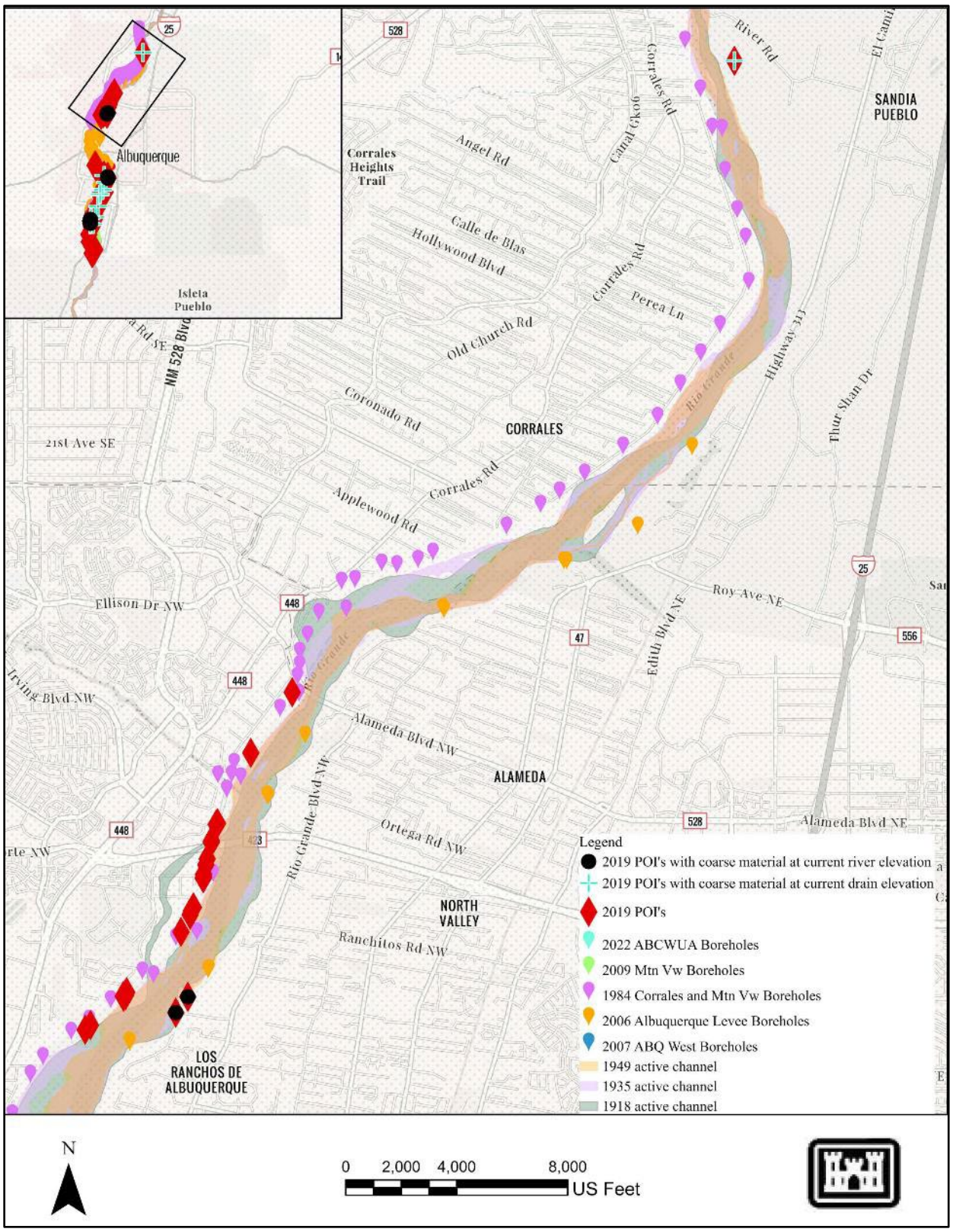

Figure 8. 2019 issue locations associated with coarser sediment: Corrales Siphon to Los Ranchos. Also shown are the historical active channel locations from 1918, 1935, and 1949. Background imagery is from ESRI accessed on 18 October 2023.

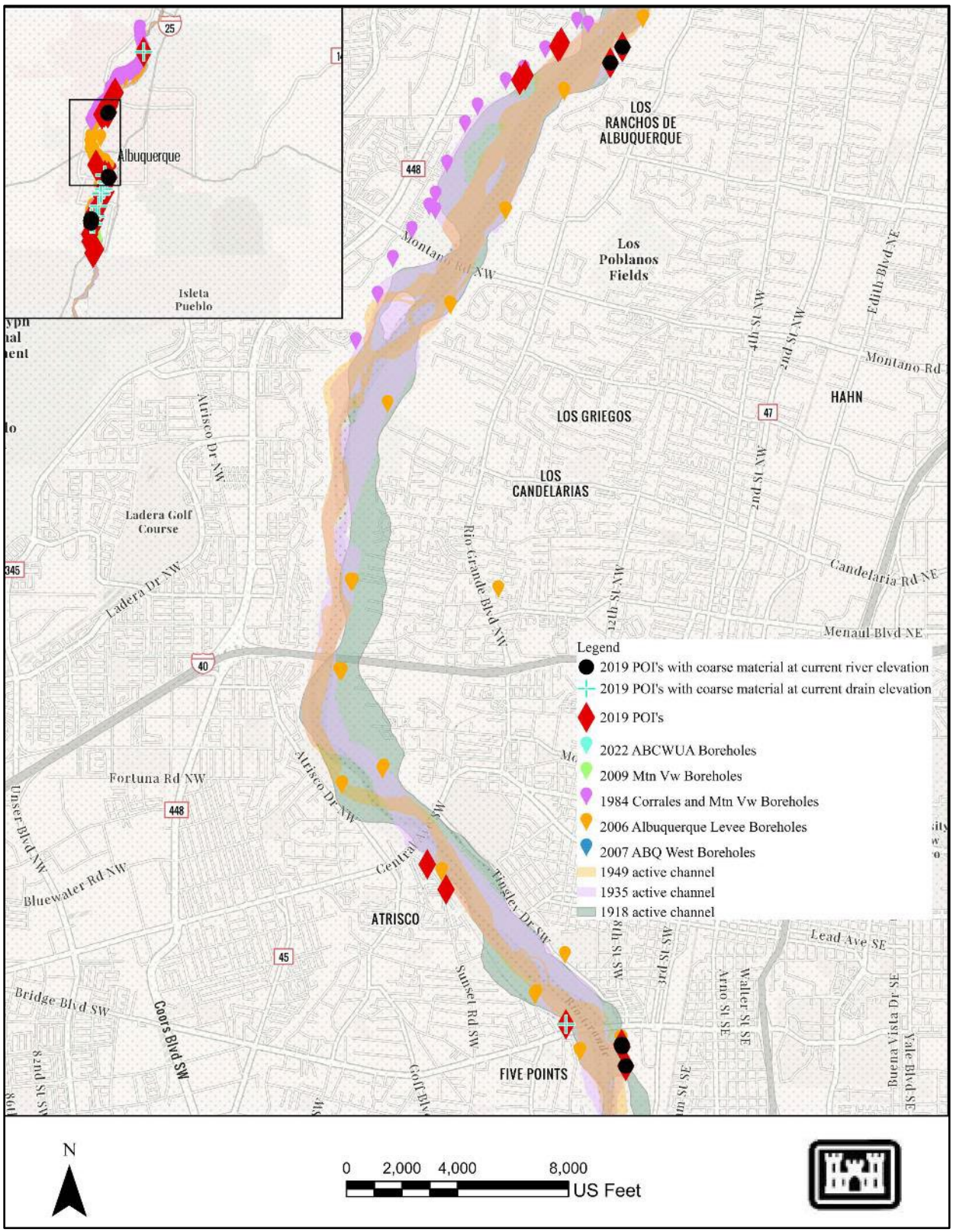

Figure 9. 2019 issue locations associated with coarser sediment: Los Ranchos to Bridge Blvd. Also shown are the historical active channel locations from 1918, 1935, and 1949. Background imagery is from ESRI accessed on 18 October 2023.

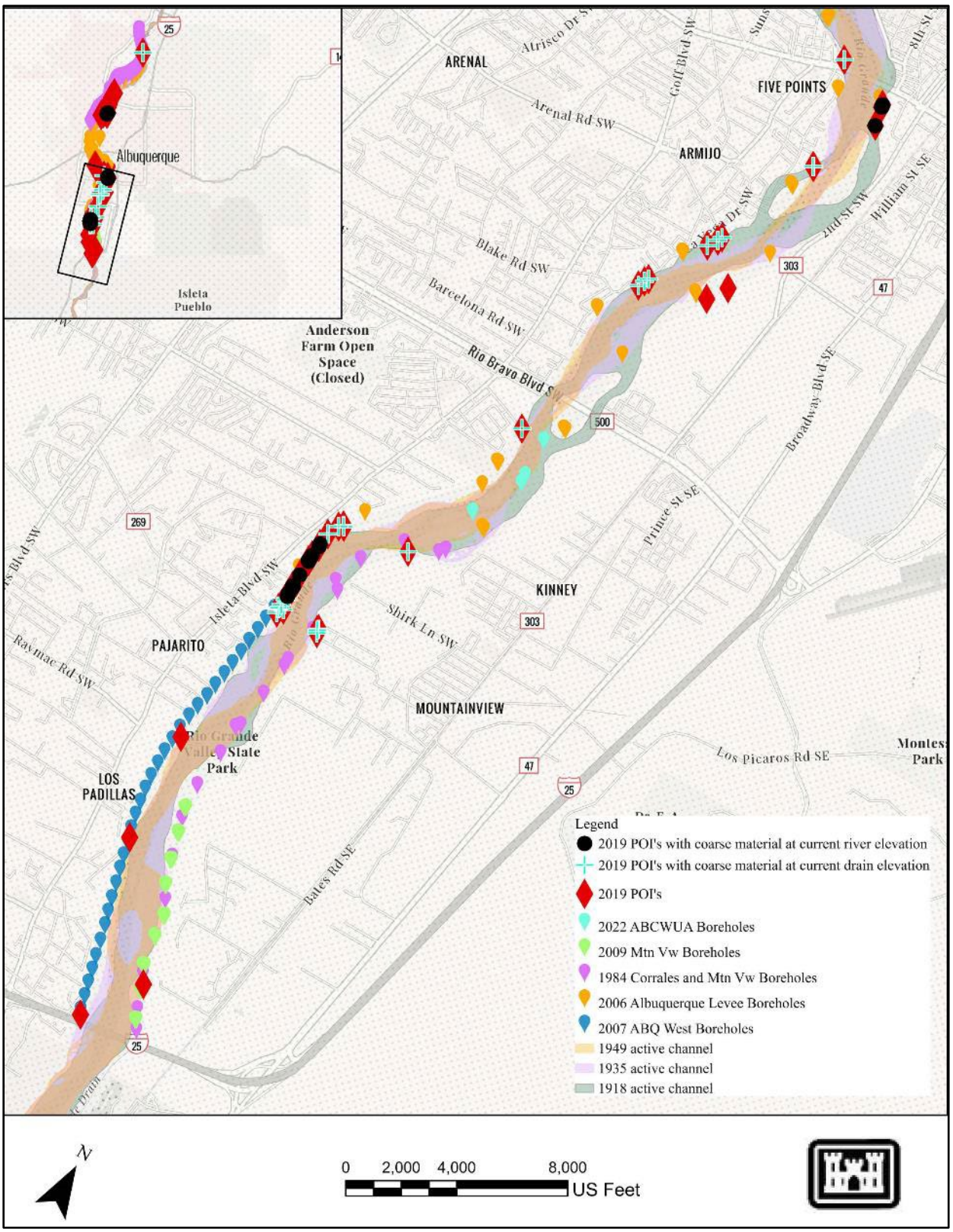

Figure 10. 2019 issue locations associated with coarser sediment: Bridge Blvd to I-25. Also shown are the historical active channel locations from 1918, 1935, and 1949. Background imagery is from ESRI accessed on 18 October 2023.

Independence Checks

Some independence checks (run-sequence and lag plots) were evaluated for the active channel distances. Underlying data is shown in more detail in Attachment 3.

The run sequence plots have a sinusoidal pattern that is more obvious in the active channel distance to the filtered 2019 issue locations than either all of the boreholes or the correlated boreholes. This seems reasonable since the points are listed from north to the south, which is the flow direction of the Rio Grande. As the Rio Grande flows it oscillates from the east to the west side in an irregular pattern that is suggestive of the plotted active channel distances. That this is more readily apparent with the 2019 issue locations and not the boreholes suggests there is a stronger correlation between the active channel and the 2019 issue locations than the active channel and the borehole locations, even the boreholes within a close proximity of the 2019 issue locations. This also suggests that the borehole stratigraphy may not be representative of the 2019 issue locations.

The sinusoidal pattern signal is strongest for the 1918 active channel distance, becoming more obfuscated in the 1935 and 1949 graphs. It is interesting that the sinusoidal pattern observed in 1918 shifts in the downstream direction in 1935 and then again in 1949, reflecting perhaps the morphological changes that were occurring in the Rio Grande during those time periods.

The lag sequence plots are interesting because they indicate that the distance to the active channels from the 2019 areas of interest are likely correlated, compared with the borehole information. The borehole plots are more uniformly spread out from the 1:1 correlation line, but the 2019 issue locations are clustered on the 1:1 correlation line. The correlated boreholes show more correlation to the active channel distance than all the boreholes together, but not as strong as the issue locations.

Linear Regressions

Regression relationships were explored between the active channel distances and the sediment sizes at various elevations correlated to cross-section features, seepage ratings, and slope stability ratings. None of the relationships plotted indicate a correlation with the active channel distance in 1918, 1935, or 1949, with R squared values all less than 0.2. Underlying data is shown in more detail in Attachment 3. The nominal bed material (d_{50}) was extracted from boreholes along the levee centerline and correlated based on depth below the levee crest to contemporary riverine features using the Wentworth (1922) classification categories. While there are no discernible trends between the grain size class and the distance to the active channel, it is interesting that the coarsest materials tend to be at the current riverside drain location. There is also more consistency in the soil classifications at the other locations compared with the current riverside drain locations.

The boreholes correlated to the 2019 issue locations generally ranged from 39 to 1800 ft away, with one location pulling information from a borehole that was over 14,000 ft away. Less than

6% of the 2019 issue locations were located within 100 feet of the correlated borehole from which the grain size information was pulled. This may explain the observed poor correlation. The average active channel widths between 1918 and 1949 in the Albuquerque area ranged from around 600 to 1300 feet (Makar and Aubuchon 2012), which if centered at an issue location indicates that a borehole range less than 650 feet from the observed 2019 issue locations would be more desirable.

Conclusions

The conducted analyses indicates that the filtered 2019 issue locations have some correlation to the observed active channel locations in 1918, 1935, and 1949, with the earliest year having stronger visual correlations, although the summary statistics of active channel distance favor the latter years. It was speculated that a stronger correlation may exist between the 2019 issue locations and active channel morphology that predates 1918, based on the morphological planform type changes between 1918 and 1949. The correlation between coarser sediment deposits and the 2019 issue locations is poor, however, and may be a result of correlated boreholes that were not closely associated with the 2019 issue locations.

The analysis suggested that there is a moderate correlation between the 2019 issue locations and zones identified as high to moderate risk for seepage and slope stability failures. Only about 43% of the 2019 issue locations had a high seepage rating and none of the 2019 issue locations had a high slope stability rating. Roughly a third of the 2019 issue locations were located in areas with a low seepage and slope stability rating. Part of the hypothesis testing was to evaluate whether historical river planforms, compared to other conditions, such as standing water or vertical gradient change, are contributing to groundwater movement that is causing seepage and slope stability issues on the riverside drains. This analysis was inconclusive in identifying a primary cause but suggests that historical channels and traditional seepage concerns (e.g., standing water, vertical gradient change, etc.) are likely both contributing culprits in the observed 2019 issue locations.

While the evaluation was focused on a flood control nexus because of a dataset that provided spatially diverse and observable links to groundwater movement, it does suggest that an increased groundwater connection through coarser sediment deposits from historical active channel locations is possible. Based on the data evaluated, the relationship is moderate at best and likely more pronounced where the current active channel has incised into the stratigraphy laid down by historical active channels. This insight would need to be tested further but if valid, advantage could be taken of historical active channel locations to develop habitat restoration that benefits from an increased flow of groundwater. Historical active channel locations may be worth the consideration, in habitat restoration however within the Floodway, as there was some groundwater connection observed. Soil moisture and groundwater connectivity are interrelated and are listed as areas of uncertainties for the Conceptual Ecological Models for endangered species (MRGESCP 2021a; MRGESCP 2021b; MRGESCP 2021c).. The increased groundwater

flow may not be as important, however, as having a floodplain overlain with finer material to minimize soil moisture losses. Generally the finer material is also brought in through a connection with the current active channel location.

Recommendations/Future Work

While a moderate correlation exists between the historical channel locations and groundwater movement based on the observed 2019 issue locations, the statistical support for a strong correlation wasn't observed. The focus of this analysis was on utilizing existing datasets to assess if a groundwater connectivity could be made. This was only partially successful and some suggestions/recommendations for future work may reach a more conclusive end.

The first recommendation is based on the observed bias in the sediment evaluations because of the distance away from the 2019 issue locations. Future work that limited the distance from which borehole information is extracted may show a higher correlation. Also, evaluations with regard to the planform location (e.g., outside of bend, straight away, etc.) and ensuring that the borehole information extracted for a given 2019 issue location comes from a similar planform location may also improve the statistical correlation. A comparison of the current active channel elevations relative to the 1918 active channel elevations may also be interesting to see if there are connections where these channels intersect and there is a historical channel slope towards the levee in the vicinity of the observed 2019 issue locations.

The second recommendation is with regard to a Rio Grande centric focus. Large floods listed by Scurlock (1998) are not limited to the spring snow-melt season (May-June), but include events that occurred in the fall, which suggests heavy monsoonal activity. The hypothesis for this work only considered Rio Grande flows but considerable sediment is also provided by ephemeral tributaries to the Rio Grande and subsequent re-working of those sediment. Parsing locations by proximity to ephemeral tributaries may also provide additional insight.

Thirdly, a comparison between existing vegetation types and historical active channel locations may also prove insightful. The larger substrate sizes tend to be about 10 feet below the levee crest. The riverside drains tend to be below this elevation, while the current river channel is around this level. It is possible therefore that certain types of vegetation may be more prevalent along paths of higher groundwater flow. A study that evaluated differences in current vegetation patterns inside and outside of the historical active channel locations may potentially provide a revealing insight on groundwater movement in the Rio Grande valley.

Finally, as a more extensive network of groundwater data becomes available, tracking groundwater movement during a spring snow-melt runoff would provide more conclusive evidence of connectivity.

References

AMEC (2006). "2-Albuquerque Levees Lab Data No Cover Sheets." AMEC Earth Environmental, Inc. for Geomachnics Southwest, Inc., Albuquerque, NM.

AMEC (2008). "Geotechnical and Hydrogeological Investigation and Analysis Report Albuquerque West Levee Project." AMEC Earth and Environmental, Inc. for Bohannan Huston, Inc., Albuquerque, NM.

ASTM (2017). "Standard Test Methods for Particle-Size Distribution (Gradation) of Soils Using Sieve Analysis." *D6913/D6913M-17*, American Society for Testing and Materials, International, West Conshohocken, PA.

AuBuchon, J., Abraham, D., and Jackson, T. (2023). "2019 Middle Rio Grande Sediment Measurements."Albuquerque, NM.

Bauer, T. (2007). "2006 Bed Material Sampling on the Middle Rio Grande, NM." U.S. Department of the Interior, Bureau of Reclamation, Technical Service Center, Denver, CO.

Bauer, T. R. (2009). "Evolution of Sediment on the Middle Rio Grande, New Mexico." *SRH-2009-32*, U.S. Department of the Interior, Bureau of Reclamation, Technical Service Center, Denver, CO.

Berry, K. L., and Lewis, K. (1997). "Historical Documentation of Middle Rio Grande Flood Protection Projects Corrales to San Marcial." University of New Mexico, Office of Contract Archaeology for the U.S. Army Corps of Engineers, Albuquerque District, Albuquerque, NM.

BHI (2009). "As-Built Constructino Plans for Albuquerque West Levee Project Bernalillo County, New Mexico." Bohannan Huston for the Middle Rio Grande Conservancy District, Albuquerque, NM.

Boberg, S., Shafike, N., Jordan, B., and Wilson, D. (2019). "2019 Middle Rio Grande High Flow Event: Report on Monitoring Efforts along the Corrales to Belen Rio Grande Corridor." U.S. Army Corps of Engineers Albuquerque District, Albuquerque, NM.

Das, B. M. (1990). *Principles of Geotechnical Engineering, Second Edition*, PWS-Kent Publishing Company, Boston, MA.

Das, B. M. (2006). *Principles of Geotechnical Engineering, International Student Edition*, Thomson Learning, Toronto, Ontario, Canada.

Delignette-Muller, M. L., and Dutang, C. (2015). "fitdistrplus: An R Package for Fitting Distributions." *Journal of Statistical Software*, 64(4), 1-34.

Erhardt, E. B., Bedrick, E. J., and Schrader, R. M. (2015). "Lecture notes for Advanced Data Analysis I (ADA) " *Stat 427/527*, University of New Mexico, Albuquerque, NM.

Fox (1984). "Sieve Analyses, Moistures and Atterberg Limits Tests for the Rio Grande Levees." Fox and Associates of New Mexico, Inc Consulting Engineers and Geologists for the U.S. Army Corps of Engineers, Albuquerque District, Albuquerque, NM.

Frost, J. (2019). "How to Identify the Distribution of Your Data." *Statistics by Jim: Making statistics intuitive*, <https://statisticsbyjim.com/hypothesis-testing/identify-distribution-data/>. (2 October 2019).

Glen, S. (2023). ""Trimean (Tukey's Trimean)" from StatisticsHowTo.com: Elementary Statistics for the rest of us." <https://www.statisticshowto.com/trimean/>. (23 August, 2023), Independent Media Associates, Inc. , Los Angeles, CA.

Grassel, K. (2002). "Taking out the Jacks: Issues of Jetty Jack Removal in Bosque and River Restoration Planning." *Water Resources Program, Publication WRP-6*, University of New Mexico, Albuquerque, NM.

Hazen (2023a). "100% Design Documents for the Construction of the Southside Water Reclamation Plant (SWRP) Outfall Restoration Project." Hazen and Sawyer for the Albuquerque Bernalillo County Water Utility Authority, Albuquerque, NM.

Hazen (2023b). "Southside Water Reclamation Plant Outfall Restoration Design Project Final Basis of Design Report 90% Design Phase." Hazen and Sawyer for the Albuquerque Bernalillo County Water Utility Authority, Albuquerque, NM.

Jimenez, R. (2009). "MRG Levee Drilling Logs." LEC, Inc., Albuquerque, NM.

Lagasse, P. F. (1980). "An Assessment of the Response of the Rio Grande to Dam Construction - Cochiti to Isleta Reach."West Point, NY.

Licon (2010). "Middle Rio Grande Flood Protection Project - Albuquerque to Belen, NM." Licon Engineering Co., Inc., Albuquerque, NM.

Makar, P., and Aubuchon, J. (2012). "Channel Conditions and Dynamics of the Middle RIo Grande River." Bureau of Reclamation, Albuquerque, NM.

Microsoft (2019a). "Average function." *Microsoft Office Help*, <<https://support.office.com/en-us/article/AVERAGE-function-047BAC88-D466-426C-A32B-8F33EB960CF6>>.

Microsoft (2019b). "KURT function." *Microsoft Office Help*, <<https://support.office.com/en-us/article/SKEW-function-BDF49D86-B1EF-4804-A046-28EAEA69C9FA>>. (22 February, 2019).

Microsoft (2019c). "SKEW function." *Microsoft Office Help*, <<https://support.office.com/en-us/article/KURT-function-BC3A265C-5DA4-4DCB-B7FD-C237789095AB>>.

Microsoft (2019d). "STDEV function." *Microsoft Office Help*, <<https://support.office.com/en-us/article/STDEV-function-51FECAAA-231E-4BBB-9230-33650A72C9B0>>. (5 September, 2019).

MRGESCP (2021a). "Draft SWFL CEM November 2021." Middle Rio Grande Endangered Species Collaborative Program, Ad Hoc group,, Albuquerque, NM.

MRGESCP (2021b). "Draft YBCU CEM November 2021." Middle Rio Grande Endangered Species Collaborative Program, Ad Hoc group,, Albuquerque, NM.

MRGESCP (2021c). "RGSM CEM June 2021." Middle Rio Grande Endangered Species Collaborative Program, Ad Hoc group,, Albuquerque, NM.

Mun, J. (2008). "Appendix C: Understanding and Choosing the Right Probability Distributions." *Advanced Analytical Models: Over 800 Models and 300 Applications from the Basel II Accord to Wall Street and Beyond*, <<https://onlinelibrary.wiley.com/doi/pdf/10.1002/9781119197096.app03>>. (26 February, 2019).

Nordin, C. F., and Beverage, J. P. (1965). "Sediment Transport in the Rio Grande New Mexico." *Geological Survey Professional Paper 462-F*, U.S. Geological Survey, Washington D.C.

Oliver, J. (2012). "Middle Rio Grande, Active Channel Features, 2012 (Metadata)." U.S. Department of the Interior, Bureau of Reclamation, Denver, CO.

Perea, J. (2006). "2006 Drilling Sites Borehole logs (1- ABQ Levees Drill Logs)." Geomechanics Southwest Inc. for the U.S. Army Corps of Engineers, Albuquerque District, Albuquerque, NM.

Schmidt, J. C., Everitt, B. L., and Richard, G. A. (2003). "Hydrology and Geomorphology of the Rio Grande and Implications for River Rehabilitation." *Special Publications Aquatic*

Fauna of the Northern Chihuahuan Desert, G. P. Garrett, and N. L. Allan, eds., Museum of Texas Tech University, Alpine, TX, 25-45.

Scurlock, D. (1998). "From the Rio to the Sierra: An Environmental History of the Middle Rio Grande Basin."Ft. Collins, CO.

Triola, M. F. (2008). *Statistics for Business Decisions, taken from Essentials of Statistics, third Edition*, Learning Solutions, New York, NY.

USACE (1986). "Middle Rio Grande Flood Protection Bernaillo to Belen, NM, General Design Memorandum No. 1 Volume A Main Report." U.S. Army Corps of Engineers, Albuquerque, NM.

USACE (2009). "Rio Grande Floodway, Albuquerque Unit Evaluation Report Albuquerque, New Mexico." U.S. Army Corps of Engineers, Albuquerque District, Albuquerque, NM.

USACE (2018). "Middle Rio Grande Flood Protection Bernalillo to Belen, New Mexico: Mountain View, Isleta and Belen units Integrated General reevaluation Report and Supplemental Environmental Impact Statement." U.S. Army Corps of Engineers, Albuquerque District, Albuquerque, NM.

Weaver, J. H. (2000). "Conquering Statistics: numbers without the Crunch."Cambridge, MA.

Wentworth, C. K. (1922). "A Scale of Grade and Class Terms for Clastic Sediments." *The Journal of Geology*, 30(5), 377-392.

Woolpert (2022). "Lidar Mapping Report Middle Rio Grande Project 2022." Woolpert for the U.S. Department of the Interior, Bureau of Reclamation, Dayton, Ohio.

Attachment 1: Collation of Datasets

The proposed analyses requires the collation of a variety of existing datasets, which are described in more detail in the sections that follow.

1918, 1935, and 1949 historical planforms

The planform dataset was developed by the U.S. Department of Interior, Bureau of Reclamation (Reclamation) based on georeferenced hand-drawn linens (1918), and aerial photography (1935 and 1949). In the process of digitizing observable features a "script" attribute field was added to differentiate between active channel, floodplain, recent changes (since the last aerial photography), etc. (Oliver 2012). Originally the dataset was developed as a personal geodatabase (RioGrandeSP83.mdb) which was converted to a file geodatabase (RioGrandeSP83.gdb) for this analysis. While all the "script" attributes were evaluated, the "active channel" and the "veg island" definitions within the "script" attribute field are assumed to provide more insight into where the potentially coarser materials were deposited.

1984 Corrales and Mountain View Levee Borehole locations

Geotechnical exploration by the U.S. Army Corps of Engineers (USACE) in 1984 was done to evaluate flood control designs in the MRG Valley. The borehole locations were digitized based on the planview locations shown in the design drawings (USACE 1986). The borehole logs didn't contain any spatial information, so the approximate locations were digitized in ArcGIS Pro (version 3.1.0) at a scale of 1:4000. Placement of borehole locations was done visually by comparing the planview locations with georeferenced imagery from 1972 and the 1985 active channel planform. Boreholes along the levee were snapped to the 2022 levee centerline, described in the section on Developed Datasets. These are shown in Figure 11.

1984 Corrales and Mountain View Levee Borehole data

The 1984 geotechnical exploration generated borehole logs and geotechnical evaluations. The borehole and geotechnical evaluations are listed in Fox (1984). For this analysis the gradation information and soil classifications were the primary source of data collated.

2002 Photogrammetry dataset

Reclamation collected aerial photography data in the January/February 2002 timeframe on the Middle Rio Grande from which a photogrammetric surface was created. The dataset was delivered in the NM SP NAD 29, central zone projection with a 1-foot contour interval vertical accuracy according to the National Map Accuracy Standards. The elevations were listed in the NGVD29 vertical datum. Part of the delivery of data from Reclamation included the extraction of the 2002 photogrammetric surface along aggradation-degradation (agg-deg) lines established within the MRG. For this analysis the 2002 agg-deg points were adjusted to the NM SP NAD 83, central zone projection using the NAVD88 vertical datum.

2006 Albuquerque Levee Borehole locations

Geotechnical exploration by USACE in 2006 was done for an evaluation report of the Albuquerque Levee units (USACE 2009). Borehole locations were digitized based on the coordinates provided at each borehole (latitude, longitude). An attribute table was created that lists the borehole name. These are shown in Figure 12.

2006 Albuquerque Levee Borehole data

The 2006 geotechnical exploration generated borehole logs and geotechnical evaluations. The borehole logs are listed under Perea (2006). The geotechnical evaluation is provided within AMEC (2006). For this analysis the gradation information and soil classifications were the primary source of data collated.

2006 Analyses

Various analyses were performed by USACE as part the evaluation report of the Albuquerque Levee units. One of the analyses (USACE 2009, Figure 22, p. 55) subdivided the Albuquerque area into 5 main reaches, which were further subdivided into subreaches. This was primarily done in order to perform a tree survey, but the subreaches were carried over into other analyses.

The geotechnical analyses utilized the subreach nomenclature and estimated a subreach seepage rating and slope stability rating (USACE 2009, Table 8, p. 68). The assigned ratings included a low (1), medium (2), and high rating (3), where a high rating indicates a high seepage rate and a low slope stability. The reaches and subreaches as presented by USACE (2009, Figure 22, p. 55) were digitized for this analysis. An attribute field was added to the subreach feature class to list the seepage and slope stability rating assigned by the geotechnical analysis (USACE 2009, Table 8, p. 68). These are shown in Figure 13.

2007 Albuquerque West Levee Borehole locations

Geotechnical exploration by the USACE in 2007 was done to prepare for the Albuquerque West Levee Construction. Approximate locations of the boreholes are shown in figures 1-3 of AMEC (2008). The figure imagery was georeferenced, and the odd boreholes approximated as part of this analysis. There are three borehole sites at each odd borehole number. These were snapped to lines digitized for the levee centerline, the riverside toe, and the landside toe. The even numbers were placed halfway between the odd borehole numbers. Boring number 34 was placed 500 feet north of boring number 23. An attribute table was created that lists the borehole name. These are shown in Figure 14.

2007 Albuquerque West Levee Borehole data

The 2007 geotechnical exploration generated borehole logs and geotechnical evaluations. AMEC (2008) provides the borehole logs and the geotechnical evaluations. For this analysis the gradation information and soil classifications were utilized.

2009 Mountain View Levee Borehole locations

Geotechnical exploration by USACE in 2009 was done as part of the General Reevaluation Report (GRR) for the Belen to Bernalillo project (USACE 2018) and included boreholes through a portion of the Mountain View levee. A file composite of the drilled coordinates (NM SP NAD 83, central zone), [see Drilled Coordinates.xlsx] was used to create a comma separated values file (called Boring_2009.csv). This was brought into ArcGIS Pro and projected using the northing and easting coordinates. Boring locations included boreholes drilled on the Isleta, Los Lunas, and Belen levee sections too. The area of interest was used to further refine the boreholes to only the ones within the Mountain View area. This feature class is called "Borings_2009_MtnVw." The attribute table contains the names of the boreholes. These are shown in Figure 14.

2009 Mountain View Levee Borehole data

The 2009 geotechnical exploration generated borehole logs and geotechnical evaluations. Jimenez (2009) provides the borehole logs and Licon (2010) contains a summary of the geotechnical evaluations. For this analysis the gradation information and soil classifications were utilized.

2019 Levee Issue Locations

An ArcGIS Collector application (Boberg et al. 2019) was created in advance of the 2019 spring snow-melt runoff that was utilized by USACE, Albuquerque District (CESPA); Reclamation, the Albuquerque Area Office, and the MRGCD to record problem sites and document locations of overbank flooding. The runoff was noted to have 79 days of flow greater than 3000 cfs at the Albuquerque USGS gage (Site ID 08330000).

Within the area of interest for this analysis there were 221 points recorded within the ArcGIS collector during the 2019 spring snow-melt runoff. The points recorded during the 2019 spring snow-melt runoff were filtered to only include locations where there were indications of increased groundwater movement, such as seeping, sand boils, tension cracks, sloughing, etc. This filtered the number of issue locations to 84, 24 of which were flagged as critical.

Filtered points primarily appear in three areas: One area on Sandia Pueblo across from the Harvey Jones channel (one point), one area between Alameda and Montano roads (10 locations on west side, two on east side – 23 points in total), and one area from Central Bridge to I-25 bridge (11 locations on west side, 5 on east side – 60 points in total. Of particular note are the 33 points along a mile section of the Albuquerque West Levee unit just downstream of the Durand outfall. The reach and sub-reach designations are shown in Figure 6.

2022 Albuquerque Area Borehole locations

Geotechnical exploration by the Albuquerque Bernalillo County Water Utility Authority (ABCWUA) in 2022 as documented in Hazen (2023a). Sheet B-01 contains the geotechnical boring information as conducted by GEOMAT. The borehole logs contained northing and eastings (NM SP NAD 83, central zone) which were used to directly digitize the borehole

locations in ArcGIS Pro. This feature class is called “Borings-ABCWUA.” These are shown in Figure 14.

2022 Albuquerque Area Borehole data

The 2022 geotechnical exploration generated borehole logs and geotechnical evaluations. Hazen (2023a) provides the borehole logs and Hazen (2023b, Appendix B, p. 62), contains the geotechnical evaluations. For this analysis the gradation information and soil classifications were utilized.

2022 LiDAR/aerial photography dataset

Reclamation collected LiDAR and aerial photography data between 25 February 2022 and 8 March 2022 on the Middle Rio Grande through their Contractor Woolpert. The dataset was delivered in the NM SP NAD 83, central zone projection. LiDAR was collected with a pulse density of 8 points per square meter and has a reported horizontal accuracy of 0.305 m at a 95% confidence level (Woolpert 2022). The reported vertical accuracy was about 0.1 m for the non-vegetated accuracy and 0.21 m for the vegetated vertical accuracy, both at the 95% confidence interval. Part of the delivery of data from Reclamation included the extraction of the 2022 LiDAR elevations along agg-deg lines established within the MRG.

A mosaiced DEM was created from the 2022 LiDAR for this analysis that was clipped to the area of interest. A hillshade rendition of the mosaiced 2022 DEM was created within ArcGIS Pro (version 3.1.0) using the 3D Analyst Tools>>Raster Surface>>Hillshade. The ESRI default settings were kept for this rendition.

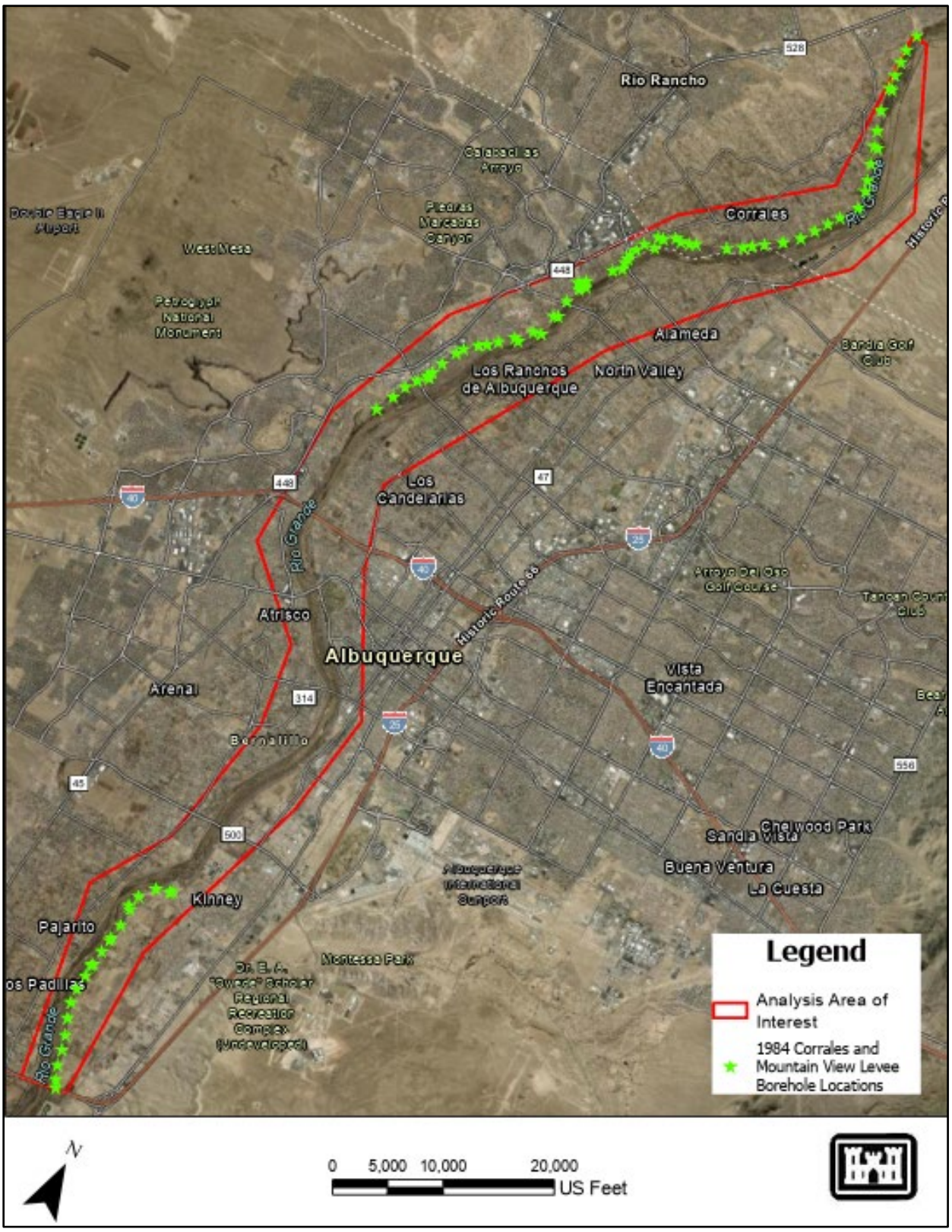

Figure 11. 1984 borehole locations within the analysis area on the MRG. Background aerial imagery is from the 2022 Middle Rio Grande Council of Government's aerial collection by Bohannon Huston from ESRI online imagery (accessed 18 August 2023).

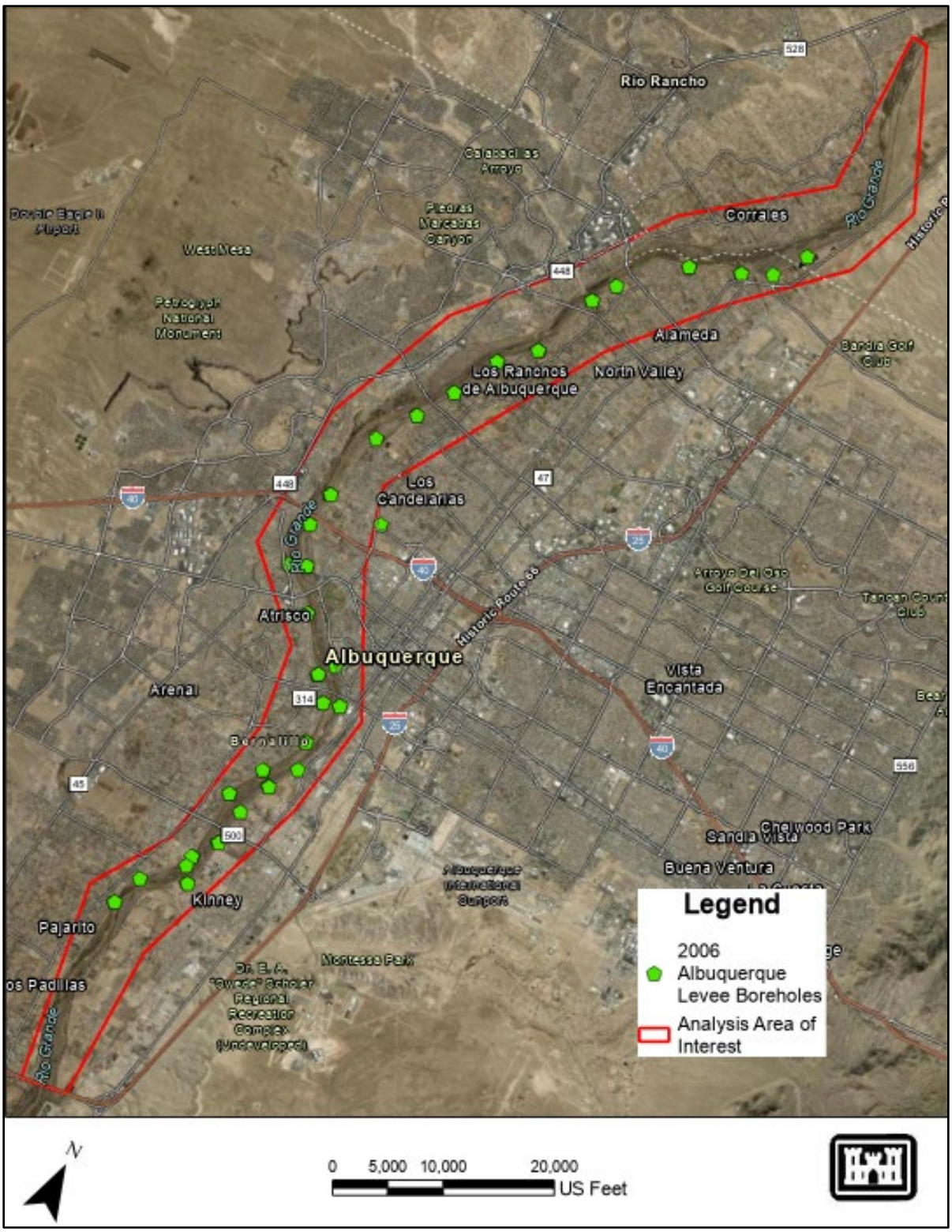

Figure 12. 2006 borehole locations within the analysis area on the MRG. Background aerial imagery is from the 2022 Middle Rio Grande Council of Government's aerial collection by Bohannon Huston from ESRI online imagery (accessed 18 August 2023).

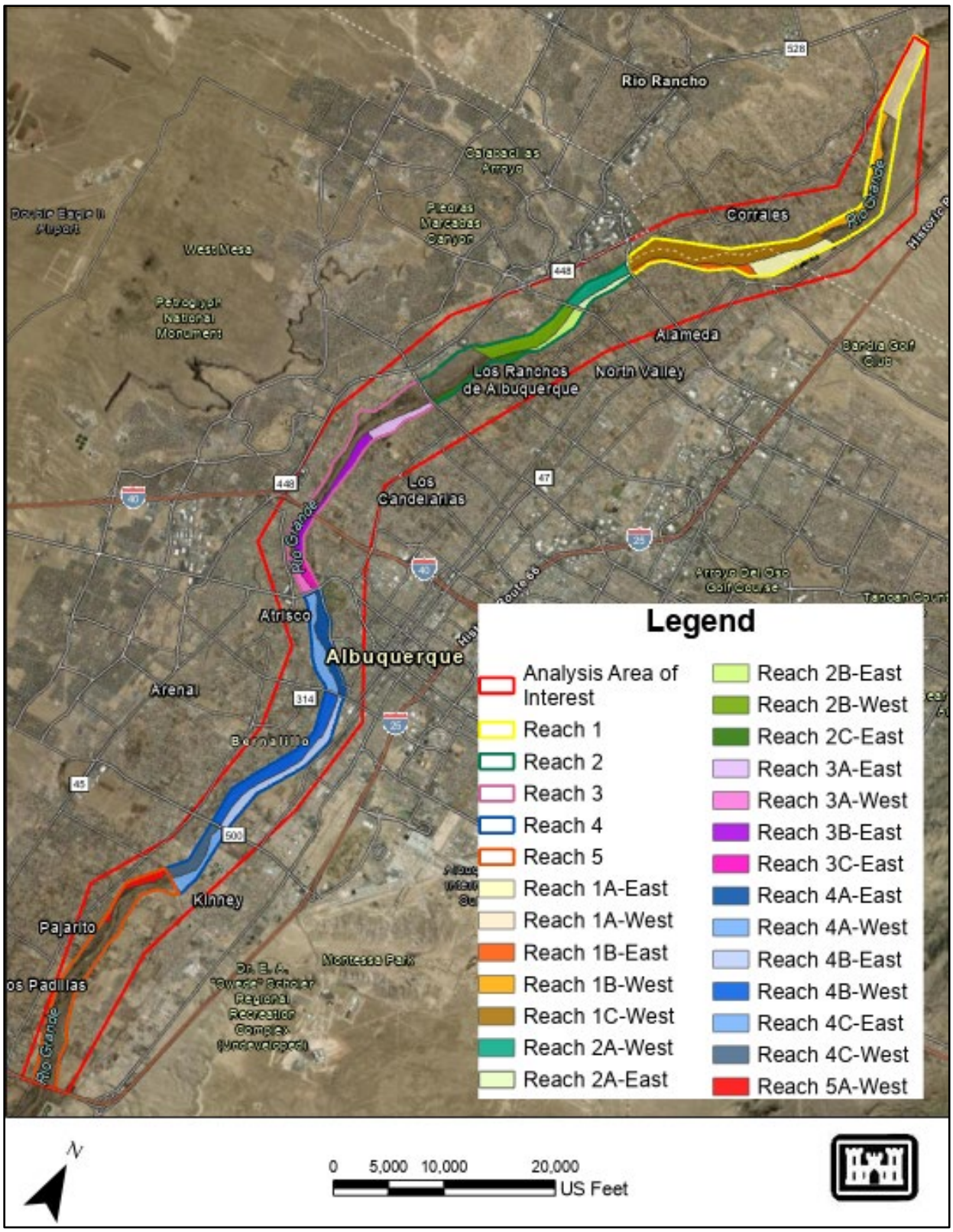

Figure 13. Reach and subreach delineations within the analysis area on the MRG. Background aerial imagery is from the 2022 Middle Rio Grande Council of Government's aerial collection by Bohannon Huston from ESRI online imagery (accessed 18 August 2023).

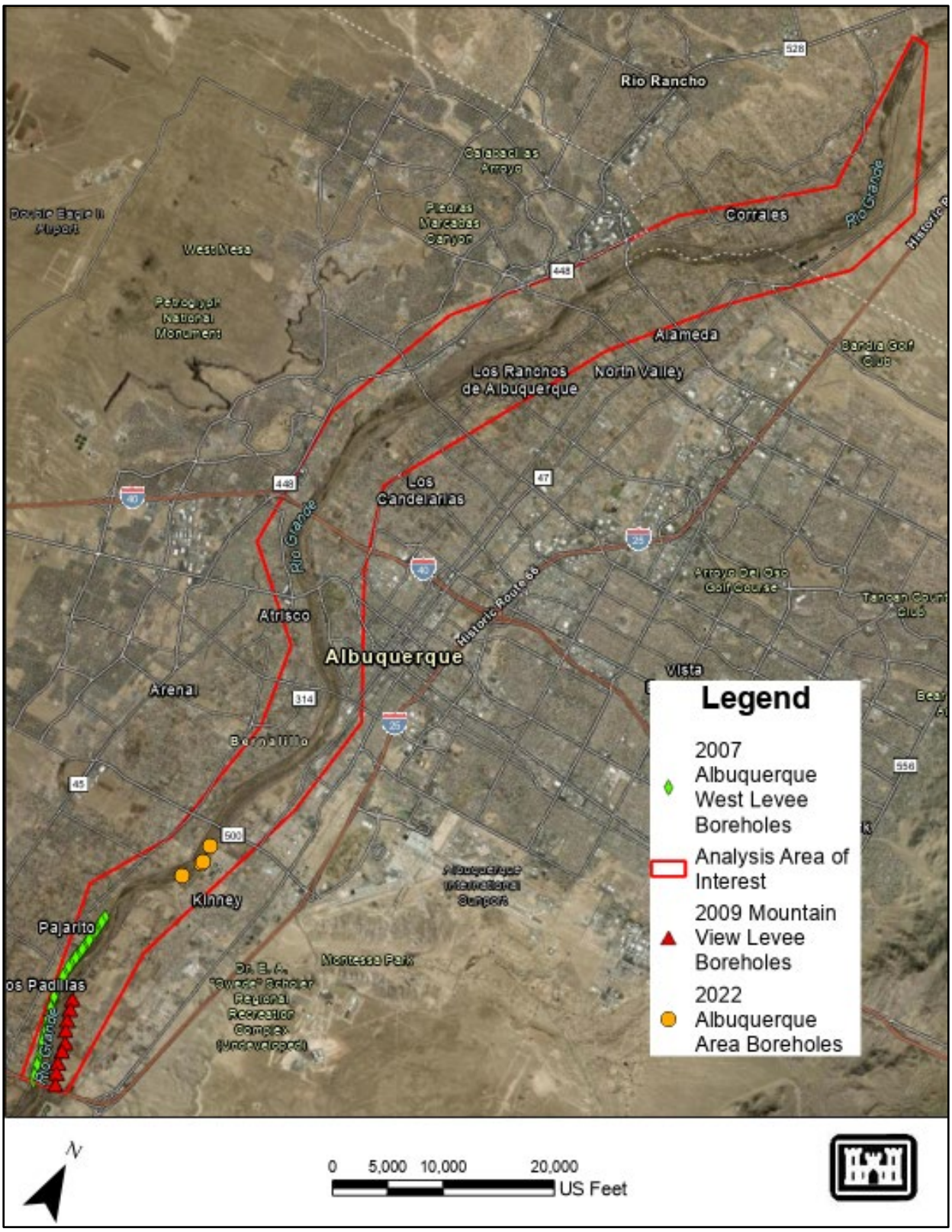

Figure 14. 2007, 2009, and 2022 borehole locations within analysis area. Background aerial imagery is from the 2022 Middle Rio Grande Council of Government's aerial collection by Bohannon Huston from ESRI online imagery (accessed 18 August 2023).

Attachment 2: Developed Datasets

The collated datasets described in Attachment 1 were utilized to extract information and create the following datasets that were utilized in the analysis to test the stated hypothesis.

2022 to 2002 Elevation Difference Dataset for the Albuquerque West Levee

The Albuquerque West Levee project was constructed in the 2008-2009 timeframe (BHI 2009). The borehole information for this section of the levee records only the depth below the surface and thus a correction is needed to assess depths below the 2022 LiDAR recorded elevation from the levee crest. To accomplish this the agg-deg lines within the Albuquerque West levee section (agg-deg 588 to 623) were utilized to extract elevation data from the 2002 photogrammetric surface (assumed borehole elevations at the time of the drilling) and the 2022 LiDAR surface (current terrain elevation) at the x, y, positions of the 2002 agg-deg data.

Since the Middle Rio Grande alignment is generally in the northern direction, plots of the easting versus elevation were made to visually inspect that there was correlation in the plots (see Figure 15). The representative plots were used to differentiate the levee section within the Albuquerque West levee unit and estimate an approximate difference between the 2022 and the 2002 levee elevations. Generally the highest elevation that was on the levee crest road was taken as the elevation representing that particular year. If the 2002 spoil levee crest was higher than the 2022 levee crest then a negative elevation difference is calculated. Elevation differences along the agg-deg lines varied from +2.1 to -2.8 feet.

The agg-deg lines upstream and downstream of each of the 2007 Albuquerque West Levee Boreholes were recorded, along with the distance between each agg-deg line and the length from the upstream agg-deg line. These were measured in ArcGIS Pro using the measure tool. Assuming a linear change in the levee height between agg-deg lines, a distance weighted formulation was utilized, as shown in Equation 1, to determine the elevation adjustment needed at each borehole. The elevation adjustment was subtracted from the 2022 elevations to reflect the approximate levee conditions at the time of the borehole investigation.

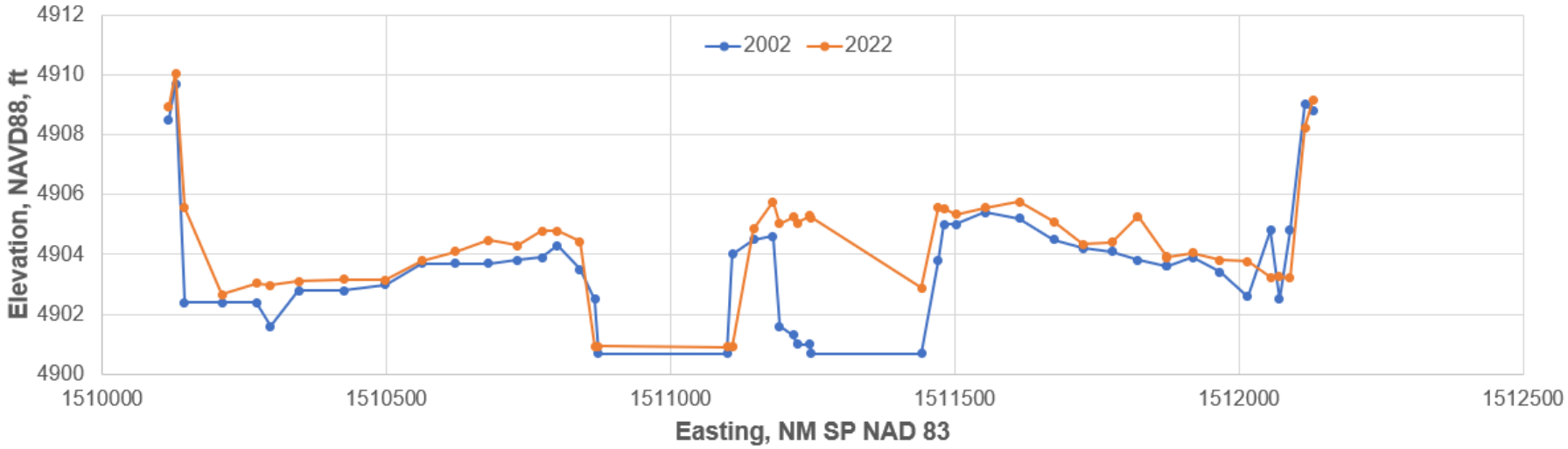

Figure 15. 2002 photogrammetric surface elevations and the 2022 LiDAR elevations. .Comparison plot is at agg-deg line 623. Cross sections are shown from west to east, so represent a right to left cross-sectional view when looking downstream.

Equation 1. Distance weighted elevation difference formulation

$$ElevDif_{BH} = \left(\frac{Dist_{ustoBH}}{Dist_{ustods}}\right)(ElevDif_{ds} - ElevDif_{us}) + ElevDif_{us}$$

Where $ElevDif_{BH}$ is the 2022 to 2002 elevation difference at a given borehole (ft, NAVD 88), $Dist_{ustoBH}$ is the distance (ft) between the upstream agg-deg line and a given borehole, $Dist_{ustods}$ is the distance (ft) between the upstream and downstream agg-deg lines, $ElevDif_{ds}$ is the 2022 to 2002 elevation difference at the downstream agg-deg line, and $ElevDif_{us}$ is the 2022 to 2002 elevation difference at the upstream agg-deg line.

2022 Feature Digitization

For this analysis a common location was developed to denote the riverside toe, landside toe, river centerline, levee centerline, and riverside drain locations. Features were drawn in ArcGIS Pro (version 3.0.2). The 2022 LiDAR, specifically the hillshade rendering, was used to delineate polylines representing the approximate feature locations. This was done zooming out to the entire area of interest and drawing lines that approximately followed the desired using the Editor function. Then working from south to north the following modifications were made:

- Vertices were adjusted on the lines representing the drains and the Rio Grande were modified using the Modify Features>>Edit Vertices features such that all vertices were situated in the areas reflecting the water surface (the hydroflattened areas of the 2022 LiDAR). This was done at a scale of 1:2000 within ArcGIS Pro. Figure 16 shows an example of the wetted water surface at the time of the LiDAR collection for both the Rio Grande and the drains.
- The delineated drains include the Atrisco Riverside Drain, the Corrales Riverside Drain, and the Upper Corrales Riverside Drain on the west side and the Albuquerque Riverside Drain on the east side. Alameda Road separates the Corrales Riverside Drain and the Upper Corrales Riverside Drain. The west side bluffs separate the Atrisco Riverside Drain from the Corrales Riverside Drain. No drains (or levees) exist in the west side bluff area (just south of the I-40 Bridge to the Oxbow Area near Taylor Ranch, NM).
- Using the Modify Features>>Copy Parallel tool the drain feature lines were offset to represent the levee crest and both the riverside and landside toes of the levee. The offset features required modification of these lines (using the Modify Features>>Edit Vertices tool). Modifications were done primarily with the 2022 LiDAR hillshade rendition. This was adjusted at a scale of 1:500 to better identify the toe locations. Figure 17 shows an example of the 2022 LiDAR hillshade rendering with the levee prism.
- The 2022 aerial photography collected with the 2022 LiDAR was also utilized to check areas that were not obvious with the hillshade, such as the top portion of Figure 17, which shows a ramp coming down from the levee into the Bosque. Some adjustment of the drains were made if the lines were observed to be outside of the hydroflattened water surface terrain as visible in the hillshade raster (see Figure 18). The river centerline was adjusted if the line crossed an island in the hillshade raster (see Figure 19).

Figure 16. 2022 LiDAR collected for Reclamation. The darkest zones represent the lowest recorded terrain in a given tile. Note there are multiple tiles, so the colors are not always balanced across the sections. These areas clearly delineate the wetted water surface of the Rio Grande and the drains at the time of the LiDAR collection. The flow direction and names of the drains are shown in the figure.

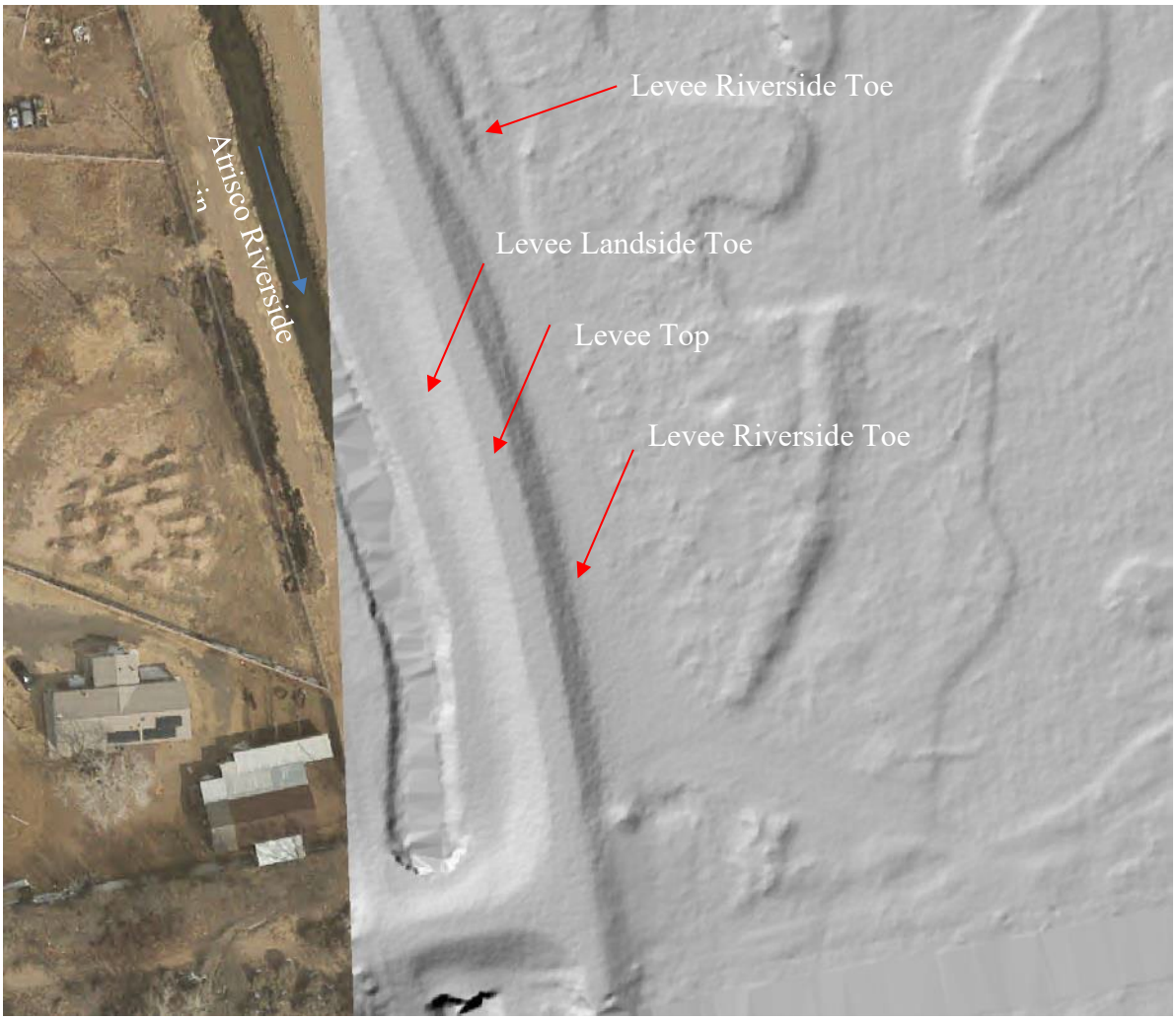

Figure 17. 2022 LiDAR hillshade rendering/aerial photography. The drain shown is the Atrisco Riverside Drain. The top Levee Riverside Toe delineation is offset to account for an earthen levee ramp into the Bosque at this location. This area is *just upstream of the I-25 river crossing on the west side.*

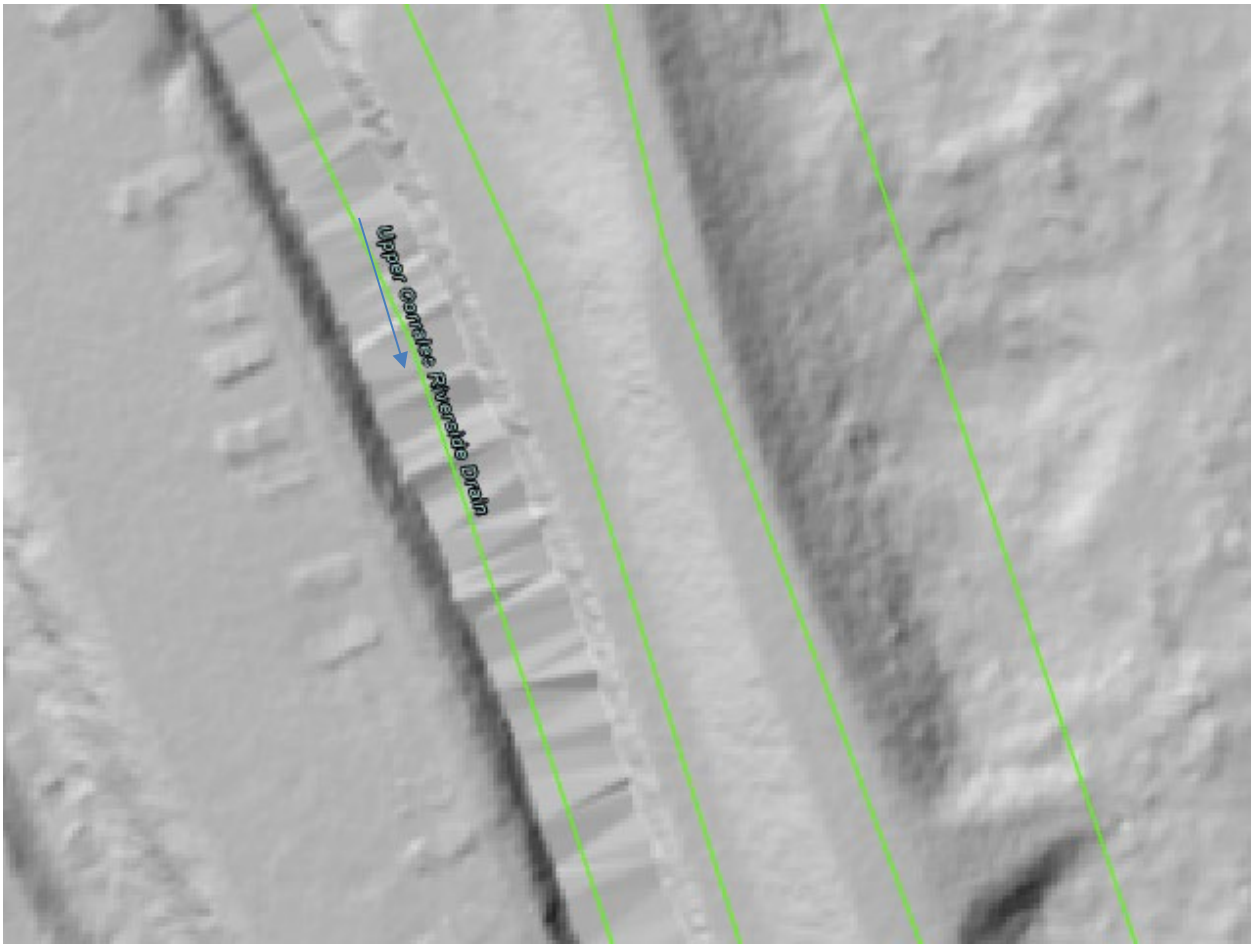

Figure 18. 2022 LiDAR hillshade rendering upstream of the Alameda Bridge on the west side. The centerline for the drain (Upper Corrales Riverside Drain) was adjusted to stay within the hydroflattened water surface of the 2022 LiDAR hillshade raster. The other lines represent the landside levee toe, the levee crest, and the riverside levee toe, as you move from left to right.

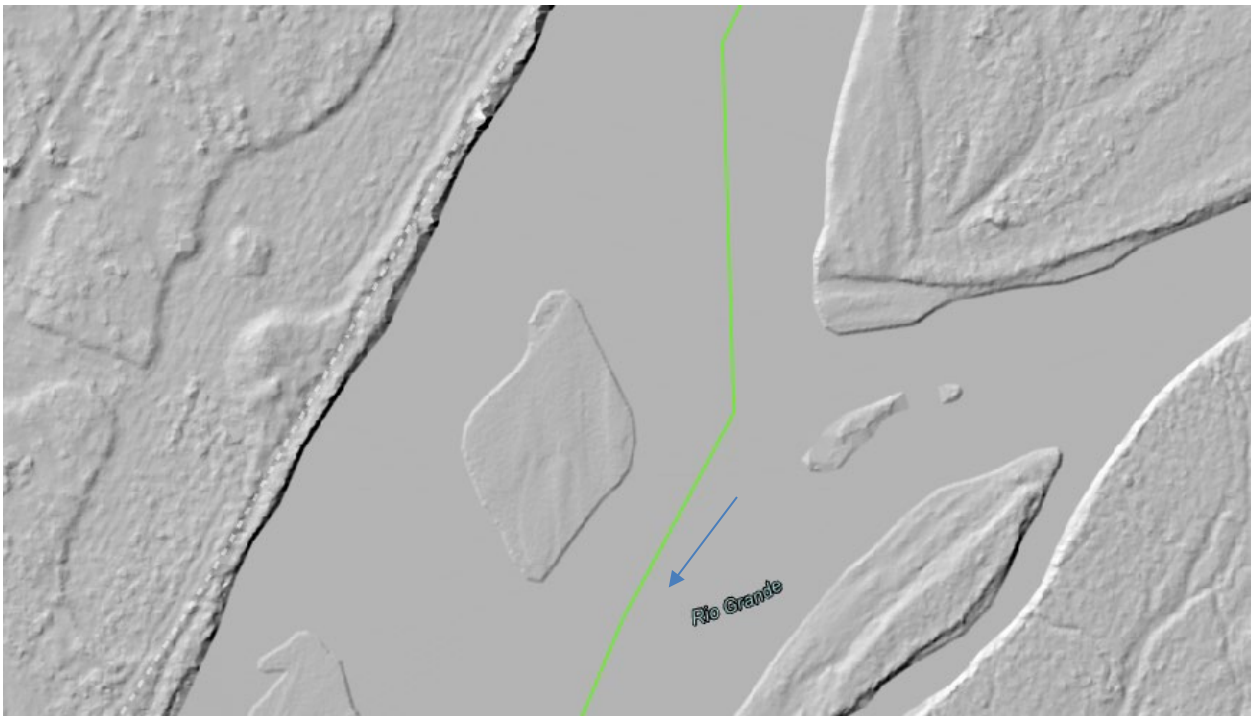

Figure 19. 2022 LiDAR hillshade rendering just upstream of the Alameda Bridge. The centerline was adjusted to avoid the islands visible above the hydroflattened water surface of the 2022 LiDAR hillshade rendering.

2022 Relative Depths

2022 LiDAR elevations were extracted at five locations for each borehole and filtered 2019 issue location. The approximate extraction locations are shown in Figure 7 of the main report. The exact locations of the features are based on the intersection of the 2022 digitized lines and a line drawn roughly perpendicular to either the borehole or the 2019 issue location, as shown in Figure 20.

An attribute field was created that lists the relative depth from the levee centerline to the other features identified in Figure 7. This is done by subtracting the field's 2022 elevation from the 2022 elevation at the levee centerline. The 2007 Albuquerque West Levee Boreholes had a readjustment of the 2022 LiDAR elevation for the levee centerline in accordance with the 2022 to 2002 Elevation Difference Dataset for the Albuquerque West Levee section. The calculated relative depths are then able to be used with the available borehole logs. The 1984 Corrales Levee Boreholes had a readjustment of the 2022 LiDAR elevations by 2.8 feet, which was the average levee height raised on that project (USACE 2018, p. ES-2). The calculated relative depths are then able to be used with the available borehole logs. All other borehole locations on the levees were assumed to be represented by the 2022 LiDAR elevations.

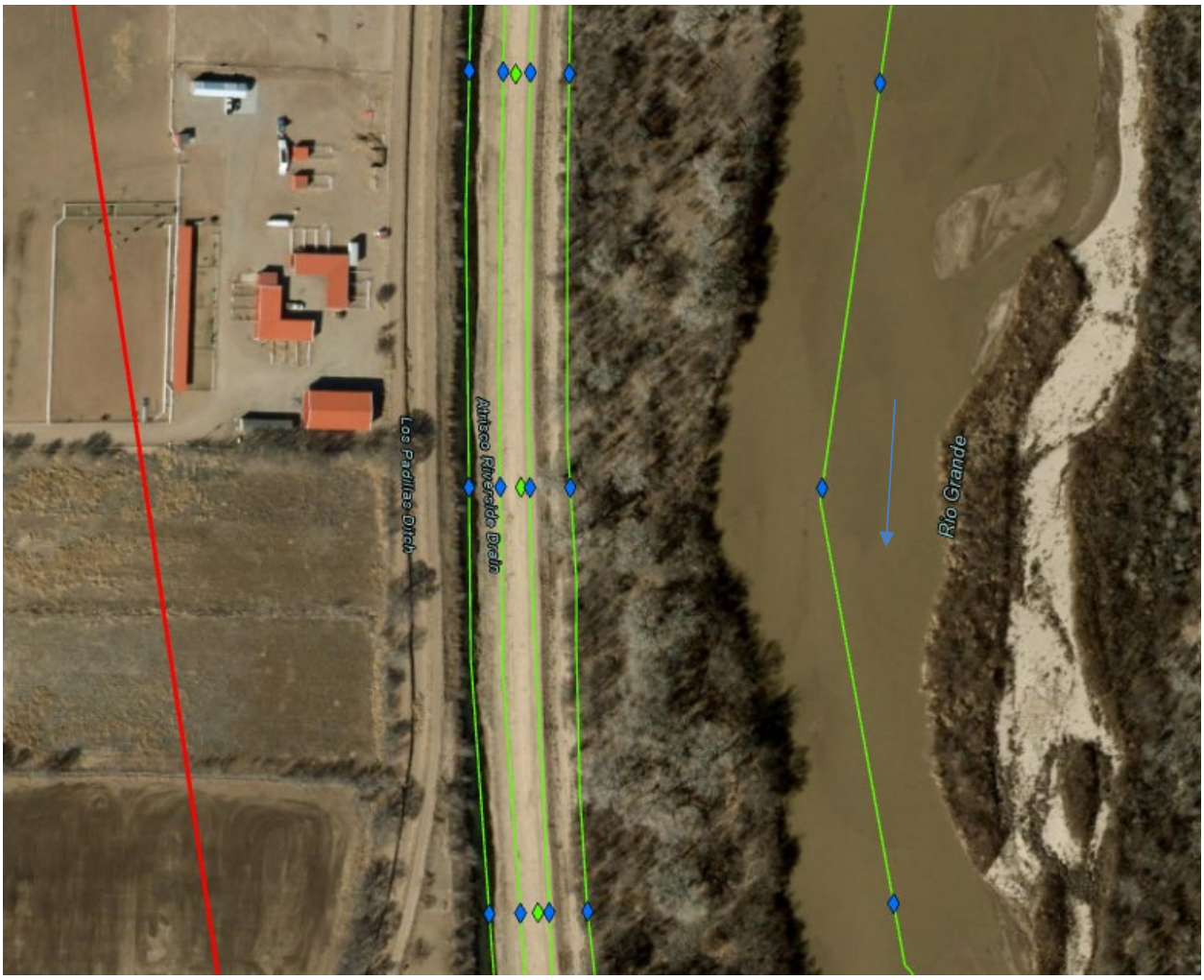

Figure 20. Point extraction of 2022 LiDAR elevations. Extraction based on the 2022 digitized lines (green lines) and borehole locations. The area shown is the Albuquerque West unit. The green diamonds are the approximate 2007 Albuquerque West Borehole locations. The blue diamonds represent the intersection of a line roughly perpendicular from the borehole to the digitized lines. The red line is the area of interest boundary. Background aerial imagery is from the 2022 Middle Rio Grande Council of Government's aerial collection by Bohannon Huston from ESRI online imagery (accessed 18August 2023).

Extraction of Soil Information from the boreholes

The 1984, 2006, 2007, 2009, and 2022 borehole information was used in conjunction with the relative depths to extract a Unified Soil Classification System (USCS) designation associated with that layer and any notes on the soil stratigraphy. Each borehole is assigned a unique entry for each of the relative depth measurement locations: Riverside Drain, Landside Toe, Levee Centerline, Riverside Toe, and River Centerline. In some situations, such as the 2007 Albuquerque West Boreholes, there were three locations drilled. These were treated as a single borehole with all three assessed when assigning the USCS at a particular depth. If there were differences in the soil stratigraphy these were noted.

Since the relative depths are in reference to the levee crest elevation, an adjustment of the relative depths for boreholes drilled at the riverside or landside levee toe was performed. For example B-09E on the 2007 Albuquerque West Boreholes is at the riverside toe, so depths are

relative to the ground surface at the riverside toe. To see what soil type it may be at the river centerline elevation (which is the water surface elevation from the 2022 LiDAR) then the depth difference between the river centerline to the levee centerline elevations (10.67 ft) and the west riverside toe to the levee centerline elevations (5.17 ft) is taken, which results in 5.5 ft. This is the depth below the surface of the riverside toe borehole (B-09E) that correlates with the location of the current active channel water surface elevation circa 2022.

The geotechnical analyses performed on the soil samples collected during the exploration of the 2006, 2007, and 2022 boreholes was utilized to extract the following information for each borehole:

- Gradation information performed through a sieve analysis (ASTM 2017). The geotechnical results were reported in terms of the percent finer per a given sieve. The #10, #16, #30, #40, #50, #100, and #200 sieves were extracted for this analysis.
- The USCS designation for the tested sample gradation. The depth for the tested sample was also listed. These were correlated with the boreholes (by number and depth) to ensure that the sample is from the same horizon as indicated in the borehole. Sometimes a sample was collected that crossed a borehole soil horizon When this situation occurred the laboratory results typically indicated two different soils with an A or B designation for the depth. To determine which sample results to use, the borehole details were considered such that the chosen soil sample correlated to the soil layer(s) (specifically the USCS nomenclature) determined from the borehole.
- The information was compiled into an Excel spreadsheet (Office 365) that included the borehole name assigned when creating the geospatial feature class representing the borehole location. The following 11 columns were added:
    - *USCS* – Records the USCS from the borehole that corresponds to the relative depths
    - *Soil description* – text that describes the borehole number and location of where data was extracted. If no east (E) or west (W) designation is listed the borehole was along the levee centerline. Depths below the surface are listed for those boreholes not along the levee centerline.
    - *USCS of gradation* – Records the USCS from the laboratory sample tested which correlates to the borehole location.
    - *Notes* – Provides notes on the depth or the sample designation listed in the borehole notes at which the lab sample was extracted. If a borehole other than the levee centerline was utilized, it is also listed.
    - *Percent Finer #10* – Lists the percent finer from the #10 sieve as reported by the geotechnical analysis for the lab sample.
    - *Percent Finer #16* – Lists the percent finer from the #16 sieve as reported by the geotechnical analysis for the lab sample.
    - *Percent Finer #30* – Lists the percent finer from the #30 sieve as reported by the geotechnical analysis for the lab sample.
    - *Percent Finer #40* – Lists the percent finer from the #40 sieve as reported by the geotechnical analysis for the lab sample.

  - *Percent Finer #50* – Lists the percent finer from the #50 sieve as reported by the geotechnical analysis for the lab sample.
  - *Percent Finer #100* – Lists the percent finer from the #100 sieve as reported by the geotechnical analysis for the lab sample.
  - *Percent Finer #200* – Lists the percent finer from the #200 sieve as reported by the geotechnical analysis for the lab sample.

Since a more standardized soil classification is utilized within the realm of sediment transport. The gradations reported from the soil samples were correlated to the following Wentworth (1922, Table 1, p. 381) categories.

- Very Coarse Sand (VCS): 1-2 mm
- Coarse Sand (CS):1-0.5 mm:
- Medium sand (MS): 0.5-0.25 mm
- Fine sand (FS): 0.25 – 0.125 mm
- Very fine sand (VFS): 0.125 – 0.0625 mm
- Fines (silts and clays): < 0.0625 mm

The following additional nine (9) columns were added to the Excel spreadsheet for a correlation of the Wentworth (1922) categories to the provided sieve openings reported in the geotechnical investigations.

- The assumed sieve openings were based on the standard dimensions (Das 1990, Table 1.5, p. 17; Das 2006, Table 2.5, p. 31) as shown below:
  - #10 – 2 mm
  - #16 – 1.18 mm
  - #30 – 0.6 mm
  - #40 – 0.425 mm
  - #50 – 0.355 mm
  - #100 – 0.15 mm
  - #200 – 0.075 mm
- Six columns were created to approximate the % of the sample that fell into the following Wentworth (Wentworth 1922, Table 1, p. 381) categories:
  - The percentages for each of the Wentworth categories were calculated as follows:
    - ~ % of sample that is VCS: percent finer #10 minus percent finer #16
    - ~ % of sample that is CS: percent finer #16 minus percent finer #30
    - ~ % of sample that is MS: percent finer #30 minus percent finer #50
    - ~ % of sample that is FS: percent finer #50 minus percent finer #100
    - ~ % of sample that is VFS: percent finer #100 minus percent finer #200
    - ~ % of sample that are Fines: percent finer #200
  - A more precise approximation could be made by looking at the actual gradation curve. The approximation was determined to be sufficient for this analysis since it would be more labor intensive to extract values at the more exact breaks.

- The last three columns extract an approximate Wentworth category associated with the percent of the gradation that is finer than the median (d_{50}) and one standard deviation (normal distribution) above (d_{84}) and below (d_{16}) the median.
    - This is determined through a series of If..then statements that evaluate the six percentages from the Wentworth category calculations. The assessment begins with an evaluation of the percent of material coarser than the #10 sieve (2 mm), This is evaluated by taking 100 minus the percent finer than the #10 sieve. If this fraction is greater than 16%, 50%. or 84%, respectively for the d_{84}, d_{50}, and d_{16} categories then a ">VCS" label is applied. From this starting point the percent of samples in the VCS, CS, MS, FS, and VFS fractions are iteratively summed until the 16%, 50%, and 84% are reached. The algorithm returns the fraction category (i.e., MS) when the 16% (d_{84}), 50% (d_{50}), and 84% (d_{16}) are reached.
    - The assessment returns the general Wentworth category, e.g., MS or CS, rather than a specific size. This provides a relative measure to understand the sediment size at a particular depth relative to a given borehole location.

Boreholes collected in 1984 and 2009 required some additional evaluation. The 1984 borehole samples only reported the percent finer associated with the #10, #40, #80, and #200 sieves. The opening diameter associated with a #80 sieve is 0.18 mm (Das 1990, Table 1.5, p. 17; Das 2006, Table 2.5, p. 31). While this provides some information on the gradation, it does not provide the detail similar to the other evaluated boreholes. The provided percent finers do bracket the required information so a linear interpolation was done based on sieve opening diameter, according to Equation 2.

Equation 2. Percent finer linear interpolation

$$PF_u = PF_{u-larger} - \left(\frac{Logdiam_{u-larger} - Logdiam_u}{Logdiam_{u-larger} - Logdiam_{u-smaller}}\right)\left(PF_{u-larger} - PF_{u-smaller}\right)$$

Where PF_u is the percent finer associated with an unreported sieve size, $PF_{u\text{-}larger}$ is the percent finer associated with the reported sieve size that is larger than the unknown value, $Pf_{u\text{-}smaller}$ is the percent finer associated with the reported sieve size that is smaller than the unknown value, $Logdiam_u$ is the log (base 10) of the unknown sieve size, $Logdiam_{u\text{-}larger}$ is the log (base 10) of the reported sieve size that is larger than the unknown sieve size, and $Logdiam_{u\text{-}smaller}$ is the log (base 10) of the reported sieve size that is smaller than the unknown sieve size. The log (base 10) transformation was done since gradation curves are typically shown on a semi-log plot. While not perfect, this approximation estimated particle sizes along the reported curve fairly well. See Figure 21 for an example of four sediment samples that are representative of what was found in the investigation. In general, the linear approximations are on or below the reported data lines. This would mean that the interpolated values would tend to reflect coarser values for the d_{16}, d_{50}, and d_{84} grain sizes. Since the goal of these grain sizes is to report a Wentworth category rather than a specific grain size, the coarser bias is reasonable since the Wentworth categories are larger than the linear interpolation bias, as can be seen in Figure 21. Specific computations for each of

the boreholes is provided in the "Linear Interpolations of the 1984 gradations" section at the end of this attachment.

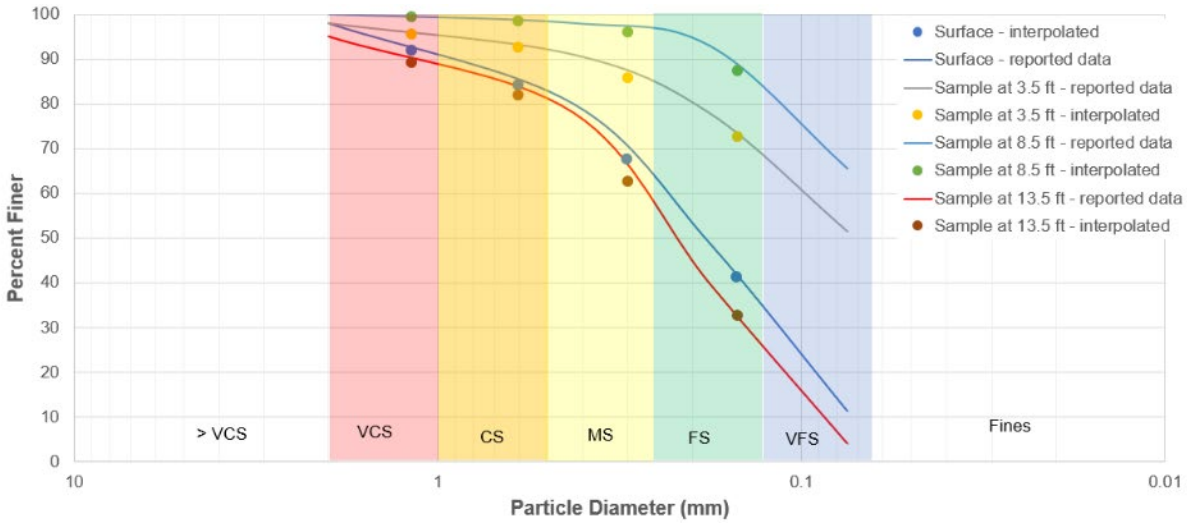

Figure 21. Comparison of reported (lines) and linearly interpolated (circles) gradation values. This is for Borehole # 2 in the 1984 geotechnical investigations. Colors represent the Wentworth categories used in this analysis: red= VCS, orange is CS, yellow is MS, green is FS, and blue is VFS. Uncolored zones reflect categories assigned when values exceeded the color banded zones.

Borehole #66B (RGL-8A2S-87) for the 1984 boreholes was drilled near the drain O&M road, so no information could be extracted related to the soil at the levee top and the east riverside toe since these locations are above the elevation of the drain O&M road. These locations had a value of "NA" (not applicable) assigned to the Soil description column.

The geotechnical investigations for the 2009 boreholes provided only information related to the percent finer for the #200 sieve. This didn't provide the opportunity for linear interpolation, so the focus for the samples from these boreholes was on identifying the correct Wentworth category for the d_{16}, d_{50}, and d_{84} grain sizes. Licon (2010) also provided "Nominal Particle Size", "D_{50}", and "D_{10}" categories, in addition to the percent finer for the #200 sieves. On closer inspection of these values the "Nominal Particle Size" is often on the larger end of the normal sieve categories (e.g., 3/8", ½", ¾", etc.) and always larger than the "D_{50}". The "D50" size is larger than the "D_{10}" size, which means the D_{50} is likely the soil particle diameter (in mm) of which 50% of the mass is finer and D_{10} is the likely the soil particle diameter (in mm) of which 10% of the mass is finer. The reported "D_{50}" size was used to manually determine the applicable Wentworth category for the d_{50} column mentioned above. The reported "D_{10}" size was used to manually determine the applicable Wentworth category for the d_{16} column mentioned above. Sometimes a value of "N/D" was reported, which was assumed to represent a not determined status. The value of "N/D" was generally provided when more than 10% of the sample passed the #200 sieve. In these situations a value of "Fines" was applied for the Wentworth category, since the # 200 sieve is very close to the sand/fine split. The determination of the d_{84} value was based on the value reported for the "Nominal Particle Size". If this was significantly larger than

the category of VCS (upper bounds of 2mm) then the d_{84} was two Wentworth categories larger than the d_{50} category. For example, the 2009 borehole 09-AD-04 sample B had a "Nominal Particle Size" of 3/8" (about 9.5 mm), which is in the gravel and larger Wentworth categories and a d_{50} Wentworth category of MS, so the d_{84} category was assigned a value of VCS to account for the skew from the presence of gravels in the sample. In some situations the "Nominal Particle Size" was not considerably larger and so only one Wentworth category larger than the d_{50} category was applied. For example, the 2009 borehole 09-AD-04 sample A had a "Nominal Particle Size" of 0.0236" (about 0.6 mm) and a d_{50} Wentworth category of FS, so the d_{84} category was assigned a value of MS to reflect the relative absence of larger gravel particles.

Borehole drilling logs and geotechnical information were not found for the following 2009 borehole locations: Borehole #2a (09-AD-02a), Borehole #7 (09-AD-07), and Borehole #8 (09-AD-08). These locations therefore were not included in the subsequent statistical analysis.

Extraction of Historical Planform Information

A geospatial analysis was conducted using ESRI's ArcGIS Pro to determine locational information related to the historical planform locations and the borehole and filtered 2019 issue locations. The following bullets detail the locational information queried. Each of the results provided a new data point that was later utilized in the statistical evaluation to assess correlation. The raw data is provided in the Raw data extraction section of this attachment. Each of these bullets were added as an attribute field that could be queried by the borehole or the filtered 2019 issue location name.

- The historical planform polygon intersected by the borehole or filtered 2019 issue location. This is based on the "script" attribute field and was done for each of the three years: 1918, 1935, and 1949. The following "scripts" attributes are utilized across the three historical planform years to denote what planform features was located at the boreholes or filtered 2019 issue locations. although not all of the features were digitized in every year. Attribute definitions are based on Oliver (2012).
    - Active channel – open water or bare earth section of the Rio Grande.
    - Vegetated island – a patch of earth surrounded by active channel that has woody vegetation present.
    - Arroyo – ephemeral tributary to the Rio Grande.
    - Flood prone – areas clearly still prone to flooding based on visual assessments.
    - Historic channel – previous channel locations that are still visible based on vegetation type or presence.
    - Island-attached to bank – previous island formation that now is part of the bankline.
    - Levee – an earthen berm constructed to manage flood flows.
    - Out of study area – area not digitized.
    - Recent channel change – section of the Rio Grande where vegetation or sedimentation differences indicate a flow change has occurred.

  - Tributary – perennial tributary to the Rio Grande, or at least had water in at the time of historical data capture.
  - Upland uses – area where flooding is not an issue, often identified by vegetation type or scarcity.
  - Ponded water – area of pooled water.
  - No data – extent of historical coverage is not provided in this section.
- The proximity (distance in feet) to "active channel" polygon (name in the "script" attribute) for the 1918, 1935, and 1949 historical channels for the boreholes and the filtered 2019 issue locations. If the borehole or filtered 2019 issue location is located in the "active channel" polygon then it is assigned a numerical value of zero.
- Identification on whether the borehole or filtered 2019 issue locations are within the vegetated island polygon within the "script" attribute for the 1918 historical planform. This is an attribute that is listed as "yes" if located within and "no" if not located within. The assumption is that those locations classified as "yes" are likely more stable from a historical perspective and would be expected to have finer soil gradations than areas of active channel locations.

An additional set of attribute values were added to the filtered 2019 issue locations as columns from which data could be queried.

- The reach/subreach from the 2006 analyses (USACE 2009) in which the filtered 2019 issue location resides.
  - The seepage rating (1, 2, or 3) associated with the assigned subreach was listed in a separate column.
  - The slope stability rating (1, 2,or 3) associated with the assigned subreach was listed in a separate column.
- The name of the closest upstream borehole, followed by columns containing the following attributes related to the soil correlated at that borehole.
  - The distance (in US feet) to the upstream borehole. Distances were measured along the levee centerline feature class.
  - The Wentworth grain classification from the upstream borehole related to the d_{16}, d_{50}, and d_{84} at the Riverside Drain.
  - The Wentworth grain classification from the upstream borehole related to the d_{16}, d_{50}, and d_{84} at the Landside Toe.
  - The Wentworth grain classification from the upstream borehole related to the d_{16}, d_{50}, and d_{84} at the Levee Centerline.
  - The Wentworth grain classification from the upstream borehole related to the d_{16}, d_{50}, and d_{84} at the Riverside Toe.
  - The Wentworth grain classification from the upstream borehole related to the d_{16}, d_{50}, and d_{84} at the River Centerline.
- The name of the closest downstream borehole, followed by columns containing the following attributes related to the soil correlated at that borehole.

- The distance (in US feet) to the downstream borehole. Distances were measured along the levee centerline feature class.
- The Wentworth grain classification from the downstream borehole related to the d_{16}, d_{50}, and d_{84} at the Riverside Drain.
- The Wentworth grain classification from the downstream borehole related to the d_{16}, d_{50}, and d_{84} at the Landside Toe.
- The Wentworth grain classification from the downstream borehole related to the d_{16}, d_{50}, and d_{84} at the Levee Centerline.
- The Wentworth grain classification from the downstream borehole related to the d_{16}, d_{50}, and d_{84} at the Riverside Toe.
- The Wentworth grain classification from the downstream borehole related to the d_{16}, d_{50}, and d_{84} at the River Centerline.

Finally, a column was added on the name of the closest borehole to the filtered 2019 issue locations. This was either the upstream or downstream borehole name, based on the shortest distance to the filtered 2019 issue location.

Linear Interpolations of the 1984 Gradations

Hole #2

Highlighted Data is interpolated

Sieve #	diam	surface % finer	3.5 ft	8.5 ft	13.5 ft
10	2	98	98	100	95
16	1.18	91.9	95.6	99.3	89.2
30	0.6	84.0	92.6	98.4	81.8
40	0.425	80	91	98	78
50	0.3	67.4	85.7	96.0	62.6
80	0.18	49	78	93	40
100	0.15	41.1	72.5	87.3	32.5
200	0.075	11.3	51.5	65.5	4.1

Data from Geotechnical Analysis

10	2	98	98	100	95
40	0.425	80	91	98	78
80	0.18	49	78	93	40
200	0.075	11.3	51.5	65.5	4.1

For copying into borehole logs

	#10	#16	#30	#40	#50	#100	#200
surface	98	91.9	84.0	80	67.4	41.1	11.3
3.5 ft	98	95.6	92.6	91	85.7	72.5	51.5
8.5 ft	100	99.3	98.4	98	96.0	87.3	65.5
13.5 ft	95	89.2	81.8	78	62.6	32.5	4.1

Hole #3

Highlighted Data is interpolated

Sieve #	diam	surface % finer	3.5 ft	8.5 ft	18.5 ft
10	2	96	99	100	52
16	1.18	92.9	98.7	99.7	50.0
30	0.6	89.0	98.2	99.2	47.3
40	0.425	87	98	99	46
50	0.3	72.8	96.0	97.4	29.0
80	0.18	52	93	95	4
100	0.15	44.9	86.9	91.6	3.4
200	0.075	17.7	63.9	78.6	1

Data from Geotechnical Analysis

10	2	96	99	100	52
40	0.425	87	98	99	46
80	0.18	52	93	95	4
200	0.075	17.7	63.9	78.6	1

For copying into borehole logs

	#10	#16	#30	#40	#50	#100	#200
surface	96	92.9	89.0	87	72.8	44.9	17.7
3.5 ft	99	98.7	98.2	98	96.0	86.9	63.9
8.5 ft	100	99.7	99.2	99	97.4	91.6	78.6
18.5 ft	52	50.0	47.3	46	29.0	3.4	1

Hole #4

Highlighted Data is interpolated

Sieve #	diam	surface % finer	3.5 ft	8.5 ft	18.5 ft
10	2	98	100	100	64
16	1.18	95.3	99.3	99.3	54.1
30	0.6	91.8	98.4	98.4	41.5
40	0.425	90	98	98	35
50	0.3	81.1	96.4	96.8	23.2
80	0.18	68	94	95	6
100	0.15	61.7	88.1	93.6	5.1
200	0.075	37.6	65.5	88.4	1.5

Data from Geotechnical Analysis

10	2	98	100	100	64
40	0.425	90	98	98	35
80	0.18	68	94	95	6
200	0.075	37.6	65.5	88.4	1.5

For copying into borehole logs

	#10	#16	#30	#40	#50	#100	#200
surface	98	95.3	91.8	90	81.1	61.7	37.6
3.5 ft	100	99.3	98.4	98	96.4	88.1	65.5
8.5 ft	100	99.3	98.4	98	96.8	93.6	88.4
18.5 ft	64	54.1	41.5	35	23.2	5.1	1.5

Hole # 5 &7

Highlighted Data is interpolated

		Hole #5			Hole #7	
		3.5 ft	8.5 ft	13.5 ft	surface	4 ft
Sieve #	diam	% finer				
10	2	97	100	99	100	99
16	1.18	95.3	99.7	92.5	98.3	92.2
30	0.6	93.1	99.2	84.2	96.1	83.5
40	0.425	92	99	80	95	79
50	0.3	88.4	97.8	60.5	93.4	52.6
80	0.18	83	96	32	91	14
100	0.15	77.8	95.0	26.0	88.8	11.1
200	0.075	58.1	91	3.4	80.4	0.2

Data from Geotechnical Analysis

10	2	97	100	99	100	99
40	0.425	92	99	80	95	79
80	0.18	83	96	32	91	14
200	0.075	58.1	91	3.4	80.4	0.2

For copying into borehole logs

		#10	#16	#30	#40	#50	#100	#200
Hole # 5	3.5 ft	97	95.3	93.1	92	88.4	77.8	58.1
Hole # 5	8.5 ft	100	99.7	99.2	99	97.8	95.0	91
Hole # 5	13.5 ft	99	92.5	84.2	80	60.5	26.0	3.4
Hole #7	surface	100	98.3	96.1	95	93.4	88.8	80.4
Hole #7	4 ft	99	92.18662	83.45296	79	52.64791	11.12607	0.2

Hole # 6

Highlighted Data is interpolated

Sieve #	diam	surface % finer	3.5 ft	8.5 ft	13.5 ft
10	2	94	100	97	100
16	1.18	89.2	99.7	96.3	98.3
30	0.6	83.1	99.2	95.4	96.1
40	0.425	80	99	95	95
50	0.3	65.8	98.2	93.4	81.2
80	0.18	45	97	91	61
100	0.15	39.2	90.9	86.6	59.6
200	0.075	17.2	67.7	69.7	54.4

Data from Geotechnical Analysis

10	2	94	100	97	100
40	0.425	80	99	95	95
80	0.18	45	97	91	61
200	0.075	17.2	67.7	69.7	54.4

For copying into borehole logs

	#10	#16	#30	#40	#50	#100	#200
surface	94	89.2	83.1	80	65.8	39.2	17.2
3.5 ft	100	99.7	99.2	99	98.2	90.9	67.7
8.5 ft	97	96.3	95.4	95	93.4	86.6	69.7
13.5 ft	100	98.3	96.1	95	81.2	59.6	54.4

Hole # 8

Highlighted Data is interpolated

Sieve #	diam	surface % finer	3.5 ft	12.5 ft	17 ft
10	2	91	97	96	59
16	1.18	88.6	95.0	85.8	45.4
30	0.6	85.6	92.3	72.7	27.9
40	0.425	84	91	66	19
50	0.3	79.1	78.4	43.3	12.5
80	0.18	72	60	10	3
100	0.15	68.0	47.9	8.1	2.5
200	0.075	52.9	1.8	0.8	0.6

Data from Geotechnical Analysis

10	2	91	97	96	59
40	0.425	84	91	66	19
80	0.18	72	60	10	3
200	0.075	52.9	1.8	0.8	0.6

For copying into borehole logs

	#10	#16	#30	#40	#50	#100	#200
surface	91	88.6	85.6	84	79.1	68.0	52.9
3.5 ft	97	95.0	92.3	91	78.4	47.9	1.8
12.5 ft	96	85.8	72.7	66	43.3	8.1	0.8
17 ft	59	45.4	27.9	19	12.5	2.5	0.6

Hole # 9 and 10

Highlighted Data is interpolated

Sieve #	diam	Hole #9 surface % finer	8.5 ft	11.5 ft	Hole #10 surface	8.5 ft
10	2	84	100	100	100	100
16	1.18	76.2	99.7	98.6	98.3	96.9
30	0.6	66.1	99.2	96.9	96.1	93.0
40	0.425	61	99	96	95	91
50	0.3	49.2	98.6	88.3	71.5	59.0
80	0.18	32	98	77	37	12
100	0.15	27.1	95.1	65.7	30.5	9.6
200	0.075	8.5	84.2	22.5	5.9	0.5

Data from Geotechnical Analysis

10	2	84	100	100	100	100
40	0.425	61	99	96	95	91
80	0.18	32	98	77	37	12
200	0.075	8.5	84.2	22.5	5.9	0.5

For copying into borehole logs

		#10	#16	#30	#40	#50	#100	#200
Hole #9	surface	84	76.2	66.1	61	49.2	27.1	8.5
Hole #9	8.5 ft	100	99.7	99.2	99	98.6	95.1	84.2
Hole #9	11.5 ft	100	98.6	96.9	96	88.3	65.7	22.5
Hole #10	surface	100	98.3	96.1	95	71.5	30.5	5.9
Hole #10	8.5 ft	100	96.93398	93.00383	91	58.97207	9.605057	0.5

Hole # 11

Highlighted Data is interpolated

Sieve #	diam	1 ft % finer	3.5 ft	6.5 ft	13.5 ft
10	2	95	92	100	99
16	1.18	75.2	88.3	98.6	97.6
30	0.6	49.9	83.4	96.9	95.9
40	0.425	37	81	96	95
50	0.3	33.8	68.4	81.0	72.3
80	0.18	29	50	59	39
100	0.15	28.5	42.2	49.6	34.2
200	0.075	26.6	12.7	13.9	15.9

Data from Geotechnical Analysis

10	2	95	92	100	99
40	0.425	37	81	96	95
80	0.18	29	50	59	39
200	0.075	26.6	12.7	13.9	15.9

For copying into borehole logs

	#10	#16	#30	#40	#50	#100	#200
1 ft	95	75.2	49.9	37	33.8	28.5	26.6
3.5 ft	92	88.3	83.4	81	68.4	42.2	12.7
6.5 ft	100	98.6	96.9	96	81.0	49.6	13.9
13.5 ft	99	97.6	95.9	95	72.3	34.2	15.9

Hole # 12

Highlighted Data is interpolated

Sieve #	diam	at surface % finer	8.5 ft	13.5 ft
10	2	90	59	78
16	1.18	85.9	54.2	73.2
30	0.6	80.7	48.1	67.1
40	0.425	78	45	64
50	0.3	61.8	39.7	55.9
80	0.18	38	32	44
100	0.15	34.1	29.5	40.4
200	0.075	19.3	19.9	26.8

Data from Geotechnical Analysis

10	2	90	59	78
40	0.425	78	45	64
80	0.18	38	32	44
200	0.075	19.3	19.9	26.8

For copying into borehole logs

	#10	#16	#30	#40	#50	#100	#200
at surface	90	85.9	80.7	78	61.8	34.1	19.3
8.5 ft	59	54.2	48.1	45	39.7	29.5	19.9
13.5 ft	78	73.2	67.1	64	55.9	40.4	26.8

Hole # 13

Highlighted Data is interpolated

Sieve #	diam	at surface % finer	6.5 ft	13.5 ft
10	2	98	100	100
16	1.18	95.3	98.6	98.6
30	0.6	91.8	96.9	96.9
40	0.425	90	96	96
50	0.3	77.0	88.3	83.0
80	0.18	58	77	64
100	0.15	51.1	69.6	55.4
200	0.075	25.1	41.7	22.9

Data from Geotechnical Analysis

10	2	98	100	100
40	0.425	90	96	96
80	0.18	58	77	64
200	0.075	25.1	41.7	22.9

For copying into borehole logs

	#10	#16	#30	#40	#50	#100	#200
at surface	98	95.3	91.8	90	77.0	51.1	25.1
6.5 ft	100	98.6	96.9	96	88.3	69.6	41.7
13.5 ft	100	98.6	96.9	96	83.0	55.4	22.9

Hole # 14

Highlighted Data is interpolated

Sieve #	diam	4.5 ft % finer	9 ft	13.5 ft
10	2	100	93	62
16	1.18	99.0	83.5	54.5
30	0.6	97.7	71.2	44.9
40	0.425	97	65	40
50	0.3	93.8	42.7	31.5
80	0.18	89	10	19
100	0.15	86.8	8.2	16.5
200	0.075	78.4	1.4	6.8

Data from Geotechnical Analysis

10	2	100	93	62
40	0.425	97	65	40
80	0.18	89	10	19
200	0.075	78.4	1.4	6.8

For copying into borehole logs

	#10	#16	#30	#40	#50	#100	#200
4.5 ft	100	99.0	97.7	97	93.8	86.8	78.4
9 ft	93	83.5	71.2	65	42.7	8.2	1.4
13.5 ft	62	54.5	44.9	40	31.5	16.5	6.8

Hole # 15

Highlighted Data is interpolated

Sieve #	diam	at surface % finer	8.5 ft	13.5 ft
10	2	85	100	100
16	1.18	78.2	99.7	97.6
30	0.6	69.5	99.2	94.6
40	0.425	65	99	93
50	0.3	52.8	96.6	68.3
80	0.18	35	93	32
100	0.15	29.2	87.0	26.1
200	0.075	7.3	64.4	3.8

Data from Geotechnical Analysis

10	2	85	100	100
40	0.425	65	99	93
80	0.18	35	93	32
200	0.075	7.3	64.4	3.8

For copying into borehole logs

	#10	#16	#30	#40	#50	#100	#200
at surface	85	78.2	69.5	65	52.8	29.2	7.3
8.5 ft	100	99.7	99.2	99	96.6	87.0	64.4
13.5 ft	100	97.6	94.6	93	68.3	26.1	3.8

Hole # 16

Highlighted Data is interpolated

Sieve #	diam	1 ft % finer	3.5 ft	6 ft	12 ft	17 ft
10	2	82	100	100	100	98
16	1.18	72.1	99.7	99.0	100.0	94.9
30	0.6	59.5	99.2	97.7	100.0	91.0
40	0.425	53	99	97	100	89
50	0.3	39.6	98.2	94.6	99.2	65.1
80	0.18	20	97	91	98	30
100	0.15	16.8	92.9	87.1	94.9	24.2
200	0.075	4.7	77.1	72.1	82.9	2.3

Data from Geotechnical Analysis

10	2	82	100	100	100	98
40	0.425	53	99	97	100	89
80	0.18	20	97	91	98	30
200	0.075	4.7	77.1	72.1	82.9	2.3

For copying into borehole logs

	#10	#16	#30	#40	#50	#100	#200
1 ft	82	72.1	59.5	53	39.6	16.8	4.7
3.5 ft	100	99.7	99.2	99	98.2	92.9	77.1
6 ft	100	99.0	97.7	97	94.6	87.1	72.1
12 ft	100	100.0	100.0	100	99.2	94.9	82.9
17 ft	98	94.93398	91.00383	89	65.08041	24.23131	2.3

Hole # 17

Highlighted Data is interpolated

Sieve #	diam	at surface % finer	3.5 ft	8.5 ft	13.5 ft
10	2	91	81	100	90
16	1.18	85.5	70.4	99.7	81.8
30	0.6	78.6	56.9	99.2	71.3
40	0.425	75	50	99	66
50	0.3	63.6	39.5	97.0	51.8
80	0.18	47	24	94	31
100	0.15	39.6	20.3	88.4	25.3
200	0.075	11.5	6.2	67	3.6

Data from Geotechnical Analysis

10	2	91	81	100	90
40	0.425	75	50	99	66
80	0.18	47	24	94	31
200	0.075	11.5	6.2	67	3.6

For copying into borehole logs

	#10	#16	#30	#40	#50	#100	#200
at surface	91	85.5	78.6	75	63.6	39.6	11.5
3.5 ft	81	70.4	56.9	50	39.5	20.3	6.2
8.5 ft	100	99.7	99.2	99	97.0	88.4	67
13.5 ft	90	81.8	71.3	66	51.8	25.3	3.6

Hole # 19

Highlighted Data is interpolated

Sieve #	diam	1 ft % finer	3.5 ft	8.5 ft	13.5 ft
10	2	65	87	100	96
16	1.18	57.8	79.8	99.7	86.1
30	0.6	48.7	70.7	99.2	73.5
40	0.425	44	66	99	67
50	0.3	34.3	51.8	95.4	45.1
80	0.18	20	31	90	13
100	0.15	16.8	26.4	79.9	10.6
200	0.075	4.5	9	41.3	1.4

Data from Geotechnical Analysis

10	2	65	87	100	96
40	0.425	44	66	99	67
80	0.18	20	31	90	13
200	0.075	4.5	9	41.3	1.4

For copying into borehole logs

	#10	#16	#30	#40	#50	#100	#200
1 ft	65	57.8	48.7	44	34.3	16.8	4.5
3.5 ft	87	79.8	70.7	66	51.8	26.4	9
8.5 ft	100	99.7	99.2	99	95.4	79.9	41.3
13.5 ft	96	86.1	73.5	67	45.1	10.6	1.4

Hole # 20

Highlighted Data is interpolated

Sieve #	diam	5 ft % finer	10 ft
10	2	96	100
16	1.18	95.7	98.6
30	0.6	95.2	96.9
40	0.425	95	96
50	0.3	80.4	75.7
80	0.18	59	46
100	0.15	51.2	37.7
200	0.075	21.7	6.2

Data from Geotechnical Analysis

10	2	96	100
40	0.425	95	96
80	0.18	59	46
200	0.075	21.7	6.2

For copying into borehole logs

	#10	#16	#30	#40	#50	#100	#200
5 ft	96	95.7	95.2	95	80.4	51.2	21.7
10 ft	100	98.6	96.9	96	75.7	37.7	6.2

Hole # 21

Highlighted Data is interpolated

Sieve #	diam	4 ft % finer	7 ft	12 ft
10	2	88	98	100
16	1.18	77.8	96.0	99.3
30	0.6	64.7	93.3	98.4
40	0.425	58	92	98
50	0.3	46.2	87.1	96.0
80	0.18	29	80	93
100	0.15	24.4	71.3	88.5
200	0.075	7	38	71.4

Data from Geotechnical Analysis

10	2	88	98	100
40	0.425	58	92	98
80	0.18	29	80	93
200	0.075	7	38	71.4

For copying into borehole logs

	#10	#16	#30	#40	#50	#100	#200
4 ft	88	77.8	64.7	58	46.2	24.4	7
7 ft	98	96.0	93.3	92	87.1	71.3	38
12 ft	100	99.3	98.4	98	96.0	88.5	71.4

Hole # 22

Highlighted Data is interpolated

Sieve #	diam	1 ft % finer	13 ft
10	2	87	100
16	1.18	78.1	98.6
30	0.6	66.8	96.9
40	0.425	61	96
50	0.3	48.8	89.9
80	0.18	31	81
100	0.15	25.9	72.1
200	0.075	6.4	38.5

Data from Geotechnical Analysis

10	2	87	100
40	0.425	61	96
80	0.18	31	81
200	0.075	6.4	38.5

For copying into borehole logs

	#10	#16	#30	#40	#50	#100	#200
1 ft	87	78.1	66.8	61	48.8	25.9	6.4
13 ft	100	98.6	96.9	96	89.9	72.1	38.5

Hole # 23

Highlighted Data is interpolated

Sieve #	diam	4 ft % finer	9 ft	13 ft
10	2	92	99	99
16	1.18	85.2	96.6	97.6
30	0.6	76.5	93.6	95.9
40	0.425	72	92	95
50	0.3	59.0	83.5	91.8
80	0.18	40	71	87
100	0.15	32.6	65.1	81.7
200	0.075	4.6	42.8	61.6

Data from Geotechnical Analysis

10	2	92	99	99
40	0.425	72	92	95
80	0.18	40	71	87
200	0.075	4.6	42.8	61.6

For copying into borehole logs

	#10	#16	#30	#40	#50	#100	#200
4 ft	92	85.2	76.5	72	59.0	32.6	4.6
9 ft	99	96.6	93.6	92	83.5	65.1	42.8
13 ft	99	97.6	95.9	95	91.8	81.7	61.6

Hole # 24

Highlighted Data is interpolated

Sieve #	diam	5 ft % finer	10 ft
10	2	95	99
16	1.18	89.5	98.0
30	0.6	82.6	96.7
40	0.425	79	96
50	0.3	62.0	92.4
80	0.18	37	87
100	0.15	32.7	80.6
200	0.075	16.5	56.4

Data from Geotechnical Analysis

10	2	95	99
40	0.425	79	96
80	0.18	37	87
200	0.075	16.5	56.4

For copying into borehole logs

	#10	#16	#30	#40	#50	#100	#200
5 ft	95	89.5	82.6	79	62.0	32.7	16.5
10 ft	99	98.0	96.7	96	92.4	80.6	56.4

Hole # 25

Highlighted Data is interpolated

		5 ft	10 ft	15 ft
Sieve #	diam	% finer		
10	2	94	100	95
16	1.18	91.6	98.0	79.7
30	0.6	88.6	95.3	60.0
40	0.425	87	94	50
50	0.3	74.0	70.5	35.8
80	0.18	55	36	15
100	0.15	49.9	30.4	12.8
200	0.075	30.4	9.1	4.2

Data from Geotechnical Analysis

10	2	94	100	95
40	0.425	87	94	50
80	0.18	55	36	15
200	0.075	30.4	9.1	4.2

For copying into borehole logs

	#10	#16	#30	#40	#50	#100	#200
5 ft	94	91.6	88.6	87	74.0	49.9	30.4
10 ft	100	98.0	95.3	94	70.5	30.4	9.1
15 ft	95	79.7	60.0	50	35.8	12.8	4.2

Hole # 26

Highlighted Data is interpolated

Sieve #	diam	5 ft % finer	10 ft
10	2	99	100
16	1.18	97.3	99.0
30	0.6	95.1	97.7
40	0.425	94	97
50	0.3	75.4	88.5
80	0.18	48	76
100	0.15	43.3	66.2
200	0.075	25.2	29.1

Data from Geotechnical Analysis

10	2	99	100
40	0.425	94	97
80	0.18	48	76
200	0.075	25.2	29.1

For copying into borehole logs

	#10	#16	#30	#40	#50	#100	#200
5 ft	99	97.3	95.1	94	75.4	43.3	25.2
10 ft	100	99.0	97.7	97	88.5	66.2	29.1

Hole # 27

Highlighted Data is interpolated

Sieve #	diam	at surface % finer	2 ft	8.5 ft
10	2	99	99	100
16	1.18	94.9	93.5	97.3
30	0.6	89.7	86.6	93.8
40	0.425	87	83	92
50	0.3	69.2	63.1	75.0
80	0.18	43	34	50
100	0.15	34.9	27.6	40.6
200	0.075	4.1	3.1	4.7

Data from Geotechnical Analysis

10	2	99	99	100
40	0.425	87	83	92
80	0.18	43	34	50
200	0.075	4.1	3.1	4.7

For copying into borehole logs

	#10	#16	#30	#40	#50	#100	#200
at surface	99	94.9	89.7	87	69.2	34.9	4.1
2 ft	99	93.5	86.6	83	63.1	27.6	3.1
8.5 ft	100	97.3	93.8	92	75.0	40.6	4.7

Hole # 27 OL

Highlighted Data is interpolated

Sieve #	diam	at surface % finer	3.5 ft	5 ft	7.5 ft
10	2	86	98	73	100
16	1.18	78.5	94.3	65.5	99.0
30	0.6	68.9	89.4	55.9	97.7
40	0.425	64	87	51	97
50	0.3	52.2	79.7	42.9	88.1
80	0.18	35	69	31	75
100	0.15	31.5	64.9	28.9	62.2
200	0.075	18.3	49.4	20.9	13.6

Data from Geotechnical Analysis

10	2	86	98	73	100
40	0.425	64	87	51	97
80	0.18	35	69	31	75
200	0.075	18.3	49.4	20.9	13.6

For copying into borehole logs

	#10	#16	#30	#40	#50	#100	#200
at surface	86	78.5	68.9	64	52.2	31.5	18.3
3.5 ft	98	94.3	89.4	87	79.7	64.9	49.4
5 ft	73	65.5	55.9	51	42.9	28.9	20.9
7.5 ft	100	99.0	97.7	97	88.1	62.2	13.6

Hole # 28

Highlighted Data is interpolated

Sieve #	diam	at surface % finer	2 ft	13.5 ft
10	2	90	100	99
16	1.18	84.5	98.0	86.7
30	0.6	77.6	95.3	71.0
40	0.425	74	94	63
50	0.3	62.6	87.1	47.2
80	0.18	46	77	24
100	0.15	38.7	73.0	19.6
200	0.075	11	57.7	2.8

Data from Geotechnical Analysis

10	2	90	100	99
40	0.425	74	94	63
80	0.18	46	77	24
200	0.075	11	57.7	2.8

For copying into borehole logs

	#10	#16	#30	#40	#50	#100	#200
at surface	90	84.5	77.6	74	62.6	38.7	11
2 ft	100	98.0	95.3	94	87.1	73.0	57.7
13.5 ft	99	86.7	71.0	63	47.2	19.6	2.8

Hole # 30

Highlighted Data is interpolated

Sieve #	diam	5 ft % finer	10 ft
10	2	96	98
16	1.18	92.9	96.0
30	0.6	89.0	93.3
40	0.425	87	92
50	0.3	81.3	87.1
80	0.18	73	80
100	0.15	67.7	77.6
200	0.075	47.5	68.3

Data from Geotechnical Analysis

10	2	96	98
40	0.425	87	92
80	0.18	73	80
200	0.075	47.5	68.3

For copying into borehole logs

	#10	#16	#30	#40	#50	#100	#200
5 ft	96	92.9	89.0	87	81.3	67.7	47.5
10 ft	98	96.0	93.3	92	87.1	77.6	68.3

Hole # 31

Highlighted Data is interpolated

Sieve #	diam	5 ft % finer	10 ft	15 ft
10	2	99	100	98
16	1.18	97.0	99.0	90.8
30	0.6	94.3	97.7	81.7
40	0.425	93	97	77
50	0.3	84.5	93.8	62.0
80	0.18	72	89	40
100	0.15	66.1	84.6	36.1
200	0.075	43.7	67.9	21.4

Data from Geotechnical Analysis

10	2	99	100	98
40	0.425	93	97	77
80	0.18	72	89	40
200	0.075	43.7	67.9	21.4

For copying into borehole logs

	#10	#16	#30	#40	#50	#100	#200
5 ft	99	97.0	94.3	93	84.5	66.1	43.7
10 ft	100	99.0	97.7	97	93.8	84.6	67.9
15 ft	98	90.8	81.7	77	62.0	36.1	21.4

Hole # 33

Highlighted Data is interpolated

Sieve #	diam	5 ft % finer	15 ft
10	2	95	99
16	1.18	87.5	94.2
30	0.6	77.9	88.1
40	0.425	73	85
50	0.3	58.0	66.8
80	0.18	36	40
100	0.15	30.3	33.9
200	0.075	8.6	10.7

Data from Geotechnical Analysis

10	2	95	99
40	0.425	73	85
80	0.18	36	40
200	0.075	8.6	10.7

For copying into borehole logs

	#10	#16	#30	#40	#50	#100	#200
5 ft	95	87.5	77.9	73	58.0	30.3	8.6
15 ft	99	94.2	88.1	85	66.8	33.9	10.7

Hole # 34

Highlighted Data is interpolated

Sieve #	diam	5 ft % finer	10 ft
10	2	99	97
16	1.18	95.6	85.1
30	0.6	91.2	69.8
40	0.425	89	62
50	0.3	71.6	47.8
80	0.18	46	27
100	0.15	41.0	22.2
200	0.075	21.8	3.8

Data from Geotechnical Analysis

10	2	99	97
40	0.425	89	62
80	0.18	46	27
200	0.075	21.8	3.8

For copying into borehole logs

	#10	#16	#30	#40	#50	#100	#200
5 ft	99	95.6	91.2	89	71.6	41.0	21.8
10 ft	97	85.1	69.8	62	47.8	22.2	3.8

Hole # 35

Highlighted Data is interpolated

Sieve #	diam	5 ft % finer	10 ft
10	2	99	100
16	1.18	96.6	96.6
30	0.6	93.6	92.2
40	0.425	92	90
50	0.3	85.9	83.5
80	0.18	77	74
100	0.15	67.1	65.8
200	0.075	29.6	34.4

Data from Geotechnical Analysis

10	2	99	100
40	0.425	92	90
80	0.18	77	74
200	0.075	29.6	34.4

For copying into borehole logs

	#10	#16	#30	#40	#50	#100	#200
5 ft	99	96.6	93.6	92	85.9	67.1	29.6
10 ft	100	96.6	92.2	90	83.5	65.8	34.4

Hole # 36

Highlighted Data is interpolated

Sieve #	diam	5 ft % finer	10 ft
10	2	96	97
16	1.18	88.2	93.3
30	0.6	78.1	88.4
40	0.425	73	86
50	0.3	54.8	71.8
80	0.18	28	51
100	0.15	24.6	45.1
200	0.075	11.5	22.7

Data from Geotechnical Analysis

10	2	96	97
40	0.425	73	86
80	0.18	28	51
200	0.075	11.5	22.7

For copying into borehole logs

	#10	#16	#30	#40	#50	#100	#200
5 ft	96	88.2	78.1	73	54.8	24.6	11.5
10 ft	97	93.3	88.4	86	71.8	45.1	22.7

Hole # 37

Highlighted Data is interpolated

Sieve #	diam	5 ft % finer	10 ft
10	2	96	99
16	1.18	91.9	97.0
30	0.6	86.7	94.3
40	0.425	84	93
50	0.3	75.1	88.9
80	0.18	62	83
100	0.15	58.2	78.3
200	0.075	43.9	60.4

Data from Geotechnical Analysis

10	2	96	99
40	0.425	84	93
80	0.18	62	83
200	0.075	43.9	60.4

For copying into borehole logs

	#10	#16	#30	#40	#50	#100	#200
5 ft	96	91.9	86.7	84	75.1	58.2	43.9
10 ft	99	97.0	94.3	93	88.9	78.3	60.4

Hole # 38

Highlighted Data is interpolated

Sieve #	diam	5 ft % finer	10 ft
10	2	85	96
16	1.18	79.9	89.5
30	0.6	73.3	81.2
40	0.425	70	77
50	0.3	54.6	62.0
80	0.18	32	40
100	0.15	27.9	34.9
200	0.075	12.4	15.6

Data from Geotechnical Analysis

10	2	85	96
40	0.425	70	77
80	0.18	32	40
200	0.075	12.4	15.6

For copying into borehole logs

	#10	#16	#30	#40	#50	#100	#200
5 ft	85	79.9	73.3	70	54.6	27.9	12.4
10 ft	96	89.5	81.2	77	62.0	34.9	15.6

Hole # 39

Highlighted Data is interpolated

Sieve #	diam	2 ft % finer	5 ft	10 ft
10	2	93	96	100
16	1.18	78.4	92.3	99.7
30	0.6	59.6	87.4	99.2
40	0.425	50	85	99
50	0.3	37.4	77.3	98.6
80	0.18	19	66	98
100	0.15	16.3	60.3	95.4
200	0.075	5.8	38.5	85.7

Data from Geotechnical Analysis

10	2	93	96	100
40	0.425	50	85	99
80	0.18	19	66	98
200	0.075	5.8	38.5	85.7

For copying into borehole logs

	#10	#16	#30	#40	#50	#100	#200
2 ft	93	78.4	59.6	50	37.4	16.3	5.8
5 ft	96	92.3	87.4	85	77.3	60.3	38.5
10 ft	100	99.7	99.2	99	98.6	95.4	85.7

Hole # 40

Highlighted Data is interpolated

Sieve #	diam	5 ft % finer	10 ft
10	2	99	97
16	1.18	97.3	91.9
30	0.6	95.1	85.3
40	0.425	94	82
50	0.3	88.3	63.8
80	0.18	80	37
100	0.15	72.2	33.2
200	0.075	42.6	18.9

Data from Geotechnical Analysis

10	2	99	97
40	0.425	94	82
80	0.18	80	37
200	0.075	42.6	18.9

For copying into borehole logs

	#10	#16	#30	#40	#50	#100	#200
5 ft	99	97.3	95.1	94	88.3	72.2	42.6
10 ft	97	91.9	85.3	82	63.8	33.2	18.9

Hole # 41

Highlighted Data is interpolated

Sieve #	diam	5 ft % finer	10 ft
10	2	98	98
16	1.18	92.9	94.9
30	0.6	86.3	91.0
40	0.425	83	89
50	0.3	68.4	82.5
80	0.18	47	73
100	0.15	41.1	66.6
200	0.075	18.5	42.1

Data from Geotechnical Analysis

10	2	98	98
40	0.425	83	89
80	0.18	47	73
200	0.075	18.5	42.1

For copying into borehole logs

	#10	#16	#30	#40	#50	#100	#200
5 ft	98	92.9	86.3	83	68.4	41.1	18.5
10 ft	98	94.9	91.0	89	82.5	66.6	42.1

Hole # 42

Highlighted Data is interpolated

Sieve #	diam	5 ft % finer
10	2	99
16	1.18	97.0
30	0.6	94.3
40	0.425	93
50	0.3	78.0
80	0.18	56
100	0.15	47.1
200	0.075	13.4

Data from Geotechnical Analysis

10	2	99
40	0.425	93
80	0.18	56
200	0.075	13.4

For copying into borehole logs

	#10	#16	#30	#40	#50	#100	#200
5 ft	99	97.0	94.3	93	78.0	47.1	13.4

Hole # 43

Highlighted Data is interpolated

Sieve #	diam	at surface % finer	3 ft
10	2	100	99
16	1.18	99.7	98.7
30	0.6	99.2	98.2
40	0.425	99	98
50	0.3	98.2	92.7
80	0.18	97	85
100	0.15	95.3	70.5
200	0.075	88.9	15.4

Data from Geotechnical Analysis

10	2	100	99
40	0.425	99	98
80	0.18	97	85
200	0.075	88.9	15.4

For copying into borehole logs

	#10	#16	#30	#40	#50	#100	#200
at surface	100	99.7	99.2	99	98.2	95.3	88.9
3 ft	99	98.7	98.2	98	92.7	70.5	15.4

Hole # 44

Highlighted Data is interpolated

Sieve #	diam	at surface % finer	0.5 ft	8.5 ft
10	2	97	73	100
16	1.18	92.9	59.7	98.6
30	0.6	87.7	42.7	96.9
40	0.425	85	34	96
50	0.3	75.3	25.1	87.1
80	0.18	61	12	74
100	0.15	55.5	10.0	63.0
200	0.075	34.8	2.5	21.4

Data from Geotechnical Analysis

10	2	97	73	100
40	0.425	85	34	96
80	0.18	61	12	74
200	0.075	34.8	2.5	21.4

For copying into borehole logs

	#10	#16	#30	#40	#50	#100	#200
at surface	97	92.9	87.7	85	75.3	55.5	34.8
0.5 ft	73	59.7	42.7	34	25.1	10.0	2.5
8.5 ft	100	98.6	96.9	96	87.1	63.0	21.4

Hole # 45

Highlighted Data is interpolated

Sieve #	diam	at surface % finer	8.5 ft
10	2	96	100
16	1.18	88.5	100.0
30	0.6	78.9	100.0
40	0.425	74	100
50	0.3	52.1	86.2
80	0.18	20	66
100	0.15	16.8	54.2
200	0.075	4.6	9.1

Data from Geotechnical Analysis

10	2	96	100
40	0.425	74	100
80	0.18	20	66
200	0.075	4.6	9.1

For copying into borehole logs

	#10	#16	#30	#40	#50	#100	#200
at surface	96	88.5	78.9	74	52.1	16.8	4.6
8.5 ft	100	100.0	100.0	100	86.2	54.2	9.1

Hole # 46

Highlighted Data is interpolated

Sieve #	diam	5 ft	7 ft
10	2	100	100
16	1.18	98.0	99.0
30	0.6	95.3	97.7
40	0.425	94	97
50	0.3	80.6	92.9
80	0.18	61	87
100	0.15	55.8	82.4
200	0.075	36.1	64.8

Data from Geotechnical Analysis

10	2	100	100
40	0.425	94	97
80	0.18	61	87
200	0.075	36.1	64.8

For copying into borehole logs

	#10	#16	#30	#40	#50	#100	#200
5 ft	100	98.0	95.3	94	80.6	55.8	36.1
7 ft	100	99.0	97.7	97	92.9	82.4	64.8

Hole # 47

Highlighted Data is interpolated

Sieve #	diam	at surface % finer	3 ft	8.5 ft
10	2	100	100	100
16	1.18	98.6	99.0	99.0
30	0.6	96.9	97.7	97.7
40	0.425	96	97	97
50	0.3	93.2	82.4	86.1
80	0.18	89	61	70
100	0.15	83.2	51.7	62.9
200	0.075	61.3	16.4	36.1

Data from Geotechnical Analysis

10	2	100	100	100
40	0.425	96	97	97
80	0.18	89	61	70
200	0.075	61.3	16.4	36.1

For copying into borehole logs

	#10	#16	#30	#40	#50	#100	#200
at surface	100	98.6	96.9	96	93.2	83.2	61.3
3 ft	100	99.0	97.7	97	82.4	51.7	16.4
8.5 ft	100	99.0	97.7	97	86.1	62.9	36.1

Hole # 48

Highlighted Data is interpolated

Sieve #	diam	at surface	4 ft
10	2	100	100
16	1.18	99.0	99.0
30	0.6	97.7	97.7
40	0.425	97	97
50	0.3	89.3	86.9
80	0.18	78	72
100	0.15	71.3	64.4
200	0.075	45.6	35.5

Data from Geotechnical Analysis

10	2	100	100
40	0.425	97	97
80	0.18	78	72
200	0.075	45.6	35.5

For copying into borehole logs

	#10	#16	#30	#40	#50	#100	#200
at surface	100	99.0	97.7	97	89.3	71.3	45.6
4 ft	100	99.0	97.7	97	86.9	64.4	35.5

Hole # 49

Highlighted Data is interpolated

Sieve #	diam	at surface % finer	2.5 ft	8.5 ft
10	2	100	98	91
16	1.18	98.3	92.5	90.0
30	0.6	96.1	85.6	88.7
40	0.425	95	82	88
50	0.3	88.9	63.4	56.4
80	0.18	80	36	10
100	0.15	75.5	31.7	8.0
200	0.075	58.3	15.2	0.6

Data from Geotechnical Analysis

10	2	100	98	91
40	0.425	95	82	88
80	0.18	80	36	10
200	0.075	58.3	15.2	0.6

For copying into borehole logs

	#10	#16	#30	#40	#50	#100	#200
at surface	100	98.3	96.1	95	88.9	75.5	58.3
2.5 ft	98	92.5	85.6	82	63.4	31.7	15.2
8.5 ft	91	90.0	88.7	88	56.4	8.0	0.6

Hole # 50

Highlighted Data is interpolated

Sieve #	diam	at surface % finer	2 ft	8.5 ft
10	2	100	100	96
16	1.18	98.6	99.7	87.8
30	0.6	96.9	99.2	77.3
40	0.425	96	99	72
50	0.3	88.3	98.2	48.5
80	0.18	77	97	14
100	0.15	71.7	92.7	11.4
200	0.075	51.7	76.4	1.5

Data from Geotechnical Analysis

10	2	100	100	96
40	0.425	96	99	72
80	0.18	77	97	14
200	0.075	51.7	76.4	1.5

For copying into borehole logs

	#10	#16	#30	#40	#50	#100	#200
at surface	100	98.6	96.9	96	88.3	71.7	51.7
2 ft	100	99.7	99.2	99	98.2	92.7	76.4
8.5 ft	96	87.8	77.3	72	48.5	11.4	1.5

Hole # 51

Highlighted Data is interpolated

Sieve #	diam	at surface % finer	11.5 ft	18.5 ft
10	2	100	100	97
16	1.18	96.9	96.3	93.9
30	0.6	93.0	91.4	90.0
40	0.425	91	89	88
50	0.3	78.4	63.5	60.0
80	0.18	60	26	19
100	0.15	52.0	21.1	15.4
200	0.075	21.8	2.3	1.8

Data from Geotechnical Analysis

10	2	100	100	97
40	0.425	91	89	88
80	0.18	60	26	19
200	0.075	21.8	2.3	1.8

For copying into borehole logs

	#10	#16	#30	#40	#50	#100	#200
at surface	100	96.9	93.0	91	78.4	52.0	21.8
11.5 ft	100	96.3	91.4	89	63.5	21.1	2.3
18.5 ft	97	93.9	90.0	88	60.0	15.4	1.8

Hole # 52

Highlighted Data is interpolated

Sieve #	diam	at surface % finer	3.5 ft	9 ft	13.5 ft
10	2	94	99	96	58
16	1.18	92.0	97.3	93.6	44.4
30	0.6	89.3	95.1	90.6	26.9
40	0.425	88	94	89	18
50	0.3	80.3	83.5	78.9	12.7
80	0.18	69	68	64	5
100	0.15	63.2	62.5	53.7	4.2
200	0.075	41	41.7	14.4	1.3

Data from Geotechnical Analysis

10	2	94	99	96	58
40	0.425	88	94	89	18
80	0.18	69	68	64	5
200	0.075	41	41.7	14.4	1.3

For copying into borehole logs

	#10	#16	#30	#40	#50	#100	#200
at surface	94	92.0	89.3	88	80.3	63.2	41
3.5 ft	99	97.3	95.1	94	83.5	62.5	41.7
9 ft	96	93.6	90.6	89	78.9	53.7	14.4
13.5 ft	58	44.4	26.9	18	12.7	4.2	1.3

Hole # 53

Highlighted Data is interpolated

Sieve #	diam	at surface % finer	2 ft	7 ft	13.5 ft
10	2	100	100	100	100
16	1.18	100.0	97.6	98.3	95.2
30	0.6	100.0	94.6	96.1	89.1
40	0.425	100	93	95	86
50	0.3	96.4	76.0	93.0	59.2
80	0.18	91	51	90	20
100	0.15	81.8	43.3	87.0	16.5
200	0.075	46.8	13.9	75.8	3.2

Data from Geotechnical Analysis

10	2	100	100	100	100
40	0.425	100	93	95	86
80	0.18	91	51	90	20
200	0.075	46.8	13.9	75.8	3.2

For copying into borehole logs

	#10	#16	#30	#40	#50	#100	#200
at surface	100	100.0	100.0	100	96.4	81.8	46.8
2 ft	100	97.6	94.6	93	76.0	43.3	13.9
7 ft	100	98.3	96.1	95	93.0	87.0	75.8
13.5 ft	100	95.2	89.1	86	59.2	16.5	3.2

Hole # 54

Highlighted Data is interpolated

Sieve #	diam	at surface % finer	8.5 ft	13.5 ft
10	2	99	100	97
16	1.18	97.6	99.7	76.9
30	0.6	95.9	99.2	51.1
40	0.425	95	99	38
50	0.3	93.0	94.1	26.2
80	0.18	90	87	9
100	0.15	87.0	81.3	7.5
200	0.075	75.6	59.4	2

Data from Geotechnical Analysis

10	2	99	100	97
40	0.425	95	99	38
80	0.18	90	87	9
200	0.075	75.6	59.4	2

For copying into borehole logs

	#10	#16	#30	#40	#50	#100	#200
at surface	99	97.6	95.9	95	93.0	87.0	75.6
8.5 ft	100	99.7	99.2	99	94.1	81.3	59.4
13.5 ft	97	76.9	51.1	38	26.2	7.5	2

Hole # 55

Highlighted Data is interpolated

Sieve #	diam	at surface % finer	2 ft	8 ft	18.5 ft
10	2	100	100	100	82
16	1.18	99.7	98.0	99.7	66.7
30	0.6	99.2	95.3	99.2	47.0
40	0.425	99	94	99	37
50	0.3	96.2	74.9	96.6	26.1
80	0.18	92	47	93	10
100	0.15	85.2	39.2	84.1	8.4
200	0.075	59.4	9.7	50.3	2.1

Data from Geotechnical Analysis

10	2	100	100	100	82
40	0.425	99	94	99	37
80	0.18	92	47	93	10
200	0.075	59.4	9.7	50.3	2.1

For copying into borehole logs

	#10	#16	#30	#40	#50	#100	#200
at surface	100	99.7	99.2	99	96.2	85.2	59.4
2 ft	100	98.0	95.3	94	74.9	39.2	9.7
8 ft	100	99.7	99.2	99	96.6	84.1	50.3
18.5 ft	82	66.7	47.0	37	26.1	8.4	2.1

Hole # 56

Highlighted Data is interpolated

Sieve #	diam	at surface % finer	2.5 ft	7.5 ft	18.5 ft
10	2	100	92	100	96
16	1.18	100.0	86.2	99.3	85.4
30	0.6	100.0	78.8	98.4	71.9
40	0.425	100	75	98	65
50	0.3	99.2	57.6	94.4	45.1
80	0.18	98	32	89	16
100	0.15	93.5	29.0	81.2	13.3
200	0.075	76.3	17.8	51.5	2.8

Data from Geotechnical Analysis

10	2	100	92	100	96
40	0.425	100	75	98	65
80	0.18	98	32	89	16
200	0.075	76.3	17.8	51.5	2.8

For copying into borehole logs

	#10	#16	#30	#40	#50	#100	#200
at surface	100	100.0	100.0	100	99.2	93.5	76.3
2.5 ft	92	86.2	78.8	75	57.6	29.0	17.8
7.5 ft	100	99.3	98.4	98	94.4	81.2	51.5
18.5 ft	96	85.4	71.9	65	45.1	13.3	2.8

Hole # 57

Highlighted Data is interpolated

Sieve #	diam	at surface % finer	3.5 ft	8.5 ft	13 ft
10	2	100	91	100	99
16	1.18	99.7	86.9	98.6	97.0
30	0.6	99.2	81.7	96.9	94.3
40	0.425	99	79	96	93
50	0.3	98.2	66.0	80.6	71.1
80	0.18	97	47	58	39
100	0.15	95.3	43.3	50.8	32.4
200	0.075	88.9	29.3	23.4	7.2

Data from Geotechnical Analysis

10	2	100	91	100	99
40	0.425	99	79	96	93
80	0.18	97	47	58	39
200	0.075	88.9	29.3	23.4	7.2

For copying into borehole logs

	#10	#16	#30	#40	#50	#100	#200
at surface	100	99.7	99.2	99	98.2	95.3	88.9
3.5 ft	91	86.9	81.7	79	66.0	43.3	29.3
8.5 ft	100	98.6	96.9	96	80.6	50.8	23.4
13 ft	99	97.0	94.3	93	71.1	32.4	7.2

Hole # 58

Highlighted Data is interpolated

Sieve #	diam	5 ft % finer	10 ft	15 ft
10	2	96	100	86
16	1.18	94.6	99.0	75.1
30	0.6	92.9	97.7	61.1
40	0.425	92	97	54
50	0.3	87.9	90.9	39.4
80	0.18	82	82	18
100	0.15	78.0	73.5	15.2
200	0.075	62.6	41.2	4.6

Data from Geotechnical Analysis

10	2	96	100	86
40	0.425	92	97	54
80	0.18	82	82	18
200	0.075	62.6	41.2	4.6

For copying into borehole logs

	#10	#16	#30	#40	#50	#100	#200
5 ft	96	94.6	92.9	92	87.9	78.0	62.6
10 ft	100	99.0	97.7	97	90.9	73.5	41.2
15 ft	86	75.1	61.1	54	39.4	15.2	4.6

Hole # 59

Highlighted Data is interpolated

		5 ft	10 ft	15 ft
Sieve #	diam	% finer		
10	2	99	100	98
16	1.18	94.6	99.7	91.2
30	0.6	88.9	99.2	82.5
40	0.425	86	99	78
50	0.3	71.0	91.3	63.4
80	0.18	49	80	42
100	0.15	40.4	66.4	35.5
200	0.075	7.9	14.7	10.8

Data from Geotechnical Analysis

10	2	99	100	98
40	0.425	86	99	78
80	0.18	49	80	42
200	0.075	7.9	14.7	10.8

For copying into borehole logs

	#10	#16	#30	#40	#50	#100	#200
5 ft	99	94.6	88.9	86	71.0	40.4	7.9
10 ft	100	99.7	99.2	99	91.3	66.4	14.7
15 ft	98	91.2	82.5	78	63.4	35.5	10.8

Hole # 60

Highlighted Data is interpolated

Sieve #	diam	5 ft % finer	10 ft
10	2	100	100
16	1.18	99.0	99.0
30	0.6	97.7	97.7
40	0.425	97	97
50	0.3	89.3	80.8
80	0.18	78	57
100	0.15	71.6	46.8
200	0.075	47.1	7.9

Data from Geotechnical Analysis

10	2	100	100
40	0.425	97	97
80	0.18	78	57
200	0.075	47.1	7.9

For copying into borehole logs

	#10	#16	#30	#40	#50	#100	#200
5 ft	100	99.0	97.7	97	89.3	71.6	47.1
10 ft	100	99.0	97.7	97	80.8	46.8	7.9

Hole # 61

Highlighted Data is interpolated

		5 ft	10 ft
Sieve #	diam	% finer	
10	2	90	94
16	1.18	74.3	84.8
30	0.6	54.2	73.0
40	0.425	44	67
50	0.3	31.4	55.2
80	0.18	13	38
100	0.15	11.3	35.3
200	0.075	4.7	24.8

Data from Geotechnical Analysis

10	2	90	94
40	0.425	44	67
80	0.18	13	38
200	0.075	4.7	24.8

For copying into borehole logs

	#10	#16	#30	#40	#50	#100	#200
5 ft	90	74.3	54.2	44	31.4	11.3	4.7
10 ft	94	84.8	73.0	67	55.2	35.3	24.8

Hole # 62

Highlighted Data is interpolated

		5 ft	10 ft
Sieve #	diam	% finer	
10	2	100	98
16	1.18	98.6	84.7
30	0.6	96.9	67.7
40	0.425	96	59
50	0.3	78.6	40.4
80	0.18	53	13
100	0.15	44.8	10.7
200	0.075	13.4	1.8

Data from Geotechnical Analysis

10	2	100	98
40	0.425	96	59
80	0.18	53	13
200	0.075	13.4	1.8

For copying into borehole logs

	#10	#16	#30	#40	#50	#100	#200
5 ft	100	98.6	96.9	96	78.6	44.8	13.4
10 ft	98	84.7	67.7	59	40.4	10.7	1.8

Hole # 63

Highlighted Data is interpolated

Sieve #	diam	5 ft % finer	10 ft
10	2	99	98
16	1.18	90.8	93.9
30	0.6	80.3	88.7
40	0.425	75	86
50	0.3	58.8	66.1
80	0.18	35	37
100	0.15	31.3	30.3
200	0.075	17.1	4.8

Data from Geotechnical Analysis

10	2	99	98
40	0.425	75	86
80	0.18	35	37
200	0.075	17.1	4.8

For copying into borehole logs

	#10	#16	#30	#40	#50	#100	#200
5 ft	99	90.8	80.3	75	58.8	31.3	17.1
10 ft	98	93.9	88.7	86	66.1	30.3	4.8

Hole # 64

Highlighted Data is interpolated

		5 ft	10 ft
Sieve #	diam	% finer	
10	2	100	100
16	1.18	98.3	99.0
30	0.6	96.1	97.7
40	0.425	95	97
50	0.3	80.0	89.7
80	0.18	58	79
100	0.15	50.4	75.6
200	0.075	21.7	62.8

Data from Geotechnical Analysis

10	2	100	100
40	0.425	95	97
80	0.18	58	79
200	0.075	21.7	62.8

For copying into borehole logs

	#10	#16	#30	#40	#50	#100	#200
5 ft	100	98.3	96.1	95	80.0	50.4	21.7
10 ft	100	99.0	97.7	97	89.7	75.6	62.8

Hole # 65

Highlighted Data is interpolated

Sieve #	diam	5 ft % finer	10 ft
10	2	99	99
16	1.18	95.9	97.0
30	0.6	92.0	94.3
40	0.425	90	93
50	0.3	73.8	81.2
80	0.18	50	64
100	0.15	46.2	63.9
200	0.075	31.7	63.4

Data from Geotechnical Analysis

10	2	99	99
40	0.425	90	93
80	0.18	50	64
200	0.075	31.7	63.4

For copying into borehole logs

	#10	#16	#30	#40	#50	#100	#200
5 ft	99	95.9	92.0	90	73.8	46.2	31.7
10 ft	99	97.0	94.3	93	81.2	63.9	63.4

Hole # 66

Highlighted Data is interpolated

		5 ft	10 ft
Sieve #	diam	% finer	
10	2	100	99
16	1.18	97.6	98.3
30	0.6	94.6	97.4
40	0.425	93	97
50	0.3	67.9	86.5
80	0.18	31	71
100	0.15	27.8	64.2
200	0.075	15.4	38.4

Data from Geotechnical Analysis

10	2	100	99
40	0.425	93	97
80	0.18	31	71
200	0.075	15.4	38.4

For copying into borehole logs

	#10	#16	#30	#40	#50	#100	#200
5 ft	100	97.6	94.6	93	67.9	27.8	15.4
10 ft	99	98.3	97.4	97	86.5	64.2	38.4

Hole # 66B

Highlighted Data is interpolated

Sieve #	diam	at surface % finer	12 ft
10	2	100	100
16	1.18	97.6	99.0
30	0.6	94.6	97.7
40	0.425	93	97
50	0.3	82.1	93.4
80	0.18	66	88
100	0.15	60.6	80.4
200	0.075	40.1	51.4

Data from Geotechnical Analysis

10	2	100	100
40	0.425	93	97
80	0.18	66	88
200	0.075	40.1	51.4

For copying into borehole logs

	#10	#16	#30	#40	#50	#100	#200
at surface	100	97.6	94.6	93	82.1	60.6	40.1
12 ft	100	99.0	97.7	97	93.4	80.4	51.4

Raw Data Extraction

Data Extraction: This information is pulled from GIS datasets

2019 Issue locations

Planform Script

OID/FID	1918		1935		1949	
1	no data	7	flood prone	4	upland uses	12
2	no data	7	flood prone	4	upland uses	12
4	no data	7	flood prone	4	upland uses	12
5	no data	7	flood prone	4	upland uses	12
6	no data	7	flood prone	4	upland uses	12
8	no data	7	flood prone	4	historic channel	5
14	no data	7	flood prone	4	upland uses	12
15	no data	7	flood prone	4	upland uses	12
16	no data	7	flood prone	4	upland uses	12
17	no data	7	flood prone	4	upland uses	12
19	active channel	2	flood prone	4	upland uses	12
20	no data	7	flood prone	4	upland uses	12
23	no data	7	flood prone	4	upland uses	12
24	no data	7	flood prone	4	upland uses	12
31	no data	7	flood prone	4	upland uses	12
33	no data	7	flood prone	4	upland uses	12
36	vegetated island	13	flood prone	4	upland uses	12
55	no data	7	out of study area	8	upland uses	12
60	no data	7	flood prone	4	upland uses	12
63	active channel	2	flood prone	4	upland uses	12
64	active channel	2	flood prone	4	upland uses	12
66	no data	7	flood prone	4	historic channel	5
67	no data	7	flood prone	4	upland uses	12
68	no data	7	flood prone	4	upland uses	12
69	no data	7	flood prone	4	upland uses	12
70	no data	7	flood prone	4	upland uses	12
71	no data	7	flood prone	4	upland uses	12
72	no data	7	flood prone	4	upland uses	12
73	no data	7	flood prone	4	upland uses	12
89	no data	7	flood prone	4	upland uses	12
90	active channel	2	flood prone	4	upland uses	12
91	no data	7	flood prone	4	upland uses	12
98	no data	7	flood prone	4	upland uses	12
103	no data	7	flood prone	4	upland uses	12
107	no data	7	flood prone	4	upland uses	12
108	active channel	2	flood prone	4	upland uses	12
110	no data	7	flood prone	4	upland uses	12
121	active channel	2	flood prone	4	upland uses	12
123	no data	7	flood prone	4	upland uses	12
125	no data	7	flood prone	4	upland uses	12
126	no data	7	flood prone	4	historic channel	5

OID/FID	1918		1935		1949	
127	active channel	2	flood prone	4	upland uses	12
128	active channel	2	flood prone	4	upland uses	12
131	no data	7	flood prone	4	upland uses	12
132	no data	7	flood prone	4	upland uses	12
134	no data	7	flood prone	4	upland uses	12
139	no data	7	flood prone	4	upland uses	12
152	no data	7	flood prone	4	upland uses	12
159	no data	7	flood prone	4	upland uses	12
163	no data	7	flood prone	4	upland uses	12
164	active channel	2	flood prone	4	historic channel	5
166	no data	7	flood prone	4	upland uses	12
176	no data	7	flood prone	4	upland uses	12
179	no data	7	flood prone	4	upland uses	12
180	no data	7	flood prone	4	upland uses	12
183	active channel	2	flood prone	4	upland uses	12
185	no data	7	flood prone	4	upland uses	12
186	no data	7	flood prone	4	upland uses	12
189	active channel	2	flood prone	4	upland uses	12
190	active channel	2	flood prone	4	historic channel	5
191	active channel	2	flood prone	4	upland uses	12
194	no data	7	out of study area	8	upland uses	12
195	no data	7	flood prone	4	upland uses	12
196	no data	7	flood prone	4	upland uses	12
197	active channel	2	out of study area	8	upland uses	12
198	vegetated island	13	flood prone	4	upland uses	12
199	vegetated island	13	flood prone	4	upland uses	12
200	vegetated island	13	flood prone	4	upland uses	12
201	vegetated island	13	flood prone	4	upland uses	12
202	vegetated island	13	flood prone	4	upland uses	12
203	vegetated island	13	flood prone	4	upland uses	12
204	vegetated island	13	flood prone	4	upland uses	12
205	no data	7	flood prone	4	upland uses	12
206	no data	7	flood prone	4	upland uses	12
207	no data	7	flood prone	4	upland uses	12
208	no data	7	flood prone	4	upland uses	12
209	no data	7	flood prone	4	upland uses	12
210	no data	7	flood prone	4	upland uses	12
211	no data	7	flood prone	4	upland uses	12
213	vegetated island	13	flood prone	4	upland uses	12
214	active channel	2	out of study area	8	upland uses	12
216	no data	7	flood prone	4	upland uses	12
217	active channel	2	flood prone	4	upland uses	12
221	no data	7	flood prone	4	upland uses	12

Data Extraction: This information is pulled from GIS datasets

Borehole locations

#	Borehole name	Planform Script 1918		1935		1949	
1	B-1	no data	7	flood prone	4	historic channel	5
2	B-10	no data	7	flood prone	4	historic channel	5
3	B-11	no data	7	flood prone	4	historic channel	5
4	B-12	no data	7	flood prone	4	historic channel	5
5	B-13	no data	7	historic channel	5	historic channel	5
6	B-14	no data	7	flood prone	4	upland uses	12
7	B-15	no data	7	flood prone	4	upland uses	12
8	B-16	no data	7	flood prone	4	historic channel	5
9	B-17	no data	7	flood prone	4	upland uses	12
10	B-18	no data	7	flood prone	4	upland uses	12
11	B-19	no data	7	flood prone	4	historic channel	5
12	B-2	no data	7	flood prone	4	historic channel	5
13	B-20	no data	7	flood prone	4	upland uses	12
14	B-21	no data	7	flood prone	4	upland uses	12
15	B-22	no data	7	flood prone	4	upland uses	12
16	B-23	no data	7	flood prone	4	upland uses	12
17	B-24	no data	7	flood prone	4	upland uses	12
18	B-25	no data	7	flood prone	4	upland uses	12
19	B-26	no data	7	flood prone	4	upland uses	12
20	B-27	no data	7	historic channel	5	upland uses	12
21	B-28	no data	7	historic channel	5	upland uses	12
22	B-29	no data	7	historic channel	5	upland uses	12
23	B-3	no data	7	flood prone	4	historic channel	5
24	B-30	active channel	2	historic channel	5	upland uses	12
25	B-31	active channel	2	historic channel	5	upland uses	12
26	B-32	no data	7	flood prone	4	upland uses	12
27	B-33	no data	7	historic channel	5	upland uses	12
28	B-34	no data	7	flood prone	4	upland uses	12
29	B-4	no data	7	flood prone	4	historic channel	5
30	B-5	no data	7	flood prone	4	historic channel	5
31	B-6	no data	7	flood prone	4	historic channel	5
32	B-7	no data	7	flood prone	4	historic channel	5
33	B-8	no data	7	flood prone	4	historic channel	5
34	B-9	no data	7	flood prone	4	historic channel	5
35	8HSA-01	no data	7	flood prone	4	upland uses	12
36	8HSA-02	no data	7	flood prone	4	historic channel	5
37	8HSA-03	no data	7	historic channel	5	historic channel	5
38	8HSA-04	no data	7	historic channel	5	historic channel	5
39	8HSA-05	no data	7	flood prone	4	historic channel	5
40	8HSA-06	no data	7	active channel	2	active channel	2
41	8HSA-07	active channel	2	recent channel change	10	historic channel	5
42	8HSA-08	no data	7	flood prone	4	out of study area	8
43	8HSA-09	active channel	2	recent channel change	10	historic channel	5
44	8HSA-10	vegetated island	13	recent channel change	10	historic channel	5
45	8HSA-11	active channel	2	flood prone	4	upland uses	12
46	8HSA-12	active channel	2	flood prone	4	historic channel	5
47	8HSA-13	no data	7	historic channel	5	historic channel	5
48	8HSA-14	no data	7	historic channel	5	historic channel	5
49	8HSA-15	no data	7	flood prone	4	upland uses	12
50	8HSA-16	no data	7	historic channel	5	historic channel	5
51	8HSA-17	no data	7	historic channel	5	historic channel	5
52	8HSA-18	no data	7	flood prone	4	historic channel	5
53	8HSA-19	active channel	2	historic channel	5	historic channel	5

#	Borehole name	1918		1935		1949	
54	8HSA-20	active channel	2	active channel	2	historic channel	5
55	8HSA-21	vegetated island	13	flood prone	4	historic channel	5
56	8HSA-23	active channel	2	historic channel	5	historic channel	5
57	8HSA-25	no data	7	active channel	2	historic channel	5
58	8HSA-26	no data	7	historic channel	5	upland uses	12
59	8HSA-27	active channel	2	flood prone	4	upland uses	12
60	8HSA-28	active channel	2	historic channel	5	upland uses	12
61	8HSA-29	active channel	2	historic channel	5	historic channel	5
62	8HSA-30	no data	7	flood prone	4	historic channel	5
63	8HSA-31	no data	7	flood prone	4	upland uses	12
64	8HSA-32	no data	7	historic channel	5	historic channel	5
65	8HSA-33	active channel	2	historic channel	5	historic channel	5
66	8HSA-34	active channel	2	historic channel	5	historic channel	5
67	8HSA-35	active channel	2	active channel	2	historic channel	5
68	8HSA-36	active channel	2	active channel	2	historic channel	5
69	8HSA-37	active channel	2	active channel	2	historic channel	5
70	8HSA-38	active channel	2	historic channel	5	historic channel	5
71	8HSA-39	active channel	2	recent channel change	10	historic channel	5
72	8HSA-40	active channel	2	historic channel	5	historic channel	5
73	8HSA-41	active channel	2	active channel	2	historic channel	5
74	8HSA-42	active channel	2	active channel	2	historic channel	5
75	8HSA-43	active channel	2	active channel	2	historic channel	5
76	8HSA-44	active channel	2	active channel	2	historic channel	5
77	8HSA-47	no data	7	historic channel	5	historic channel	5
78	8HSA-48	no data	7	flood prone	4	upland uses	12
79	8HSA-49	no data	7	historic channel	5	historic channel	5
80	8HSA-50	no data	7	historic channel	5	historic channel	5
81	8HSA-51	no data	7	historic channel	5	historic channel	5
82	8HSA-52	no data	7	historic channel	5	historic channel	5
83	8HSA-53	no data	7	historic channel	5	historic channel	5
84	8HSA-54	no data	7	historic channel	5	historic channel	5
85	8HSA-57	no data	7	flood prone	4	historic channel	5
86	8HSA-58	no data	7	flood prone	4	historic channel	5
87	8HSA-67	active channel	2	flood prone	4	historic channel	5
88	8HSA-22	vegetated island	13	historic channel	5	historic channel	5
89	8HSA-66	active channel	2	flood prone	4	historic channel	5
90	8HSA-65	active channel	2	historic channel	5	historic channel	5
91	8HSA-64	no data	7	flood prone	4	upland uses	12
92	8HSA-63	no data	7	flood prone	4	historic channel	5
93	8HSA-61	no data	7	flood prone	4	upland uses	12
94	8HSA-62	no data	7	flood prone	4	upland uses	12
95	8HSA-24	active channel	2	flood prone	4	upland uses	12
96	RGL-8A-1	no data	7	out of study area	8	out of study area	8
97	RGL-8A2s-2	no data	7	flood prone	4	upland uses	12
98	RGL-8A2S-3	no data	7	flood prone	4	upland uses	12
99	RGL-8A2S-4	no data	7	flood prone	4	upland uses	12
100	RGL-8A2S-5	no data	7	flood prone	4	upland uses	12
101	RGL-8A-7	no data	7	historic channel	5	historic channel	5
102	RGL-8A2S-6	no data	7	flood prone	4	upland uses	12
103	RGL-8A2S-8	no data	7	flood prone	4	upland uses	12
104	RGL-8A2S-9	no data	7	flood prone	4	upland uses	12
105	RGL-8A-10	active channel	2	active channel	2	active channel	2
106	RGL-8A2S-11	active channel	2	flood prone	4	upland uses	12
107	RGL-8A2S-12	no data	7	flood prone	4	upland uses	12
108	RGL-8A2S-13	no data	7	flood prone	4	upland uses	12
109	RGL-8A2S-14	no data	7	flood prone	4	upland uses	12
110	RGL-8A2S-15	no data	7	flood prone	4	upland uses	12
111	RGL-8A2S-16	no data	7	flood prone	4	historic channel	5

#	Borehole name	1918		1935		1949	
112	RGL-8A2S-17	no data	7	historic channel	5	historic channel	5
113	RGL-8A2S-18	no data	7	flood prone	4	upland uses	12
114	RGL-8A2S-19	no data	7	flood prone	4	upland uses	12
115	RGL-8A2S-21	active channel	2	flood prone	4	upland uses	12
116	RGL-8A2S-22	no data	7	historic channel	5	historic channel	5
117	RGL-8A2S-23	no data	7	flood prone	4	upland uses	12
118	RGL-8A2S-24	no data	7	flood prone	4	upland uses	12
119	RGL-8A2S-25	no data	7	flood prone	4	upland uses	12
120	RGL-8A2S-26	no data	7	historic channel	5	historic channel	5
121	RGL-8A2S-27	no data	7	historic channel	5	historic channel	5
122	RGL-8A2S-28	no data	7	flood prone	4	out of study area	8
123	RGL-8A2S-29	no data	7	historic channel	5	historic channel	5
124	RGL-8A2S-31	no data	7	flood prone	4	out of study area	8
125	RGL-8A-30	active channel	2	active channel	2	active channel	2
126	RGL-8A2S-32	active channel	2	historic channel	5	historic channel	5
127	RGL-8A2S-33	active channel	2	flood prone	4	historic channel	5
128	RGL-8A2S-34	no data	7	flood prone	4	upland uses	12
129	RGL-8A2S-35	no data	7	flood prone	4	upland uses	12
130	RGL-8A2S-36	no data	7	flood prone	4	upland uses	12
131	RGL-8A-31	no data	7	historic channel	5	historic channel	5
132	RGL-8A2S-38	no data	7	flood prone	4	upland uses	12
133	RGL-8A-42	no data	7	active channel	2	active channel	2
134	RGL-8A2S-41	no data	7	out of study area	8	upland uses	12
135	RGL-8A-40	no data	7	out of study area	8	out of study area	8
136	RGL-8A-44	no data	7	out of study area	8	out of study area	8
137	RGL-8A2S-43	no data	7	out of study area	8	upland uses	12
138	RGL-8A2S-45	active channel	2	out of study area	8	upland uses	12
139	RGL-8A2S-47	vegetated island	13	flood prone	4	upland uses	12
140	RGL-8A-46	vegetated island	13	active channel	2	historic channel	5
141	RGL-8A2S-48	vegetated island	13	flood prone	4	upland uses	12
142	RGL-8A-49	active channel	2	active channel	2	vegetated island	13
143	RGL-8A2S-50	no data	7	flood prone	4	upland uses	12
144	RGL-8A-52	active channel	2	active channel	2	active channel	2
145	RGL-8A2S-54	no data	7	flood prone	4	upland uses	12
146	RGL-8A2S-53	no data	7	flood prone	4	upland uses	12
147	RGL-8A2S-51	no data	7	flood prone	4	upland uses	12
148	RGL-8A2S-56	no data	7	active channel	2	historic channel	5
149	RGL-8A2S-58	no data	7	active channel	2	historic channel	5
150	RGL-8A2S-59	active channel	2	active channel	2	historic channel	5
151	RGL-8A2S-61	no data	7	historic channel	5	historic channel	5
152	RGL-8A2S-60	no data	7	active channel	2	historic channel	5
153	RGL-8A-62	no data	7	historic channel	5	historic channel	5
154	RGL-8A2S-63	no data	7	historic channel	5	historic channel	5
155	RGL-8A2S-64	no data	7	historic channel	5	historic channel	5
156	RGL-8A2S-65	no data	7	active channel	2	active channel	2
157	RGL-8A2S-66	no data	7	active channel	2	historic channel	5
158	RGL-8A-68	no data	7	active channel	2	historic channel	5
159	RGL-8A2S-67	no data	7	flood prone	4	upland uses	12
160	RGL-8A2S-69	no data	7	flood prone	4	upland uses	12
161	RGL-8A2S-70	no data	7	flood prone	4	upland uses	12
162	RGL-8A2S-71	no data	7	flood prone	4	upland uses	12
163	RGL-8A-72	active channel	2	historic channel	5	historic channel	5
164	RGL-8A2S-73	no data	7	flood prone	4	upland uses	12
165	RGL-8A2S-75	no data	7	flood prone	4	historic channel	5
166	RGL-8A-74	no data	7	recent channel change	10	active channel	2
167	RGL-8A2S-76	no data	7	flood prone	4	upland uses	12
168	RGL-8A2S-77	active channel	2	flood prone	4	historic channel	5
169	RGL-8A-78	active channel	2	active channel	2	active channel	2

#	Borehole name	1918		1935		1949	
170	RGL-8A2S-79	no data	7	flood prone	4	upland uses	12
171	RGL-8A2S-81	no data	7	historic channel	5	historic channel	5
172	RGL-8A2S-80	no data	7	flood prone	4	upland uses	12
173	RGL-8A2S-82	no data	7	flood prone	4	upland uses	12
174	RGL-8A2S-83	no data	7	flood prone	4	upland uses	12
175	RGL-8A2S-84	no data	7	flood prone	4	upland uses	12
176	RGL-8A2S-85	no data	7	flood prone	4	upland uses	12
177	RGL-8A2S-86	no data	7	flood prone	4	upland uses	12
178	RGL-8A2S-87	no data	7	historic channel	5	out of study area	8
179	BOREHOLE #9	no data	7	flood prone	4	upland uses	12
180	BOREHOLE #6	no data	7	flood prone	4	upland uses	12
181	BOREHOLE #5	no data	7	flood prone	4	upland uses	12
182	BOREHOLE #4	no data	7	flood prone	4	upland uses	12
183	BOREHOLE #3	no data	7	flood prone	4	upland uses	12
184	BOREHOLE #1	no data	7	flood prone	4	upland uses	12
185	Boring B-3	active channel	2	recent channel change	10	historic channel	5
186	Boring B-2	active channel	2	recent channel change	10	historic channel	5
187	Boring B-1	active channel	2	recent channel change	10	historic channel	5
188	Boring B-4	active channel	2	active channel	2	active channel	2

Data Extraction: This information is pulled from GIS datasets

2019 Issue locations

	Distance to Active Channel					Geotechnical Analyses		Riverside Drain						Landside Toe						Levee Centerline						Riverside Toe						River Centerline					
OID/FID	1918	1935	1949	1918 "vegetated island" planform		2006 seepage rating	2006 slope stability rating	d16		d50		d84		d16		d50		d84		d16		d50		d84		d16		d50		d84		d16		d50		d84	
1	92.86358	70.92042	41.04354	no	2	3	2	Fines	6	VFS	5	CS	2	Fines	6	VFS	5	MS	3	VFS	5	FS	4	MS	3	Fines	6	FS	4	CS	2	FS	4	MS	3	VCS	1
2	96.76152	75.22538	42.06561	no	2	3	2	Fines	6	VFS	5	CS	2	Fines	6	VFS	5	MS	3	VFS	5	FS	4	MS	3	Fines	6	FS	4	CS	2	FS	4	MS	3	VCS	1
4	99.58102	77.91251	45.68734	no	2	3	2	Fines	6	VFS	5	CS	2	Fines	6	VFS	5	MS	3	VFS	5	FS	4	MS	3	Fines	6	FS	4	CS	2	FS	4	MS	3	VCS	1
5	25.3674	20.64512	20.34469	no	2	3	2	Fines	6	VFS	5	CS	2	Fines	6	VFS	5	MS	3	VFS	5	FS	4	MS	3	Fines	6	FS	4	CS	2	FS	4	MS	3	VCS	1
6	126.9131	116.9597	61.00488	no	2	3	2	Fines	6	VFS	5	CS	2	Fines	6	VFS	5	MS	3	VFS	5	FS	4	MS	3	Fines	6	FS	4	CS	2	FS	4	MS	3	VCS	1
8	111.6677	48.95077	193.7544	no	2	3	1	FS	4	FS	4	MS	3	Fines	6	VFS	5	MS	3	Fines	6	VFS	5	MS	3	Fines	6	FS	4	FS	4	FS	4	FS	4	MS	3
14	133.5891	105.495	112.1879	no	2	3	2	FS	4	MS	3	MS	3	Fines	6	FS	4	MS	3	Fines	6	FS	4	MS	3	Fines	6	FS	4	MS	3	Fines	6	FS	4	FS	4
15	136.4831	104.3773	112.7199	no	2	3	2	FS	4	MS	3	MS	3	Fines	6	FS	4	MS	3	Fines	6	FS	4	MS	3	Fines	6	FS	4	MS	3	Fines	6	FS	4	FS	4
16	133.9547	124.0645	67.80263	no	2	3	2	Fines	6	VFS	5	CS	2	Fines	6	VFS	5	MS	3	VFS	5	FS	4	MS	3	Fines	6	FS	4	CS	2	FS	4	MS	3	VCS	1
17	91.35538	69.40761	39.66951	no	2	3	2	Fines	6	VFS	5	CS	2	Fines	6	VFS	5	MS	3	VFS	5	FS	4	MS	3	Fines	6	FS	4	CS	2	FS	4	MS	3	VCS	1
19	0	21.0478	20.98841	no	2	3	2	Fines	6	VFS	5	CS	2	Fines	6	VFS	5	MS	3	VFS	5	FS	4	MS	3	Fines	6	FS	4	CS	2	FS	4	MS	3	VCS	1
20	4.297663	136.1891	225.9217	no	2	1	2	FS	4	MS	3	MS	3	VFS	5	FS	4	MS	3	Fines	6	FS	4	>VCS	0	VFS	5	FS	4	MS	3	VFS	5	FS	4	MS	3
23	131.085	89.23158	108.6078	no	2	3	2	FS	4	MS	3	MS	3	Fines	6	FS	4	MS	3	Fines	6	FS	4	MS	3	Fines	6	FS	4	MS	3	Fines	6	FS	4	FS	4
24	91.65375	52.36993	68.82176	no	2	3	1	VFS	5	FS	4	FS	4	Fines	6	Fines	6	VFS	5	Fines	6	Fines	6	FS	4	Fines	6	Fines	6	VFS	5	Fines	6	Fines	6	VFS	5
31	15.02349	159.495	237.0574	no	2	1	2	FS	4	MS	3	MS	3	VFS	5	FS	4	MS	3	Fines	6	FS	4	>VCS	0	VFS	5	FS	4	MS	3	VFS	5	FS	4	MS	3
33	190.6821	148.8355	141.2277	no	2	1	1	Fines	6	VFS	5	MS	3	Fines	6	VFS	5	MS	3	Fines	6	VFS	5	MS	3	Fines	6	VFS	5	MS	3	Fines	6	Fines	6	FS	4
36	131.8598	96.34771	76.12079	yes	1	1	1	Fines	6	VFS	5	MS	3	Fines	6	VFS	5	FS	4	Fines	6	VFS	5	FS	4	Fines	6	VFS	5	FS	4	Fines	6	VFS	5	MS	3
55	132.3774	95.44099	89.79686	no	2	1	1	Fines	6	VFS	5	MS	3	Fines	6	VFS	5	FS	4	Fines	6	VFS	5	FS	4	Fines	6	VFS	5	FS	4	Fines	6	VFS	5	MS	3
60	82.25007	63.14397	103.0593	no	2	1	2	VFS	5	FS	4	MS	3	Fines	6	VFS	5	MS	3	Fines	6	FS	4	MS	3	Fines	6	FS	4	MS	3	Fines	6	FS	4	MS	3
63	0	39.51307	75.12039	no	2	1	2	FS	4	MS	3	>VCS	0	Fines	6	VFS	5	FS	4	Fines	6	VFS	5	MS	3	Fines	6	FS	4	MS	3	Fines	6	VFS	5	FS	4
64	0	86.9074	197.3761	no	2	1	2	FS	4	MS	3	MS	3	VFS	5	FS	4	MS	3	Fines	6	FS	4	>VCS	0	VFS	5	FS	4	MS	3	VFS	5	FS	4	MS	3
66	88.38952	57.1704	65.08376	no	2	3	2	FS	4	MS	3	MS	3	Fines	6	FS	4	MS	3	Fines	6	FS	4	MS	3	Fines	6	FS	4	MS	3	Fines	6	FS	4	FS	4
67	136.6278	102.3335	112.2309	no	2	3	2	FS	4	MS	3	MS	3	Fines	6	FS	4	MS	3	Fines	6	FS	4	MS	3	Fines	6	FS	4	MS	3	Fines	6	FS	4	FS	4
68	140.8321	107.2855	116.4204	no	2	3	2	FS	4	MS	3	MS	3	Fines	6	FS	4	MS	3	Fines	6	FS	4	MS	3	Fines	6	FS	4	MS	3	Fines	6	FS	4	FS	4
69	137.439	116.2477	79.32713	no	2	3	2	FS	4	MS	3	MS	3	Fines	6	FS	4	MS	3	Fines	6	FS	4	MS	3	Fines	6	FS	4	MS	3	Fines	6	FS	4	FS	4
70	131.3249	121.4811	65.06998	no	2	3	2	Fines	6	VFS	5	CS	2	Fines	6	VFS	5	MS	3	VFS	5	FS	4	MS	3	Fines	6	FS	4	CS	2	FS	4	MS	3	VCS	1
71	92.56288	70.39622	42.0624	no	2	3	2	Fines	6	VFS	5	CS	2	Fines	6	VFS	5	MS	3	VFS	5	FS	4	MS	3	Fines	6	FS	4	CS	2	FS	4	MS	3	VCS	1
72	89.10655	67.48737	35.57677	no	2	3	2	Fines	6	VFS	5	CS	2	Fines	6	VFS	5	MS	3	VFS	5	FS	4	MS	3	Fines	6	FS	4	CS	2	FS	4	MS	3	VCS	1
73	101.3975	79.78659	41.55442	no	2	3	2	Fines	6	VFS	5	CS	2	Fines	6	VFS	5	MS	3	VFS	5	FS	4	MS	3	Fines	6	FS	4	CS	2	FS	4	MS	3	VCS	1
89	30.14114	88.96152	86.23417	no	2	2	2	FS	4	FS	4	MS	3	Fines	6	FS	4	CS	2	VFS	5	FS	4	MS	3	VFS	5	FS	4	MS	3	Fines	6	MS	3	>VCS	0
90	0	63.40733	52.46574	no	2	2	2	FS	4	FS	4	MS	3	Fines	6	FS	4	CS	2	VFS	5	FS	4	MS	3	VFS	5	FS	4	MS	3	Fines	6	MS	3	>VCS	0
91	205.2434	199.7218	196.1192	no	2	2	2	VFS	5	FS	4	MS	3	FS	4	CS	2	>VCS	0	Fines	6	FS	4	MS	3	VFS	5	MS	3	>VCS	0	VFS	5	FS	4	MS	3
98	106.7682	57.97823	63.15588	no	2	3	1	Fines	6	Fines	6	MS	3	Fines	6	FS	4	MS	3	Fines	6	FS	4	MS	3	Fines	6	FS	4	MS	3	Fines	6	Fines	6	MS	3
103	210.9887	147.5617	148.9704	no	2	2	2	VFS	5	FS	4	MS	3	FS	4	CS	2	>VCS	0	Fines	6	FS	4	MS	3	VFS	5	MS	3	>VCS	0	VFS	5	FS	4	MS	3
107	55.07682	67.44866	91.27672	no	2	3	2	FS	4	CS	2	>VCS	0	FS	4	FS	4	CS	2	Fines	6	VFS	5	FS	4	FS	4	MS	3	CS	2	FS	4	FS	4	CS	2
108	0	46.32144	54.25428	no	2	3	2	FS	4	CS	2	>VCS	0	FS	4	FS	4	CS	2	Fines	6	VFS	5	FS	4	FS	4	MS	3	CS	2	FS	4	FS	4	CS	2
110	101.5657	80.29585	44.48647	no	2	3	2	Fines	6	VFS	5	CS	2	Fines	6	VFS	5	MS	3	VFS	5	FS	4	MS	3	Fines	6	FS	4	CS	2	FS	4	MS	3	VCS	1
121	0	47.03994	82.5883	no	2	1	2	FS	4	MS	3	>VCS	0	Fines	6	VFS	5	FS	4	Fines	6	VFS	5	MS	3	Fines	6	FS	4	MS	3	Fines	6	VFS	5	FS	4
123	4.237537	135.6432	226.5511	no	2	1	2	FS	4	MS	3	MS	3	VFS	5	FS	4	MS	3	Fines	6	FS	4	>VCS	0	VFS	5	FS	4	MS	3	VFS	5	FS	4	MS	3
125	46.35685	56.22559	52.80423	no	2	2	2	VFS	5	MS	3	>VCS	0	Fines	6	FS	4	MS	3	Fines	6	MS	3	>VCS	0	Fines	6	FS	4	>VCS	0	VFS	5	FS	4	CS	2
126	42.25523	56.47117	78.64927	no	2	3	2	FS	4	CS	2	>VCS	0	FS	4	FS	4	CS	2	Fines	6	VFS	5	FS	4	FS	4	MS	3	CS	2	FS	4	FS	4	CS	2
127	0	49.507	57.45503	no	2	3	2	FS	4	CS	2	>VCS	0	FS	4	FS	4	CS	2	Fines	6	VFS	5	FS	4	FS	4	MS	3	CS	2	FS	4	FS	4	CS	2
128	0	28.32075	28.01722	no	2	3	2	Fines	6	VFS	5	CS	2	Fines	6	VFS	5	MS	3	VFS	5	FS	4	MS	3	Fines	6	FS	4	CS	2	FS	4	MS	3	VCS	1
131	131.7094	99.61141	107.9428	no	2	3	2	FS	4	MS	3	MS	3	Fines	6	FS	4	MS	3	Fines	6	FS	4	MS	3	Fines	6	FS	4	MS	3	Fines	6	FS	4	FS	4
132	134.6263	107.2673	113.5557	no	2	3	2	FS	4	MS	3	MS	3	Fines	6	FS	4	MS	3	Fines	6	FS	4	MS	3	Fines	6	FS	4	MS	3	Fines	6	FS	4	FS	4
134	58.62344	35.73357	34.82389	no	2	3	1	Fines	6	Fines	6	VFS	5	Fines	6	VFS	5	FS	4	Fines	6	VFS	5	MS	3	Fines	6	VFS	5	FS	4	Fines	6	Fines	6	VFS	5
139	176.7338	193.0576	179.1106	no	2	2	2	FS	4	MS	3	>VCS	0	Fines	6	VFS	5	MS	3	Fines	6	Fines	6	VFS	5	Fines	6	Fines	6	FS	4	Fines	6	VFS	5	FS	4
152	31.02398	90.58519	87.63854	no	2	2	2	FS	4	FS	4	MS	3	Fines	6	FS	4	CS	2	VFS	5	FS	4	MS	3	VFS	5	FS	4	MS	3	Fines	6	MS	3	>VCS	0
159	54.34931	94.97946	15.08445	no	2	3	1	MS	3	VCS	1	>VCS	0	VFS	5	VFS	5	MS	3	Fines	6	VFS	5	MS	3	Fines	6	VFS	5	MS	3	VFS	5	VFS	5	MS	3
163	109.4209	66.77232	62.19709	no	2	3	2	FS	4	FS	4	MS	3	Fines	6	VFS	5	FS	4	Fines	6	CS	2	>VCS	0	VFS	5	FS	4	CS	2	FS	4	MS	3	VCS	1
164	0	10.58424	73.38544	no	2	3	2	FS	4	FS	4	MS	3	Fines	6	VFS	5	FS	4	Fines	6	CS	2	>VCS	0	VFS	5	FS	4	CS	2	FS	4	MS	3	VCS	1
166	32.79024	47.37329	78.74729	no	2	3	2	FS	4	CS	2	>VCS	0	FS	4	FS	4	CS	2	Fines	6	VFS	5	FS	4	FS	4	MS	3	CS	2	FS	4	FS	4	CS	2
176	29.15141	76.83356	74.48451	no	2	2	2	FS	4	FS	4	MS	3	Fines	6	FS	4	CS	2	VFS	5	FS	4	MS	3	VFS	5	FS	4	MS	3	Fines	6	MS	3	>VCS	0
179	47.06852	86.2148	102.913	no	2	3	1	FS	4	CS	2	>VCS	0	VFS	5	FS	4	MS	3	Fines	6	Fines	6	VFS	5	VFS	5	FS	4	MS	3	Fines	6	Fines	6	VFS	5
180	50.37645	70.6349	105.2229	no	2	3	1	FS	4	CS	2	>VCS	0	VFS	5	FS	4	MS	3	Fines	6	Fines	6	VFS	5	VFS	5	FS	4	MS	3	Fines	6	Fines	6	VFS	5
183	0	22.81179	30.67771	no	2	1	2	FS	4	MS	3	MS	3	VFS	5	FS	4	MS	3	Fines	6	FS	4	>VCS	0	VFS	5	FS	4	MS	3	VFS	5	FS	4	MS	3
185	111.259	46.29111	53.41985	no	2	1	2	VFS	5	FS	4	MS	3	Fines	6	VFS	5	MS	3	Fines	6	FS	4	MS	3	Fines	6	FS	4	MS	3	Fines	6	FS	4	MS	3
186	36.2883	37.73009	45.44497	no	2	1	2	FS	4	MS	3	CS	2	Fines	6	Fines	6	MS	3	Fines	6	FS	4	MS	3	Fines	6	FS	4	MS	3	Fines	6	FS	4	MS	3

Wentworth classifications for the 2019 issue locations

OID/FID	Distance to Active Channel			1918 "vegetated island" planform		Geotechnical Analyses		Riverside Drain				Landside Toe				Levee Centerline				Riverside Toe				River Centerline			
	1918	1935	1949			2006 seepage rating	2006 slope stability rating	d16		d50		d84		d16		d50		d84		d16		d50		d84		d16		d50		d84	
189	0	31.67623	28.76228	no	2	3	2	Fines	6	VFS	5	CS	2	Fines	6	VFS	5	MS	3	VFS	5	FS	4	MS	3	Fines	6	FS	4	CS	2	FS	4	MS	3	VCS	1
190	0	17.9185	19.56967	no	2	3	2	Fines	6	VFS	5	CS	2	Fines	6	VFS	5	MS	3	VFS	5	FS	4	MS	3	Fines	6	FS	4	CS	2	FS	4	MS	3	VCS	1
191	0	26.19258	22.9255	no	2	3	2	Fines	6	VFS	5	CS	2	Fines	6	VFS	5	MS	3	VFS	5	FS	4	MS	3	Fines	6	FS	4	CS	2	FS	4	MS	3	VCS	1
194	128.9783	85.29664	78.69995	no	2	1	1	Fines	6	VFS	5	MS	3	Fines	6	VFS	5	FS	4	Fines	6	VFS	5	FS	4	Fines	6	VFS	5	FS	4	Fines	6	VFS	5	MS	3
195	132.015	63.18194	66.68917	no	2	1	1	VFS	5	FS	4	MS	3	VFS	5	FS	4	CS	2	VFS	5	FS	4	CS	2	VFS	5	FS	4	CS	2	VFS	5	FS	4	MS	3
196	133.5257	111.4511	83.94992	no	2	3	2	FS	4	MS	3	MS	3	Fines	6	FS	4	MS	3	Fines	6	FS	4	MS	3	Fines	6	FS	4	MS	3	Fines	6	FS	4	FS	4
197	0	48.95908	51.11907	no	2	1	1	Fines	6	VFS	5	MS	3	Fines	6	VFS	5	FS	4	Fines	6	VFS	5	FS	4	Fines	6	VFS	5	FS	4	Fines	6	VFS	5	MS	3
198	150.4713	110.2791	92.29842	yes	1	1	1	Fines	6	FS	4	MS	3	Fines	6	FS	4	MS	3	VFS	5	FS	4	CS	2	VFS	5	FS	4	CS	2	Fines	6	FS	4	MS	3
199	149.6537	130.8858	131.7661	yes	1	1	1	Fines	6	FS	4	MS	3	Fines	6	FS	4	MS	3	VFS	5	FS	4	CS	2	VFS	5	FS	4	CS	2	Fines	6	FS	4	MS	3
200	145.4485	109.9892	121.0972	yes	1	1	1	Fines	6	FS	4	MS	3	Fines	6	FS	4	MS	3	VFS	5	FS	4	CS	2	VFS	5	FS	4	CS	2	Fines	6	FS	4	MS	3
201	130.9118	76.47405	78.97541	yes	1	1	1	Fines	6	FS	4	MS	3	Fines	6	FS	4	MS	3	VFS	5	FS	4	CS	2	VFS	5	FS	4	CS	2	Fines	6	FS	4	MS	3
202	136.8508	90.53168	88.89947	yes	1	1	1	Fines	6	FS	4	MS	3	Fines	6	FS	4	MS	3	VFS	5	FS	4	CS	2	VFS	5	FS	4	CS	2	Fines	6	FS	4	MS	3
203	126.6485	80.15938	77.98838	yes	1	1	1	Fines	6	FS	4	MS	3	Fines	6	FS	4	MS	3	VFS	5	FS	4	CS	2	VFS	5	FS	4	CS	2	Fines	6	FS	4	MS	3
204	95.33902	54.49161	57.14103	yes	1	1	1	Fines	6	Fines	6	FS	4	Fines	6	VFS	5	MS	3	Fines	6	VFS	5	MS	3	Fines	6	VFS	5	MS	3	Fines	6	VFS	5	MS	3
205	149.7508	42.40001	50.85268	no	2	1	1	Fines	6	Fines	6	Fines	6	Fines	6	VFS	5	MS	3	VFS	5	MS	3	VCS	1	VFS	5	MS	3	VCS	1	Fines	6	VFS	5	MS	3
206	149.4048	52.26479	55.15711	no	2	1	1	Fines	6	Fines	6	Fines	6	Fines	6	VFS	5	MS	3	VFS	5	MS	3	VCS	1	VFS	5	MS	3	VCS	1	Fines	6	VFS	5	MS	3
207	65.90452	149.5689	111.6563	no	2	1	1	Fines	6	FS	4	MS	3	Fines	6	VFS	5	FS	4	Fines	6	VFS	5	FS	4	Fines	6	VFS	5	FS	4	Fines	6	VFS	5	FS	4
208	137.1382	116.072	68.46357	no	2	3	2	Fines	6	VFS	5	CS	2	Fines	6	VFS	5	MS	3	VFS	5	FS	4	MS	3	Fines	6	FS	4	CS	2	FS	4	MS	3	VCS	1
209	65.25767	199.2624	164.6422	no	2	1	1	Fines	6	FS	4	MS	3	Fines	6	VFS	5	FS	4	Fines	6	VFS	5	FS	4	Fines	6	VFS	5	FS	4	Fines	6	VFS	5	FS	4
210	143.948	46.10859	49.06387	no	2	1	1	Fines	6	Fines	6	Fines	6	Fines	6	VFS	5	MS	3	VFS	5	MS	3	VCS	1	VFS	5	MS	3	VCS	1	Fines	6	VFS	5	MS	3
211	182.8695	69.3834	70.00756	no	2	1	1	VFS	5	FS	4	CS	2	VFS	5	FS	4	VCS	1	VFS	5	FS	4	VCS	1	VFS	5	FS	4	VCS	1	VFS	5	FS	4	CS	2
213	146.0029	117.934	123.9398	yes	1	1	1	Fines	6	FS	4	MS	3	Fines	6	FS	4	MS	3	VFS	5	FS	4	CS	2	VFS	5	FS	4	CS	2	Fines	6	FS	4	MS	3
214	0	50.89955	56.25387	no	2	1	1	Fines	6	VFS	5	MS	3	Fines	6	VFS	5	FS	4	Fines	6	VFS	5	FS	4	Fines	6	VFS	5	FS	4	Fines	6	VFS	5	MS	3
216	2.404813	34.8858	36.24105	no	2	1	2	FS	4	MS	3	MS	3	VFS	5	FS	4	MS	3	Fines	6	FS	4	>VCS	0	VFS	5	FS	4	MS	3	VFS	5	FS	4	MS	3
217	0	23.69503	29.16043	no	2	1	2	FS	4	MS	3	MS	3	VFS	5	FS	4	MS	3	Fines	6	FS	4	>VCS	0	VFS	5	FS	4	MS	3	VFS	5	FS	4	MS	3
221	38.43334	70.94559	92.92929	no	2	3	1	FS	4	CS	2	>VCS	0	VFS	5	FS	4	MS	3	Fines	6	Fines	6	VFS	5	VFS	5	FS	4	MS	3	Fines	6	Fines	6	VFS	5

Data Extraction: This information is pulled from GIS datasets

Borehole locations

#	Borehole name	Correlated to issue location	Distance to Active Channel			1918 "vegetated island" planform	
			1918	1935	1949		
1	B-1	Yes	283.4509	61.58239	512.4243	no	2
2	B-10	No	237.3967	270.6605	27.73642	no	2
3	B-11	No	255.3859	234.0865	28.02694	no	2
4	B-12	No	202.3594	192.4487	19.77015	no	2
5	B-13	No	116.1175	121.2261	30.73045	no	2
6	B-14	Yes	142.0855	67.04214	64.08295	no	2
7	B-15	No	79.01801	142.4362	104.7876	no	2
8	B-16	No	220.5633	177.4814	155.3566	no	2
9	B-17	No	384.1337	250.453	250.1396	no	2
10	B-18	No	410.0022	309.3138	309.6907	no	2
11	B-19	No	384.9598	303.5336	172.6353	no	2
12	B-2	No	428.3568	205.1393	685.0279	no	2
13	B-20	No	339.2316	204.0775	130.3579	no	2
14	B-21	No	279.7258	29.33443	51.61552	no	2
15	B-22	Yes	324.7467	185.9749	241.5216	no	2
16	B-23	No	315.6619	425.464	362.0564	no	2
17	B-24	No	263.4086	233.9995	307.1816	no	2
18	B-25	No	238.2155	73.41982	414.3241	no	2
19	B-26	No	200.4589	116.6852	672.1403	no	2
20	B-27	No	83.97494	116.2474	792.7085	no	2
21	B-28	No	130.8415	209.1407	939.5504	no	2
22	B-29	No	249.7362	216.3986	989.6885	no	2
23	B-3	No	613.5459	315.2212	680.375	no	2
24	B-30	No	0	67.80172	772.7203	no	2
25	B-31	No	0	144.8457	492.6525	no	2
26	B-32	No	254.225	156.9218	334.2392	no	2
27	B-33	Yes	391.5668	247.2686	324.1826	no	2
28	B-34	No	405.37	290.94	324.29	no	2
29	B-4	No	732.2308	354.5426	682.8346	no	2
30	B-5	No	665.7383	347.7402	528.363	no	2
31	B-6	No	514.3137	264.4302	251.1364	no	2
32	B-7	No	489.9477	112.6304	108.5627	no	2
33	B-8	No	393.2074	62.02065	76.11948	no	2
34	B-9	No	247.4783	144.0818	110.9633	no	2
35	8HSA-01	Yes	107.5833	66.78744	72.87354	no	2
36	8HSA-02	Yes	56.91945	7.157497	14.2939	no	2
37	8HSA-03	Yes	356.0039	369.0486	352.2722	no	2
38	8HSA-04	No	248.9161	189.9637	164.2051	no	2
39	8HSA-05	Yes	314.8966	255.235	224.6139	no	2
40	8HSA-06	No	89.63335	0	0	no	2
41	8HSA-07	No	0	70.26949	252.0778	no	2
43	8HSA-09	No	0	14.95197	352.2763	no	2
44	8HSA-10	No	47.72318	839.9602	708.8517	yes	1
45	8HSA-11	No	0	896.0346	785.9662	no	2
46	8HSA-12	No	0	17.26323	601.7021	no	2
47	8HSA-13	No	472.7194	341.0514	430.8922	no	2
48	8HSA-14	Yes	504.7939	374.423	467.5415	no	2
49	8HSA-15	No	551.232	421.7964	522.6935	no	2
50	8HSA-16	No	446.3824	107.4763	498.8541	no	2
51	8HSA-17	Yes	22.25356	169.1737	160.4105	no	2
52	8HSA-18	Yes	71.70388	215.2818	203.3387	no	2
53	8HSA-19	No	0	24.87171	80.73315	no	2
54	8HSA-20	No	0	0	39.57787	no	2
55	8HSA-21	Yes	310.0366	384.4351	285.5232	yes	1

#	Borehole name	Correlated to issue location	Distance to Active Channel 1918	1935	1949	1918 "vegetated island" planform	
56	8HSA-23	Yes	0	17.06356	135.464	no	2
57	8HSA-25	No	116.6425	0	213.7204	no	2
58	8HSA-26	No	166.0792	45.8906	254.9383	no	2
59	8HSA-27	No	0	141.0307	371.8584	no	2
60	8HSA-28	Yes	0	92.37124	315.9993	no	2
61	8HSA-29	No	0	57.42166	278.6759	no	2
62	8HSA-30	Yes	240.5645	109.9302	122.2858	no	2
63	8HSA-31	No	280.4485	150.8184	163.5259	no	2
64	8HSA-32	No	28.98351	77.3317	678.2846	no	2
65	8HSA-33	No	0	1120.064	29.82831	no	2
66	8HSA-34	No	0	1148.362	70.56354	no	2
67	8HSA-35	No	0	0	605.2605	no	2
68	8HSA-36	No	0	0	562.9691	no	2
69	8HSA-37	No	0	0	648.6662	no	2
70	8HSA-38	No	0	132.5819	457.6856	no	2
71	8HSA-39	No	0	63.11368	389.3392	no	2
72	8HSA-40	No	0	167.3343	490.7937	no	2
73	8HSA-41	No	0	0	332.1275	no	2
74	8HSA-42	No	0	0	289.1903	no	2
75	8HSA-43	No	0	0	371.6493	no	2
76	8HSA-44	No	0	0	999.7383	no	2
77	8HSA-47	No	99.9092	87.92692	229.8832	no	2
78	8HSA-48	No	140.6521	129.7886	271.3459	no	2
79	8HSA-49	No	7.570516	35.82138	273.0344	no	2
80	8HSA-50	No	52.24591	80.50682	317.1976	no	2
81	8HSA-51	No	87.63011	154.2109	95.75299	no	2
82	8HSA-52	No	125.2229	195.8735	137.3424	no	2
83	8HSA-53	No	146.0646	109.8554	154.7095	no	2
84	8HSA-54	Yes	148.5963	108.7809	141.7778	no	2
85	8HSA-57	Yes	432.1377	540.2727	649.2331	no	2
86	8HSA-58	No	809.4471	799.0533	769.8661	no	2
87	8HSA-67	No	0	145.034	150.9215	no	2
88	8HSA-22	No	414.9163	278.5056	179.4539	yes	1
89	8HSA-66	No	0	195.292	201.1688	no	2
90	8HSA-65	No	0	333.5359	133.7847	no	2
91	8HSA-64	No	293.6105	315.7597	261.3528	no	2
92	8HSA-63	No	214.453	237.1254	184.4723	no	2
93	8HSA-61	No	335.6388	389.177	495.8062	no	2
94	8HSA-62	No	338.4727	471.6687	576.3931	no	2
95	8HSA-24	No	0	61.63232	174.516	no	2
96	RGL-8A-1	No	98.68179	124.7731	122.5847	no	2
97	RGL-8A2s-2	No	428.616	485.8422	494.1942	no	2
98	RGL-8A2S-3	No	413.0188	254.1094	273.9356	no	2
99	RGL-8A2S-4	No	171.6984	90.66299	175.8096	no	2
100	RGL-8A2S-5	No	483.8913	471.2765	463.1289	no	2
101	RGL-8A-7	No	201.0809	187.4989	189.785	no	2
102	RGL-8A2S-6	No	535.102	211.3391	239.8056	no	2
103	RGL-8A2S-8	No	612.8905	364.3931	354.8227	no	2
104	RGL-8A2S-9	No	175.9561	231.9854	262.552	no	2
105	RGL-8A-10	No	0	0	0	no	2
106	RGL-8A2S-11	No	0	162.9949	310.7231	no	2
107	RGL-8A2S-12	No	343.854	397.8654	432.0193	no	2
108	RGL-8A2S-13	No	494.2838	555.1461	570.5227	no	2
109	RGL-8A2S-14	No	529.6797	413.858	428.8267	no	2
110	RGL-8A2S-15	No	597.2092	415.3721	500.9189	no	2
111	RGL-8A2S-16	No	443.2101	70.78655	285.2555	no	2
112	RGL-8A2S-17	No	712.2229	53.96264	78.65603	no	2

#	Borehole name	Correlated to issue location	Distance to Active Channel 1918	1935	1949	1918 "vegetated island" planform	
113	RGL-8A2S-18	No	601.2567	215.8712	246.6224	no	2
114	RGL-8A2S-19	No	97.57191	137.995	165.875	no	2
115	RGL-8A2S-21	No	0	75.6913	263.0273	no	2
116	RGL-8A2S-22	No	373.6609	255.6855	436.2396	no	2
117	RGL-8A2S-23	No	545.4675	646.2983	678.4807	no	2
118	RGL-8A2S-24	No	279.1891	162.6373	320.7371	no	2
119	RGL-8A2S-25	No	605.1366	144.6854	1288.997	no	2
120	RGL-8A2S-26	No	256.8346	79.14571	1089.468	no	2
121	RGL-8A2S-27	No	89.00233	119.543	853.5708	no	2
122	RGL-8A2S-28	No	247.6753	431.8979	1033.567	no	2
123	RGL-8A2S-29	No	99.04385	511.6813	745.9607	no	2
124	RGL-8A2S-31	No	306.5734	753.0828	731.6451	no	2
125	RGL-8A-30	No	0	0	0	no	2
126	RGL-8A2S-32	No	0	319.9332	444.3317	no	2
127	RGL-8A2S-33	No	0	132.0075	733.8504	no	2
128	RGL-8A2S-34	No	169.0644	65.90614	670.9772	no	2
129	RGL-8A2S-35	No	291.3088	85.45776	409.9361	no	2
130	RGL-8A2S-36	Yes	469.1939	350.2501	239.1454	no	2
131	RGL-8A-31	No	271.7176	91.5887	104.7033	no	2
132	RGL-8A2S-38	No	322.6025	165.7072	211.7168	no	2
133	RGL-8A-42	No	52.25949	0	0	no	2
134	RGL-8A2S-41	Yes	401.1715	86.37305	97.86131	no	2
135	RGL-8A-40	No	508.1615	209.3395	256.4163	no	2
136	RGL-8A-44	No	876.9314	560.1816	552.1473	no	2
137	RGL-8A2S-43	No	434.0348	259.2277	188.937	no	2
138	RGL-8A2S-45	Yes	0	125.2455	140.0592	no	2
139	RGL-8A2S-47	Yes	357.9701	174.9464	237.1175	yes	1
140	RGL-8A-46	No	95.72183	0	15.10151	yes	1
141	RGL-8A2S-48	Yes	97.33092	167.3283	159.3862	yes	1
142	RGL-8A-49	No	0	0	74.86587	no	2
143	RGL-8A2S-50	Yes	194.2349	122.9101	192.6824	no	2
144	RGL-8A-52	No	0	0	0	no	2
145	RGL-8A2S-54	No	199.071	187.5528	567.7721	no	2
146	RGL-8A2S-53	Yes	174.5743	565.3044	399.6883	no	2
147	RGL-8A2S-51	Yes	229.4337	155.4784	132.6266	no	2
148	RGL-8A2S-56	No	85.6379	0	802.9471	no	2
149	RGL-8A2S-58	No	77.4937	0	947.2175	no	2
150	RGL-8A2S-59	No	0	0	903.6551	no	2
151	RGL-8A2S-61	No	498.0959	206.5786	593.3507	no	2
152	RGL-8A2S-60	No	152.6799	0	583.7194	no	2
153	RGL-8A-62	No	388.7414	71.89442	336.9146	no	2
154	RGL-8A2S-63	No	995.3899	1028.323	1185.112	no	2
155	RGL-8A2S-64	No	211.0104	227.222	855.8142	no	2
156	RGL-8A2S-65	No	164.0141	0	0	no	2
157	RGL-8A2S-66	No	139.1401	0	144.0299	no	2
158	RGL-8A-68	No	214.5879	0	524.3098	no	2
159	RGL-8A2S-67	No	249.9305	101.2597	501.7183	no	2
160	RGL-8A2S-69	Yes	122.6667	316.9097	43.57187	no	2
161	RGL-8A2S-70	No	34.36272	383.3114	581.1709	no	2
162	RGL-8A2S-71	No	203.3832	440.5315	926.5553	no	2
163	RGL-8A-72	No	0	80.5512	567.2405	no	2
164	RGL-8A2S-73	Yes	188.2136	95.19547	315.4089	no	2
165	RGL-8A2S-75	No	325.8207	182.8044	23.12954	no	2
166	RGL-8A-74	No	301.1648	51.38349	0	no	2
167	RGL-8A2S-76	No	88.00601	199.6234	67.78769	no	2
168	RGL-8A2S-77	No	0	73.42728	64.07595	no	2
169	RGL-8A-78	No	0	0	0	no	2

#	Borehole name	Correlated to issue location	Distance to Active Channel			1918 "vegetated island" planform	
			1918	1935	1949		
170	RGL-8A2S-79	No	435.176	440.7435	393.5465	no	2
171	RGL-8A2S-81	No	417.5326	425.8831	822.5557	no	2
172	RGL-8A2S-80	No	692.8356	674.8135	706.7094	no	2
173	RGL-8A2S-82	No	266.4409	221.7269	546.9599	no	2
174	RGL-8A2S-83	No	208.2232	84.07091	134.2963	no	2
175	RGL-8A2S-84	No	47.18918	93.95253	68.89481	no	2
176	RGL-8A2S-85	Yes	308.5179	180.1716	195.2304	no	2
177	RGL-8A2S-86	No	222.2903	78.47504	89.42956	no	2
178	RGL-8A2S-87	No	246.6759	332.1266	318.4416	no	2
179	BOREHOLE #9	No	490.5902	509.7311	721.402	no	2
180	BOREHOLE #6	No	118.1905	13.66811	252.7111	no	2
181	BOREHOLE #5	No	268.3917	115.1477	119.9268	no	2
182	BOREHOLE #4	No	45.90418	93.13154	67.48353	no	2
183	BOREHOLE #3	No	177.1397	204.5923	175.6494	no	2
184	BOREHOLE #1	No	168.6793	134.1403	151.6978	no	2
185	Boring B-3	No	0	285.4037	209.8748	no	2
186	Boring B-2	No	0	196.0307	119.4857	no	2
187	Boring B-1	No	0	118.9972	121.1763	no	2
188	Boring B-4	No	0	0	0	no	2

Attachment 3: Statistical Analyses Details

The previous collated and developed datasets provide additional information at the 84 issue locations identified from the 2019 spring snow-melt runoff. These 84 issue locations and their associated attributes represent the sample fields from which relations are assessed to determine if there is a correlation that can potentially explain the observed problem sites. Four statistical methods are utilized to evaluate the correlation in order to assess the level of uncertainty. These include frequency distributions, summary statistics, independence checks, and regression relationships. The underlying assumption with the statistical analysis is that the 2019 issue locations and their associated attributes identified are representative of the overall population within the analysis area, that they are independent and discrete datasets, and they share similar distribution characteristics. Additional details on each of the assessed statistical methods are provided in the sections that follow.

Frequency Distributions

Frequency distributions are often used to gain an idea of the statistical distribution for a particular relationship (Weaver 2000). This was assessed for the following sample sets:

- Planform type (1918, 1935, and 1949) at the filtered 2019 issue locations
- Planform type (1918, 1935, and 1949) at the borehole locations
- Distance to active channel (1918, 1935, and 1949) for the filtered 2019 issue locations
- Distance to active channel (1918, 1935, and 1949) for the borehole locations
- Distance to active channel (1918, 1935, and 1949) for the borehole locations correlated with the filtered 2019 issue locations

The sample sets are separated into class sizes (bins) and the number of each sample that fits within that particular bin are summed together. The number in each bin divided by the overall sample number represents the relative frequency distribution. When displayed graphically at the correct bin size, this gives insight into the probability density function (pdf). Incrementally summing the values in each bin from lowest to highest provide a cumulative frequency that when viewed graphically gives insight into the cumulative distribution function (cdf). The pdf's and cdf's can provide an indication on whether a particular correlation is normally distributed, skewed either towards high or low numbers (log-normal or gamma distribution), or has a more uniform distribution.

A combination of Microsoft Excel tools (Office 365) and coding in R (R Studio, version 1.4.1103) were utilized to produce the plots to assess the potential distribution of the sample sets. A code was written in R (version 3.4.3) by B. Summers (USACE – SPA) to provide visualization of the datasets and assess the fit for the normal, lognormal, and gamma distributions. The code builds upon work of others (Delignette-Muller and Dutang 2015; Erhardt et al. 2015) and has

been tweaked to evaluate the measured distance from the boreholes or the 2019 points of interest to the active channels digitized in 1918, 1935, and 1949. The R code reads comma delimited files of the parameters, identified by a header row. The code provides a visualization of the sample shape through use of histograms, violin plots, boxplots, comparison to theoretical distributions, and computation of sample set fit to theoretical distributions.

The following sections provide additional details related to the developed of the frequency distribution evaluations.

Planform type plots

The relationship between the 1918, 1935, and 1949 historical planforms and the 2019 issue locations is important to assess if there is a definable distribution pattern. The relationship between the historical planforms and the boreholes is also of interest, primarily to assess whether this has a different or similar distribution as the relationship between the 2019 issue locations. The historical planforms were digitized with consistent nomenclature regarding the planform type. This provides the ability to compare between years and compare between locations (issue locations, boreholes, and boreholes correlated with the issue locations). In order to take advantage of graphical evaluation techniques, the unique planform types were assigned a numerical value. The following textural to numerical relationships were utilized for this analysis:

- Active channel – 2
- Vegetated island – 13
- Arroyo – 3
- Flood prone – 4
- Historic channel – 5
- Island-attached to bank – 1
- Levee – 6
- Out of study area – 8
- Recent channel change – 10
- Tributary – 11
- Upland uses – 12
- Ponded water – 9
- No data – 7

The bin classification is by units of 1 since each integer from 1 through 13 represents a unique planform type. Both the Data>>Data Analysis>>Descriptive Statistics and the Data>>Data Analysis>> Histogram feature within Microsoft Excel (Office 365) were utilized for this analysis. The cumulative percentage is clicked to be on for these analyses. The results from the histogram analysis are then plotted using tools in Excel. The graphical results from these evaluations are shown below. The specific computations are provided in the Planform type computations section.

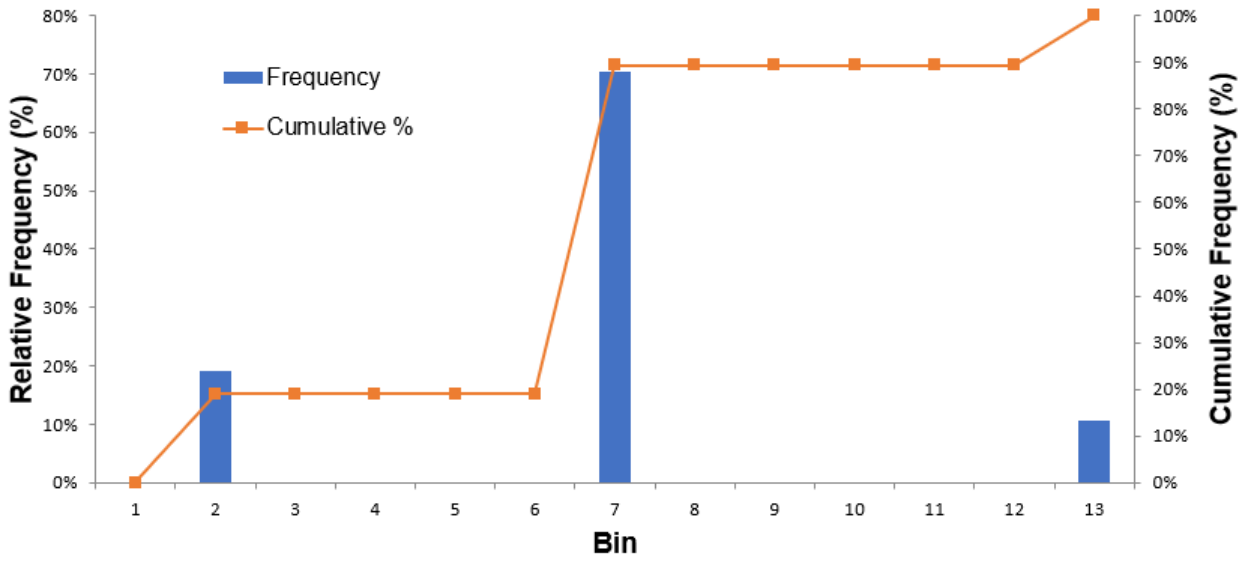

Figure 22. 1918 planform type at the 2019 issue locations.

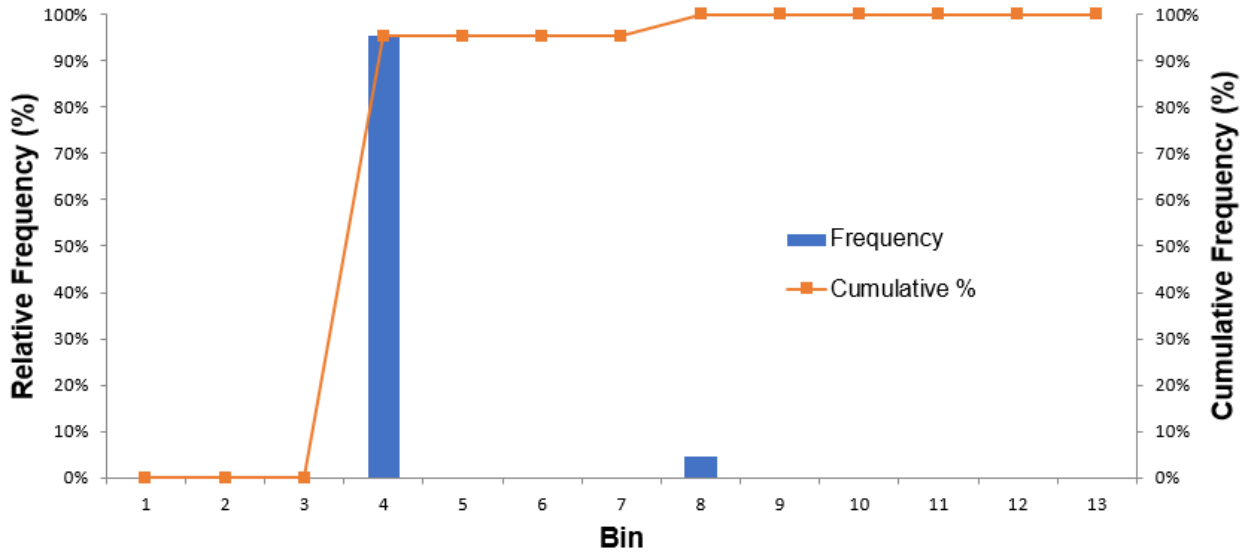

Figure 23. 1935 planform type at the 2019 issue locations.

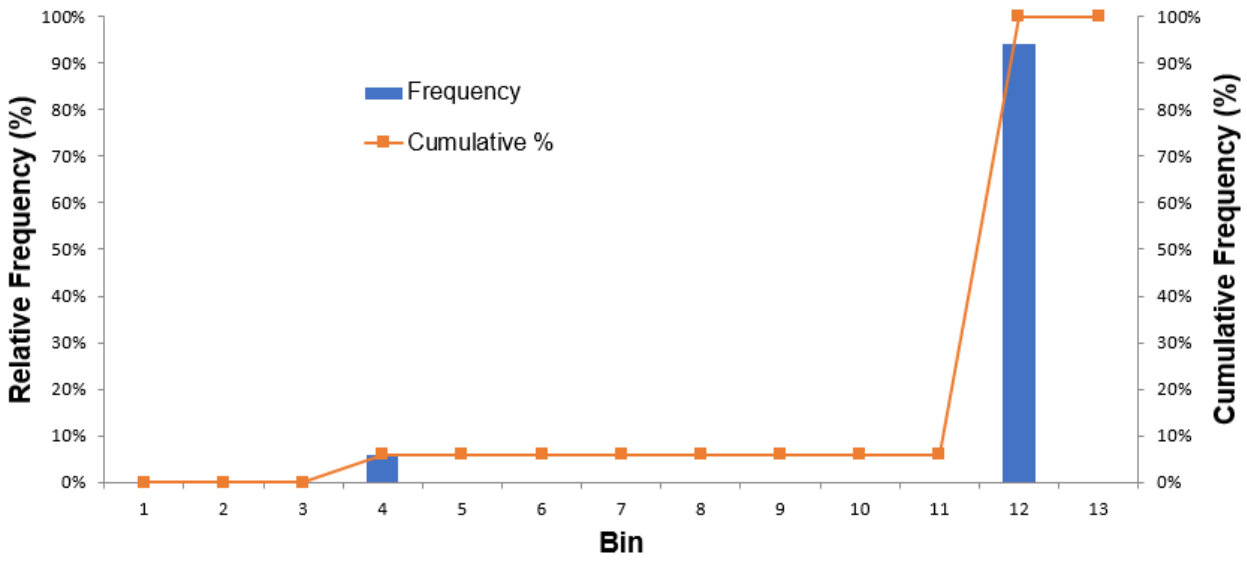

Figure 24. 1949 planform type at the 2019 issue locations.

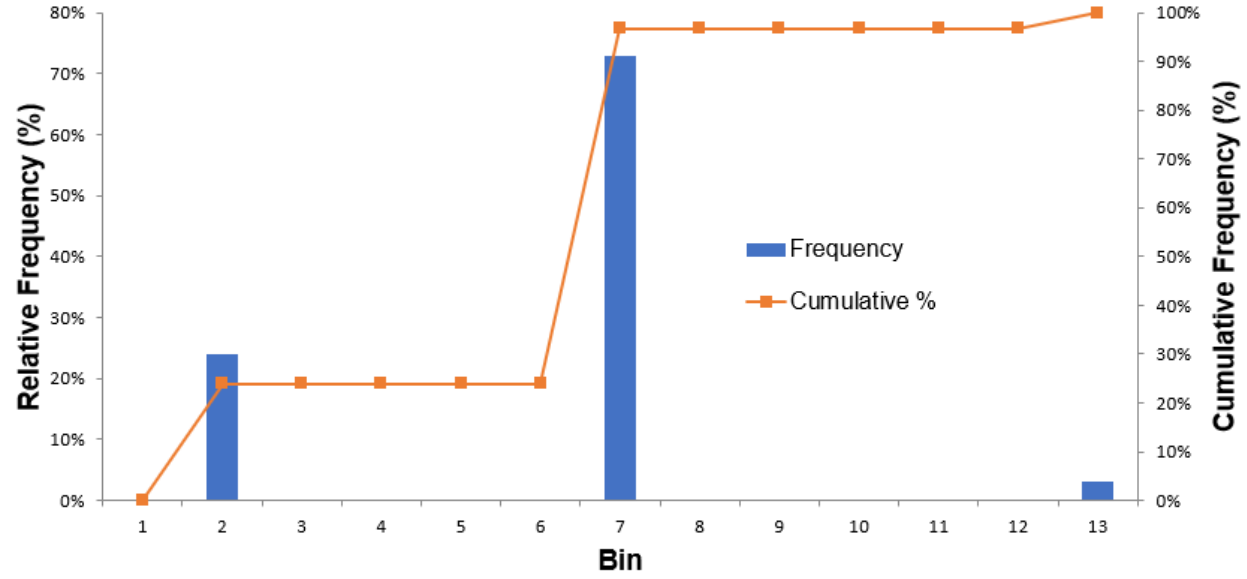

Figure 25. 1918 planform type at the borehole locations..

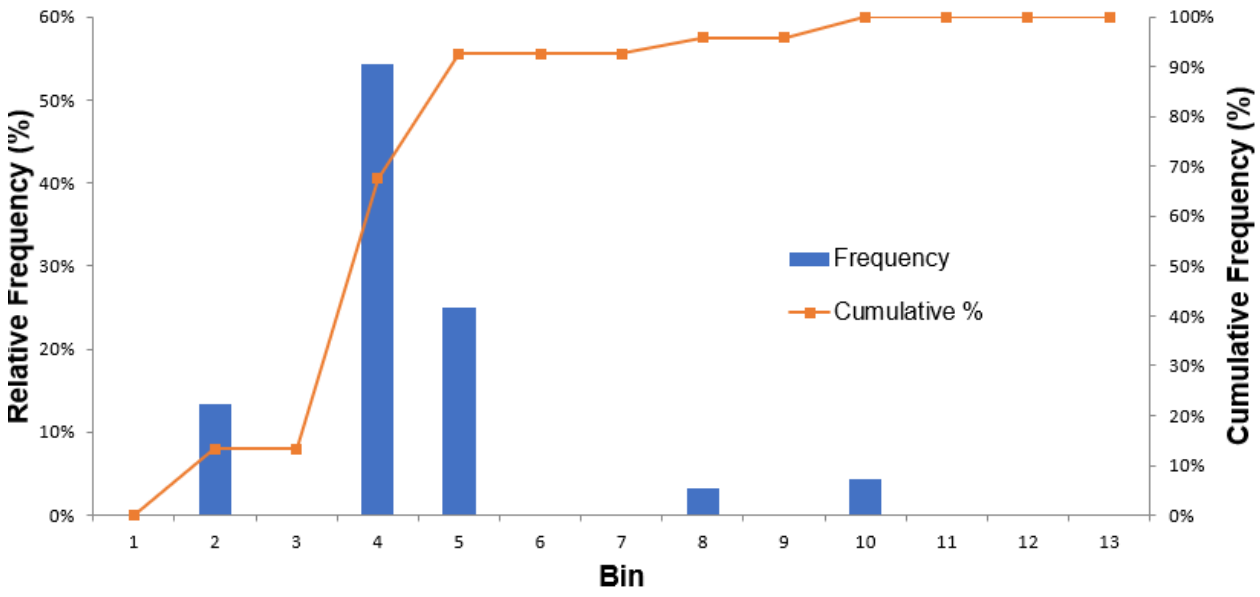

Figure 26. 1935 planform type at the borehole locations.

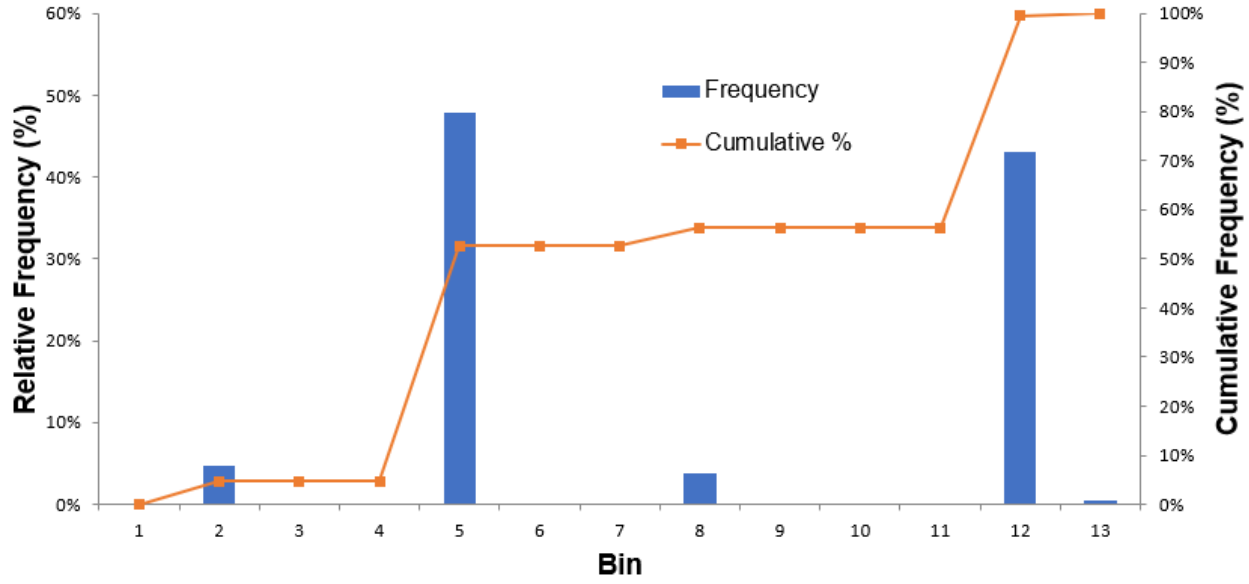

Figure 27. 1949 planform type at the borehole locations.

Planform type computations

The following graphics show the specific computations behind the generation of the relative and cumulative frequency plot for the planform types.

1918 Planform Statistics

Descriptive Statistics

Column1	
Mean	6.690476
Standard Error	0.320452
Median	7
Mode	7
Standard Deviation	2.936994
Sample Variance	8.625932
Kurtosis	0.719332
Skewness	0.297807
Range	11
Minimum	2
Maximum	13
Sum	562
Count	84

Histogram

Bin	Frequency	Cumulative %	Relative Frequency %
1	0	0.00%	0.00%
2	16	19.05%	19.05%
3	0	19.05%	0.00%
4	0	19.05%	0.00%
5	0	19.05%	0.00%
6	0	19.05%	0.00%
7	59	89.29%	70.24%
8	0	89.29%	0.00%
9	0	89.29%	0.00%
10	0	89.29%	0.00%
11	0	89.29%	0.00%
12	0	89.29%	0.00%
13	9	100.00%	10.71%
More	0	100.00%	

Figure 28. 1918 Planform type computations at the 2019 areas of interest.

1935 Planform Statistics

Descriptive Statistics

Column1	
Mean	4.190476
Standard Error	0.093501
Median	4
Mode	4
Standard Deviation	0.856952
Sample Variance	0.734366
Kurtosis	17.12297
Skewness	4.326169
Range	4
Minimum	4
Maximum	8
Sum	352
Count	84

Histogram

Bin	Frequency	Cumulative %	Relative Frequency %
1	0	0.00%	0.00%
2	0	0.00%	0.00%
3	0	0.00%	0.00%
4	80	95.24%	95.24%
5	0	95.24%	0.00%
6	0	95.24%	0.00%
7	0	95.24%	0.00%
8	4	100.00%	4.76%
9	0	100.00%	0.00%
10	0	100.00%	0.00%
11	0	100.00%	0.00%
12	0	100.00%	0.00%
13	0	100.00%	0.00%
More	0	100.00%	

Figure 29. 1935 Planform type computations at the 2019 areas of interest.

1949 Planform Statistics

Descriptive Statistics

Column1	
Mean	11.58333
Standard Error	0.181793
Median	12
Mode	12
Standard Deviation	1.666165
Sample Variance	2.776104
Kurtosis	12.67593
Skewness	-3.79139
Range	7
Minimum	5
Maximum	12
Sum	973
Count	84

Histogram

Bin	Frequency	Cumulative %	Relative Frequency %
1	0	0.00%	0.00%
2	0	0.00%	0.00%
3	0	0.00%	0.00%
4	0	0.00%	0.00%
5	5	5.95%	5.95%
6	0	5.95%	0.00%
7	0	5.95%	0.00%
8	0	5.95%	0.00%
9	0	5.95%	0.00%
10	0	5.95%	0.00%
11	0	5.95%	0.00%
12	79	100.00%	94.05%
13	0	100.00%	0.00%
More	0	100.00%	

Figure 30. 1949 Planform type computations at the 2019 areas of interest.

1918 Planform Statistics

Descriptive Statistics

Column1	
Mean	5.994681
Standard Error	0.180941
Median	7
Mode	7
Standard Deviation	2.480938
Sample Variance	6.155052
Kurtosis	0.748038
Skewness	-0.23596
Range	11
Minimum	2
Maximum	13
Sum	1127
Count	188

Histogram

Bin	Frequency	Cumulative %	Relative Frequency %
1	0	0.00%	0.00%
2	45	23.94%	23.94%
3	0	23.94%	0.00%
4	0	23.94%	0.00%
5	0	23.94%	0.00%
6	0	23.94%	0.00%
7	137	96.81%	72.87%
8	0	96.81%	0.00%
9	0	96.81%	0.00%
10	0	96.81%	0.00%
11	0	96.81%	0.00%
12	0	96.81%	0.00%
13	6	100.00%	3.19%
More	0	100.00%	

Figure 31. 1918 Planform type computations at the borehole locations.

1935 Planform Statistics

Descriptive Statistics

Column1	
Mean	4.367021
Standard Error	0.119932
Median	4
Mode	4
Standard Deviation	1.644429
Sample Variance	2.704147
Kurtosis	4.422676
Skewness	1.693111
Range	8
Minimum	2
Maximum	10
Sum	821
Count	188

Histogram

Bin	Frequency	Cumulative %	Relative Frequency %
1	0	0.00%	0.00%
2	25	13.30%	13.30%
3	0	13.30%	0.00%
4	102	67.55%	54.26%
5	47	92.55%	25.00%
6	0	92.55%	0.00%
7	0	92.55%	0.00%
8	6	95.74%	3.19%
9	0	95.74%	0.00%
10	8	100.00%	4.26%
11	0	100.00%	0.00%
12	0	100.00%	0.00%
13	0	100.00%	0.00%
More	0	100.00%	

Figure 32. 1935 Planform type computations at the borehole locations.

1949 Planform Statistics

Descriptive Statistics

Column1	
Mean	8.026596
Standard Error	0.26425
Median	5
Mode	5
Standard Deviation	3.623207
Sample Variance	13.12763
Kurtosis	-1.75981
Skewness	0.083993
Range	11
Minimum	2
Maximum	13
Sum	1509
Count	188

Histogram

Bin	Frequency	Cumulative %	Relative Frequency %
1	0	0.00%	0.00%
2	9	4.79%	4.79%
3	0	4.79%	0.00%
4	0	4.79%	0.00%
5	90	52.66%	47.87%
6	0	52.66%	0.00%
7	0	52.66%	0.00%
8	7	56.38%	3.72%
9	0	56.38%	0.00%
10	0	56.38%	0.00%
11	0	56.38%	0.00%
12	81	99.47%	43.09%
13	1	100.00%	0.53%
More	0	100.00%	

Figure 33. 1949 Planform type computations at the borehole locations.

Distance to Active Channel Plots

The distances to the active channel were graphically evaluated for both the 2019 issue locations and the borehole locations using the developed R Code (provided in the R code section of this Attachment). The graphical visualization of distributions through employment of the R code evaluated the distribution through the development of histograms, violin plots, box plots, four-quadrant pdf and cdf plots, as well as specific goodness of fit values with computed p values. It should be noted that zero values cannot be present when evaluating a lognormal distribution, so all zero distance values were changed to a value of one, in order to evaluate the distribution fits within the R code.

The four-quadrant pdf and cdf plots measure the goodness of fit to the theoretical gamma and lognormal distributions. The first plot is a histogram of the sample data plotted against theoretical pdfs for both the gamma and lognormal distributions. The second is an evaluation of the sample cdf compared with the theoretical cdfs for the gamma and lognormal distributions (Weaver 2000). These two plots provide a visualization of how well the theoretical distributions fit the sample data. The two other plots [quantile-quantile (Q-Q) and probability-probability (P-P) plots] provide the ability to assess lack of fit at the distribution tails (Q-Q plots) and at the distribution center (P-P plots) (Delignette-Muller and Dutang 2015).

Specific computations related to the specific good ness of fit values are provided in the Distance to Active Channel Computations section.

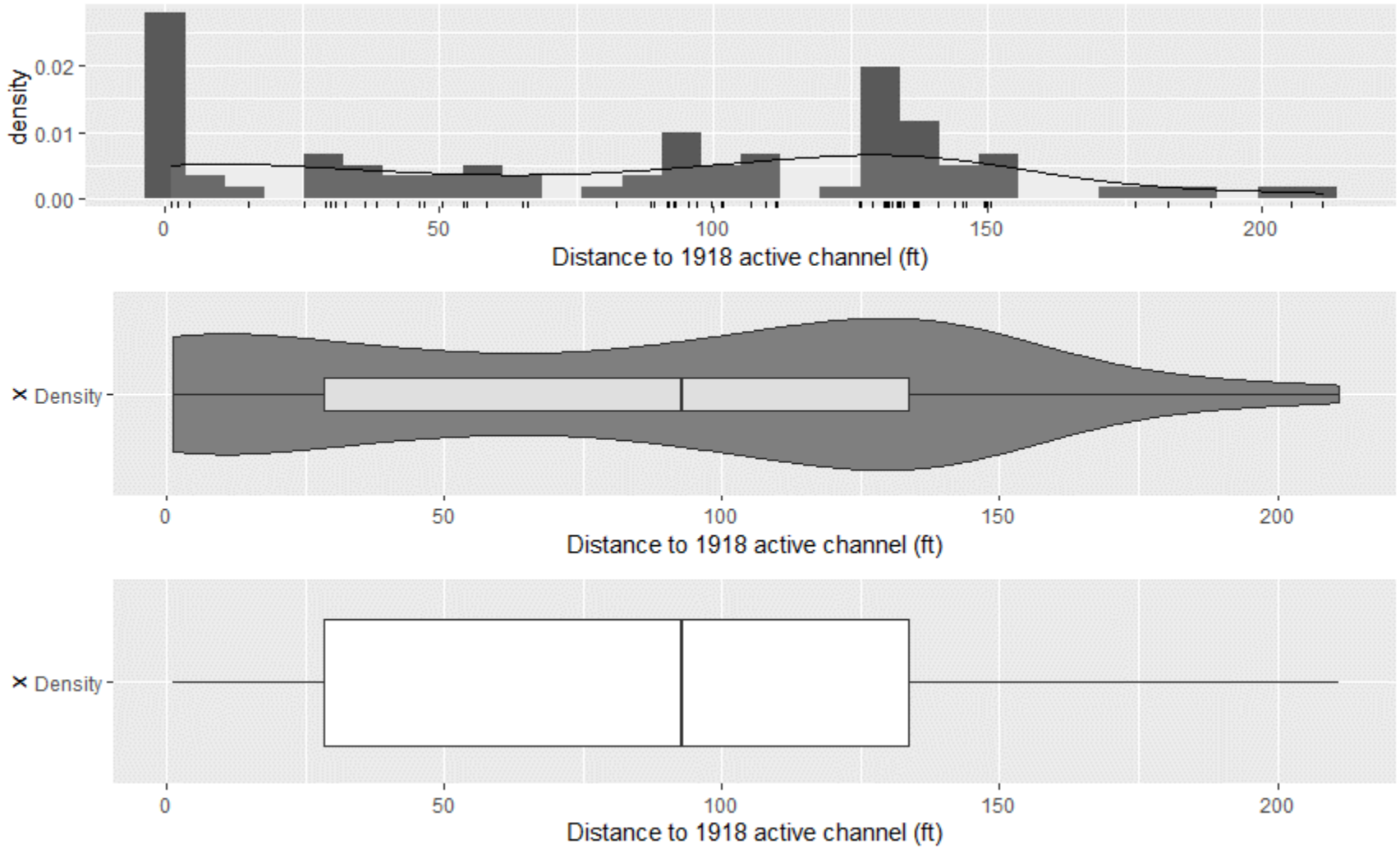

Figure 34. Active channel distances from the 1918 active channel to the 2019 points of interest. The top plot is a histogram. The bottom is a box and whisker plot, where the box represents the first and third quartiles and the line in the box represents the median value. The whiskers extend to 1.5 times the interquartile range. The middle graph is a violin plot combining aspects of the box and whisker and histogram.

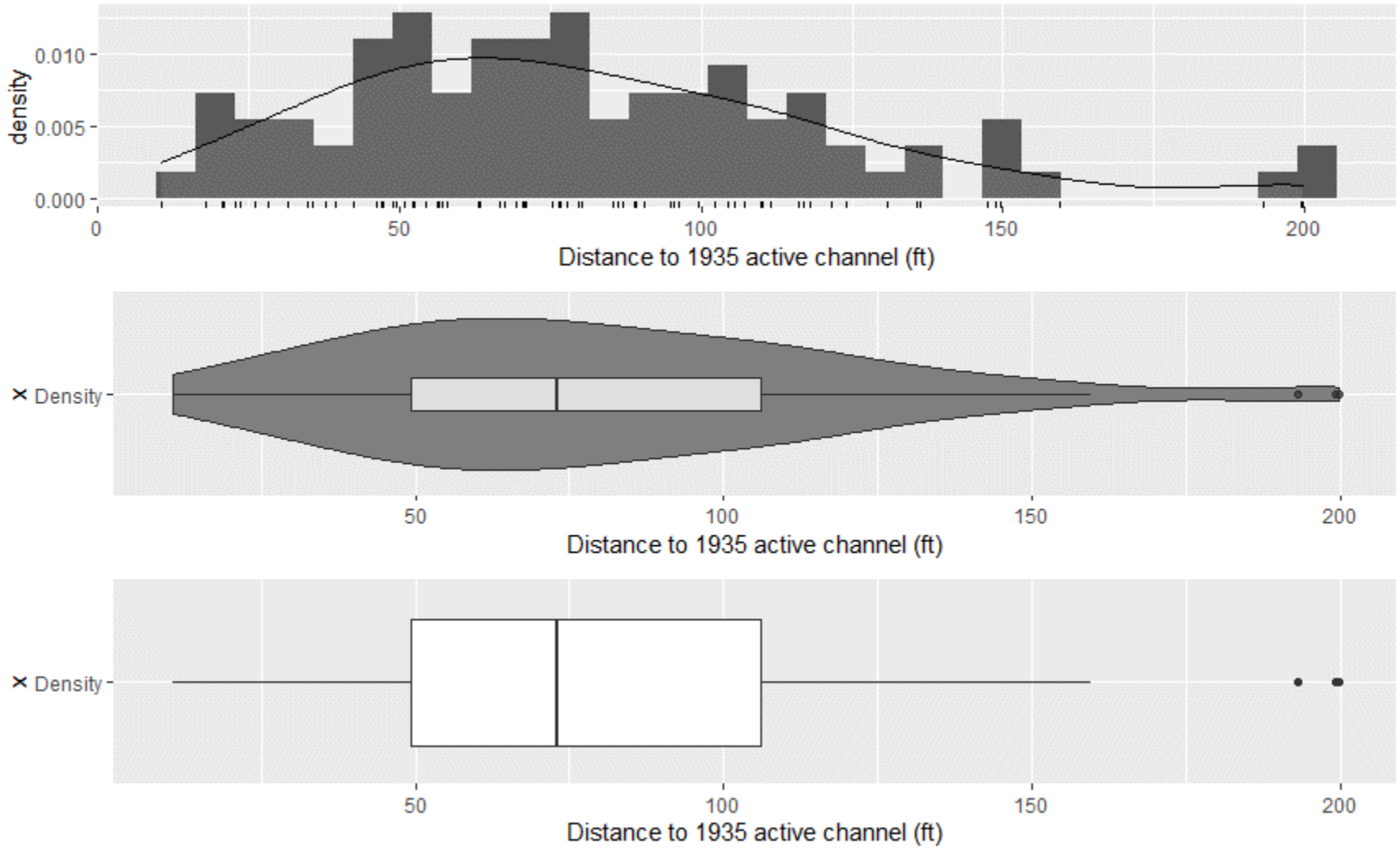

Figure 35. Active channel distances from the 1935 active channel to the 2019 points of interest. The top plot is a histogram. The bottom is a box and whisker plot, where the box represents the first and third quartiles and the line in the box represents the median value. The whiskers extend to 1.5 times the interquartile range. The middle graph is a violin plot combining aspects of the box and whisker and histogram.

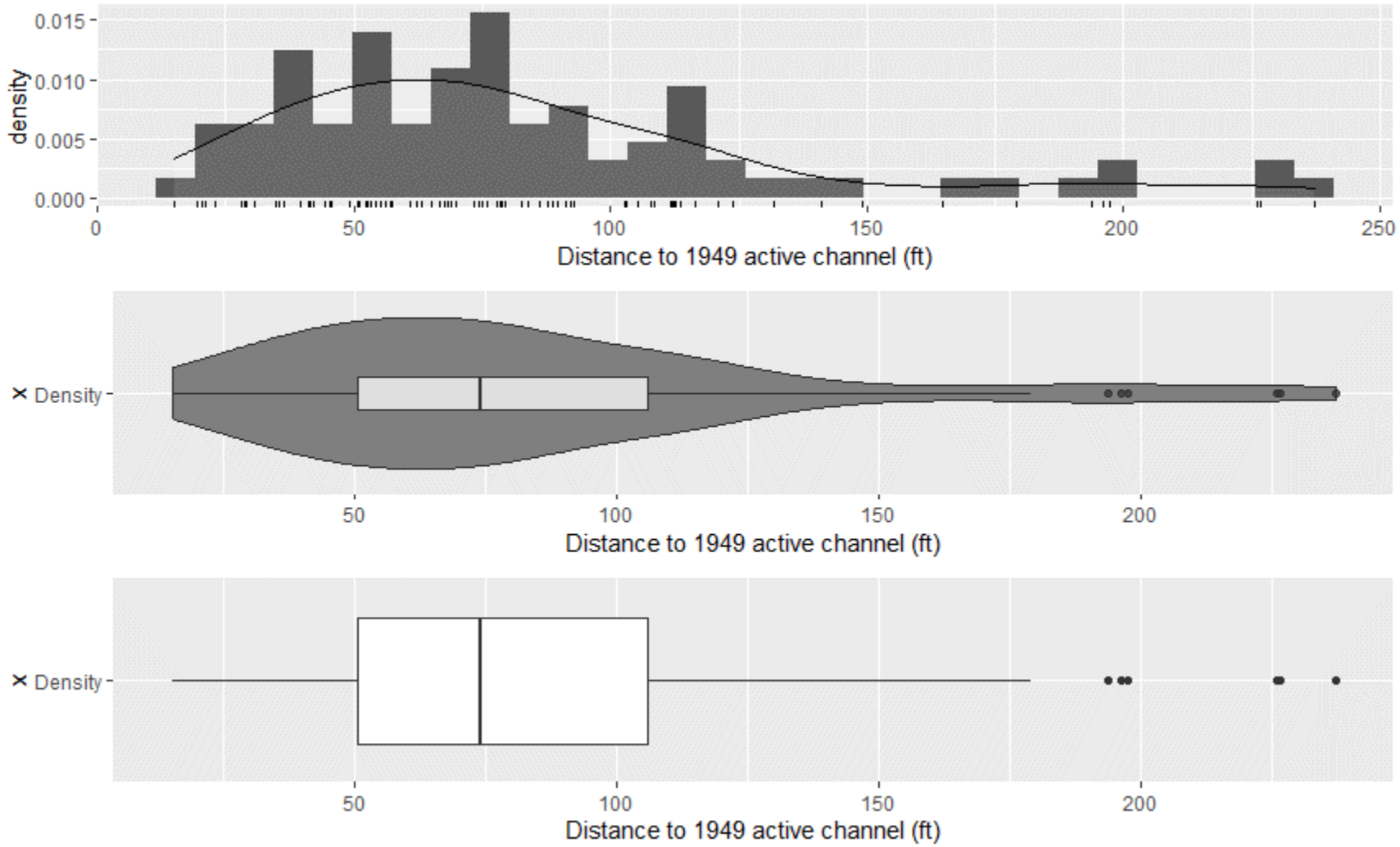

Figure 36. Active channel distances from the 1949 active channel to the 2019 points of interest. The top plot is a histogram. The bottom is a box and whisker plot, where the box represents the first and third quartiles and the line in the box represents the median value. The whiskers extend to 1.5 times the interquartile range. The middle graph is a violin plot combining aspects of the box and whisker and histogram.

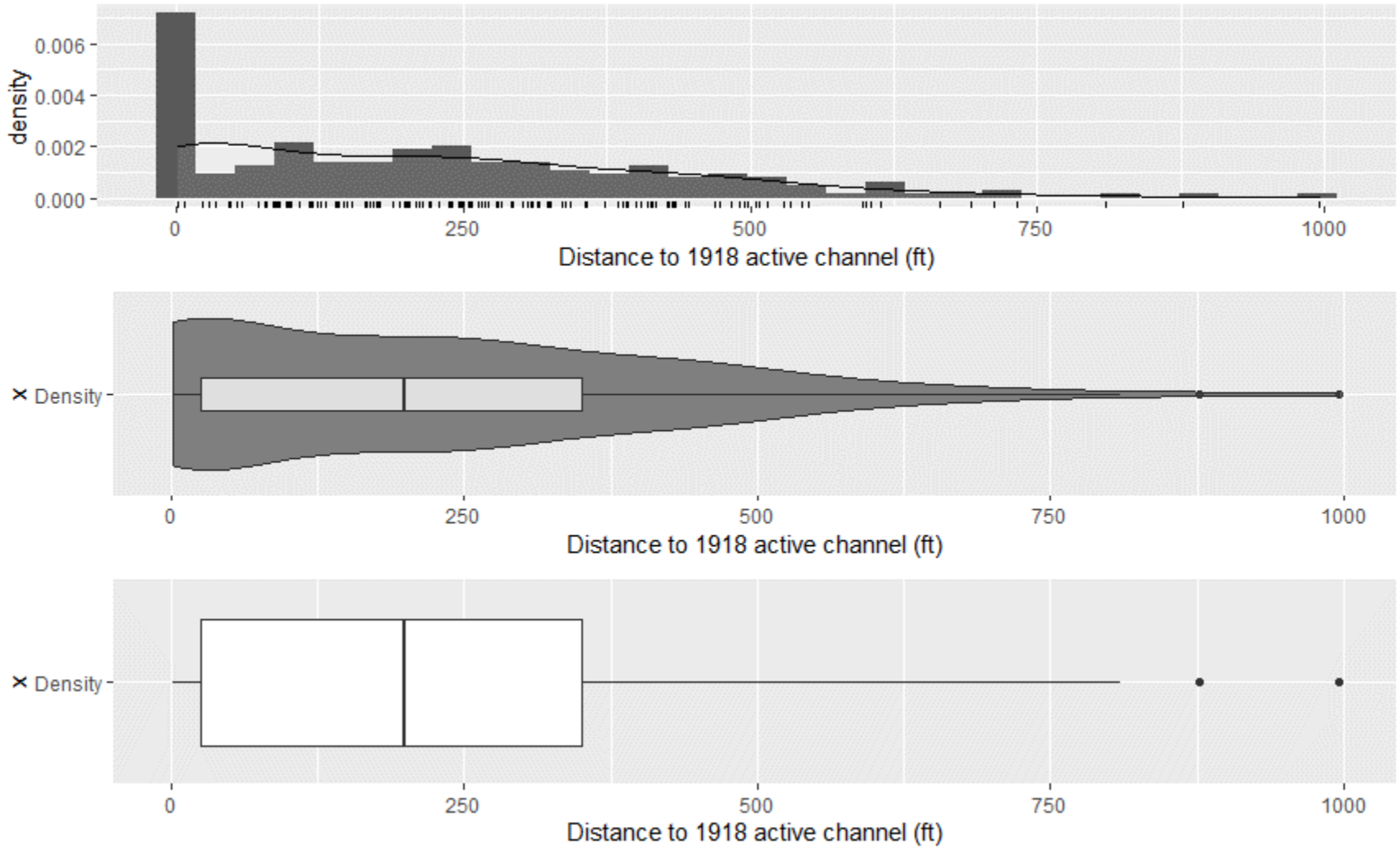

Figure 37. Active channel distances from the 1918 active channel to the borehole locations. The top plot is a histogram. The bottom is a box and whisker plot, where the box represents the first and third quartiles and the line in the box represents the median value. The whiskers extend to 1.5 times the interquartile range. The middle graph is a violin plot combining aspects of the box and whisker and histogram.

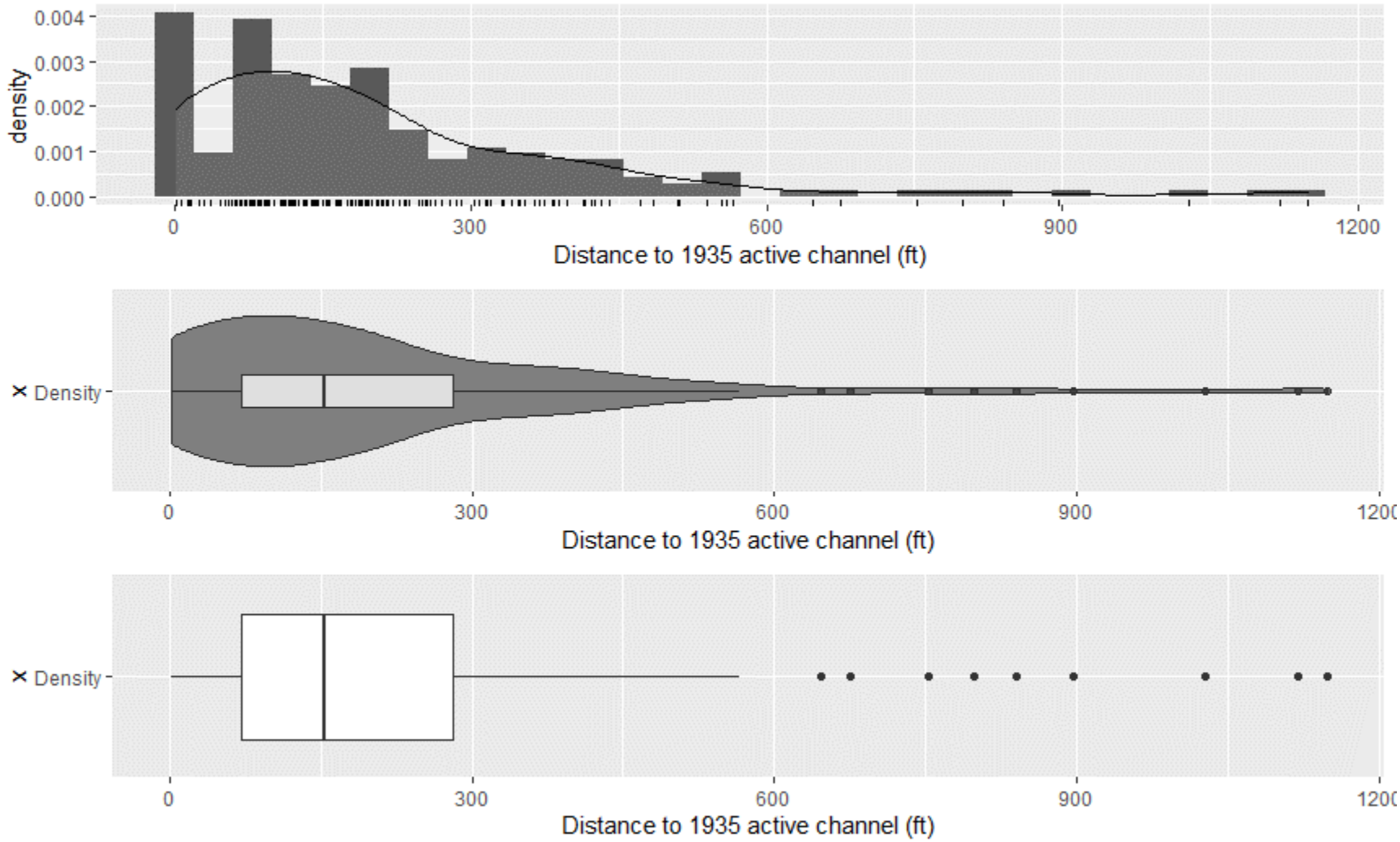

Figure 38. Active channel distances from the 1935 active channel to the borehole locations. The top plot is a histogram. The bottom is a box and whisker plot, where the box represents the first and third quartiles and the line in the box represents the median value. The whiskers extend to 1.5 times the interquartile range. The middle graph is a violin plot combining aspects of the box and whisker and histogram.

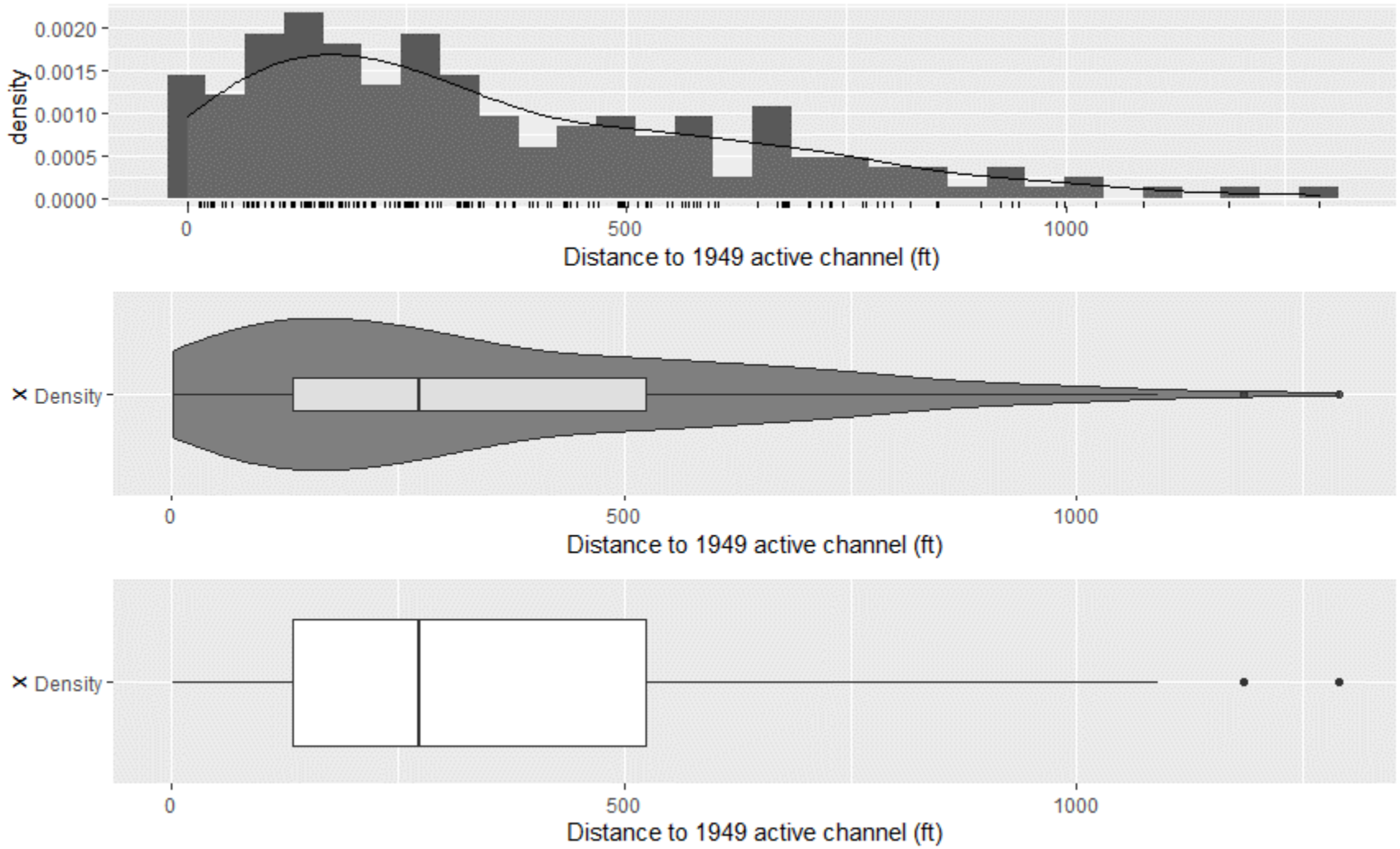

Figure 39. Active channel distances from the 1949 active channel to the borehole locations. The top plot is a histogram. The bottom is a box and whisker plot, where the box represents the first and third quartiles and the line in the box represents the median value. The whiskers extend to 1.5 times the interquartile range. The middle graph is a violin plot combining aspects of the box and whisker and histogram.

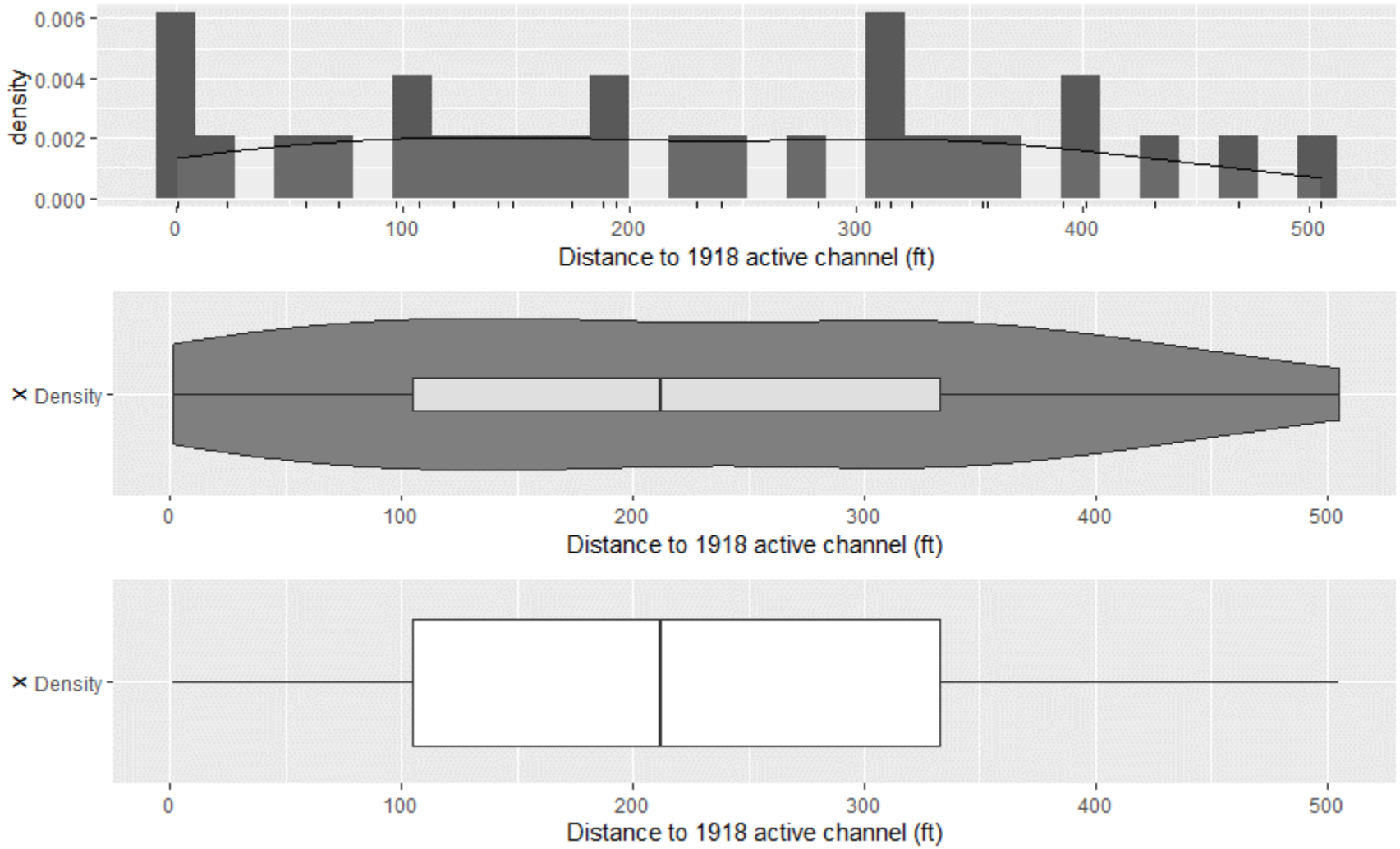

Figure 40. Active channel distances from the 1918 active channel to the correlated borehole locations. The top plot is a histogram. The bottom is a box and whisker plot, where the box represents the first and third quartiles and the line in the box represents the median value. The whiskers extend to 1.5 times the interquartile range. The middle graph is a violin plot combining aspects of the box and whisker and histogram.

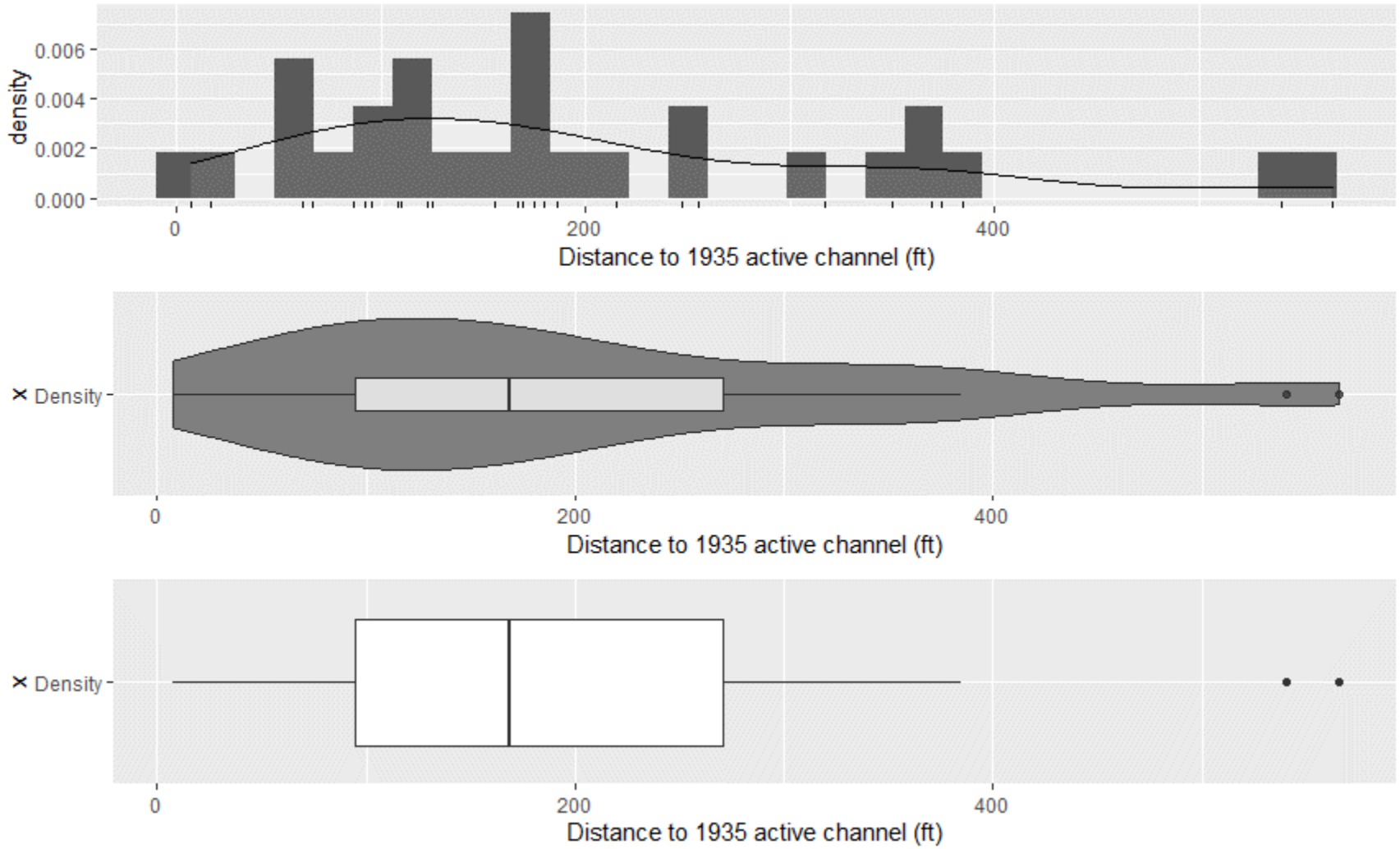

Figure 41. Active channel distances from the 1935 active channel to the correlated borehole locations. The top plot is a histogram. The bottom is a box and whisker plot, where the box represents the first and third quartiles and the line in the box represents the median value. The whiskers extend to 1.5 times the interquartile range. The middle graph is a violin plot combining aspects of the box and whisker and histogram.

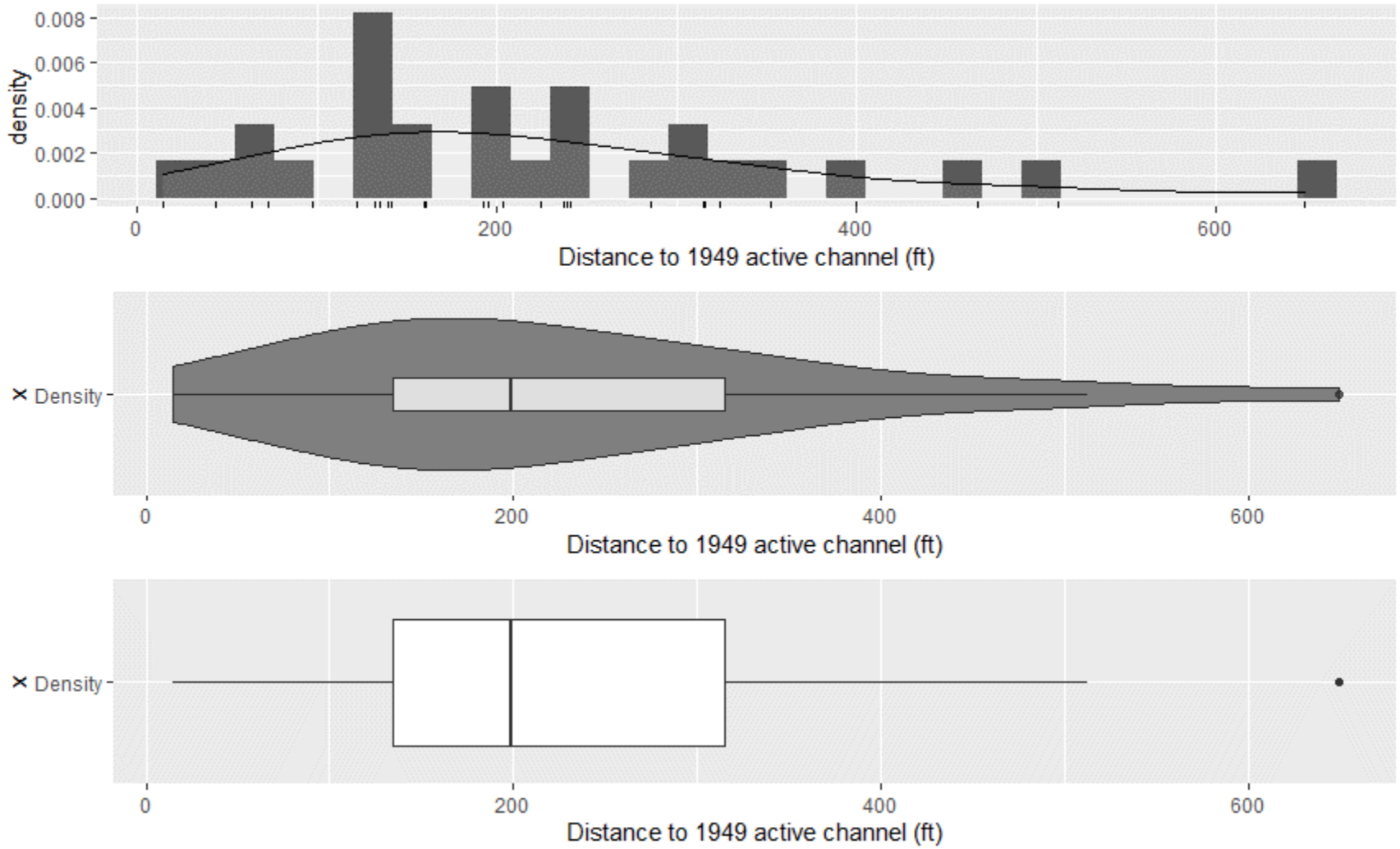

Figure 42. Active channel distances from the 1949 active channel to the correlated borehole locations. The top plot is a histogram. The bottom is a box and whisker plot, where the box represents the first and third quartiles and the line in the box represents the median value. The whiskers extend to 1.5 times the interquartile range. The middle graph is a violin plot combining aspects of the box and whisker and histogram.

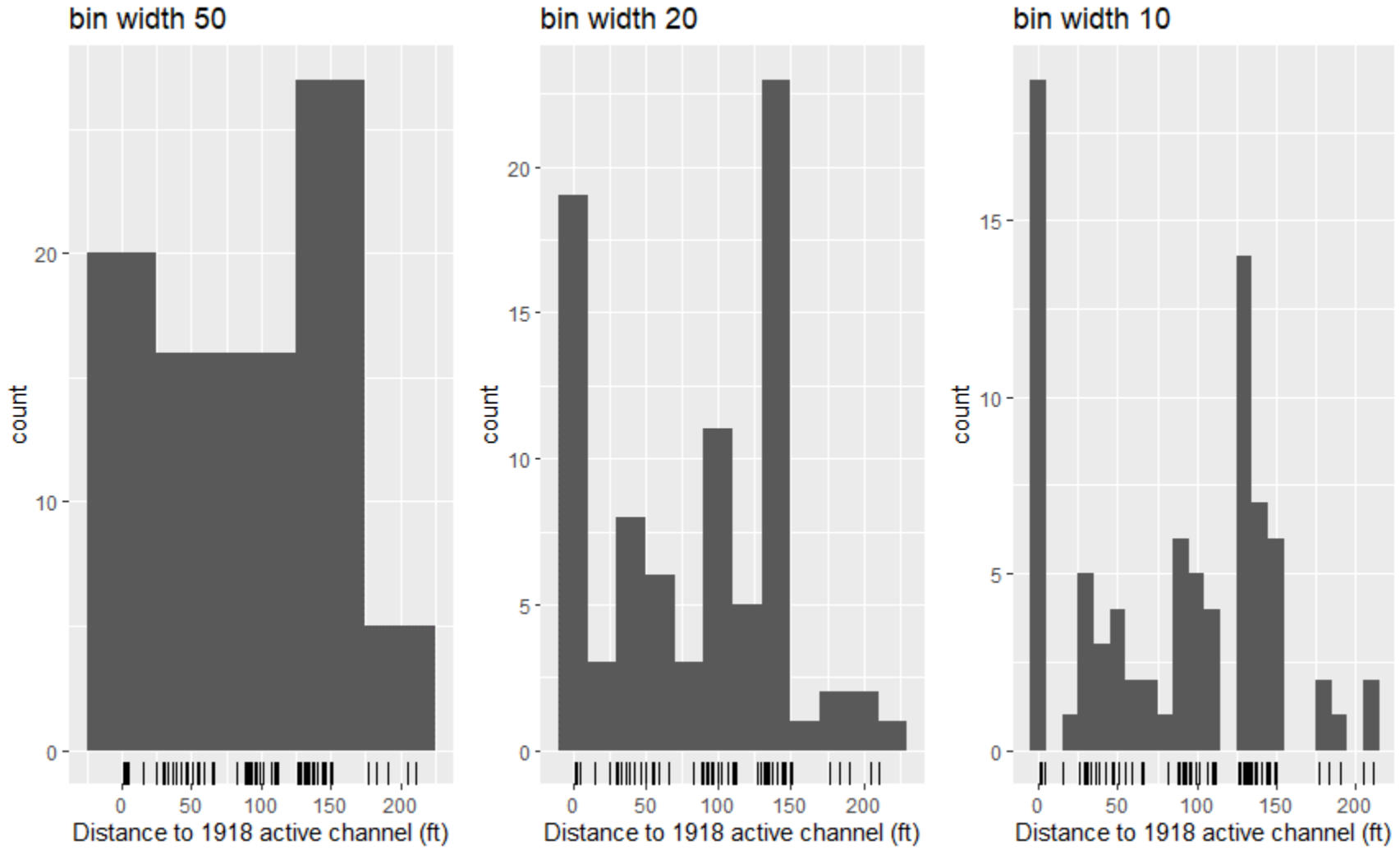

Figure 43. Histograms of 1918 active channel distance from the 2019 issue locations.

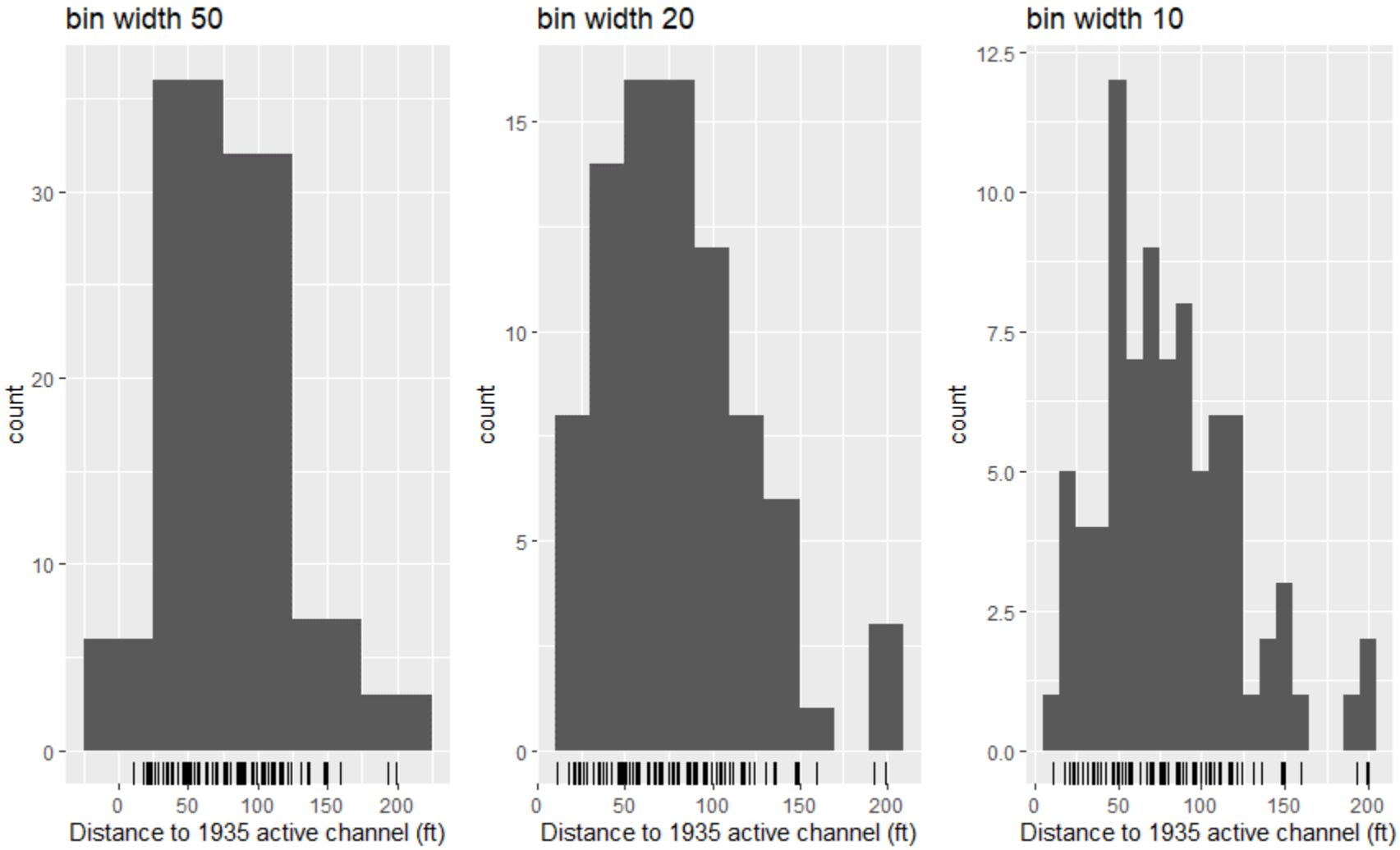

Figure 44. Histograms of the 1935 active channel distance from the 2019 issue locations.

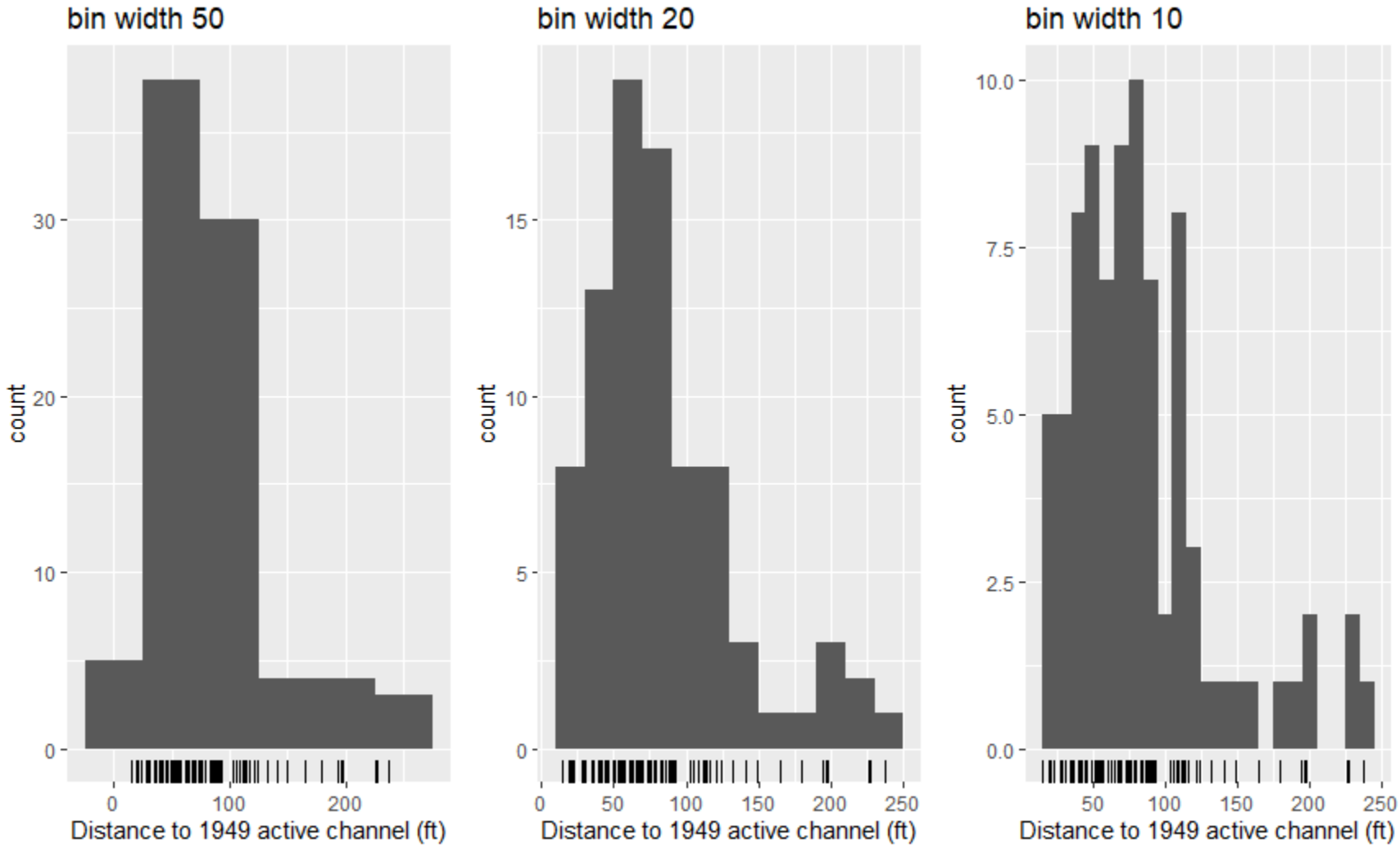

Figure 45. Histograms of the 1949 active channel distance from the 2019 issue locations.

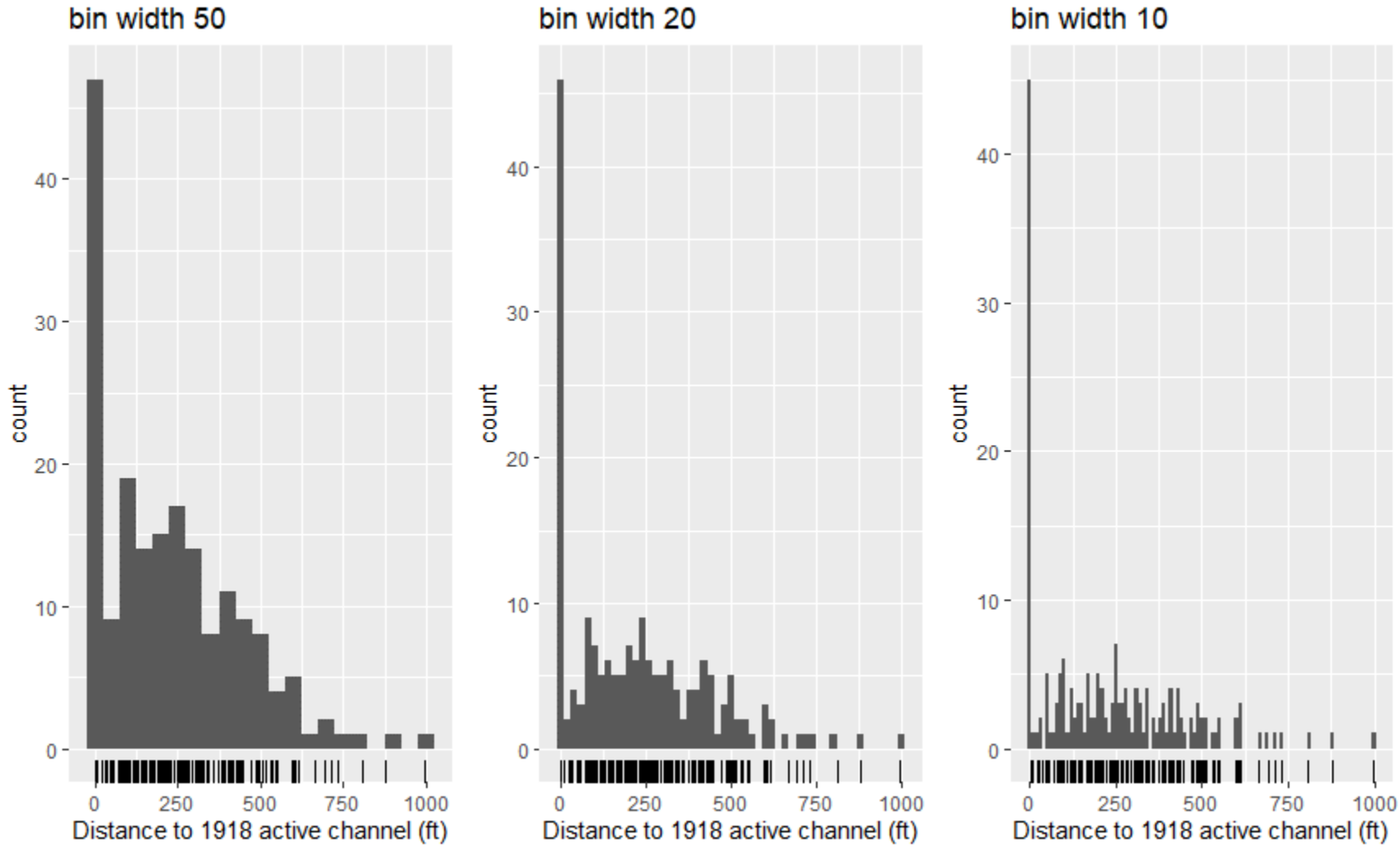

Figure 46. Histograms of the 1918 active channel distance from the borehole locations.

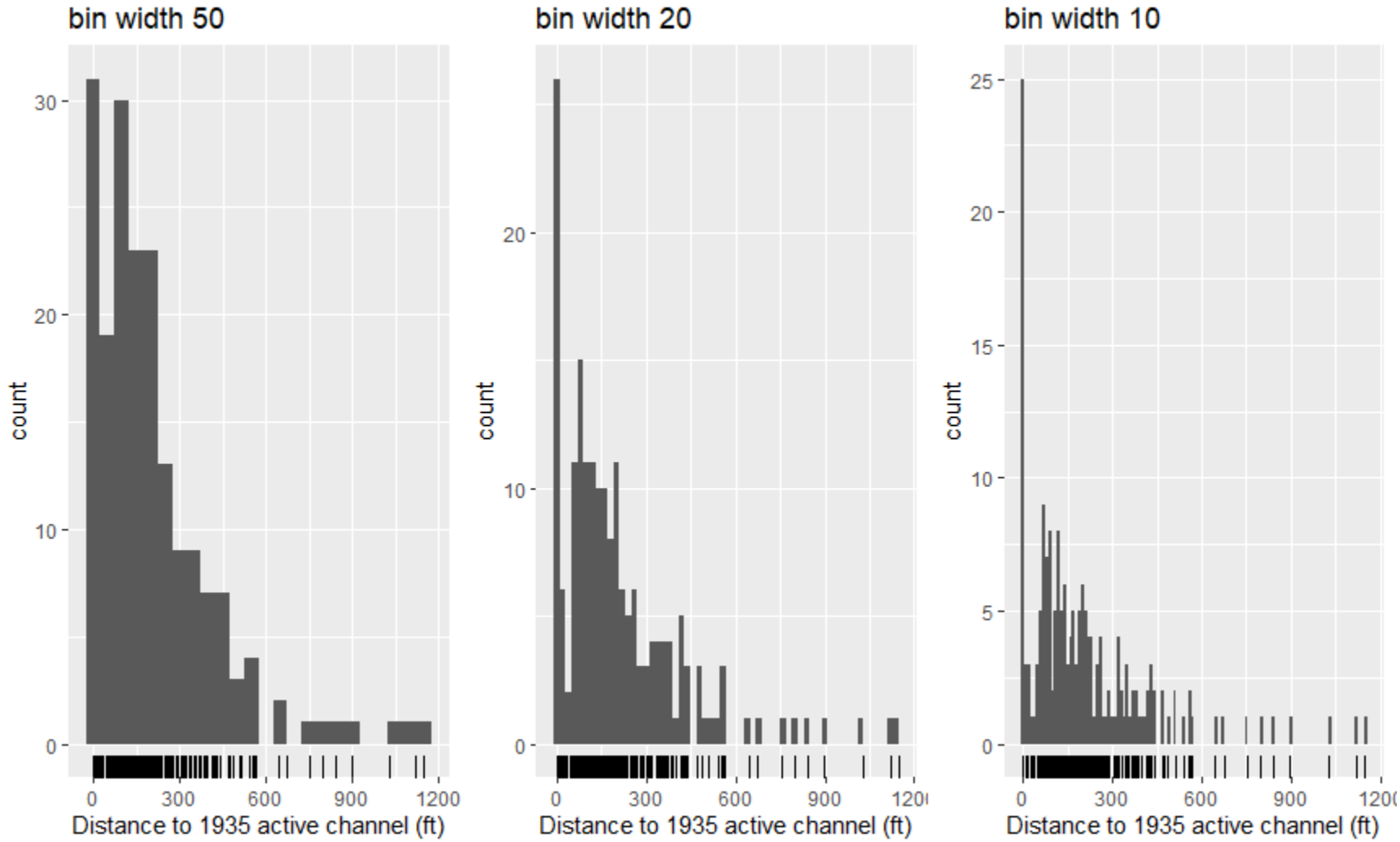

Figure 47. Histograms of the 1935 active channel distance from the borehole locations.

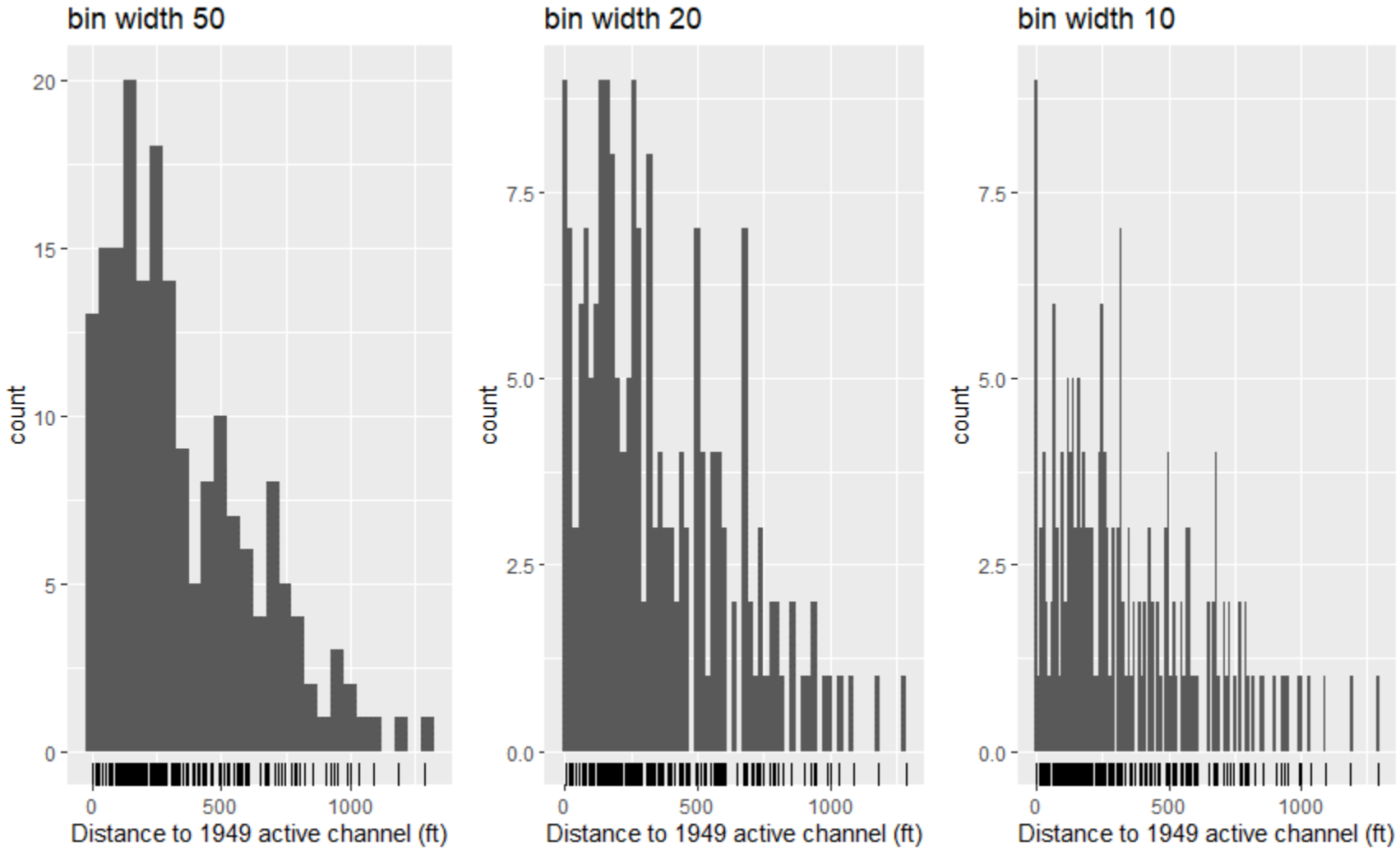

Figure 48. Histograms of the 1949 active channel distance from the borehole locations.

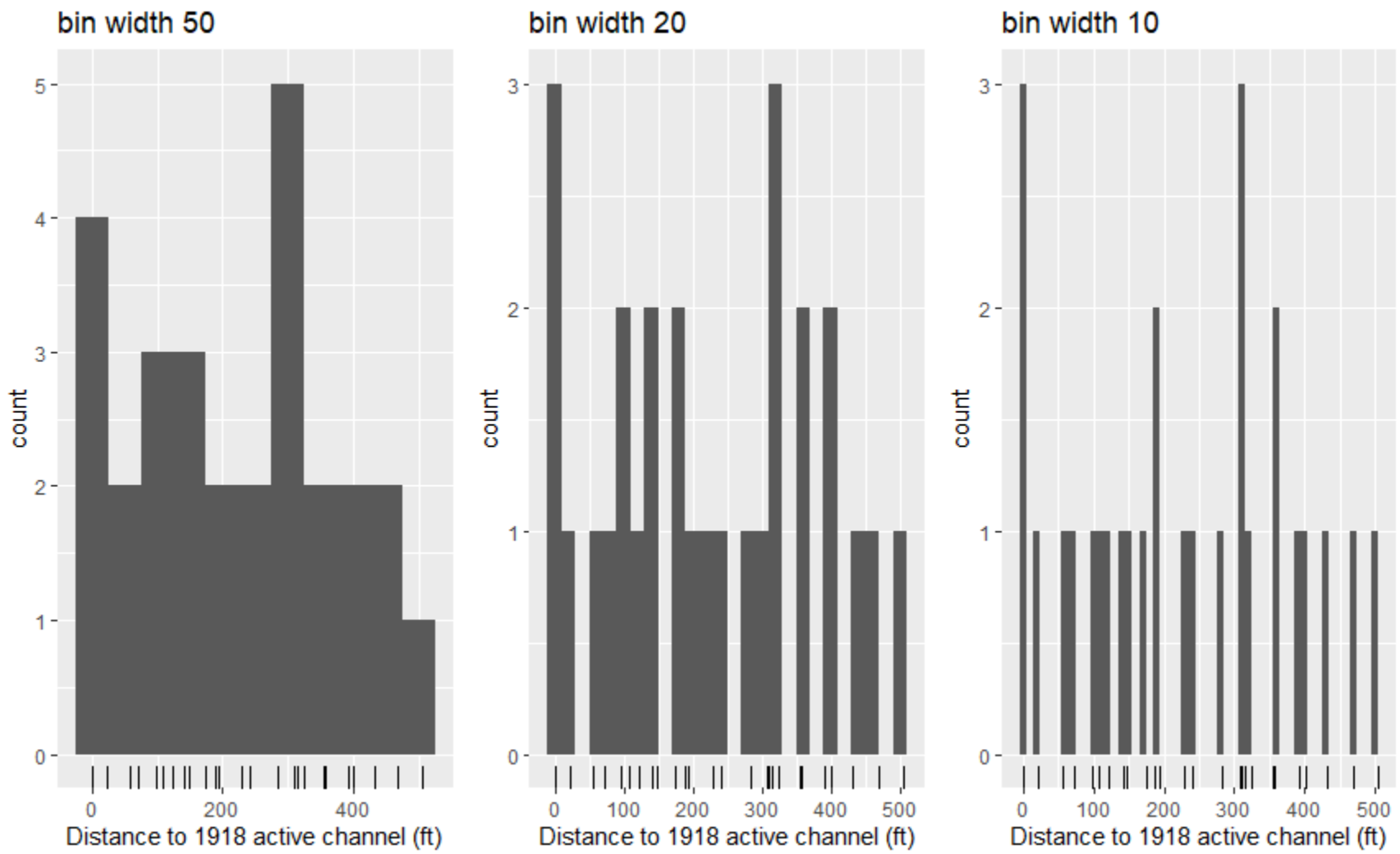

Figure 49. Histograms of the 1918 active channel distance from the correlated borehole locations.

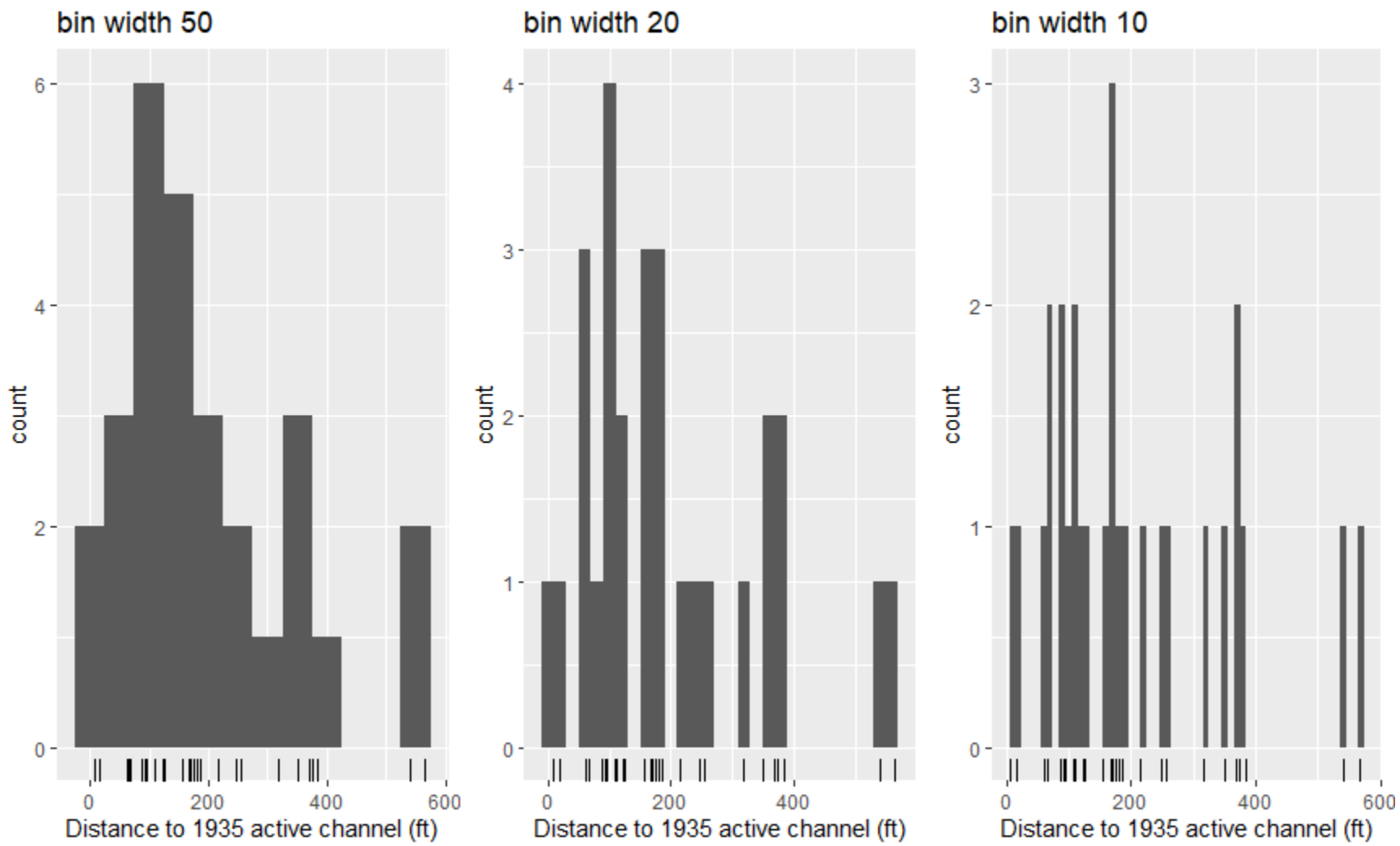

Figure 50. Histograms of the 1935 active channel distance from the correlated borehole locations.

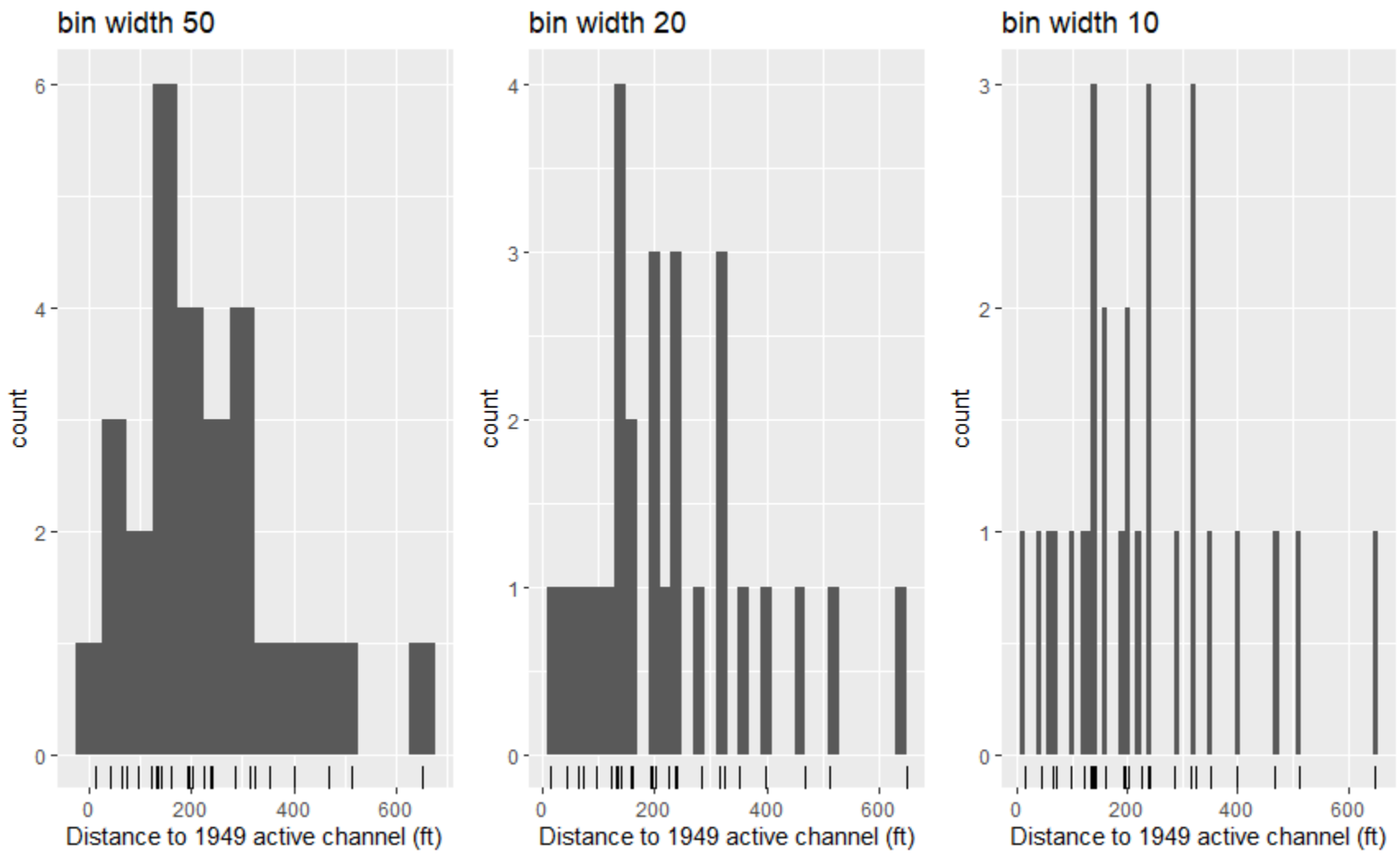

Figure 51. Histograms of the 1949 active channel distance from the correlated borehole locations.

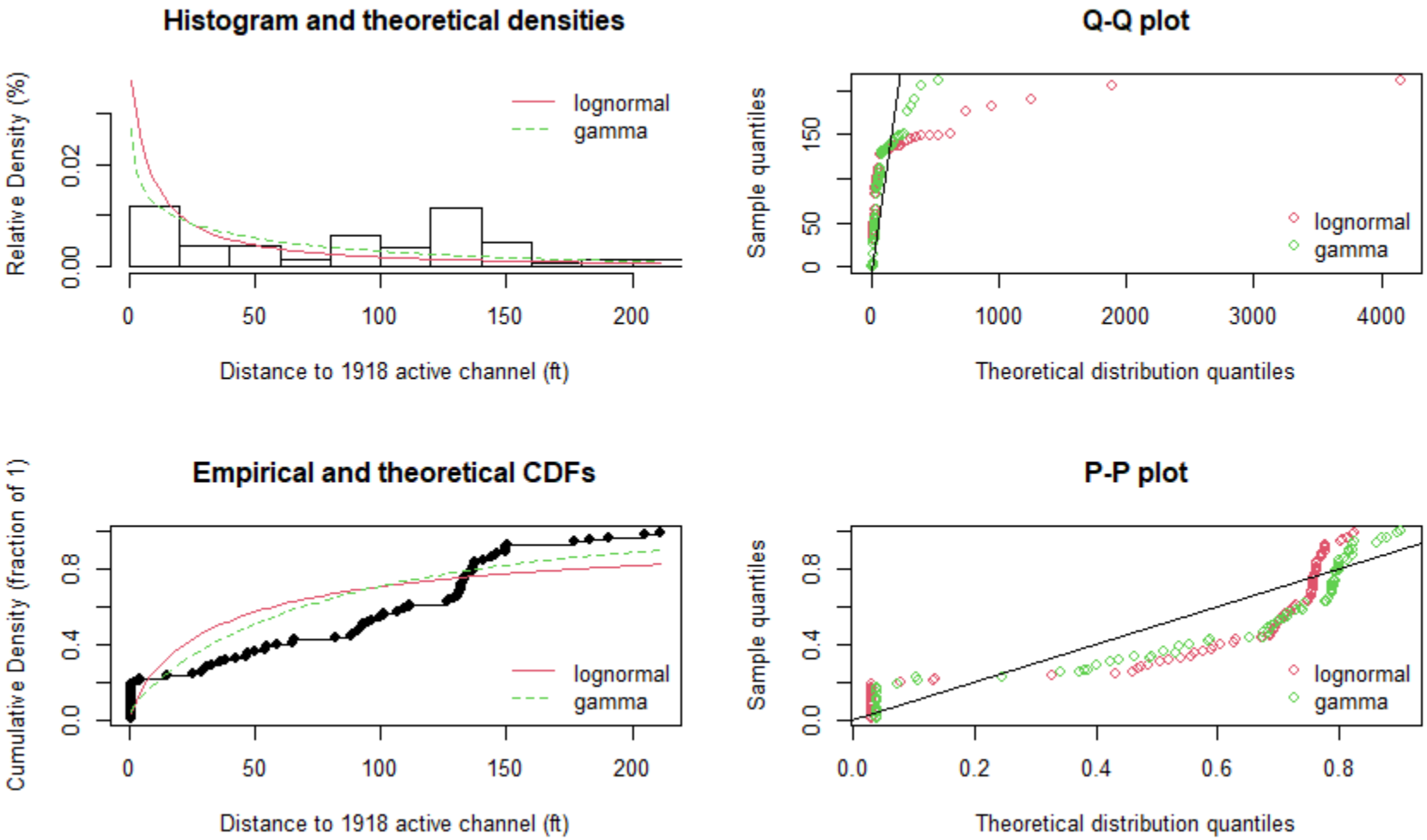

Figure 52. Goodness of fit plots: 1918 active channel distance to 2019 points of interest. The two graphs on the left show the theoretical gamma and lognormal distributions plotted against the sample set PDF (top plot) and CDF (bottom plot). The two graphs on the right evaluate the sample set against the theoretical distributions by assessing fit at the distribution tails (Q-Q plot) and center (P-P plot).

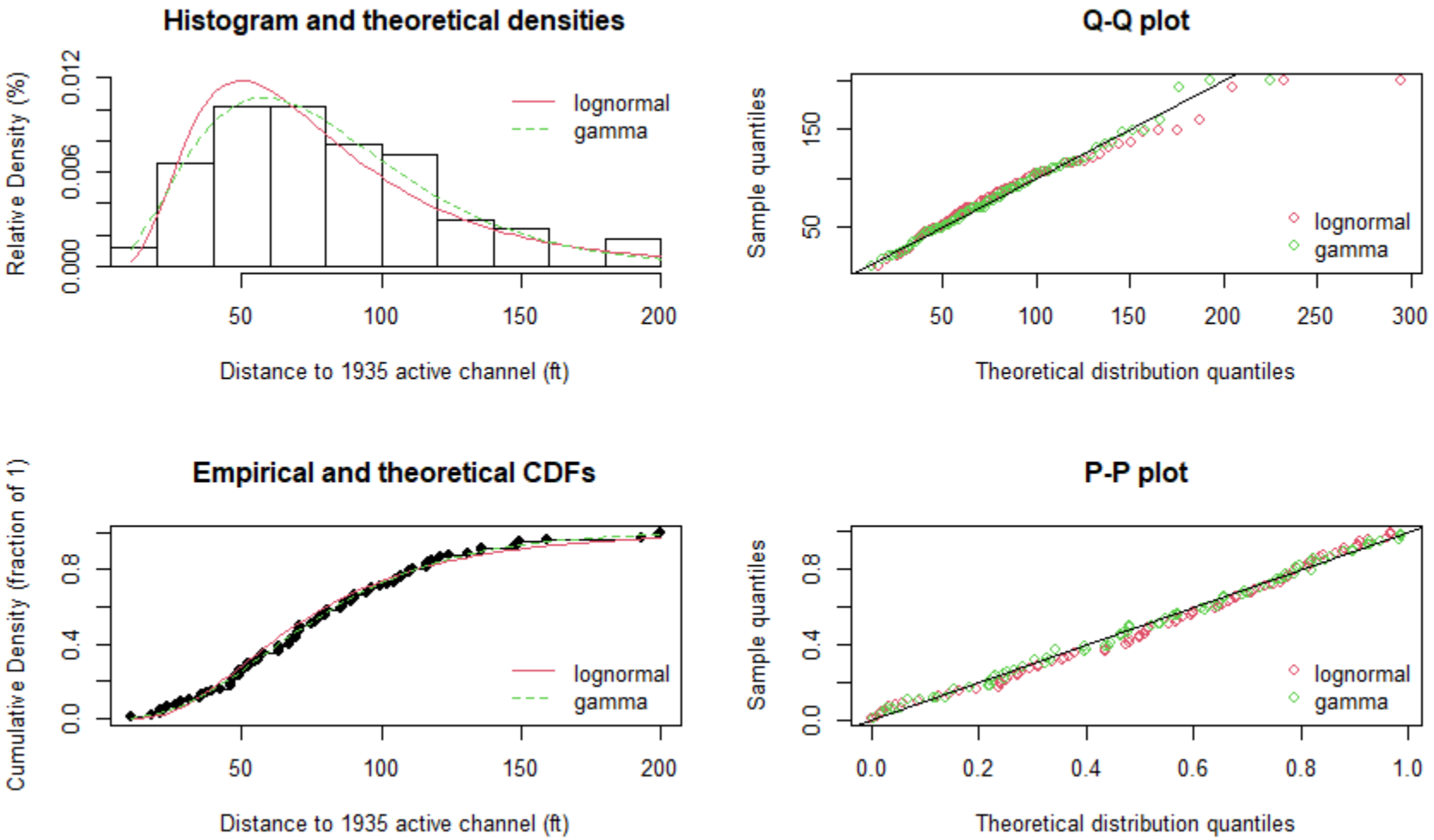

Figure 53. Goodness of fit plots: 1935 active channel distance to 2019 points of interest. The two graphs on the left show the theoretical gamma and lognormal distributions plotted against the sample set PDF (top plot) and CDF (bottom plot). The two graphs on the right evaluate the sample set against the theoretical distributions by assessing fit at the distribution tails (Q-Q plot) and center (P-P plot).

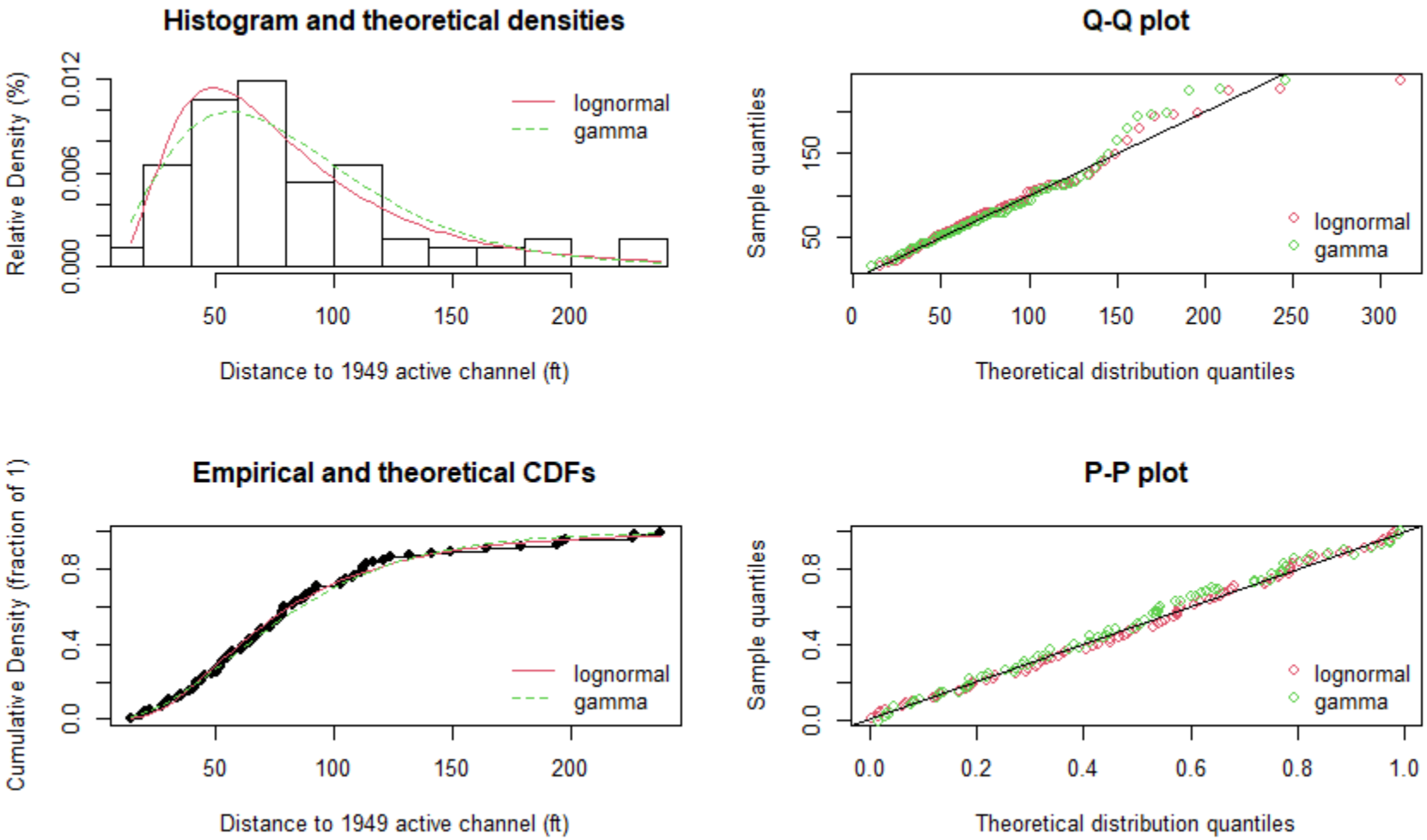

Figure 54. Goodness of fit plots: 1949 active channel distance to 2019 points of interest. The two graphs on the left show the theoretical gamma and lognormal distributions plotted against the sample set PDF (top plot) and CDF (bottom plot). The two graphs on the right evaluate the sample set against the theoretical distributions by assessing fit at the distribution tails (Q-Q plot) and center (P-P plot).

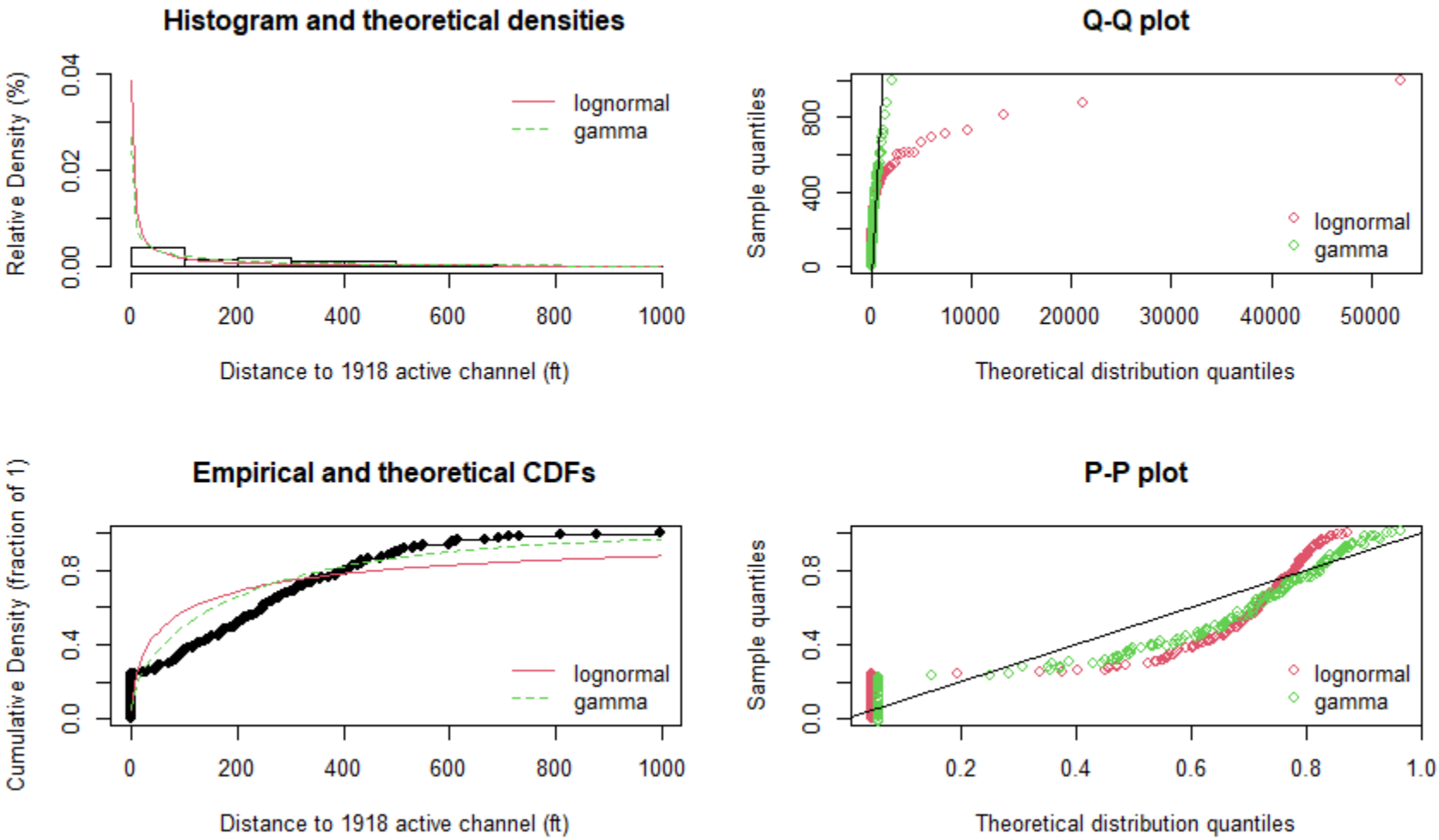

Figure 55. Goodness of fit plots: 1918 active channel distance to borehole locations. The two graphs on the left show the theoretical gamma and lognormal distributions plotted against the sample set PDF (top plot) and CDF (bottom plot). The two graphs on the right evaluate the sample set against the theoretical distributions by assessing fit at the distribution tails (Q-Q plot) and center (P-P plot).

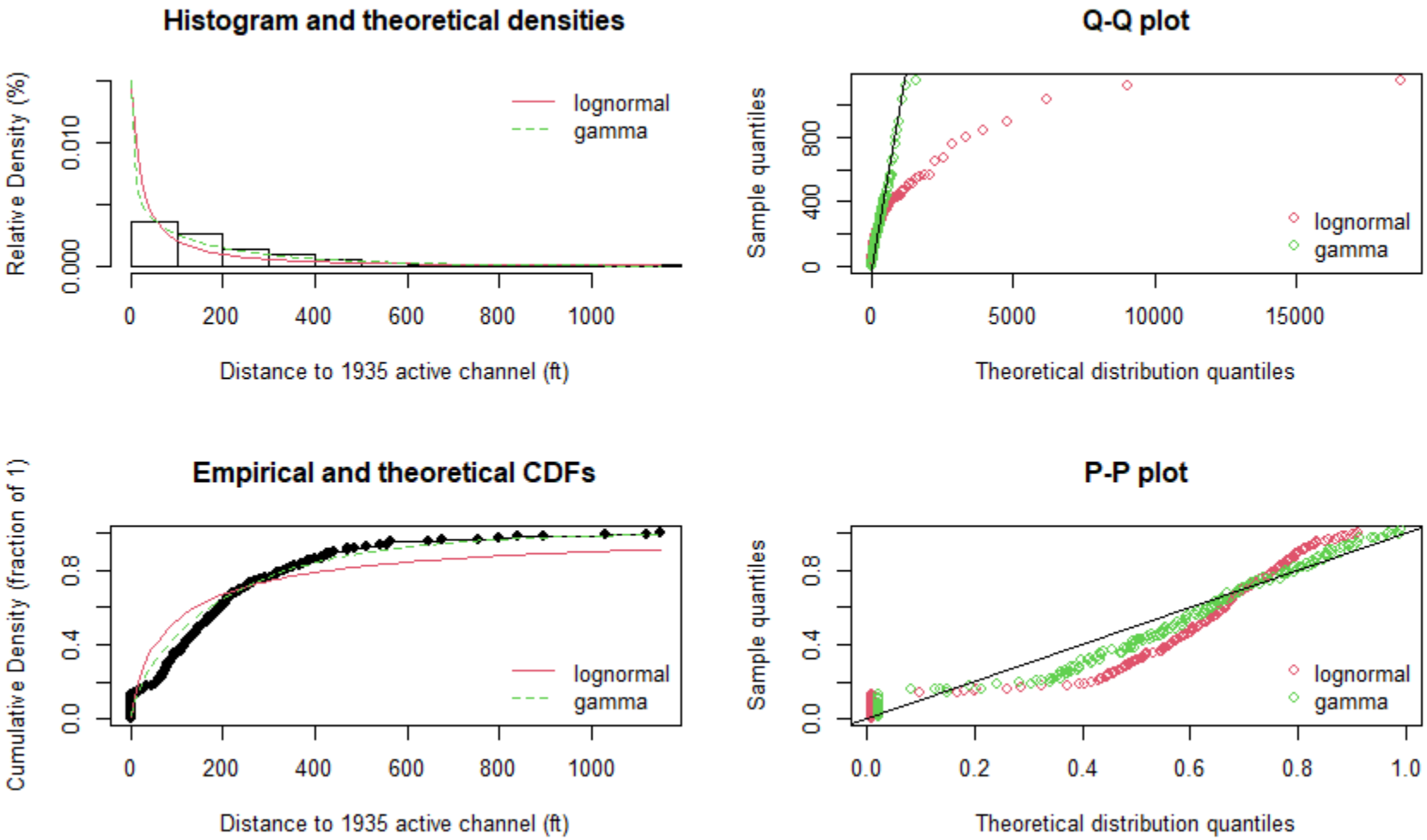

Figure 56. Goodness of fit plots: 1935 active channel distance to borehole locations. The two graphs on the left show the theoretical gamma and lognormal distributions plotted against the sample set PDF (top plot) and CDF (bottom plot). The two graphs on the right evaluate the sample set against the theoretical distributions by assessing fit at the distribution tails (Q-Q plot) and center (P-P plot).

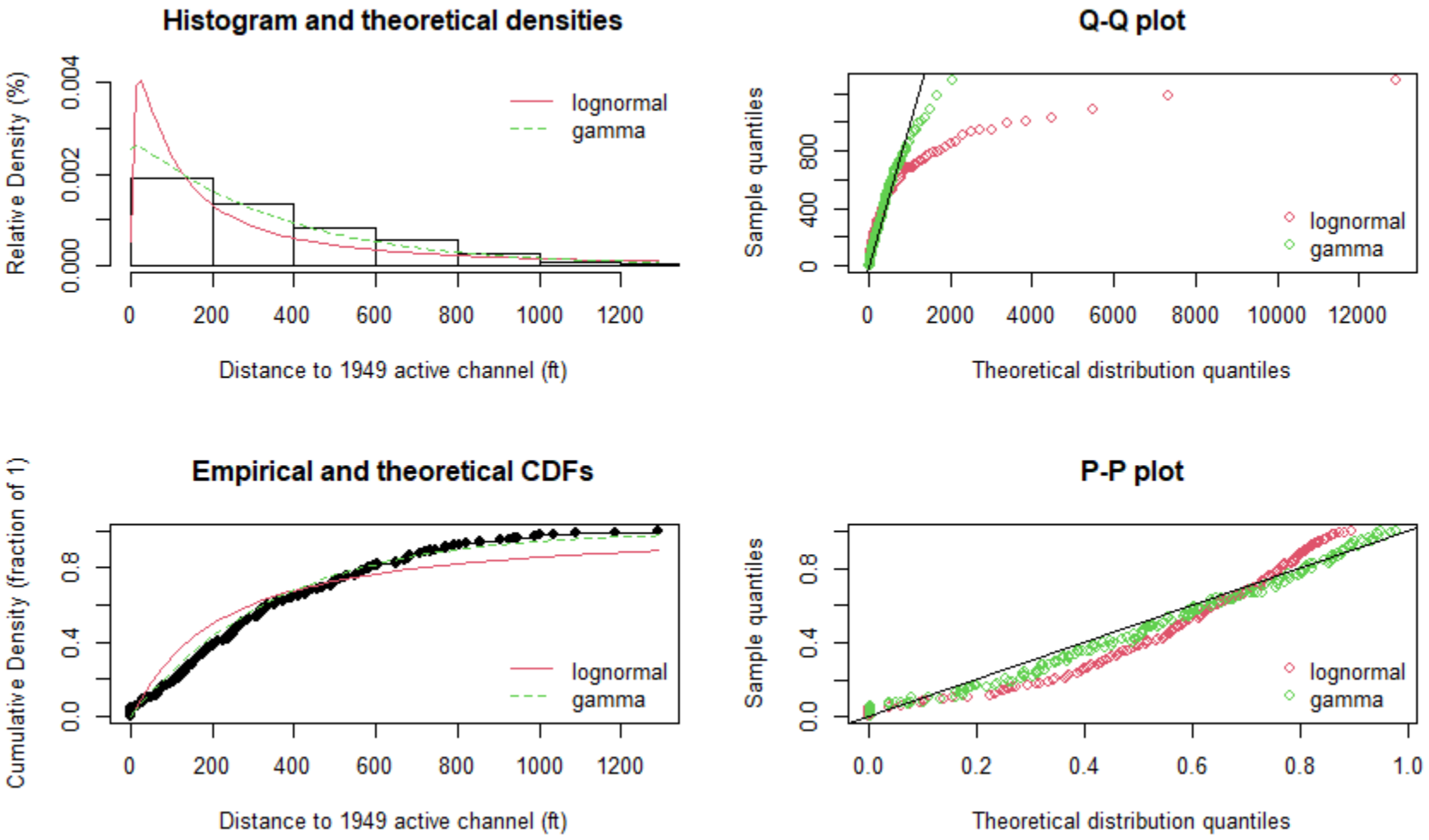

Figure 57. Goodness of fit plots: 1949 active channel distance to borehole locations. The two graphs on the left show the theoretical gamma and lognormal distributions plotted against the sample set PDF (top plot) and CDF (bottom plot). The two graphs on the right evaluate the sample set against the theoretical distributions by assessing fit at the distribution tails (Q-Q plot) and center (P-P plot).

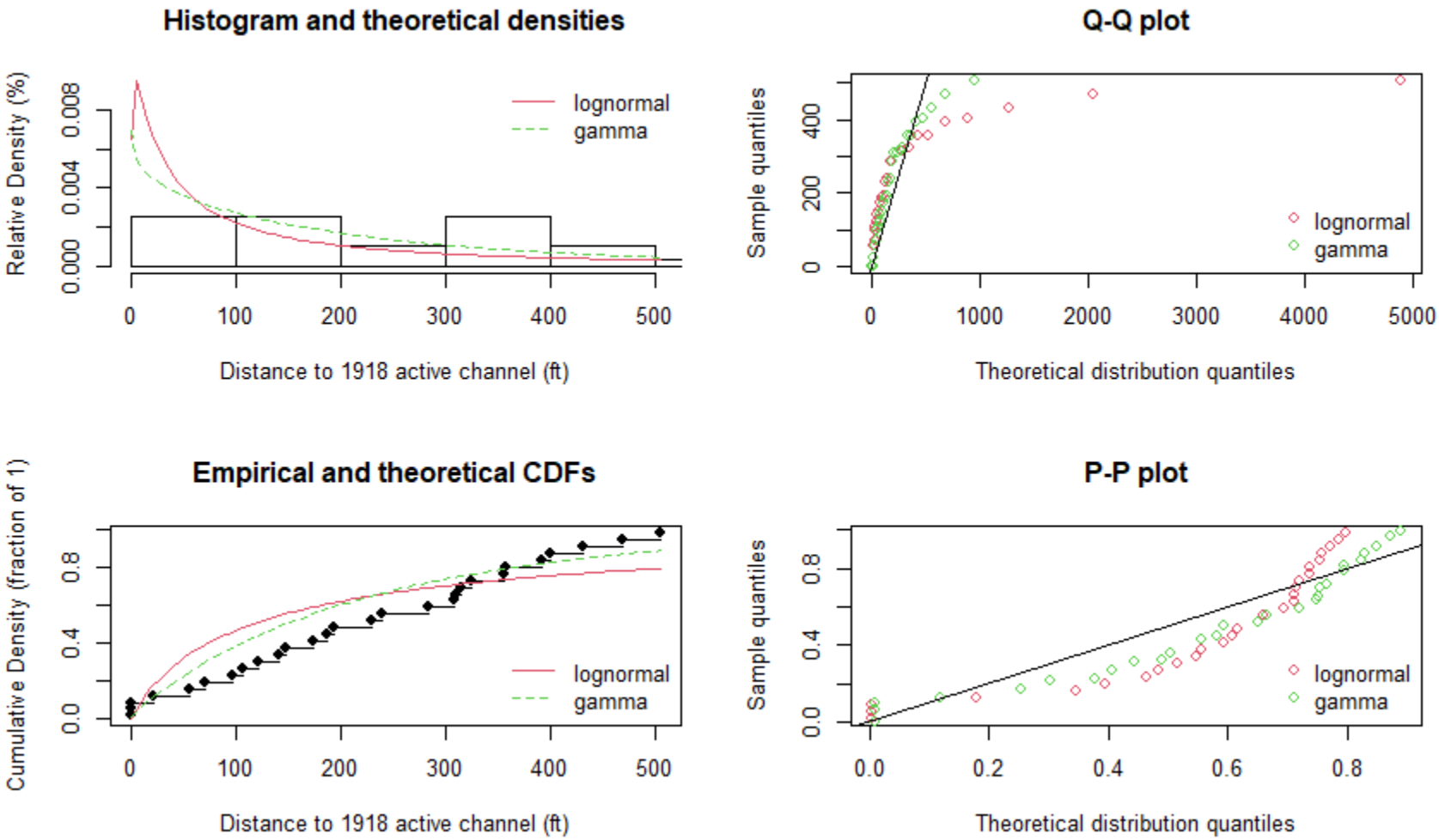

Figure 58. Goodness of fit plots:1918 active channel distance to correlated borehole locations. The two graphs on the left show the theoretical gamma and lognormal distributions plotted against the sample set PDF (top plot) and CDF (bottom plot). The two graphs on the right evaluate the sample set against the theoretical distributions by assessing fit at the distribution tails (Q-Q plot) and center (P-P plot).

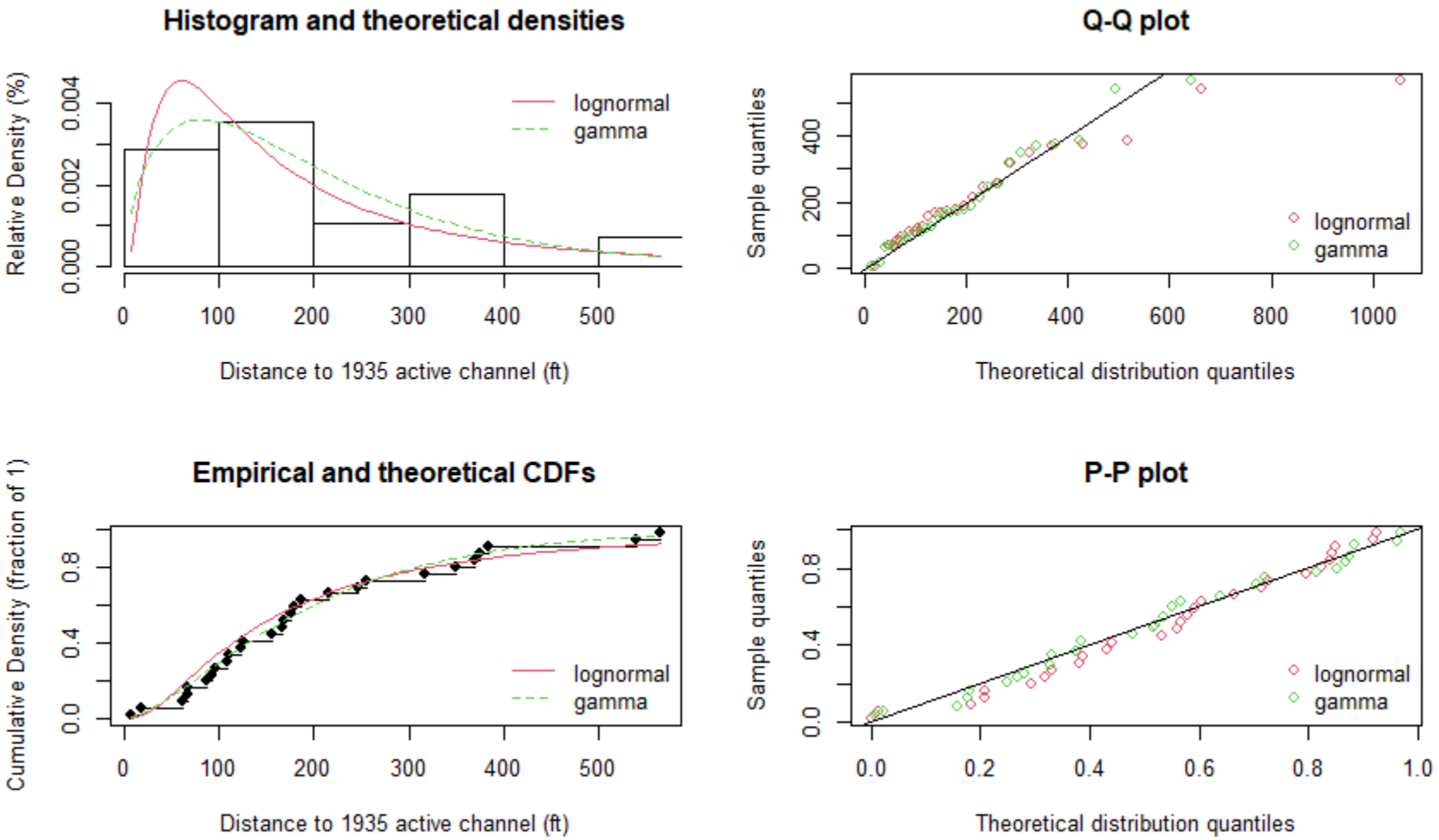

Figure 59. Goodness of fit plots: 1935 active channel distance to correlated borehole locations. The two graphs on the left show the theoretical gamma and lognormal distributions plotted against the sample set PDF (top plot) and CDF (bottom plot). The two graphs on the right evaluate the sample set against the theoretical distributions by assessing fit at the distribution tails (Q-Q plot) and center (P-P plot).

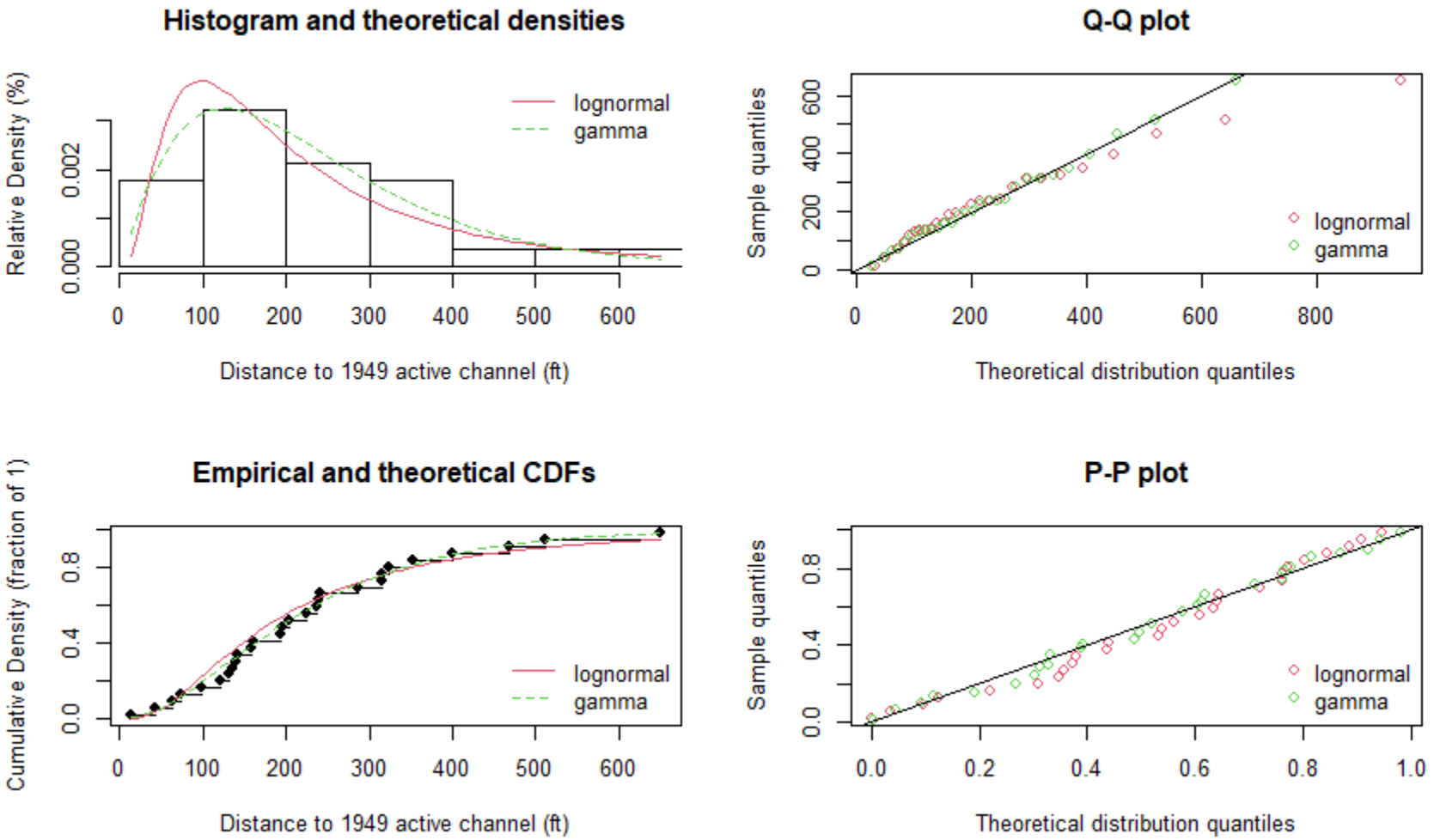

Figure 60. Goodness of fit plots:1949 active channel distance to correlated borehole locations. The two graphs on the left show the theoretical gamma and lognormal distributions plotted against the sample set PDF (top plot) and CDF (bottom plot). The two graphs on the right evaluate the sample set against the theoretical distributions by assessing fit at the distribution tails (Q-Q plot) and center (P-P plot).

Distance to Active Channel Computations

Comparison of the sample sets to theoretical distribution function conditions (Mun 2008) can help assess the best fitting theoretical distribution to the sample data (Delignette-Muller and Dutang 2015; Erhardt et al. 2015; Frost 2019; Mun 2008). This was done to check the normal, log-normal, and gamma distributions for the tested sample sets. This provides a more quantitative assessment of distribution fit than just a visual assessment. The null hypothesis for each of these tests is that the data fits the theoretical distribution. Thus, high p-values indicate that the null hypothesis cannot be rejected. Small p-values (<0.005) indicate that the null hypothesis can be rejected as the provided sample data does not fit that theoretical distribution (Frost 2019). The last function of the code was to provide the best-fit distribution parameters for the gamma and lognormal distributions. The computations performed for this analysis are provided in the figures below.

```
Fitting of the distribution ' gamma ' by maximum likelihood
Parameters :
      estimate  Std. Error
shape 3.58847800 0.528831373
rate  0.04467483 0.007063089
Loglikelihood:  -425.5853   AIC:  855.1706   BIC:  860.0323
Correlation matrix:
       shape     rate
shape 1.0000000 0.9313484
rate  0.9313484 1.0000000

> fln <- fitdist(Amer.R$Dist1935, "lnorm")
> summary (fln)
Fitting of the distribution ' lnorm ' by maximum likelihood
Parameters :
      estimate Std. Error
meanlog 4.240299 0.06270076
sdlog   0.574662 0.04433553
Loglikelihood:  -428.8422   AIC:  861.6844   BIC:  866.546
Correlation matrix:
      meanlog sdlog
meanlog      1    0
sdlog        0    1

Test of fit for the Gamma distribution

data:  Amer.R$Dist1935
V = -0.82355, p-value = 0.5603

> lnorm_test(Amer.R$Dist1935) # lognormal test for untransformed data

            Test for the lognormal distribution based on a transformation to normality

data:  Amer.R$Dist1935
p-value = 0.03235

> normal_test(Amer.R$Dist1935) #n

            Correlation test for normality

data:  Amer.R$Dist1935
R = 0.99079, p-value = 0.005767
alternative hypothesis: Amer.R$Dist1935 does not follow a normal distribution.
```

Figure 61. Distribution fits: 1918 active channel distance from 2019 points of interest.

```
Fitting of the distribution ' gamma ' by maximum likelihood
Parameters :
      estimate  Std. Error
shape 3.58847800 0.528831373
rate  0.04467483 0.007063089
Loglikelihood:  -425.5853   AIC:  855.1706   BIC:  860.0323
Correlation matrix:
       shape     rate
shape 1.0000000 0.9313484
rate  0.9313484 1.0000000

> fln <- fitdist(Amer.R$Dist1935, "lnorm")
> summary (fln)
Fitting of the distribution ' lnorm ' by maximum likelihood
Parameters :
      estimate Std. Error
meanlog 4.240299 0.06270076
sdlog   0.574662 0.04433553
Loglikelihood:  -428.8422   AIC:  861.6844   BIC:  866.546
Correlation matrix:
      meanlog sdlog
meanlog      1    0
sdlog        0    1

Test of fit for the Gamma distribution

data:  Amer.R$Dist1935
V = -0.82355, p-value = 0.5603

> lnorm_test(Amer.R$Dist1935) # lognormal test for untransformed data

            Test for the lognormal distribution based on a transformation to normality

data:  Amer.R$Dist1935
p-value = 0.03235

> normal_test(Amer.R$Dist1935) #normal test for untransformed data

            Correlation test for normality

data:  Amer.R$Dist1935
R = 0.99079, p-value = 0.005767
```

Figure 62. Distribution fits: 1935 active channel distance from 2019 points of interest.

```
Fitting of the distribution ' gamma ' by maximum likelihood
Parameters :
      estimate  Std. Error
shape 3.13502829 0.459115411
rate  0.03776083 0.005992987
Loglikelihood:  -432.7403   AIC:  869.4807   BIC:  874.3423
Correlation matrix:
       shape     rate
shape 1.000000 0.921659
rate  0.921659 1.000000

> fln <- fitdist(Amer.R$Dist1949, "lnorm")
> summary (fln)
Fitting of the distribution ' lnorm ' by maximum likelihood
Parameters :
       estimate Std. Error
meanlog 4.2511688 0.06460344
sdlog   0.5921003 0.04568095
Loglikelihood:  -432.2664   AIC:  868.5327   BIC:  873.3944
Correlation matrix:
      meanlog sdlog
meanlog      1    0
sdlog        0    1

>
> #distribution tests for sample set
> gamma_test(Amer.R$Dist1949) #gamma test for untransformed data

              Test of fit for the Gamma distribution

data:  Amer.R$Dist1949
V = 1.2444, p-value = 0.3789

> lnorm_test(Amer.R$Dist1949) # lognormal test for untransformed data

              Test for the lognormal distribution based on a transformation to normality

data:  Amer.R$Dist1949
p-value = 0.599

> normal_test(Amer.R$Dist1949) #normal test for untransformed data

              Correlation test for normality

data:  Amer.R$Dist1949
R = 0.97323, p-value = 0.000103
alternative hypothesis: Amer.R$Dist1949 does not follow a normal distribution.
```

Figure 63. Distribution fits: 1949 active channel distance from 2019 points of interest.

```
Fitting of the distribution ' gamma ' by maximum likelihood
Parameters :
       estimate   Std. Error
shape 0.494837607 0.0370569071
rate  0.002212214 0.0001810947
Loglikelihood:  -1156.911   AIC:  2317.821   BIC:  2324.283
Correlation matrix:
       shape     rate
shape 1.0000000 0.4740543
rate  0.4740543 1.0000000

> fln <- fitdist(Amer.R$Dist1918, "lnorm")
> summary (fln)
Fitting of the distribution ' lnorm ' by maximum likelihood
Parameters :
      estimate Std. Error
meanlog 4.124976  0.1772683
sdlog   2.424108  0.1253475
Loglikelihood:  -1202.294   AIC:  2408.587   BIC:  2415.05
Correlation matrix:
      meanlog sdlog
meanlog      1    0
sdlog        0    1



Test of fit for the Gamma distribution

data:  Amer.R$Dist1918
V = -5.2818, p-value = 0.0001879

> lnorm_test(Amer.R$Dist1918) # lognormal test for untransformed data

            Test for the lognormal distribution based on a transformation to normality

data:  Amer.R$Dist1918
p-value < 2.2e-16

> normal_test(Amer.R$Dist1918) #normal test for untransformed data

            Correlation test for normality

data:  Amer.R$Dist1918
R = 0.99505, p-value = 0.003845
alternative hypothesis: Amer.R$Dist1918 does not follow a normal distribution.
```

Figure 64. Distribution fits: 1918 active channel distance from borehole locations.

```
Fitting of the distribution ' gamma ' by maximum likelihood
Parameters :
       estimate   Std. Error
shape 0.686270305 0.0564278204
rate  0.003294926 0.0003436835
Loglikelihood:  -1175.198   AIC:  2354.397   BIC:  2360.859
Correlation matrix:
       shape     rate
shape 1.0000000 0.6525377
rate  0.6525377 1.0000000

> fln <- fitdist(Amer.R$Dist1935, "lnorm")
> summary (fln)
Fitting of the distribution ' lnorm ' by maximum likelihood
Parameters :
      estimate Std. Error
meanlog 4.456063  0.1412327
sdlog   1.931329  0.0998665
Loglikelihood:  -1221.71   AIC:  2447.421   BIC:  2453.883
Correlation matrix:
          meanlog       sdlog
meanlog  1.000000e+00 -4.008717e-10
sdlog   -4.008717e-10  1.000000e+00


Test of fit for the Gamma distribution

data:  Amer.R$Dist1935
V = -2.8468, p-value = 0.04412

> lnorm_test(Amer.R$Dist1935) # lognormal test for untransformed data

            Test for the lognormal distribution based on a transformation to normality

data:  Amer.R$Dist1935
p-value = 9.943e-16

> normal_test(Amer.R$Dist1935) #norm

            Correlation test for normality

data:  Amer.R$Dist1935
R = 0.95521, p-value = 1.58e-07
alternative hypothesis: Amer.R$Dist1935 does not follow a normal distribution.
```

Figure 65. Distribution fits: 1935 active channel distance from borehole locations.

```
Fitting of the distribution ' gamma ' by maximum likelihood
Parameters :
       estimate   Std. Error
shape 1.027531279 0.0820060121
rate  0.002938163 0.0002578838
Loglikelihood:  -1282.264   AIC:  2568.529   BIC:  2574.991
Correlation matrix:
       shape     rate
shape 1.0000000 0.7050375
rate  0.7050375 1.0000000

> fln <- fitdist(Amer.R$Dist1949, "lnorm")
> summary (fln)
Fitting of the distribution ' lnorm ' by maximum likelihood
Parameters :
      estimate Std. Error
meanlog 5.297470 0.10941916
sdlog   1.496285 0.07737088
Loglikelihood:  -1331.327   AIC:  2666.653   BIC:  2673.116
Correlation matrix:
          meanlog       sdlog
meanlog 1.000000e+00 2.406141e-10
sdlog   2.406141e-10 1.000000e+00
Test of fit for the Gamma distribution

data:  Amer.R$Dist1949
V = -4.1622, p-value = 0.00325

> lnorm_test(Amer.R$Dist1949) # lognormal test for untransformed data

            Test for the lognormal distribution based on a transformation to normality

data:  Amer.R$Dist1949
p-value = 1.282e-15

> normal_test(Amer.R$Dist1949) #normal test for untransformed data

            Correlation test for normality

data:  Amer.R$Dist1949
R = 0.98469, p-value = 4.407e-05
alternative hypothesis: Amer.R$Dist1949 does not follow a normal distribution.
```

Figure 66. Distribution fits: 1949 active channel distance from borehole locations.

```
Fitting of the distribution ' gamma ' by maximum likelihood
Parameters :
       estimate  Std. Error
shape 0.881997002 0.193231585
rate  0.003948511 0.001063933
Loglikelihood:  -179.2938   AIC:  362.5876   BIC:  365.252
Correlation matrix:
        shape     rate
shape 1.0000000 0.7192763
rate  0.7192763 1.0000000

> fln <- fitdist(Amer.R$Dist1918, "lnorm")
> summary (fln)
Fitting of the distribution ' lnorm ' by maximum likelihood
Parameters :
      estimate Std. Error
meanlog 4.744373  0.3373604
sdlog   1.785144  0.2385495
Loglikelihood:  -188.7987   AIC:  381.5974   BIC:  384.2618
Correlation matrix:
      meanlog sdlog
meanlog      1    0
sdlog        0    1
```

```
data:  Amer.R$Dist1918
V = -2.8522, p-value = 0.04372

> lnorm_test(Amer.R$Dist1918) # lognormal test for untransformed data

            Test for the lognormal distribution based on a transformation to normality

data:  Amer.R$Dist1918
p-value = 1.924e-06

> normal_test(Amer.R$Dist1918) #normal test for untransformed data

            Correlation test for normality

data:  Amer.R$Dist1918
R = 0.99825, p-value = 0.6808
alternative hypothesis: Amer.R$Dist1918 does not follow a normal distribution.
```

Figure 67. Distribution fits: 1918 active channel distance from correlated borehole locations.

```
Fitting of the distribution ' gamma ' by maximum likelihood
Parameters :
       estimate  Std. Error
shape 1.674064555 0.399699605
rate  0.008350927 0.002286809
Loglikelihood:  -174.4877   AIC:  352.9755   BIC:  355.6399
Correlation matrix:
       shape     rate
shape 1.0000000 0.8507299
rate  0.8507299 1.0000000

> fln <- fitdist(Amer.R$Dist1935, "lnorm")
> summary (fln)
Fitting of the distribution ' lnorm ' by maximum likelihood
Parameters :
       estimate Std. Error
meanlog 4.9730158  0.1788008
sdlog   0.9461249  0.1264306
Loglikelihood:  -177.4241   AIC:  358.8481   BIC:  361.5125
Correlation matrix:
      meanlog sdlog
meanlog      1    0
sdlog        0    1
```

```
Test of fit for the Gamma distribution

data:  Amer.R$Dist1935
V = -0.73787, p-value = 0.6018

> lnorm_test(Amer.R$Dist1935) # lognormal test for untransformed data

        Test for the lognormal distribution based on a transformation to normality

data:  Amer.R$Dist1935
p-value = 0.01257

> normal_test(Amer.R$Dist1935) #normal te

        Correlation test for normality

data:  Amer.R$Dist1935
R = 0.98318, p-value = 0.02036
alternative hypothesis: Amer.R$Dist1935 does not follow a normal distribution.
```

Figure 68. Distribution fits: 1935 active channel distance from correlated borehole locations.

```
Fitting of the distribution ' gamma ' by maximum likelihood
Parameters :
      estimate  Std. Error
shape 2.213687467 0.537839329
rate  0.009622499 0.002594178
Loglikelihood:  -176.1674   AIC:  356.3349   BIC:  358.9993
Correlation matrix:
       shape     rate
shape 1.0000000 0.8847916
rate  0.8847916 1.0000000

> fln <- fitdist(Amer.R$Dist1949, "lnorm")
> summary (fln)
Fitting of the distribution ' lnorm ' by maximum likelihood
Parameters :
      estimate Std. Error
meanlog 5.1955188  0.1489894
sdlog   0.7883778  0.1053507
Loglikelihood:  -178.547   AIC:  361.0941   BIC:  363.7585
Correlation matrix:
      meanlog sdlog
meanlog      1    0
sdlog        0    1


Test of fit for the Gamma distribution

data:  Amer.R$Dist1949
V = -0.66929, p-value = 0.636

> lnorm_test(Amer.R$Dist1949) # lognormal test for untransformed data

        Test for the lognormal distribution based on a transformation to normality

data:  Amer.R$Dist1949
p-value = 0.05266

> normal_test(Amer.R$Dist1949) #normal test for untransformed data

        Correlation test for normality

data:  Amer.R$Dist1949
R = 0.98652, p-value = 0.03589
alternative hypothesis: Amer.R$Dist1949 does not follow a normal distribution.
```

Figure 69. Distribution fits: 1949 active channel distance from correlated borehole locations.

R Code

```
#Load libraries
library(ggplot2)
library(gridExtra)
library(car)
library(nortest)
library(ggpubr)
library(fitdistrplus)
library(goft)
library(actuar)
library(triangle)
library(outliers)
library(robustloggamma)

#import csv file
#import values for flow bins. The bins cover the range of flow values. The value between each of these nodes was used as input values to generate the underlying distribution function.
Amer.R <- read.csv(file.choose(), head = TRUE, row.names= NULL, na.strings="NA") #navigate to .csv file.
Amer.R is a dataframe.
summary(Amer.R) #Look at data, basic stats
str(Amer.R) #know the structure of the dataframe

##1. Visualize data: This sequence of plots allow you to visually evaluate shape of data, in order:
# run chunk of code to grid.arrange to see plots.
ph <- ggplot(Amer.R, aes(x=Dist1918)) # a) histogram, with kernal density curve
ph <- ph + geom_histogram(aes(y=..density..))
ph <- ph + geom_density(alpha=0.1, fill="white")
ph <- ph + labs(x="Distance to 1918 active channel (ft)")
ph <- ph + geom_rug()

pv <- ggplot(Amer.R, aes(x="Density", y =Dist1918)) #b) violin plot,
pv <- pv + geom_violin(fill="gray50")
pv <- pv + geom_boxplot(width = 0.2, alpha = 3/4)
pv <- pv + labs(y="Distance to 1918 active channel (ft)")
ph <- ph + geom_rug()
pv <- pv + coord_flip()

pb <- ggplot(Amer.R, aes(x = "Density", y =Dist1918)) #c) boxplot - highlights outliers
pb <- pb + geom_boxplot()
pb <- pb + labs(y="Distance to 1918 active channel (ft)")
ph <- ph + geom_rug()
pb <- pb + coord_flip()

grid.arrange(ph, pv, pb, ncol=1)
```

Figure 70. First part of R code for processing statistical data for the active channel distances from the POIs, the overall boreholes, and the correlated boreholes. Green coloring reflects text that explains function of the code. Only the code for the 1918 active channel distances is shown. The 1935 and 1949 code is similar just replaces the year.

```
##histogram plots with varying bin width - adjust bin width # if needed
p1 <- ggplot(Amer.R, aes(x=Dist1918))
p1 <- p1 + geom_histogram(binwidth =50)
p1 <- p1 + geom_rug()
p1 <- p1 + labs(x="Distance to 1918 active channel (ft)")
p1 <- p1 + labs(title = "bin width 50")
print(p1)

p2 <- ggplot(Amer.R, aes(x=Dist1918))
p2 <- p2 + geom_histogram(binwidth =20)
p2 <- p2 + geom_rug()
p2 <- p2 + labs(x="Distance to 1918 active channel (ft)")
p2 <- p2 + labs(title = "bin width 20")
print(p2)

p3 <- ggplot(Amer.R, aes(x=Dist1918))
p3 <- p3 + geom_histogram(binwidth =10)
p3 <- p3 + geom_rug()
p3 <- p3 + labs(x="Distance to 1918 active channel (ft)")
p3 <- p3 + labs(title = "bin width 10")
print(p3)

# Graphics using firdistrplus package to see how data potentially fit lognormal distributions
fg <- fitdist(Amer.R$Dist1918, "gamma")
summary(fg)
fln <- fitdist(Amer.R$Dist1918, "lnorm")
summary (fln)
par(mfrow = c(2,2)) # 2x2 arrangement of figures
plot.legend <- c("lognormal", "gamma")
denscomp(list(fln, fg), legendtext = plot.legend, xlab = "Distance to 1918 active channel (ft)", ylab = "Relative
Density (%)")
qqcomp(list(fln, fg), legendtext = plot.legend, xlab = "Theoretical distribution quantiles", ylab = "Sample quantiles")
cdfcomp(list(fln, fg), legendtext = plot.legend, xlab = "Distance to 1918 active channel (ft)", ylab = "Cumulative
Density (fraction of 1)")
ppcomp(list(fln, fg), legendtext = plot.legend, xlab = "Theoretical distribution quantiles", ylab = "Sample quantiles")

#distribution tests for sample set
gamma_test(Amer.R$Dist1918) #gamma test for untransformed data
lnorm_test(Amer.R$Dist1918) # lognormal test for untransformed data
normal_test(Amer.R$Dist1918) #normal test for untransformed data
```

Figure 71. Second part of R code for processing statistical data for the active channel distances from the POIs, the overall boreholes, and the correlated boreholes. Green coloring reflects text that explains function of the code. Only the code for the 1918 active channel distances is shown. The 1935 and 1949 code is similar just replaces the year.

Summary Statistics

There are certain summary statistics that can provide an exploratory assessment of the underlying sample sets and help assess if there are any correlations. The sample sets assessed as part of this analysis include the following:

- Planform type (1918, 1935, and 1949) at the filtered 2019 issue locations
- Planform type (1918, 1935, and 1949) at the borehole locations
- Distance to active channel for 2019 issue locations (1918, 1935, and 1949 planforms)

- Distance to active channel for the borehole locations (1918, 1935, and 1949 planforms).
- Distance to active channel for the borehole locations correlated to the 2019 issue locations (1918, 1935, and 1949 planforms).
- 2019 issue locations correlated to the 1918 “vegetated island” planform
- Borehole locations correlated to the 1918 “vegetated island” planform
- The 2006 seepage rating for the 2019 issue locations
- The 2006 slope stability ratings for the 2019 issue locations
- Riverside drain d_{16} at the 2019 issue locations
- Riverside drain d_{50} at the 2019 issue locations
- Riverside drain d_{84} at the 2019 issue locations
- Landside Toe d_{16} at the 2019 issue locations
- Landside Toe d_{50} at the 2019 issue locations
- Landside Toe d_{84} at the 2019 issue locations
- Levee Centerline d_{16} at the 2019 issue locations
- Levee Centerline d_{50} at the 2019 issue locations
- Levee Centerline d_{84} at the 2019 issue locations
- Riverside Toe d_{16} at the 2019 issue locations
- Riverside Toe d_{50} at the 2019 issue locations
- Riverside Toe d_{84} at the 2019 issue locations
- River Centerline d_{16} at the 2019 issue locations
- River Centerline d_{50} at the 2019 issue locations
- River Centerline d_{84} at the 2019 issue locations

A total of 16 summary statistics were utilized in this analysis. The specific statistics and their definitions are provided in the Definitions section. The computed statistics are provided in the Summary Statistics Computation section. Patterns in the summary statistics were explored through the use of heat maps and pie charts. These are provided in the Summary Statistics Graphics section.

Colors utilized in the heat maps were chosen to help assess the degree of correlation. Reds are associated with strong correlations, while greens are weak correlations. Yellow was chosen as moderate correlation strength. The values utilized in the color formatting choices are subjective but were chosen to be consistent with the estimated error for a normal distribution. An error of 50 feet was used to represent the sample central tendency from the true sample central tendency for the active channel distance. An error of one unit was utilized in the assessment of the vegetated island planform types and the seepage/slope stability assessments. The chosen error is used to assess the minimum number of samples that are needed to have 95% confidence level in the central tendency +/- the error estimate, assuming a normal distribution. This provides a check on whether the sample size is adequate (e.g., if the computed minimum sample size is larger than the sample set size then there is a high probability that the sample set does not adequately reflect a measure of the population, which may create a bias in the underlying statistics.

The numerical values utilized for the color coding were based on the summary statistic types: first through fourth moments. The first moment of the sample set, or the central tendency (mean, mode, minimum, Q_1, median, Q_3, maximum, and Tukey's Trimean), helps understand how correlated a historical channel location is to the location of interest or the boreholes. Distances between zero and 50 ft were considered to be strongly correlated, while distances greater than 100 ft were considered to be only weakly correlated. Distance between 50 and 100 ft were assigned a moderate correlation. The 1918 vegetative islands only had a binary response, so one is strongly correlate and two is weakly correlated. The 2006 seepage and slope stability ratings were assigned a strong correlation if the central tendency had a value of three, while a moderate correlation was assigned for a value of two and a weak correlation assigned for a value of one.

The second moment of the sample, or the dispersion of the data points (standard deviation and the coefficient of variation, C_v), tell us if the central tendency is very strong or weak. A strong tendency (small values) would support the hypothesis of a strong correlation between active channel locations and the 2019 areas of interest. Distances between zero and 50 ft were considered to be strongly correlated, while distances greater than 100 ft were considered to be only weakly correlated. Distance between 50 and 100 ft were assigned a moderate correlation. For the vegetated island and seepage/slope stability assessments a strong correlation had to be less than 0.5 units. Values greater than one unit were considered weak correlations, while between a value of 0.5 and one had a moderate correlation.

The third moment of the sample is shown by the skewness. Values of zero suggest a normal distribution. Positive or negative skews would indicate there are large outlying values which would argue for a weaker correlation between active channel locations and the areas of interest. Skewness absolute values of one to zero were considered to be indicative of a strong correlation, while an absolute value greater than one is considered a weak correlation. No moderate correlations are utilized with the skew.

Finally, the fourth moment of the sample is shown by the kurtosis. The normal distribution has a kurtosis of 3, so lower values indicate a tighter grouping of the data than a normal distribution and would indicate support for a stronger correlation. Larger values suggest the data is spread out a lot more (peak is squished) and thus indicates a lower correlation. Kurtosis values of three or less are considered a strong correlation, while kurtosis values greater than three have a weak correlation. No moderate correlations are utilized with the kurtosis.

Definitions

The summary statistics explored for this analysis, along with their definitions are shown below:

- **Count** – the number of records in the sample.
- **Minimum** – minimum value from the sample.
- **Maximum** – maximum value from the sample.
- **Range** – difference between the minimum and maximum value from the sample.

- **Mean** – arithmetic average of the sample (see Equation 3)

Equation 3. Mean (Microsoft 2019a)

$$\bar{x} = \frac{\sum_{i=1}^{n} x_i}{n}$$

Where $\bar{x}$ = the sample mean, x = the individual values from the sample record, and n = the number of records in the sample.

- **Median** – middle value of the sample or the average of the middle two numbers.
- **Mode** – the value repeated most often in the sample.
- **Q_1** – the value of the sample associated with the first quartile of the data (e.g., 25% of the data is lower than this value).
- **Q_3** – the value of the sample associated with the third quartile of the data (e.g., 75% of the data is lower than this value).
- **Standard Deviation** – measure of the variation of values around the mean (see Equation 4).

Equation 4. Sample standard Deviation (Microsoft 2019d)

$$s = \sqrt{\frac{\sum(x - \bar{x})^2}{(n-1)}}$$

Where s = the sample standard deviation, x = the individual values from the sample record, $\bar{x}$ = the sample mean, and n = the number of records in the sample.

- **Skewness** – measure of the sample distribution compared to a normal distribution (see Equation 5).

Equation 5. Skewness (Microsoft 2019c)

$$skewness = \frac{n}{(n-1)(n-2)} \sum_{i=1}^{n} \left(\frac{x_i - \bar{x}}{s}\right)^3$$

Where n = the number of records in the sample, x = the individual values from the sample record, $\bar{x}$ = the sample mean, and s = the sample standard deviation.

- **Kurtosis** – measure of the peakness or flatness of a distribution compared to a normal distribution (see Equation 6).

Equation 6. Kurtosis (Microsoft 2019b)

$$Kurtosis = \left\{\frac{n(n+1)}{(n-1)(n-2)(n-3)} \sum \left(\frac{x_i - \bar{x}}{s}\right)^4\right\} - \frac{3(n-1)^2}{(n-2)(n-3)}$$

Where n = the number of records in the sample, x = the individual values from the sample record, $\bar{x}$ = the sample mean, and s = the sample standard deviation.

- **Coefficient of Variation** – description of the standard deviation relative to the mean (Triola 2008), providing a unitless comparison of values from the sample that can be compared to other samples (see Equation 7). This is also considered a more robust measure of the sample's central tendency.

  Equation 7. Coefficient of Variation (Triola 2008)

  $$CV = \frac{s}{\bar{x}} * 100\%$$

  Where CV = coefficient of variation, $\bar{x}$ = the sample mean, and s = the sample standard deviation.

- **Minimum sample number** – estimate of the minimum number of records needed to provide a 95% confidence level that the sample mean is +/- the listed value from the population mean (see Equation 8). This assumes the sample has a normal distribution.

  Equation 8. Minimum sample number (Weaver 2000)

  $$n_m = \left[\frac{z_{\alpha/2}s}{E}\right]^2$$

  Where n_m = minimum sample number to ensure sample mean is +/- X from population mean with 95% confidence (assumes sample has a normal distribution), s = the sample standard deviation, $z_{\alpha/2}$ = the z value (1.96) associated with an alpha/2 value of .025. Lookup value is 1-α/2 or (0.975), α = the area under the curve not represented by the normal distribution. The confidence interval is related to 1-α, and E = the max error (+/-) around the sample mean for estimating the population mean.

- **Error estimate** – Given the sample number, this is the error estimate (see Equation 9) of the sample mean for the population mean. Value is given for +/- the listed units.

  Equation 9. Error estimate (Weaver 2000)

  $$E = \frac{z_{\alpha/2}s}{\sqrt{n}}$$

  Where n = number of records in the sample, s = the sample standard deviation, $z_{\alpha/2}$ = the z value (1.96) associated with an alpha/2 value of .025. Lookup value is 1-α/2 or (0.975) These values assume that the sample is normally distributed, α = the area under the curve not represented by the normal distribution. The confidence interval is related to 1-α, and E = the max error (+/-) around the sample mean for estimating the population mean (assumes record is normally distributed).

- **Tukey's Trimean** – a more robust measure of the sample central tendency (see Equation 10).

Equation 10. Tukey's Trimean (Glen 2023)

$$TM = \frac{Q_1 + 2Q_2 + Q_3}{4}$$

Where TM = Tukey's trimean, Q_1 is the first quartile value of the sample set, Q_2 is the second quartile (or median) of the sample set, and Q_3 is the third quartile value of the sample set.

Summary Statistics Computations

The summary statistics computed for each of the attributes are shown in the following figures.

Distance to Active Channel: 1918 Planform Statistics

Descriptive Statistics - All

Column1	
Mean	82.88641
Standard Error	6.633063
Median	92.71323
Mode	0
Standard Deviation	60.79302
Sample Variance	3695.792
Kurtosis	-1.19679
Skewness	-0.02724
Range	210.9887
Minimum	0
Maximum	210.9887
Sum	6962.458
Count	84
Confidence Level(95.0%)	13.19289
Coefficient of Variation (CV)	73.34
min sample number for 95% CI	6
Error	50 ft
Error Estimate	13.01
Quartile 1	28 ft
Quartile 3	134 ft
Tukey's Trimean	87 ft

Distance to Active Channel: 1935 Planform Statistics

Descriptive Statistics - All

Column1	
Mean	80.32096
Standard Error	4.509059
Median	73.08548
Mode	#N/A
Standard Deviation	41.32621
Sample Variance	1707.855
Kurtosis	0.663093
Skewness	0.814571
Range	189.1376
Minimum	10.58424
Maximum	199.7218
Sum	6746.961
Count	84
Confidence Level(95.0%)	8.968337
Coefficient of Variation (CV)	51.45
min sample number for 95% CI	3
Error	50 ft
Error Estimate	8.84
Quartile 1	49 ft
Quartile 3	106 ft
Tukey's Trimean	75 ft

Figure 72. Summary statistics for the 2019 issue locations: 1918 and 1935 planforms.

Distance to Active Channel: 1949 Planform Statistics
Descriptive Statistics - All

Column1	
Mean	83.01941
Standard Error	5.419877
Median	73.93498
Mode	#N/A
Standard Deviation	49.67399
Sample Variance	2467.505
Kurtosis	1.626149
Skewness	1.32155
Range	221.973
Minimum	15.08445
Maximum	237.0574
Sum	6973.63
Count	84
Confidence Level(95.0%)	10.77992
(CV)	59.83
min sample number for 95% CI	4
Error	50 ft
Error Estimate	10.63
Quartile 1	50 ft
Quartile 3	106 ft
Tukey's Trimean	76 ft

1918 "vegetated island" planform
Descriptive Statistics - All

Column1		
Mean	1.892857	
Standard Error	0.03395	
Median	2	
Mode	2	
Standard Deviation	0.311152	
Sample Variance	0.096816	
Kurtosis	4.805219	
Skewness	-2.58676	
Range	1	
Minimum	1	
Maximum	2	
Sum	159	
Count	84	
Confidence Level(95.0%)	0.067524	Coefficient of Variation
Coefficient of Variation (CV)	16.44	
min sample number for 95% CI	1	
Error	1	unit
Error Estimate	0.07	
Quartile 1	2	unit
Quartile 3	2	unit
Tukey's Trimean	2	unit

Figure 73. Summary statistics for the 2019 issue locations: 1949 and 1918 vegetated island planform.

2006 seepage rating

Descriptive Statistics - All

Column1	
Mean	2.119048
Standard Error	0.103586
Median	3
Mode	3
Standard Deviation	0.949379
Sample Variance	0.90132
Kurtosis	-1.87361
Skewness	-0.24317
Range	2
Minimum	1
Maximum	3
Sum	178
Count	84
Confidence Level(95.0%)	0.206028
Coefficient of Variation (CV)	44.80
min sample number for 95% CI	4
Error	1 unit
Error Estimate	0.21
Quartile 1	1 unit
Quartile 3	3 unit
Tukey's Trimean	3 unit

2006 slope stability rating

Descriptive Statistics - All

Column1	
Mean	1.654762
Standard Error	0.052187
Median	2
Mode	2
Standard Deviation	0.478301
Sample Variance	0.228772
Kurtosis	-1.5992
Skewness	-0.66291
Range	1
Minimum	1
Maximum	2
Sum	139
Count	84
Confidence Level(95.0%)	0.103798
Coefficient of Variation (CV)	28.90
min sample number for 95% CI	1
Error	1 unit
Error Estimate	0.11
Quartile 1	1 unit
Quartile 3	2 unit
Tukey's Trimean	2 unit

Figure 74. Summary statistics for the 2019 issue locations: 2006 seepage and slope stability ratings.

2019 Issue Location: Riverside Drain d_{16}

Descriptive Statistics - All

Column1		
Mean	5.011905	
Standard Error	0.106439	
Median	5	
Mode	6	
Standard Deviation	0.975533	
Sample Variance	0.951664	
Kurtosis	-1.80584	
Skewness	-0.10398	
Range	3	
Minimum	3	
Maximum	6	
Sum	421	
Count	84	
Confidence Level(95.0%)	0.211704	
Coefficient of Variation (CV)	19.46	
min sample number for 95% CI	4	
Error	1	unit
Error Estimate	0.21	
Quartile 1	4	unit
Quartile 3	6	unit
Tukey's Trimean	5	unit

2019 Issue Location: Riverside Drain d_{50}

Descriptive Statistics - All

Column1		
Mean	3.940476	
Standard Error	0.126008	
Median	4	
Mode	5	
Standard Deviation	1.154887	
Sample Variance	1.333764	
Kurtosis	-0.61001	
Skewness	-0.16998	
Range	5	
Minimum	1	
Maximum	6	
Sum	331	
Count	84	
Confidence Level(95.0%)	0.250626	
Coefficient of Variation (CV)	29.31	
min sample number for 95% CI	6	
Error	1	unit
Error Estimate	0.25	
Quartile 1	3	unit
Quartile 3	5	unit
Tukey's Trimean	4	unit

Figure 75. Summary statistics for the 2019 issue locations: Riverside Drain d_{16} and d_{50}

2019 Issue Location: Riverside Drain d_{84} Descriptive Statistics - All			2019 Issue Location: Landside Toe d_{16} Descriptive Statistics - All		
Column1			*Column1*		
Mean	2.452381		Mean	5.678571	
Standard Error	0.144119		Standard Error	0.068087	
Median	3		Median	6	
Mode	3		Mode	6	
Standard Deviation	1.320868		Standard Deviation	0.624031	
Sample Variance	1.744693		Sample Variance	0.389415	
Kurtosis	1.15982		Kurtosis	1.928476	
Skewness	-0.15158		Skewness	-1.77981	
Range	6		Range	2	
Minimum	0		Minimum	4	
Maximum	6		Maximum	6	
Sum	206		Sum	477	
Count	84		Count	84	
Confidence Level(95.0%)	0.286646		Confidence Level(95.0%)	0.135423	
Coefficient of Variation (CV)	53.86		Coefficient of Variation (CV)	10.99	
min sample number for 95% CI	7		min sample number for 95% CI	2	
Error	1	unit	Error	1	unit
Error Estimate	0.29		Error Estimate	0.14	
Quartile 1	2	unit	Quartile 1	6	unit
Quartile 3	3	unit	Quartile 3	6	unit
Tukey's Trimean	3	unit	Tukey's Trimean	6	unit

Figure 76. Summary statistics for the 2019 issue locations: Riverside Drain d_{84} and Landside Toe d_{16}

2019 Issue Location: Landside Toe d_{50}
Descriptive Statistics - All

Column1		
Mean	4.47619	
Standard Error	0.072802	
Median	4.5	
Mode	5	
Standard Deviation	0.66724	
Sample Variance	0.445209	
Kurtosis	2.837334	
Skewness	-0.9082	
Range	4	
Minimum	2	
Maximum	6	
Sum	376	
Count	84	
Confidence Level(95.0%)	0.1448	
Coefficient of Variation (CV)	14.91	
min sample number for 95% CI	2	
Error	1	unit
Error Estimate	0.15	
Quartile 1	4	unit
Quartile 3	5	unit
Tukey's Trimean	5	unit

2019 Issue Location: Landside Toe d_{84}
Descriptive Statistics - All

Column1		
Mean	2.952381	
Standard Error	0.082809	
Median	3	
Mode	3	
Standard Deviation	0.758959	
Sample Variance	0.576018	
Kurtosis	4.958703	
Skewness	-1.27496	
Range	5	
Minimum	0	
Maximum	5	
Sum	248	
Count	84	
Confidence Level(95.0%)	0.164704	
Coefficient of Variation (CV)	25.71	
min sample number for 95% CI	3	
Error	1	unit
Error Estimate	0.17	
Quartile 1	3	unit
Quartile 3	3	unit
Tukey's Trimean	3	unit

Figure 77. Summary statistics for the 2019 issue locations: Landside Toe d_{50} and d_{84}.

2019 Issue Location: Levee Centerline d_{16}
Descriptive Statistics - All

Column1		
Mean	5.595238	
Standard Error	0.053877	
Median	6	
Mode	6	
Standard Deviation	0.493794	
Sample Variance	0.243832	
Kurtosis	-1.88943	
Skewness	-0.39515	
Range	1	
Minimum	5	
Maximum	6	
Sum	470	
Count	84	
Confidence Level(95.0%)	0.10716	
Coefficient of Variation (CV)	8.83	
min sample number for 95% CI	1	
Error	1	unit
Error Estimate	0.11	
Quartile 1	5	unit
Quartile 3	6	unit
Tukey's Trimean	6	unit

2019 Issue Location: Levee Centerline d_{50}
Descriptive Statistics - All

Column1		
Mean	4.25	
Standard Error	0.081006	
Median	4	
Mode	4	
Standard Deviation	0.742432	
Sample Variance	0.551205	
Kurtosis	1.754027	
Skewness	0.101787	
Range	4	
Minimum	2	
Maximum	6	
Sum	357	
Count	84	
Confidence Level(95.0%)	0.161118	
Coefficient of Variation (CV)	17.47	
min sample number for 95% CI	3	
Error	1	unit
Error Estimate	0.16	
Quartile 1	4	unit
Quartile 3	5	unit
Tukey's Trimean	4	unit

Figure 78. Summary statistics for the 2019 issue locations: Levee Centerline d_{16} and d_{50}.

2019 Issue Location: Levee Centerline d_{84}
Descriptive Statistics - All

Column1		
Mean	2.702381	
Standard Error	0.13944	
Median	3	
Mode	3	
Standard Deviation	1.277986	
Sample Variance	1.633247	
Kurtosis	0.372348	
Skewness	-0.83817	
Range	5	
Minimum	0	
Maximum	5	
Sum	227	
Count	84	
Confidence Level(95.0%)	0.27734	
Coefficient of Variation (CV)	47.29	
min sample number for 95% CI	7	
Error	1	unit
Error Estimate	0.28	
Quartile 1	2	unit
Quartile 3	3	unit
Tukey's Trimean	3	unit

2019 Issue Location: Riverside Toe d_{16}
Descriptive Statistics - All

Column1		
Mean	5.52381	
Standard Error	0.06663	
Median	6	
Mode	6	
Standard Deviation	0.610672	
Sample Variance	0.37292	
Kurtosis	-0.15596	
Skewness	-0.90572	
Range	2	
Minimum	4	
Maximum	6	
Sum	464	
Count	84	
Confidence Level(95.0%)	0.132524	
Coefficient of Variation (CV)	11.06	
min sample number for 95% CI	2	
Error	1	unit
Error Estimate	0.14	
Quartile 1	5	unit
Quartile 3	6	unit
Tukey's Trimean	6	unit

Figure 79. Summary statistics for the 2019 issue locations: Levee Centerline d_{84} and Riverside Toe d_{16}.

2019 Issue Location: Riverside Toe d_{50}
Descriptive Statistics - All

Column1		
Mean	4.059524	
Standard Error	0.064162	
Median	4	
Mode	4	
Standard Deviation	0.588058	
Sample Variance	0.345812	
Kurtosis	2.256566	
Skewness	0.71961	
Range	3	
Minimum	3	
Maximum	6	
Sum	341	
Count	84	
Confidence Level(95.0%)	0.127616	
Coefficient of Variation (CV)	14.49	
min sample number for 95% CI	2	
Error	1	unit
Error Estimate	0.13	
Quartile 1	4	unit
Quartile 3	4	unit
Tukey's Trimean	4	unit

2019 Issue Location: Riverside Toe d_{84}
Descriptive Statistics - All

Column1		
Mean	2.547619	
Standard Error	0.102192	
Median	3	
Mode	2	
Standard Deviation	0.936602	
Sample Variance	0.877223	
Kurtosis	0.832485	
Skewness	-0.32162	
Range	5	
Minimum	0	
Maximum	5	
Sum	214	
Count	84	
Confidence Level(95.0%)	0.203255	
Coefficient of Variation (CV)	36.76	
min sample number for 95% CI	4	
Error	1	unit
Error Estimate	0.21	
Quartile 1	2	unit
Quartile 3	3	unit
Tukey's Trimean	3	unit

Figure 80. Summary statistics for the 2019 issue locations: Riverside Toe d_{50} and d_{84}.

2019 Issue Location: River Centerline d_{16}
Descriptive Statistics - All

Column1		
Mean	5.22619	
Standard Error	0.097812	
Median	6	
Mode	6	
Standard Deviation	0.896461	
Sample Variance	0.803643	
Kurtosis	-1.60864	
Skewness	-0.46656	
Range	2	
Minimum	4	
Maximum	6	
Sum	439	
Count	84	
Confidence Level(95.0%)	0.194544	
Coefficient of Variation (CV)	17.15	
min sample number for 95% CI	4	
Error	1	unit
Error Estimate	0.2	
Quartile 1	4	unit
Quartile 3	6	unit
Tukey's Trimean	6	unit

2019 Issue Location: River Centerline d_{50}
Descriptive Statistics - All

Column1		
Mean	4.059524	
Standard Error	0.097812	
Median	4	
Mode	4	
Standard Deviation	0.896461	
Sample Variance	0.803643	
Kurtosis	-0.27936	
Skewness	0.600817	
Range	3	
Minimum	3	
Maximum	6	
Sum	341	
Count	84	
Confidence Level(95.0%)	0.194544	
Coefficient of Variation (CV)	22.08	
min sample number for 95% CI	4	
Error	1	unit
Error Estimate	0.2	
Quartile 1	3	unit
Quartile 3	5	unit
Tukey's Trimean	4	unit

Figure 81. Summary statistics for the 2019 issue locations: River Centerline d_{16} and d_{50}.

2019 Issue Location: River Centerline d_{84}
Descriptive Statistics - All

Column1		
Mean	2.607143	
Standard Error	0.144727	
Median	3	
Mode	3	
Standard Deviation	1.326449	
Sample Variance	1.759466	
Kurtosis	-0.83525	
Skewness	-0.22102	
Range	5	
Minimum	0	
Maximum	5	
Sum	219	
Count	84	
Confidence Level(95.0%)	0.287857	
Coefficient of Variation (CV)	50.88	
min sample number for 95% CI	7	
Error	1	unit
Error Estimate	0.29	
Quartile 1	1	unit
Quartile 3	3	unit
Tukey's Trimean	3	unit

Figure 82. Summary statistics for the 2019 issue locations: River Centerline d_{84}.

Descriptive Statistics - All

Column1		
Mean	223.5254	
Standard Error	15.18933	
Median	199.071	
Mode	0	
Standard Deviation	207.711	
Sample Variance	43143.86	
Kurtosis	0.605299	
Skewness	0.921017	
Range	995.3899	
Minimum	0	
Maximum	995.3899	
Sum	41799.25	
Count	187	
Confidence Level(95.0%)	29.96552	
Coefficient of Variation (CV)	92.93	
min sample number for 95% CI	67	
Error	50	ft
Error Estimate	29.78	
Quartile 1	26	ft
Quartile 3	350	ft
Tukey's Trimean	193	ft

Descriptive Statistics - Only Correlated boreholes

Need to select only correlated ones

Column1		
Mean	223.2374	
Standard Error	28.47813	
Median	211.8343	
Mode	0	
Standard Deviation	150.6921	
Sample Variance	22708.1	
Kurtosis	-1.06916	
Skewness	0.111334	
Range	504.7939	
Minimum	0	
Maximum	504.7939	
Sum	6250.647	
Count	28	
Confidence Level(95.0%)	58.43229	
Coefficient of Variation (CV)	67.50	
min sample number for 95% CI	35	
Error	50	ft
Error Estimate	55.82	
Quartile 1	105	ft
Quartile 3	333	ft
Tukey's Trimean	215	ft

Figure 83. Summary statistics for the 1918 active channel distance: all and correlated boreholes.

Descriptive Statistics - All

Column1		
Mean	208.158	
Standard Error	15.33623	
Median	154.2109	
Mode	0	
Standard Deviation	209.7198	
Sample Variance	43982.41	
Kurtosis	4.962629	
Skewness	1.956691	
Range	1148.362	
Minimum	0	
Maximum	1148.362	
Sum	38925.55	
Count	187	
Confidence Level(95.0%)	30.25532	
Coefficient of Variation (CV)	100.75	
min sample number for 95% CI	68	
Error	50	ft
Error Estimate	30.06	
Quartile 1	71	ft
Quartile 3	282	ft
Tukey's Trimean	165	ft

Descriptive Statistics - Only Correlated boreholes

Need to select only correlated ones

Column1		
Mean	200.4265	
Standard Error	27.64821	
Median	168.251	
Mode	#N/A	
Standard Deviation	146.3006	
Sample Variance	21403.87	
Kurtosis	0.555071	
Skewness	1.044697	
Range	558.1469	
Minimum	7.157497	
Maximum	565.3044	
Sum	5611.942	
Count	28	
Confidence Level(95.0%)	56.72945	
Coefficient of Variation (CV)	72.99	
min sample number for 95% CI	33	
Error	50	ft
Error Estimate	54.2	
Quartile 1	94	ft
Quartile 3	271	ft
Tukey's Trimean	175	ft

Figure 84. Summary statistics for the 1935 active channel distance: all and correlated boreholes.

Descriptive Statistics - All

Column1		
Mean	349.7194	
Standard Error	20.28807	
Median	273.0344	
Mode	0	
Standard Deviation	277.4352	
Sample Variance	76970.28	
Kurtosis	0.326019	
Skewness	0.930879	
Range	1288.997	
Minimum	0	
Maximum	1288.997	
Sum	65397.52	
Count	187	
Confidence Level(95.0%)	40.02431	
Coefficient of Variation (CV)	79.33	
min sample number for 95% CI	119	
Error	50	ft
Error Estimate	39.77	
Quartile 1	135	ft
Quartile 3	524	ft
Tukey's Trimean	301	ft

Descriptive Statistics - Only Correlated boreholes

Need to select only correlated ones

Column1		
Mean	230.0220395	
Standard Error	27.99819302	
Median	199.2845471	
Mode	#N/A	
Standard Deviation	148.1525118	
Sample Variance	21949.16674	
Kurtosis	1.168886946	
Skewness	1.055498541	
Range	634.9392431	
Minimum	14.2938955	
Maximum	649.2331386	
Sum	6440.617106	
Count	28	
Confidence Level(95.0%)	57.44754684	
Coefficient of Variation (CV)	64.41	
min sample number for 95% CI	34	
Error	50	ft
Error Estimate	54.88	
Quartile 1	135	ft
Quartile 3	316	ft
Tukey's Trimean	212	ft

Figure 85. Summary statistics for the 1949 active channel distance: all and correlated boreholes.

Descriptive Statistics - All

Column1		
Mean	1.967914	
Standard Error	0.012922	
Median	2	
Mode	2	
Standard Deviation	0.1767	
Sample Variance	0.031223	
Kurtosis	26.94686	
Skewness	-5.35339	
Range	1	
Minimum	1	
Maximum	2	
Sum	368	
Count	187	
Confidence Level(95.0%)	0.025492	
Coefficient of Variation (CV)	8.98	
min sample number for 95% CI	1	
Error	1	unit
Error Estimate	0.03	
Quartile 1	2	unit
Quartile 3	2	unit
Tukey's Trimean	2	unit

Descriptive Statistics - Only Correlated boreholes

Need to select only correlated ones

Column1		
Mean	1.892857	
Standard Error	0.059524	
Median	2	
Mode	2	
Standard Deviation	0.31497	
Sample Variance	0.099206	
Kurtosis	5.613785	
Skewness	-2.68646	
Range	1	
Minimum	1	
Maximum	2	
Sum	53	
Count	28	
Confidence Level(95.0%)	0.122133	
Coefficient of Variation (CV)	16.64	
min sample number for 95% CI	1	
Error	1	unit
Error Estimate	0.12	
Quartile 1	2	unit
Quartile 3	2	unit
Tukey's Trimean	2	unit

Figure 86. Summary statistics for the 1918 vegetated islands: all and correlated boreholes.

Summary Statistics Graphics

Heat maps, pie charts, and other tables used to evaluate tendencies of the summary statistics are provided below.

Table 2. Heat map of summary statistics for distance from active channel planforms. Red is used to show areas of stronger correlation [value of 50 or less for central tendency and dispersion, skewness of zero to one, and kurtosis of less than three). Green is used to show areas of weaker correlation (value greater than 100 for central tendency and dispersion, skewness values greater than an absolute value of one, and kurtosis values greater than three. Yellow is utilized to signify moderate correlation levels and contains value between the stronger (red) and weaker correlation (green) values. Note, skewness and kurtosis do not have a moderate correlation level in this analysis.

Parameter	1918 planforms			1935 planforms			1949 planforms		
	Issue Locs	All boreholes	Correlated Boreholes	Issue Locs	All boreholes	Correlated Boreholes	Issue Locs	All boreholes	Correlated Boreholes
Count	84	187	28	84	187	28	84	187	28
Range	211	995	505	189	1148	558	222	1289	635
Mean	83	224	223	80	208	200	83	350	230
Mode	0	0	0	#N/A	0	#N/A	#N/A	0	#N/A
Minimum	0	0	0	11	0	7	15	0	14
Q1	28	26	105	49	71	94	50	135	135
Median	93	199	212	73	154	168	74	273	199
Q3	134	350	333	106	282	271	106	524	316
Maximum	211	995	505	200	1148	565	237	1289	649
Standard Deviation	60.8	207.7	150.7	41.3	209.7	146.3	49.7	277.4	148.2
Skewness	0.0	0.9	0.1	0.8	2.0	1.0	1.3	0.9	1.1
Kurtosis	-1.2	0.6	-1.1	0.7	5.0	0.6	1.6	0.3	1.2
Coefficient of Variation	73.3	92.9	67.5	51.5	100.8	73.0	59.8	79.3	64.4
Min sample #	6	67	35	3	68	33	4	119	34
Error Estimate	13	30	56	9	30	54	11	40	55
Tukey's Trimean	87	193	215	75	165	175	76	301	212

Table 3. Summary statistics for 1918 vegetation island and seepage/slope stability ratings. Red is used to show areas of stronger correlation [value of one for the 1918 vegetative islands and three for the seepage and slope stability for central tendency, dispersion of less than 0.5 units, skewness of zero to one, and kurtosis of less than three). Green is used to show areas of weaker correlation (value of two for the 1918 vegetative islands and one for the seepage and slope stability for central tendency, dispersion greater than one, skewness values greater than an absolute value of one, and kurtosis values greater than three. Yellow is utilized to signify moderate correlation levels and contains value between the stronger (red) and weaker correlation (green) values. Note, skewness and kurtosis do not have a moderate correlation level in this analysis.

Parameter	1918 Vegetative Islands			2006 seepage	2006 slope stability
	Issue Locs	All boreholes	Correlated Boreholes		
Count	84	187	28	84	84
Range	1	1	1	2	1
Mean	2	2	2	2	2
Mode	2	2	2	3	2
Minimum	1	1	1	1	1
Q1	2	2	2	1	1
Median	2	2	2	3	2
Q3	2	2	2	3	2
Maximum	2	2	2	3	2
Standard Deviation	0.3	0.2	0.3	0.9	0.5
Skewness	-2.6	-5.4	-2.7	-0.2	-0.7
Kurtosis	4.8	26.9	5.6	-1.9	-1.6
Coefficient of Variation	16.4	9.0	16.6	44.8	28.9
Min sample #	1	1	1	4	1
Error Estimate	0.1	0.0	0.1	0.2	0.1
Tukey's Trimean	2	2	2	3	2

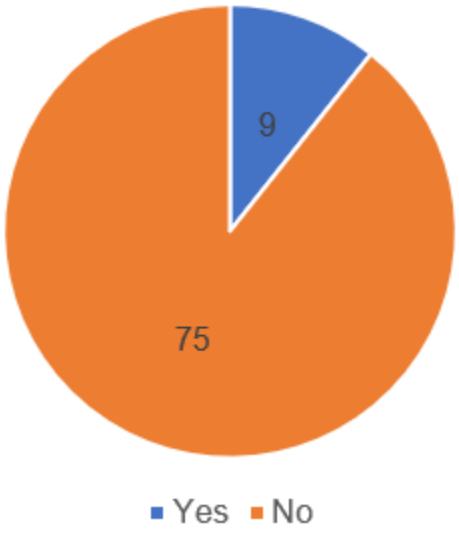

Figure 87. 2019 issue locations in areas identified as a vegetated island in 1918.

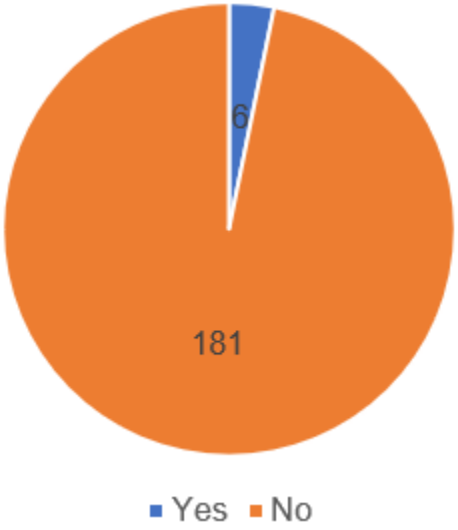

Figure 88. Borehole locations in areas identified as a vegetated island in 1918.

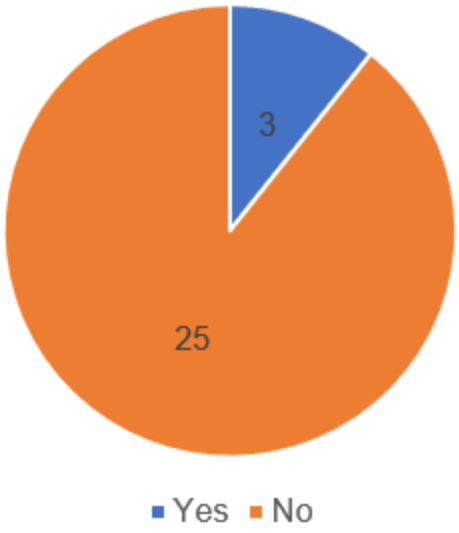

Figure 89. Correlated borehole locations identified as a vegetated island in 1918.

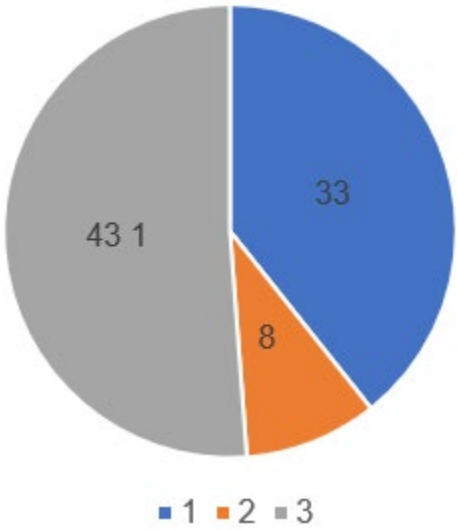

Figure 90. 2006 seepage ratings (USACE 2009) for the 2019 issue locations.

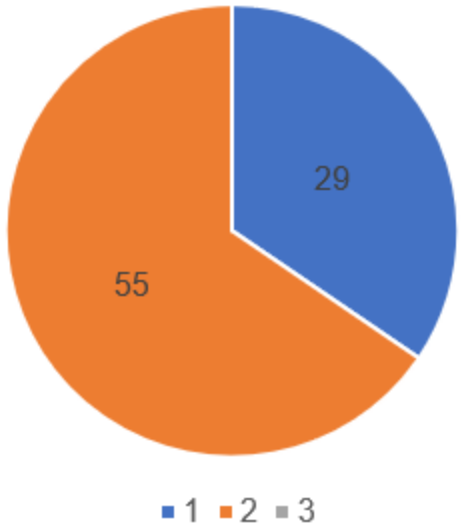

Figure 91. 2006 slope stability ratings (USACE 2009) for the 2019 issue locations.

Table 4. Summary of central tendencies for bed material sizes at the 2019 issue locations. The Wentworth grain size classifications are utilized to show the central tendency for the grain size associated where 16% of the mass is finer (d_{16}), 50% of the mass is finer (d_{50}), and 84% of the mass is finer (d_{84}). Red shaded areas reflect zones of coarser material relative to the sample set.

Statistic	Riverside Drain	Landside Levee Toe	Levee Centerline	Riverside Levee Toe	River Centerline
d_{16}					
Median	VFS	Fines	Fines	Fines	Fines
Tukey's Trimean	VFS	Fines	Fines	Fines	Fines
Q1/Q3	Fines to FS	Fines	Fines to VFS	Fines to VFS	Fines to FS
d_{50}					
Median	FS	VFS	FS	FS	FS
Tukey's Trimean	FS	VFS	FS	FS	FS
Q1/Q3	VFS to MS	VFS to FS	VFS to FS	FS	VFS to MS
d_{84}					
Median	MS	MS	MS	MS	MS
Tukey's Trimean	MS	MS	MS	MS	MS
Q1/Q3	MS to CS	MS	MS to CS	MS to CS	MS to VCS

Table 5. Summary statistics for Wentworth classification related to the 2019 issue locations. Blue is used to indicate Fines and very fine sands (VFS). Green indicates fine sands (FS) and medium sands (MS), yellow is for coarse sands (CS) and very coarse sands (VCS), and red indicates gravel and coarser grain sizes (>VCS).

Parameter	Wentworth classifications for the 2019 issue location correlations														
	Riverside Drain			Landside Toe			Levee Centerline			Riverside Toe			River Centerline		
	d16	d50	d84	d16	d50	d84	d16	d50	d84	d16	d50	d84	d16	d50	d84
Count	84	84	84	84	84	84	84	84	84	84	84	84	84	84	84
Range	3	5	6	2	4	5	1	4	5	2	3	5	2	3	5
Mean	5.0	3.9	2.5	5.7	4.5	3.0	5.6	4.3	2.7	5.5	4.1	2.5	5.2	4.1	2.6
Mode	6	5	3	6	5	3	6	4	3	6	4	2	6	4	3
Minimum	3	1	0	4	2	0	5	2	0	4	3	0	4	3	0
Q1	4	3	2	6	4	3	5	4	2	5	4	2	4	3	1
Median	5	4	3	6	4.5	3	6	4	3	6	4	3	6	4	3
Q3	6	5	3	6	5	3	6	5	3	6	4	3	6	5	3
Maximum	6	6	6	6	6	5	6	6	5	6	6	5	6	6	5
Standard Deviation	1.0	1.2	1.3	0.6	0.7	0.8	0.5	0.7	1.3	0.6	0.6	0.9	0.9	0.9	1.3
Skewness	-0.1	-0.2	-0.2	-1.8	-0.9	-1.3	-0.4	0.1	-0.8	-0.9	0.7	-0.3	-0.5	0.6	-0.2
Kurtosis	-1.8	-0.6	1.2	1.9	2.8	5.0	-1.9	1.8	0.4	-0.2	2.3	0.8	-1.6	-0.3	-0.8
Coefficient of Variation	19.5	29.3	53.9	11.0	14.9	25.7	8.8	17.5	47.3	11.1	14.5	36.8	17.2	22.1	50.9
Min sample #	4	6	7	2	2	3	1	3	7	2	2	4	4	4	7
Error Estimate	0.2	0.3	0.3	0.1	0.2	0.2	0.1	0.2	0.3	0.1	0.1	0.2	0.2	0.2	0.3
Tukey's Trimean	5.0	4.0	2.8	6.0	4.5	3.0	5.8	4.3	2.8	5.8	4.0	2.8	5.5	4.0	2.6

Independence Checks

Run-sequence and lag plots provide a visual assessment of correlation, as well as independence. Both of these plots were created by first computing the northing associated with the filtered 2019 issue locations and the boreholes (all of them and the correlated ones). The northings were then sorted so that the points lined up from north (large northing values) to south (smaller northing values). The sorted northing values were then assigned a value from one (in the north) to n (in the south). This became the northing index.

The run-sequence plots are created by plotting the northing index versus the distance to the active channel. Patterns in these plots suggest there may be a correlation or lack of independence. The run-sequence plots are shown below in the Run-Sequence Plot section.

The lag plots are created by arranging the values by the northing index (one is far north and n is far south). The lag plots graph the active channel distance for a given index number's value against the active channel distance for the next sequential index number's value. The last index value in a sample is plotted against the very first index number's value. Observed patterns suggest some degree of correlation with the active channel. Lag plots are shown below in the Lag Plot section.

Run-Sequence Plots

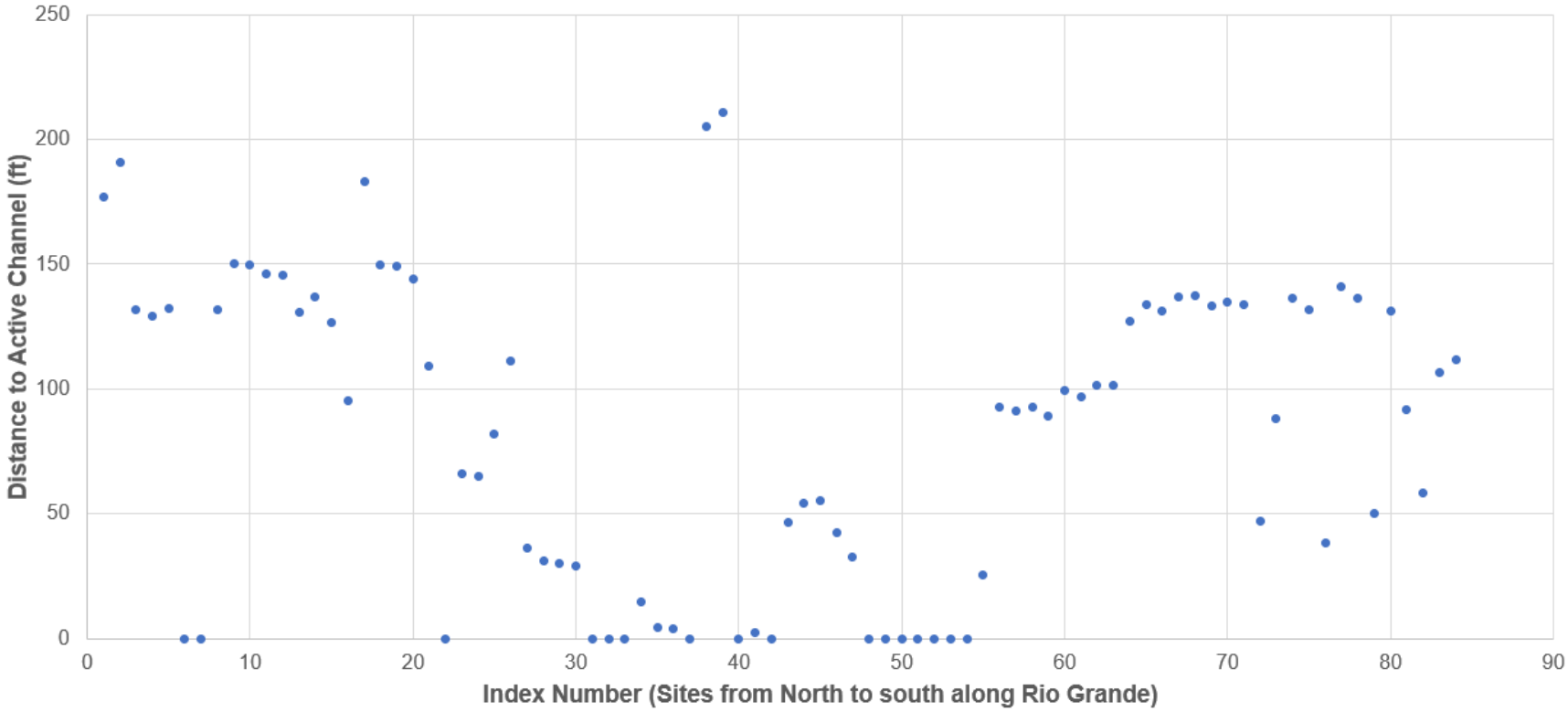

Figure 92. Run-sequence plot 1918 channel and 2019 issue locations.

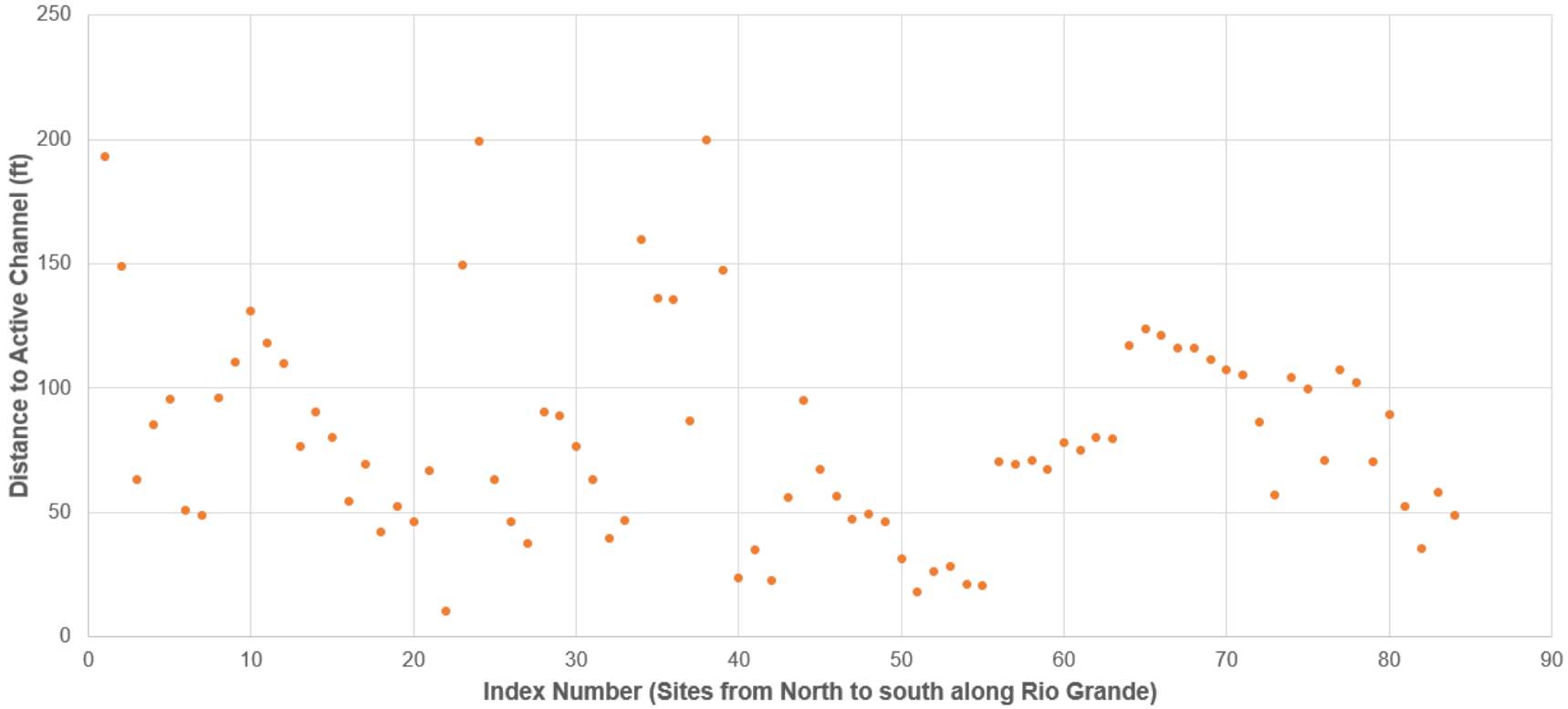

Figure 93. Run-sequence plot 1935 channel and 2019 issue locations.

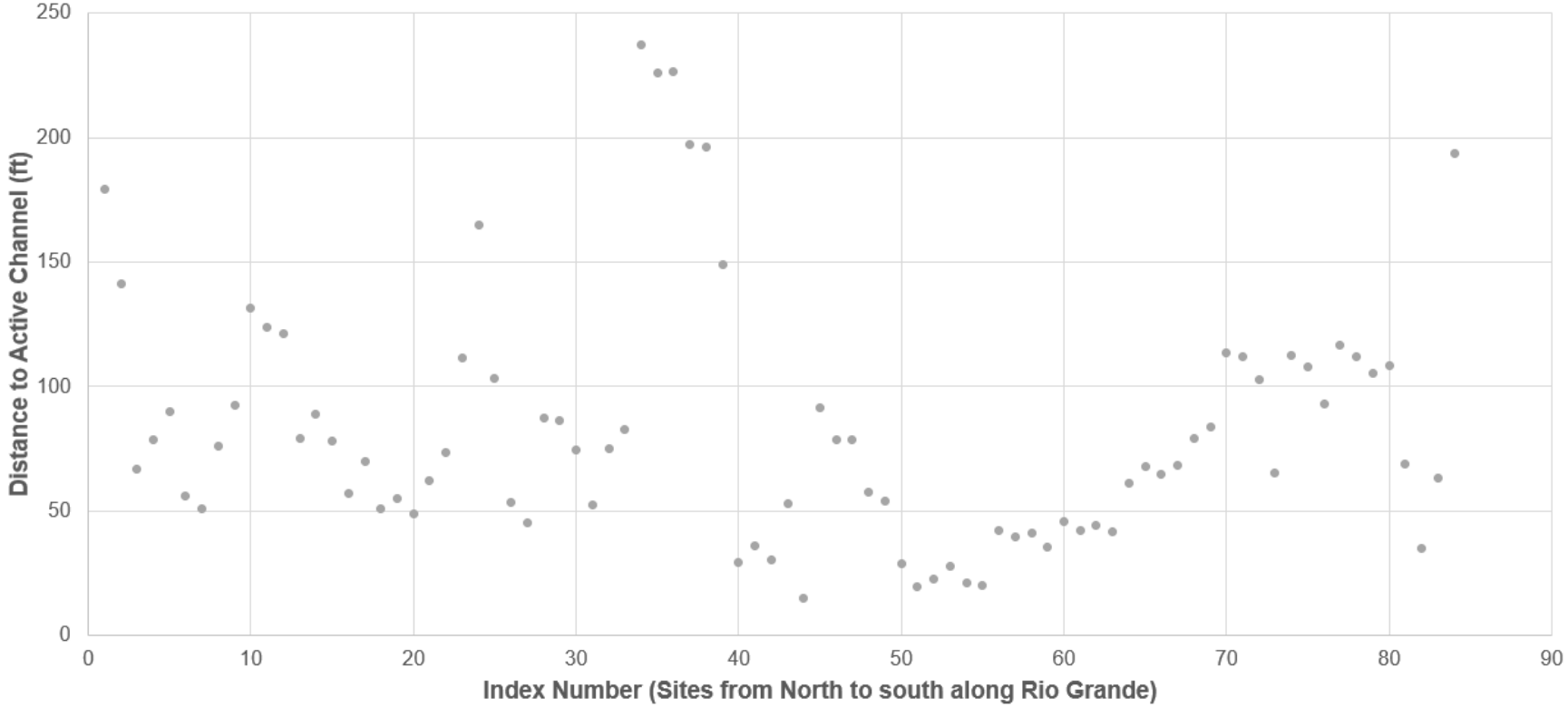

Figure 94. Run-sequence plot 1949 channel and 2019 issue locations.

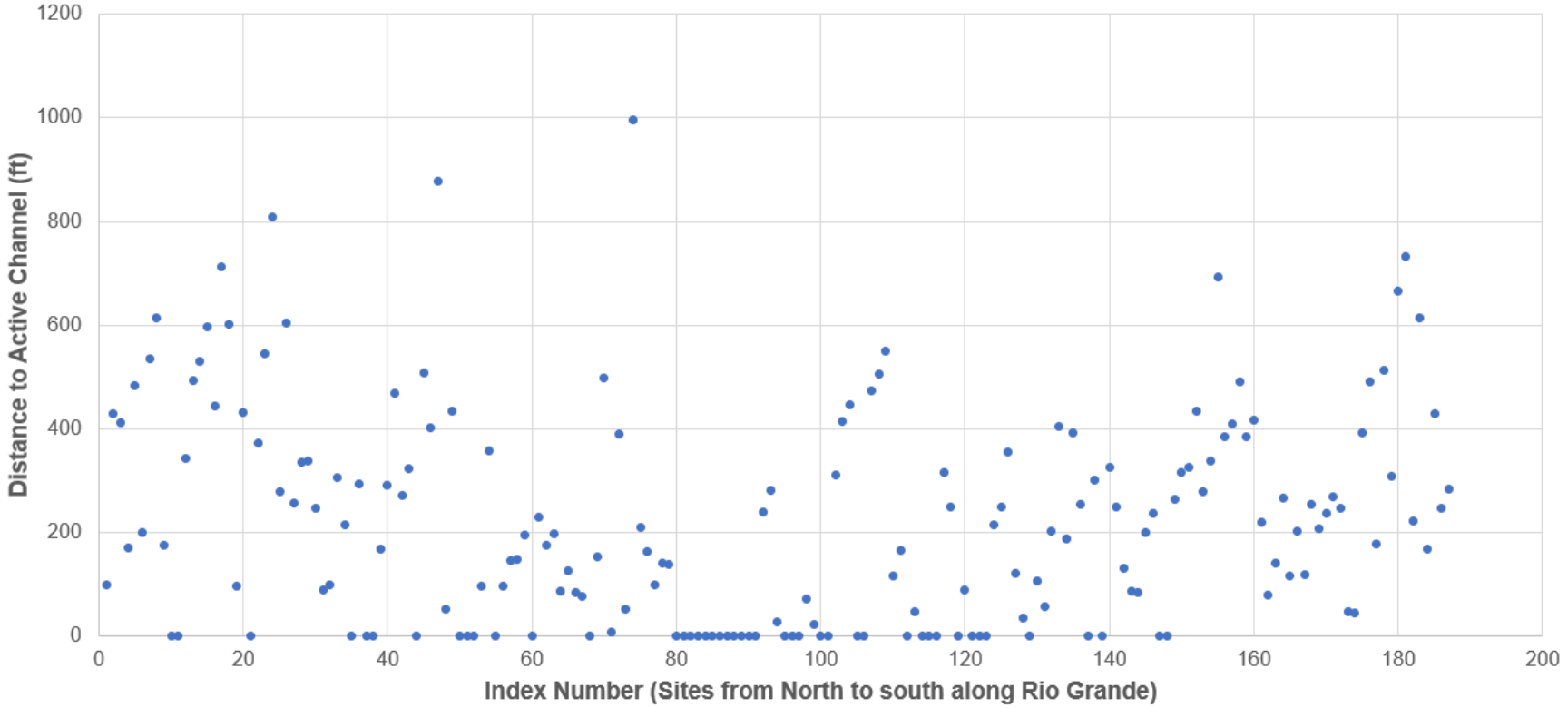

Figure 95. Run-sequence plot 1918 channel and borehole locations.

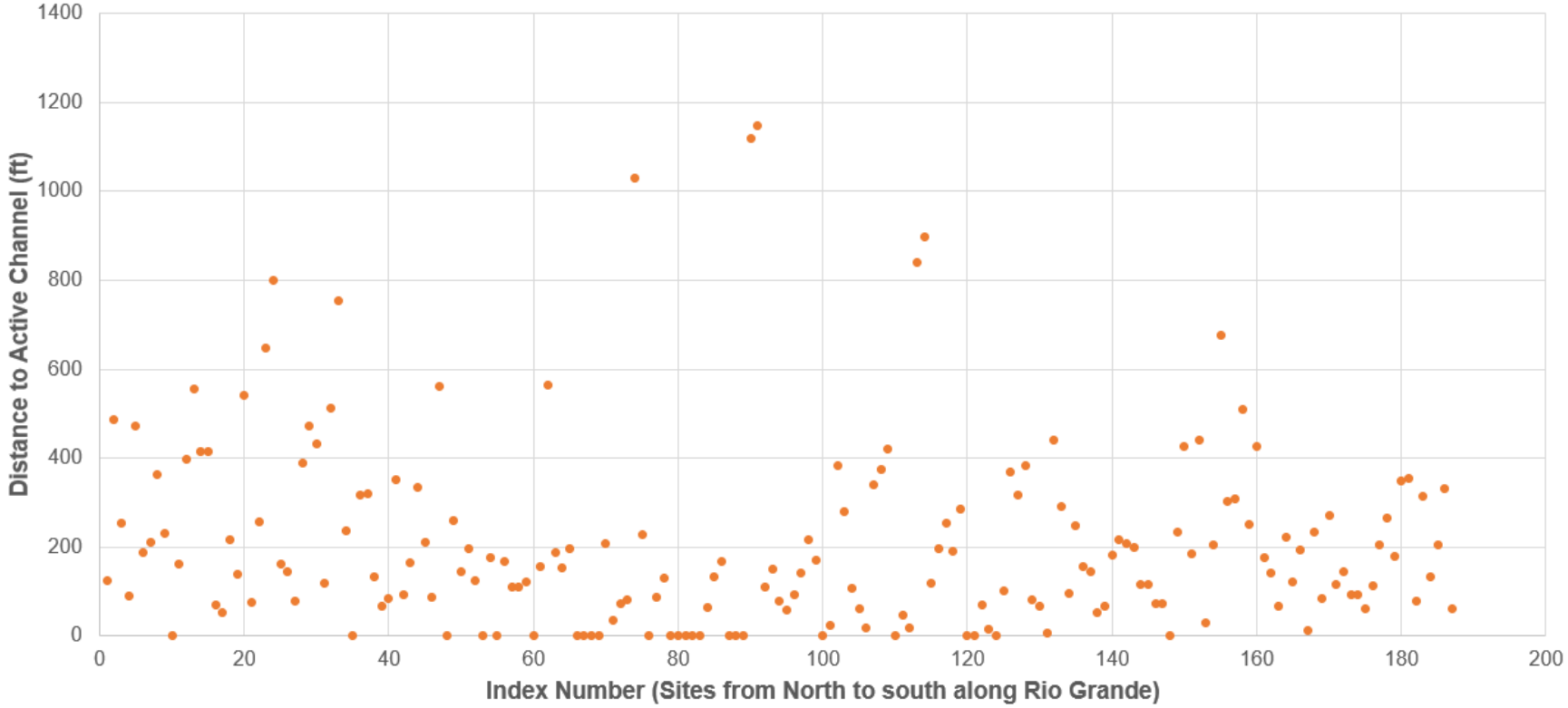

Figure 96. Run-sequence plot 1935 channel and borehole locations.

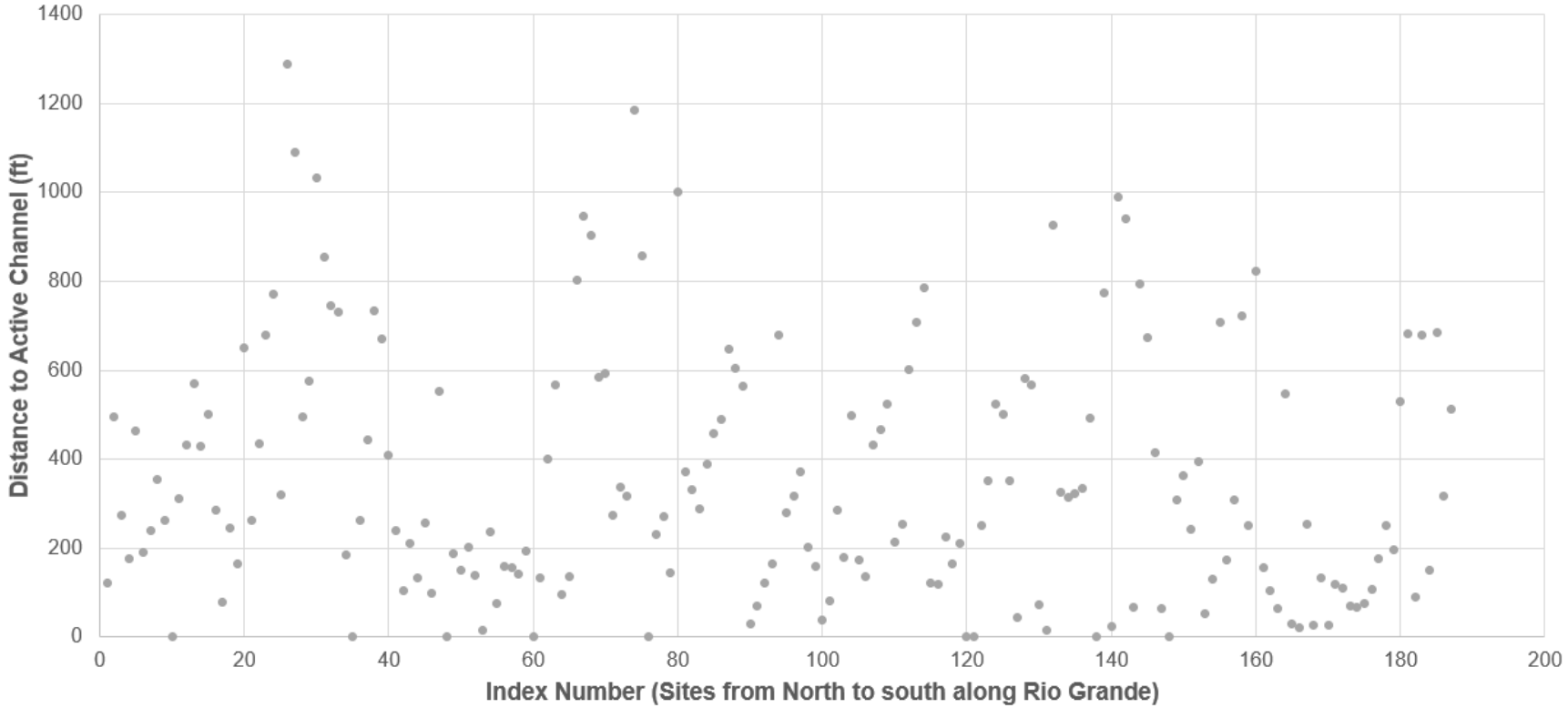

Figure 97. Run-sequence plot 1949 channel and borehole locations.

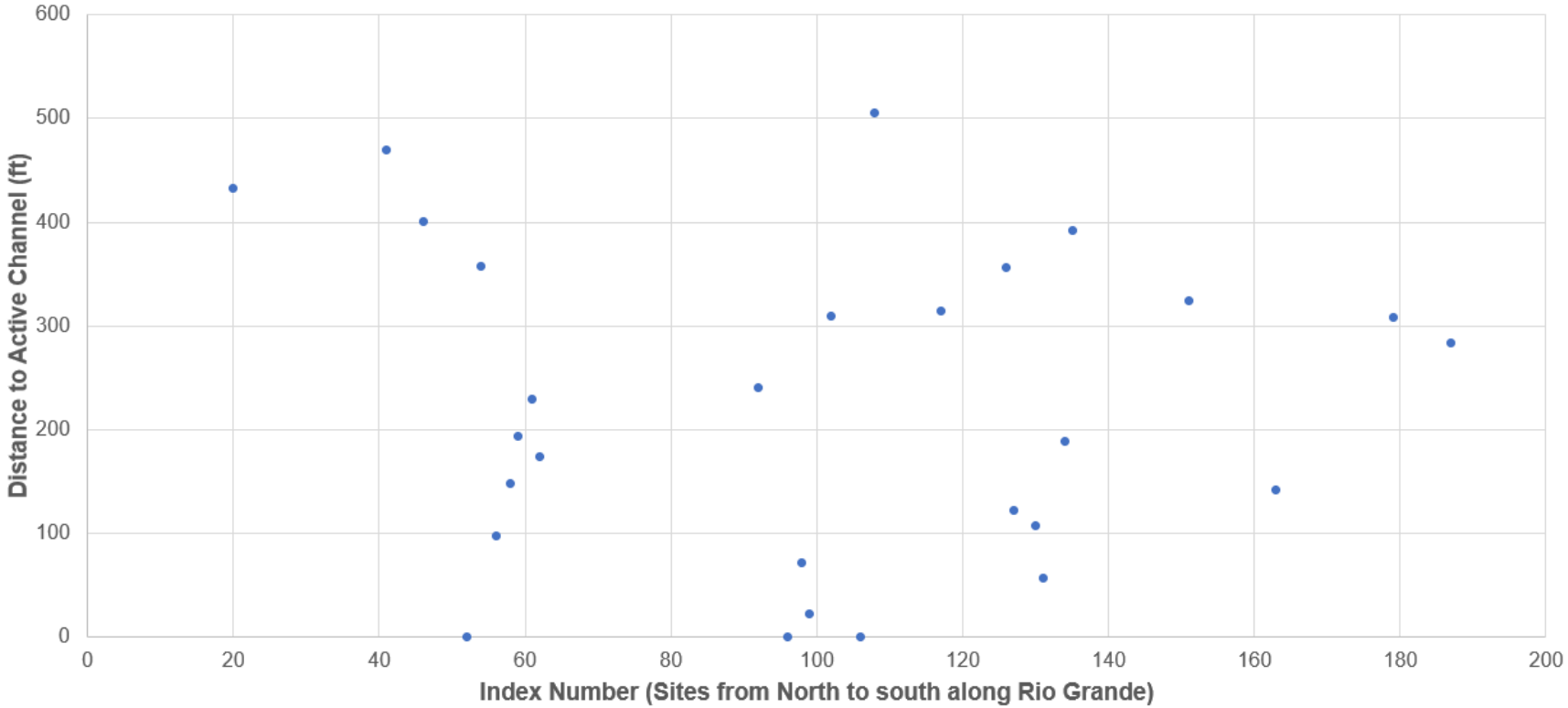

Figure 98. Run-sequence plot 1918 channel and correlated borehole locations.

Figure 99. Run-sequence plot 1935 channel and correlated borehole locations.

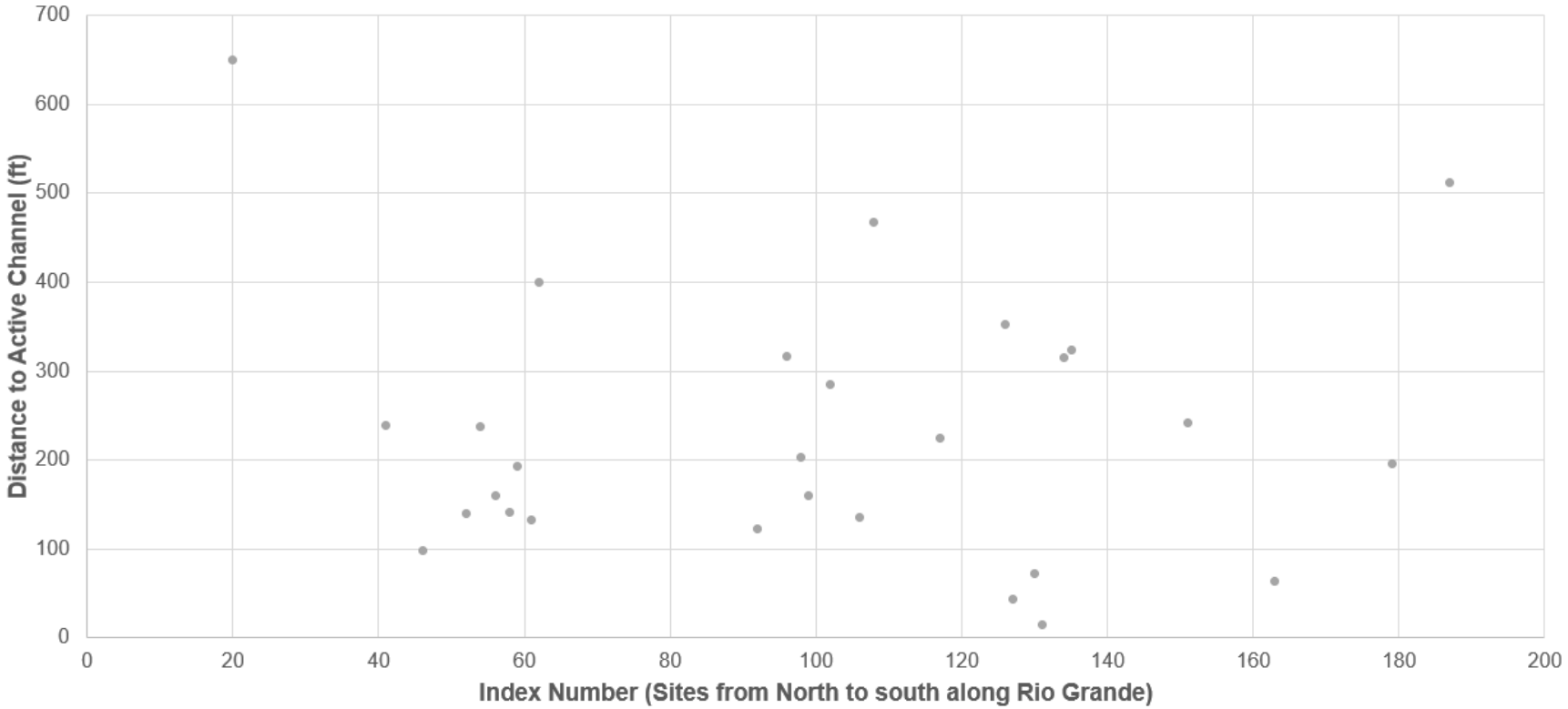

Figure 100. Run-sequence plot 1949 channel and correlated borehole locations.

Lag Plots

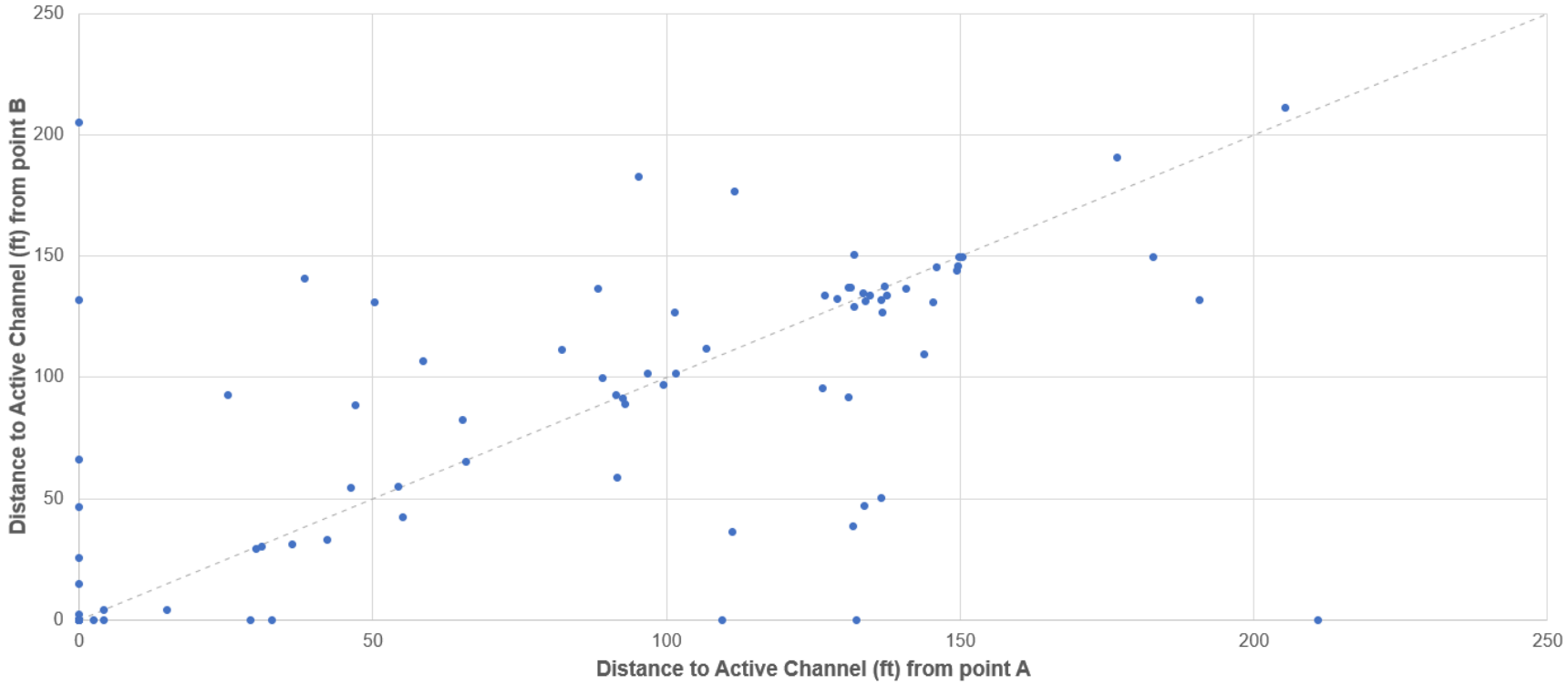

Figure 101. Lag plot 1918 channel and 2019 issue locations.

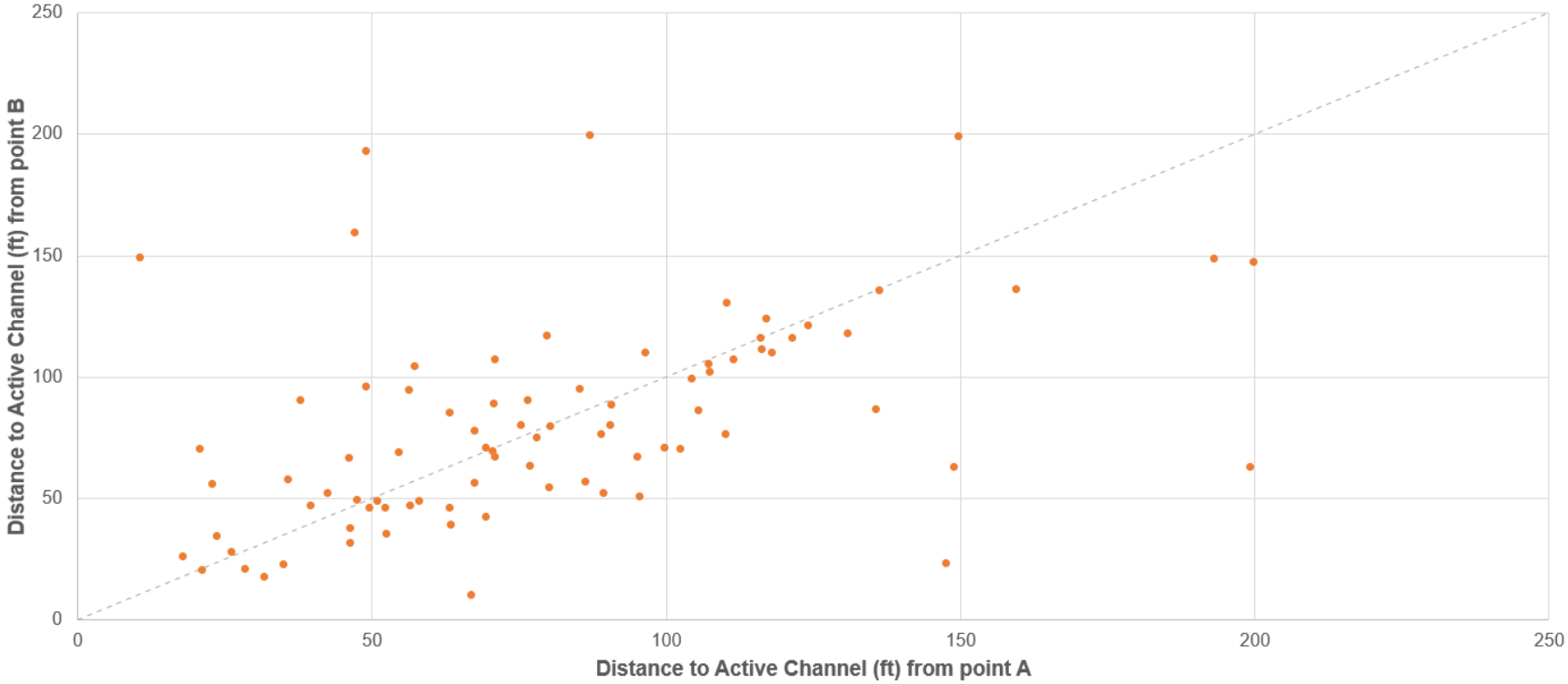

Figure 102. Lag plot 1935 channel and 2019 issue locations.

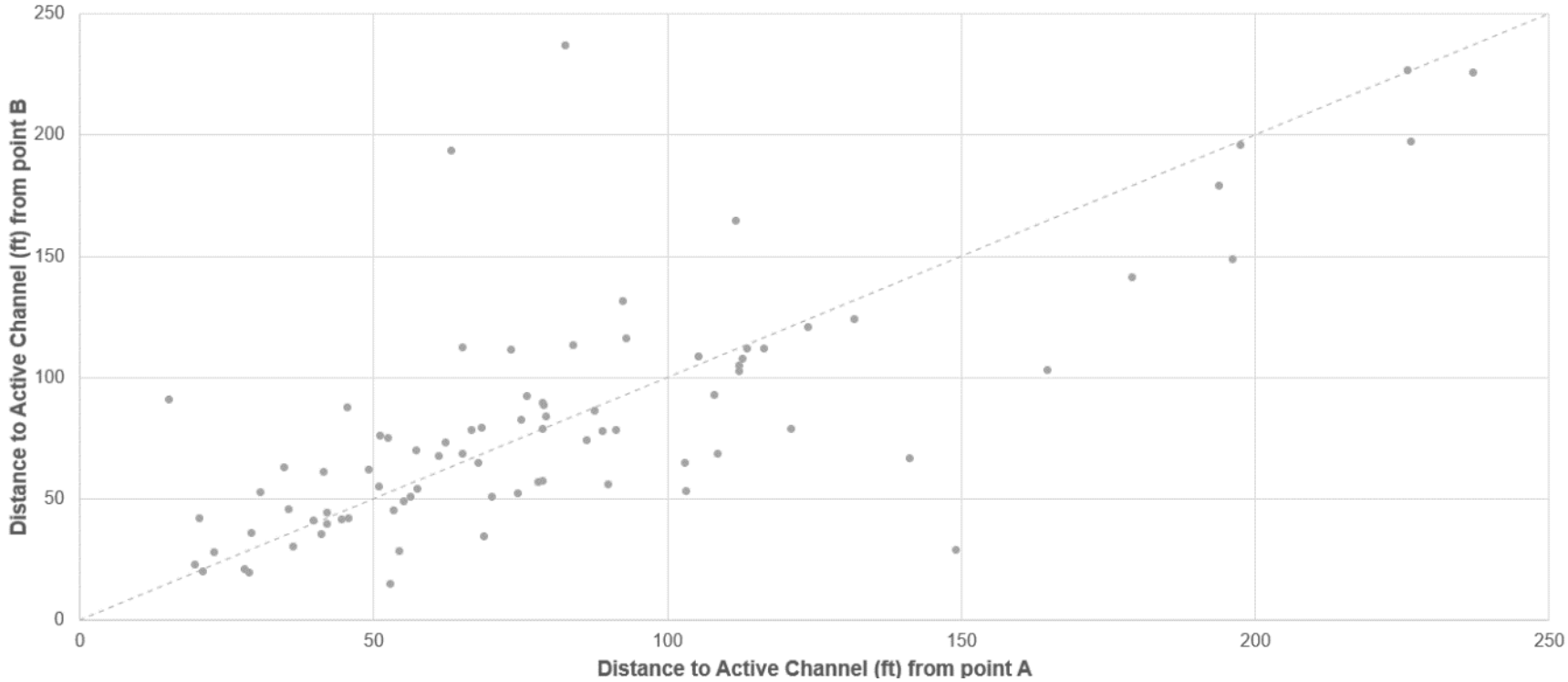

Figure 103. Lag plot 1949 channel and 2019 issue locations.

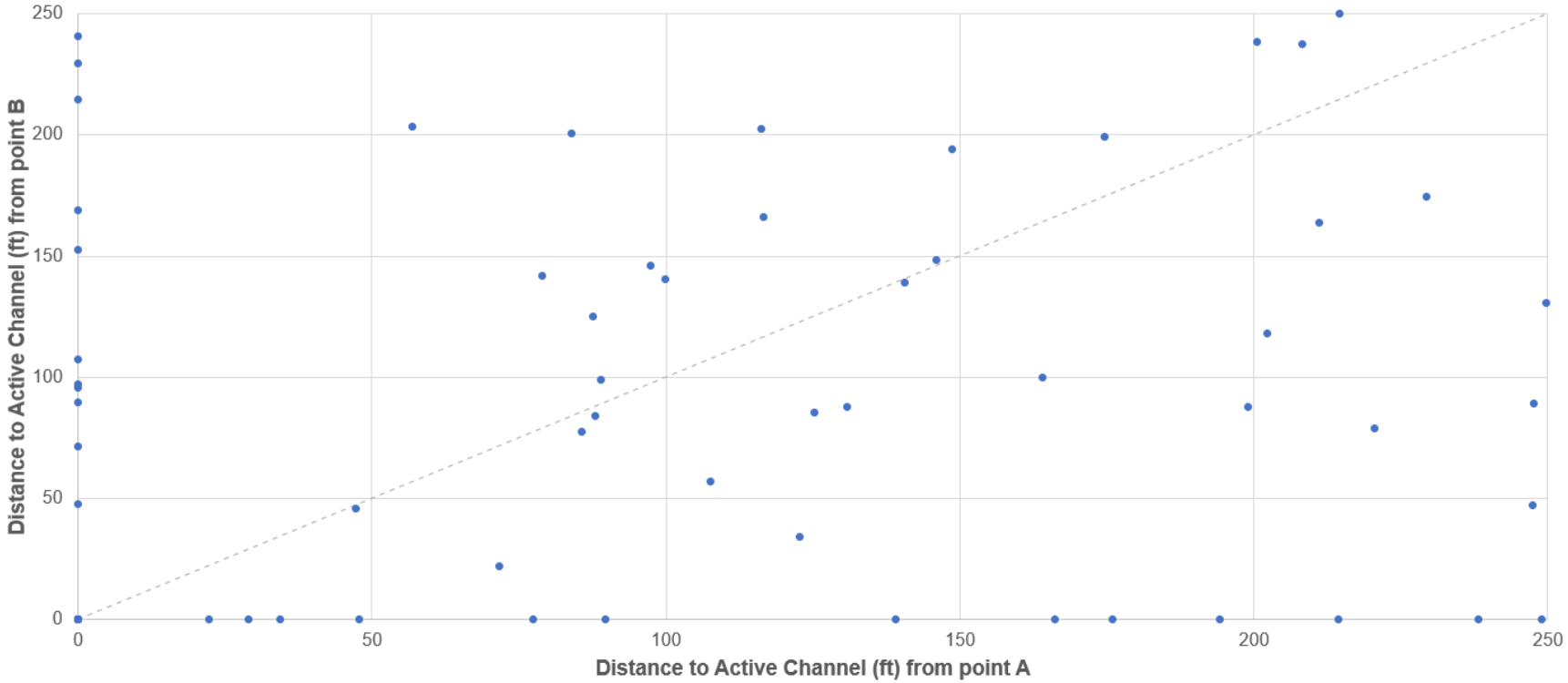

Figure 104. Lag plot 1918 channel and borehole locations.

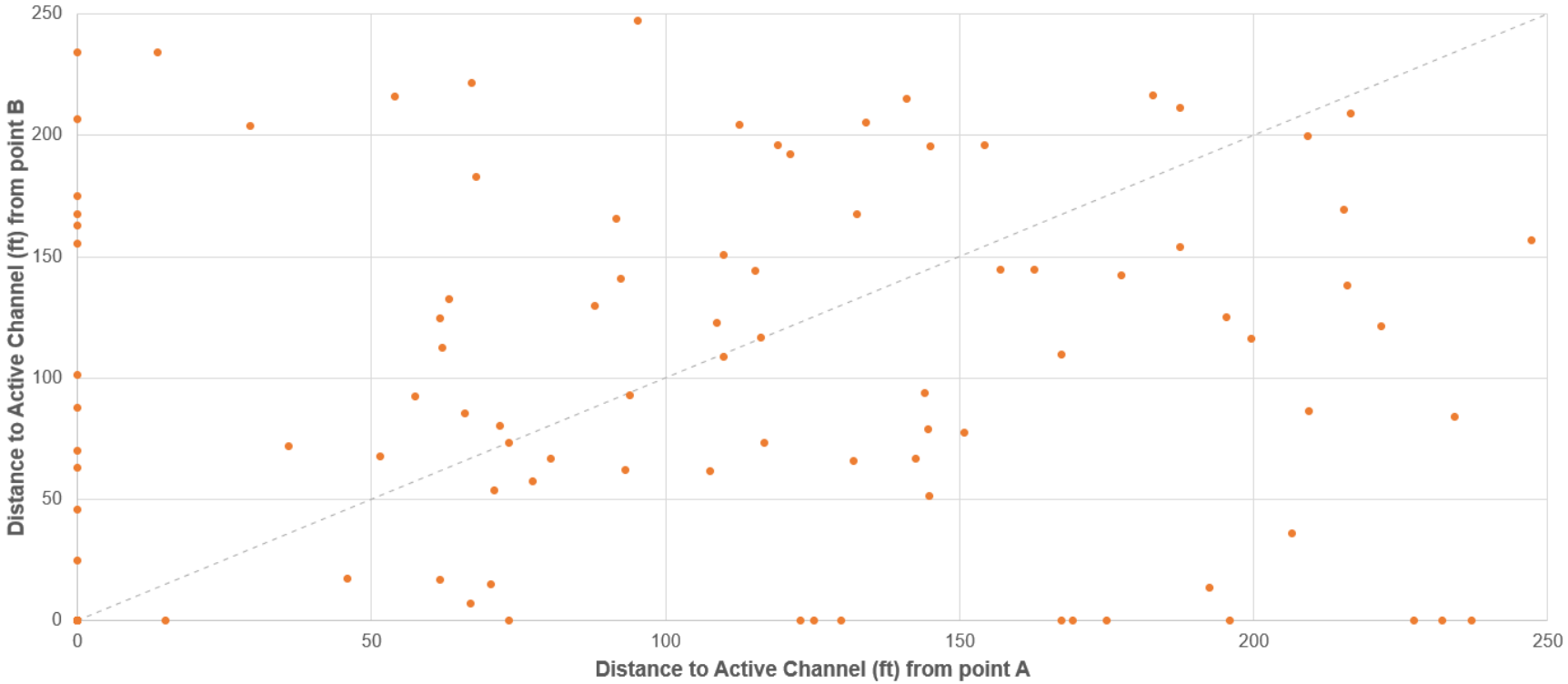

Figure 105. Lag plot 1935 channel and borehole locations.

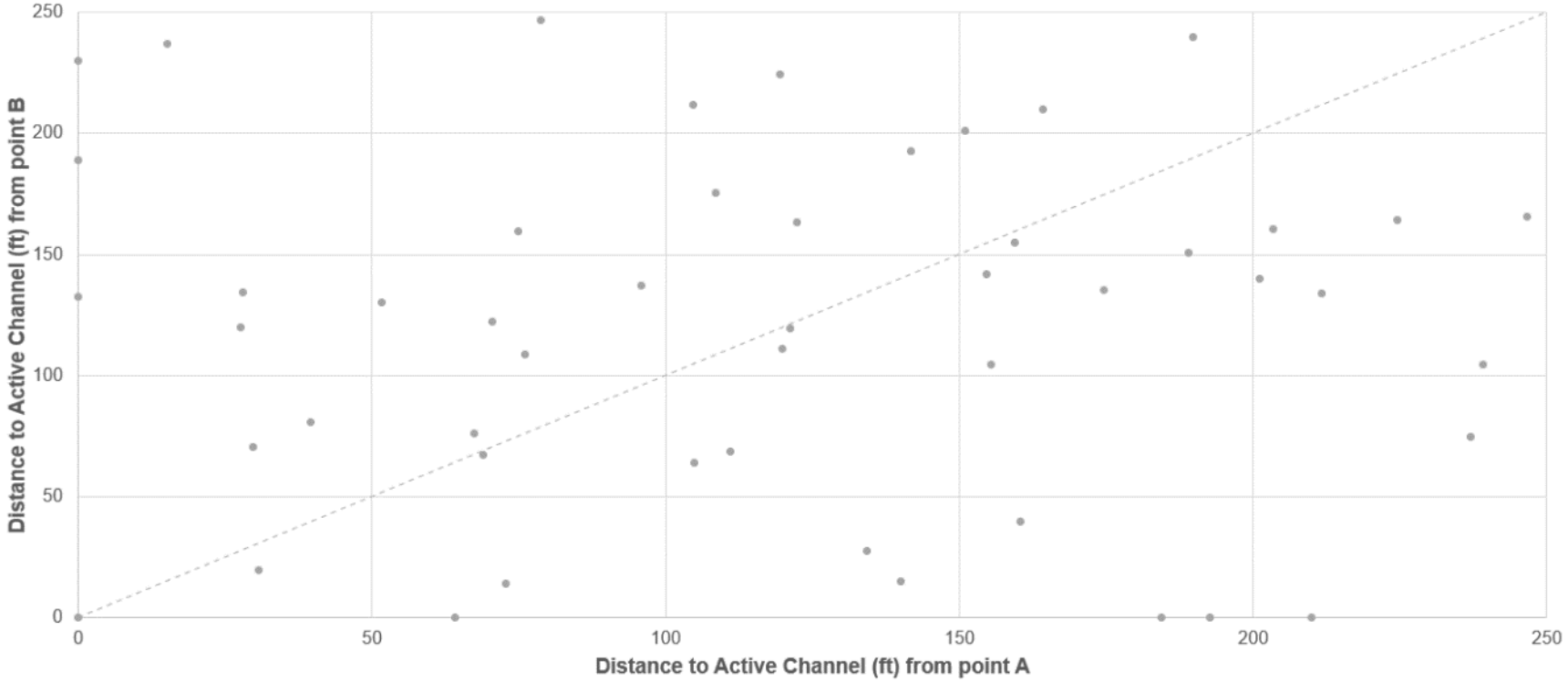

Figure 106. Lag plot 1949 channel and borehole locations.

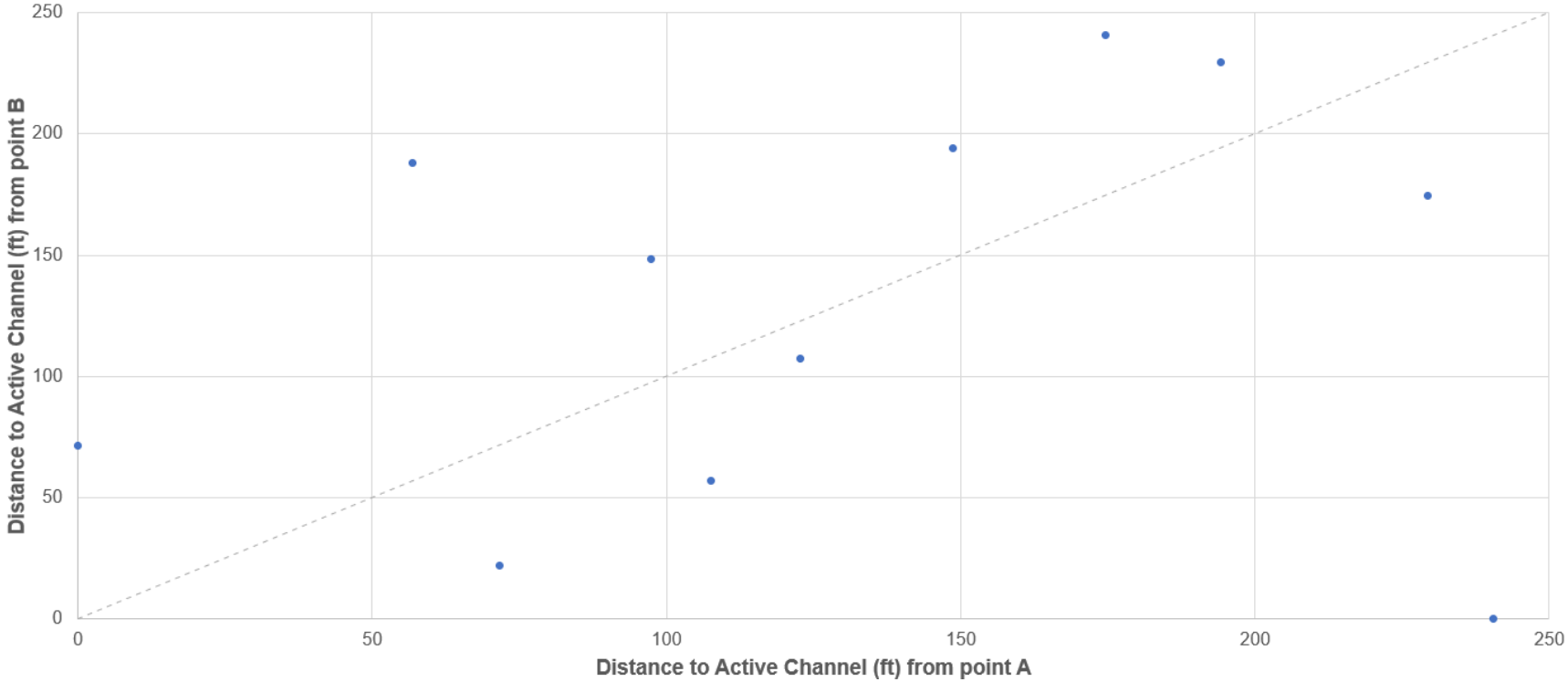

Figure 107. Lag plot 1918 channel and correlated borehole locations.

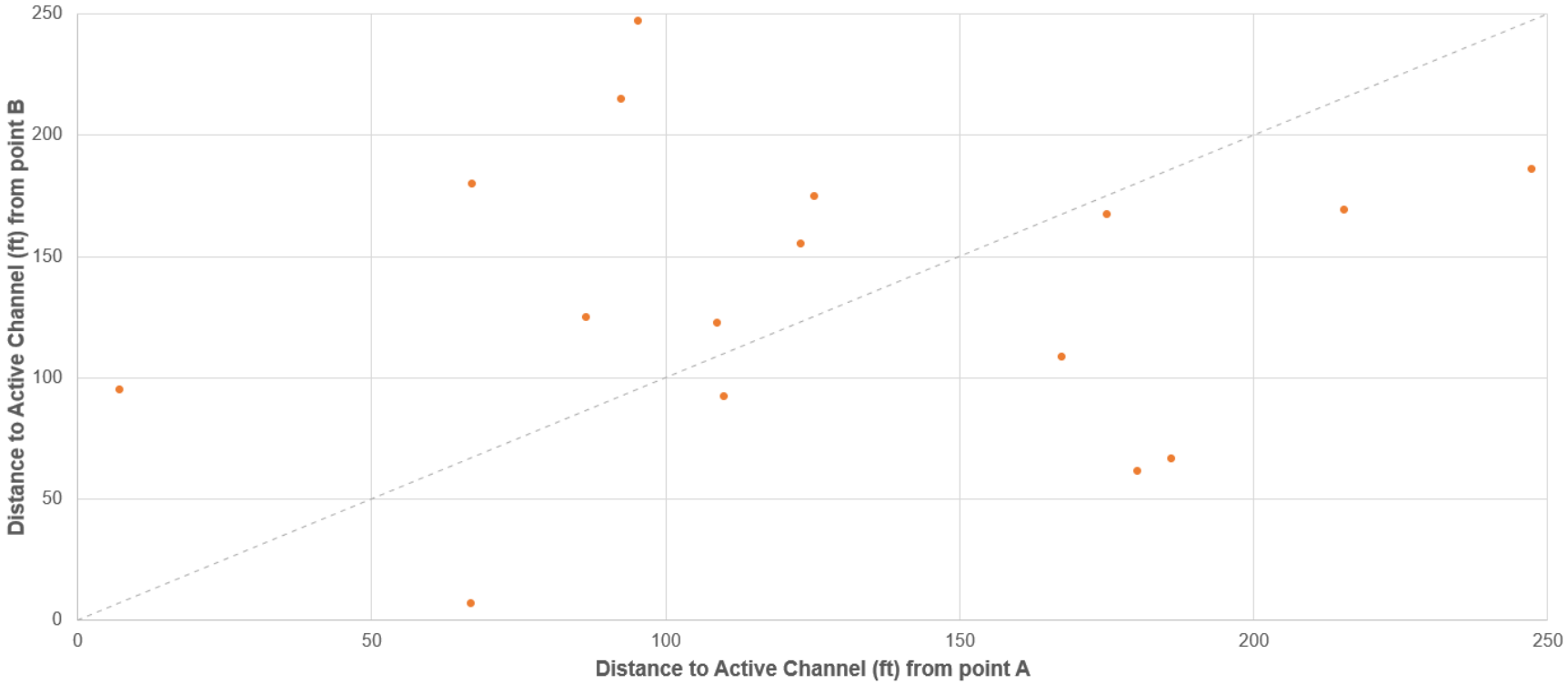

Figure 108. Lag plot 1935 channel and correlated borehole locations.

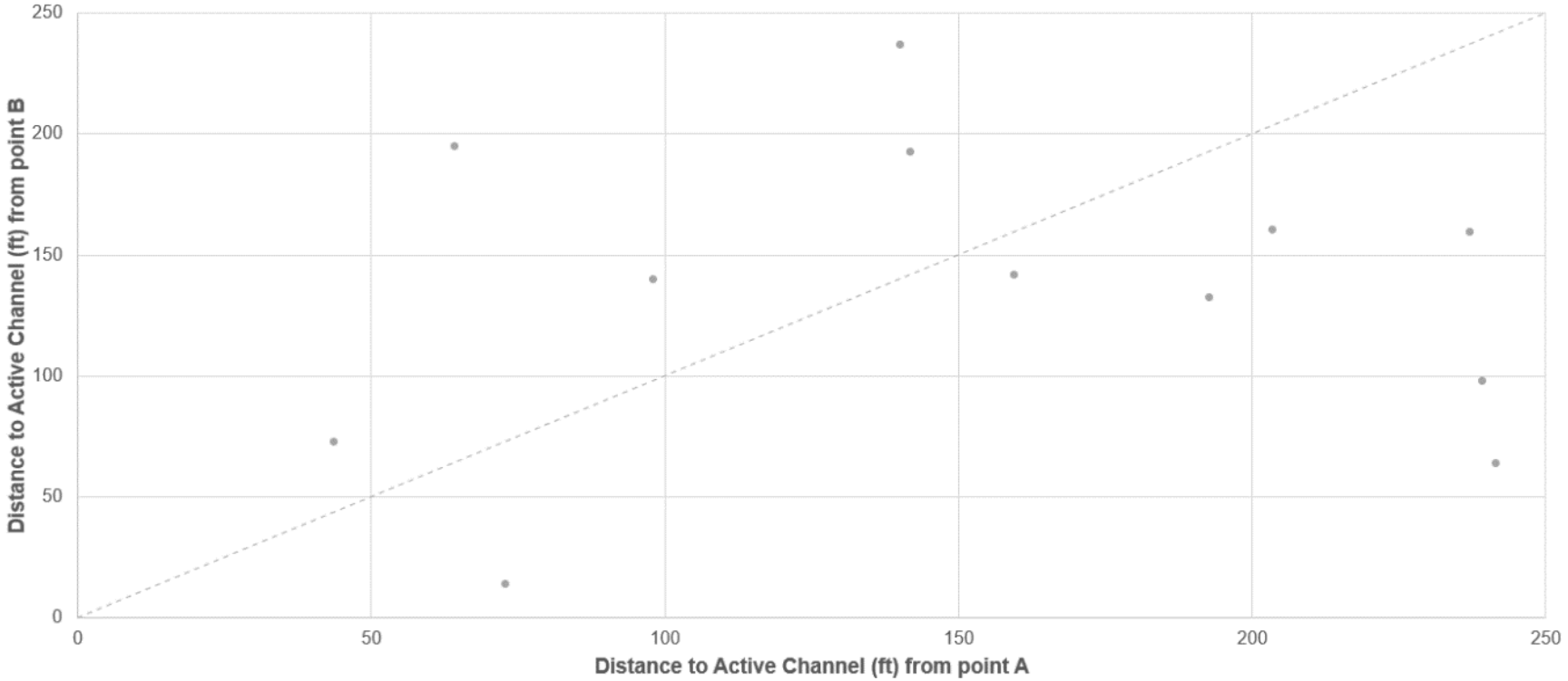

Figure 109. Lag plot 1949 channel and correlated borehole locations.

Linear Regressions

Regression equations can provide insight into the degree of correlation between two different datasets. The active channel distances from the filtered 2019 issue locations and the 1918, 1935, and 1949 active channel locations were paired with the sediment sizes and the seepage/slope stability ratings to assess if there are any discernible trends. Sediment sizes were evaluated for the current river channel, the riverside levee toe, the landside levee toe, and the riverside drain elevations. Graphs of these relationships are provided below.

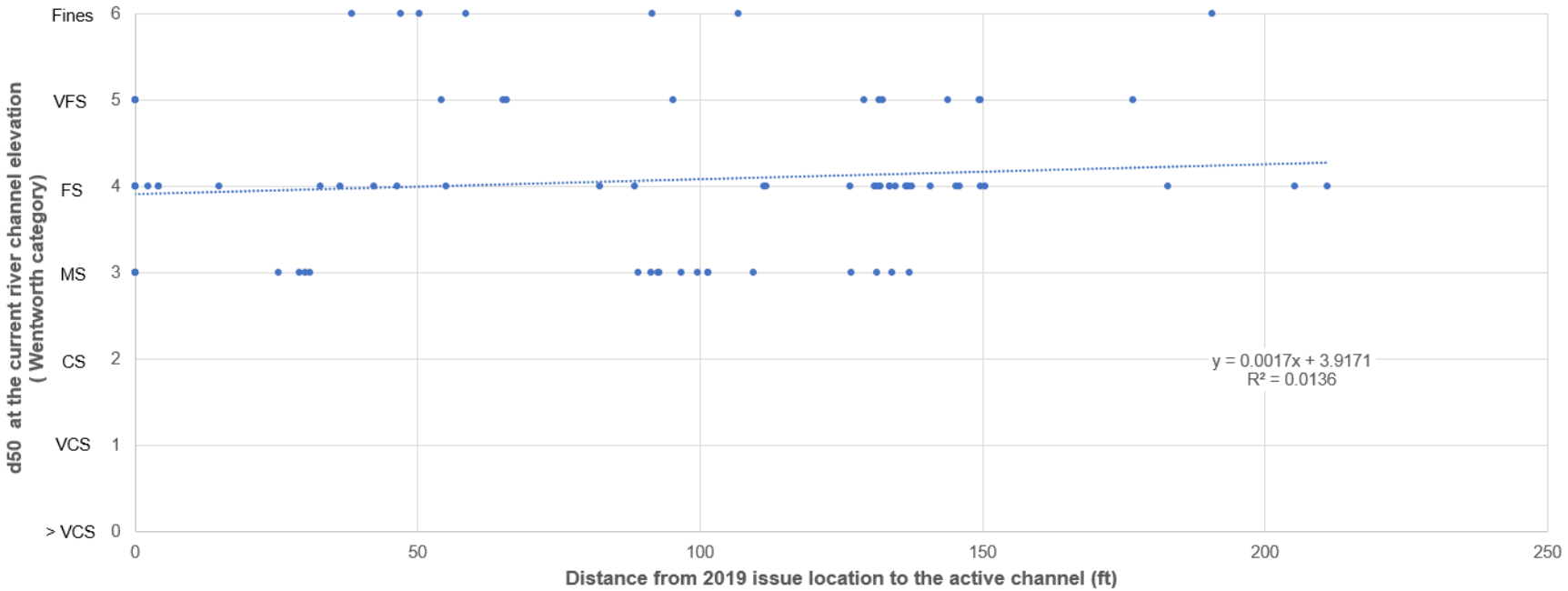

Figure 110. Linear regression 1918 active channel distance to the 2019 points of interest and d_{50} grain size at the current river channel elevation.

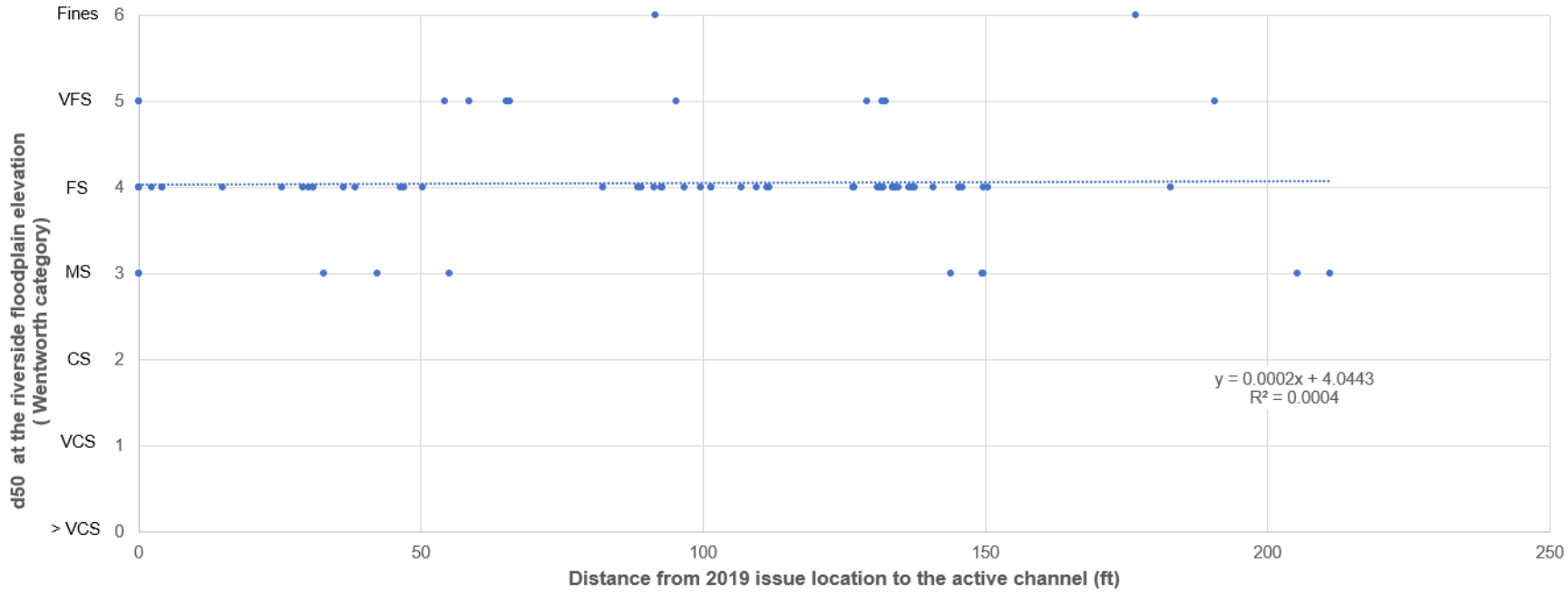

Figure 111. Linear regression of 1918 active channel distance to the 2019 points of interest and d_{50} grain size at the current riverside levee toe elevation.

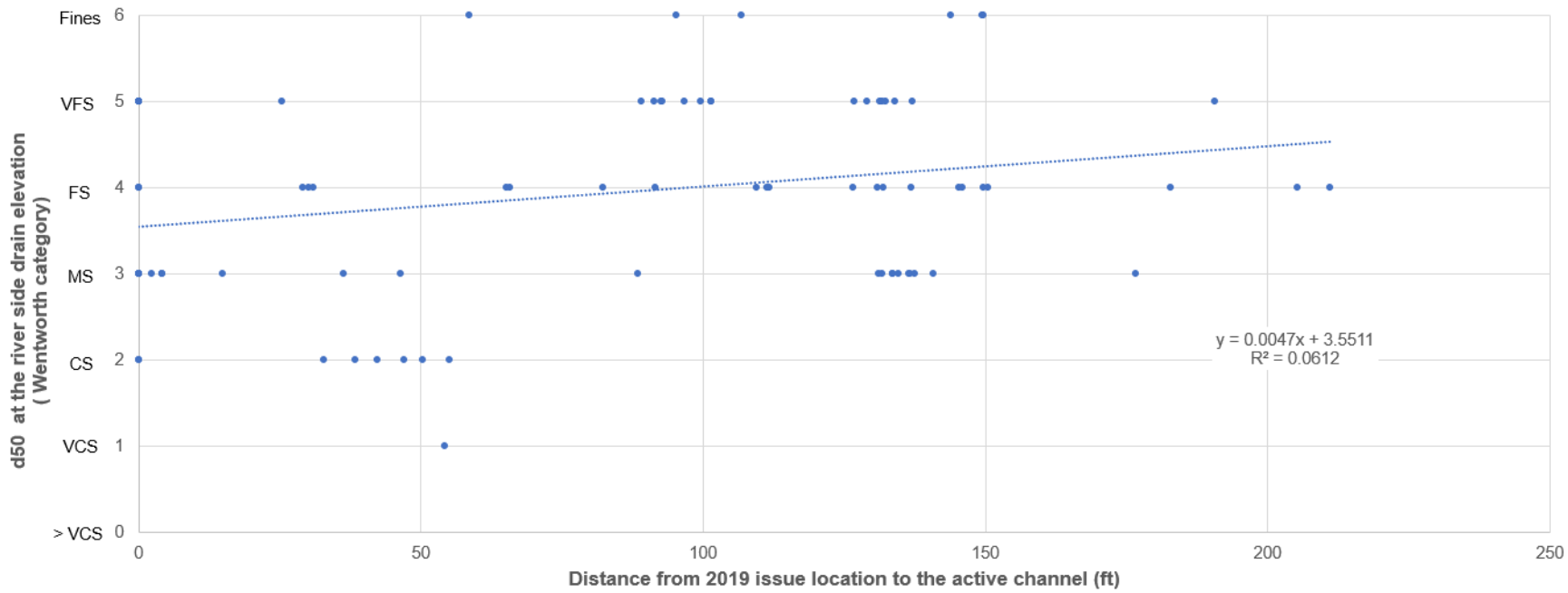

Figure 112. Linear regression of 1918 active channel distance to the 2019 points of interest and d_{50} grain size at the current riverside drain elevation.

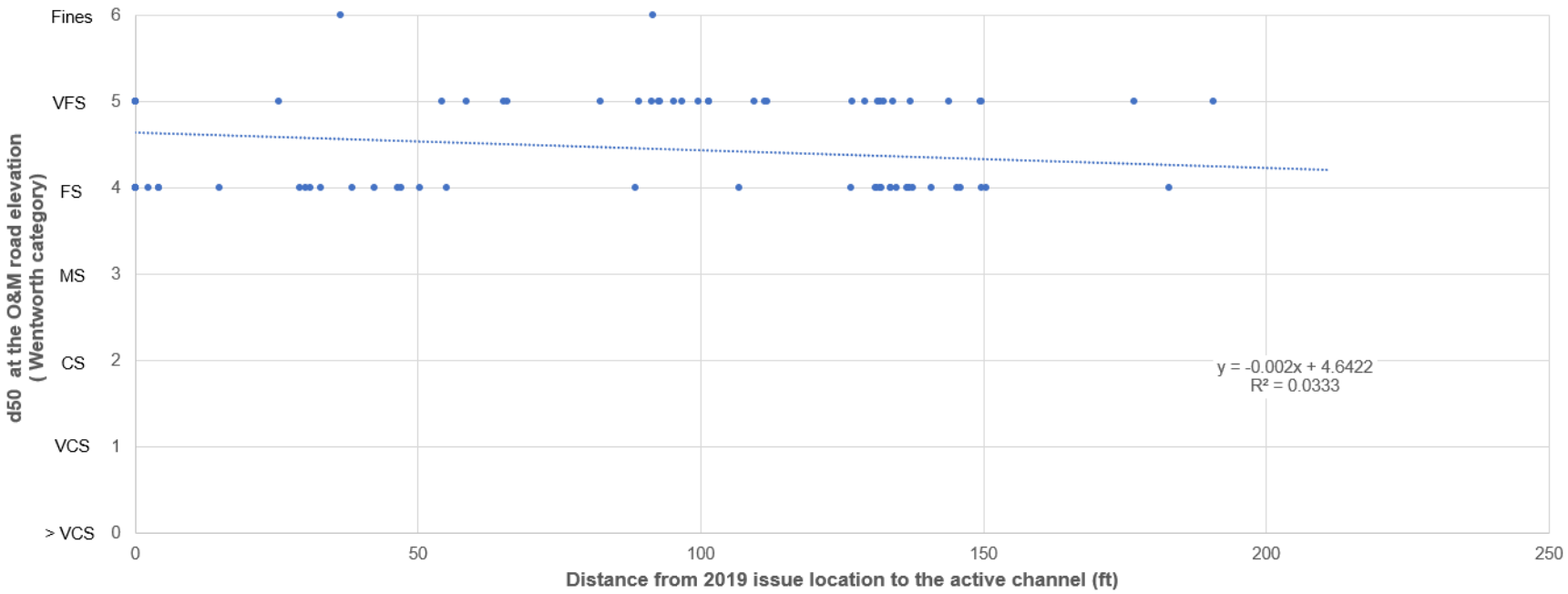

Figure 113. Linear regression of 1918 active channel distance to the 2019 points of interest and d_{50} grain size at the current landside levee toe elevation.

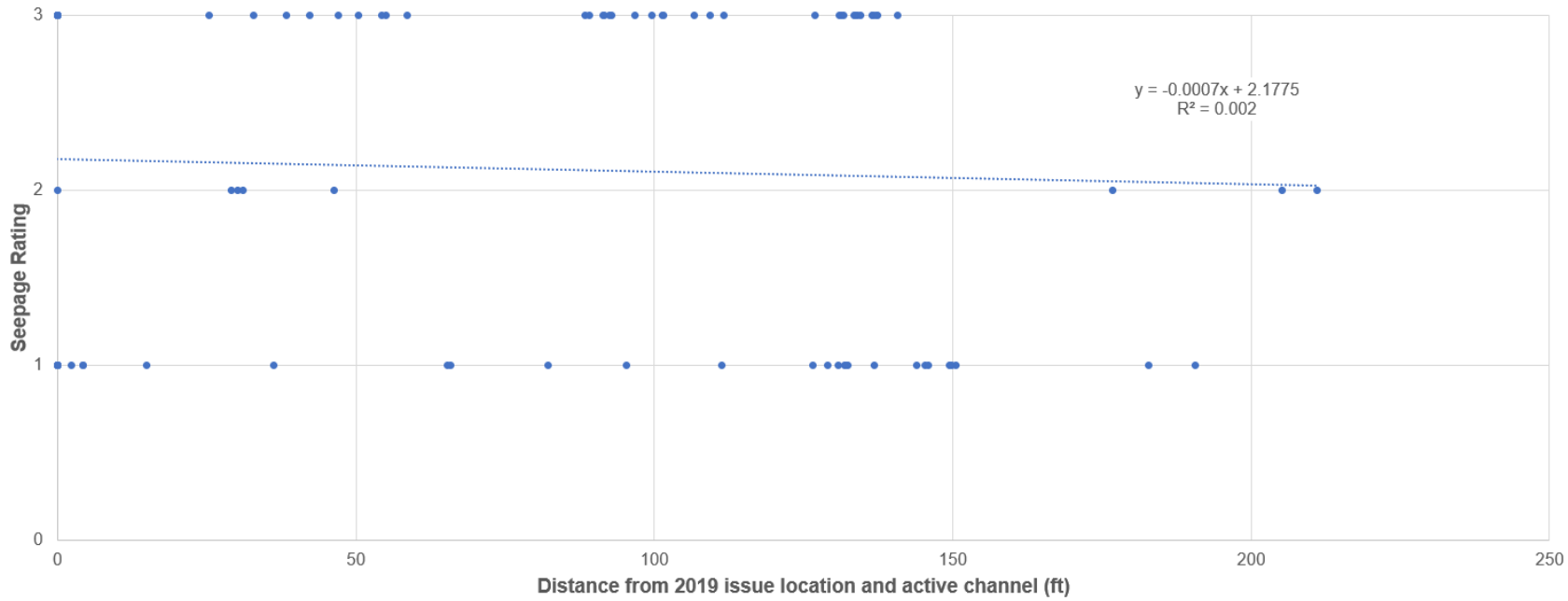

Figure 114. Linear regression of 1918 active channel distance to the 2019 points of interest and the 2006 seepage ratings.

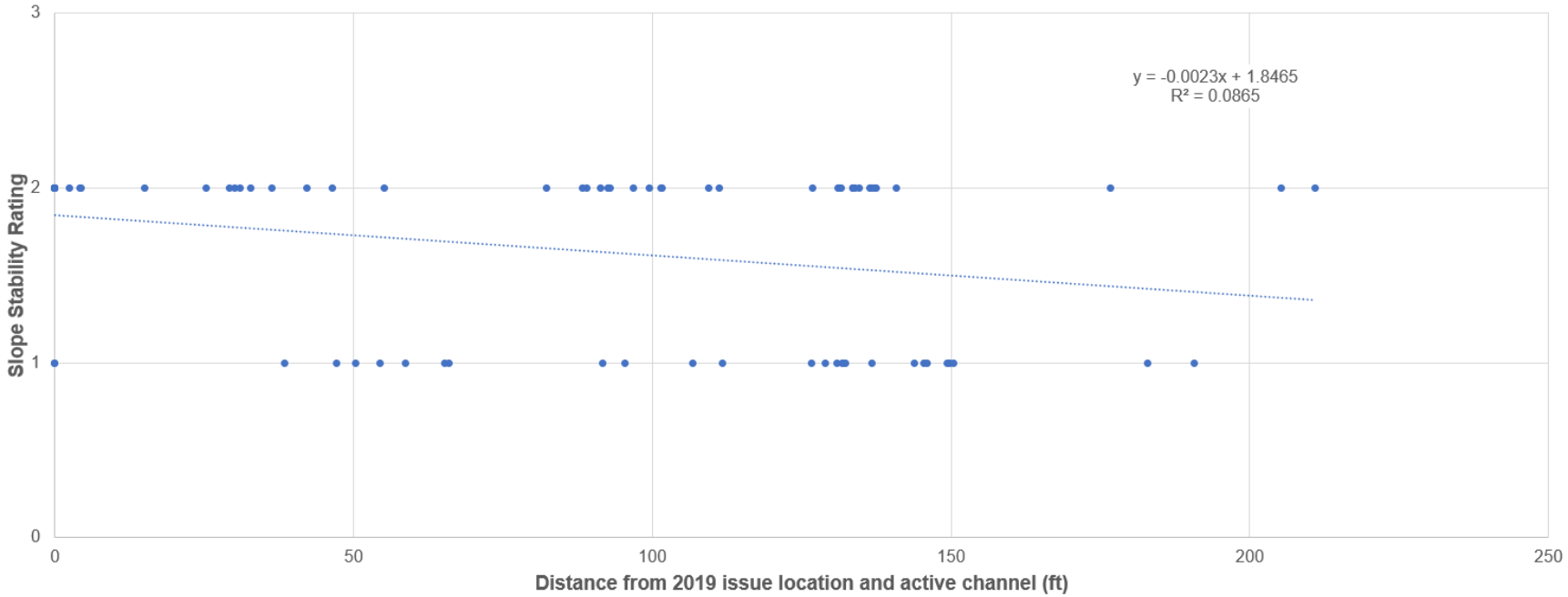

Figure 115. Linear regression of 1918 active channel distance to the 2019 points of interest and the 2006 slope stability ratings.

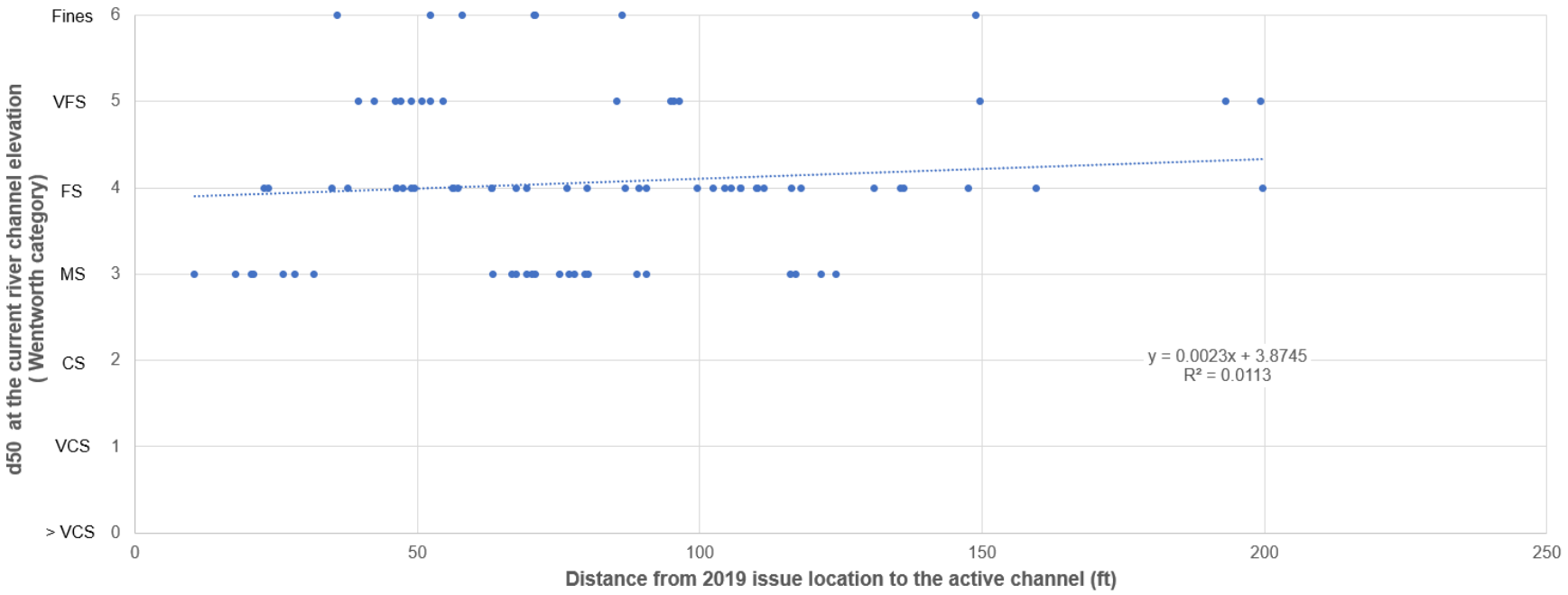

Figure 116. Linear regression of 1935 active channel distance to the 2019 points of interest and d_{50} grain size at the current river channel elevation.

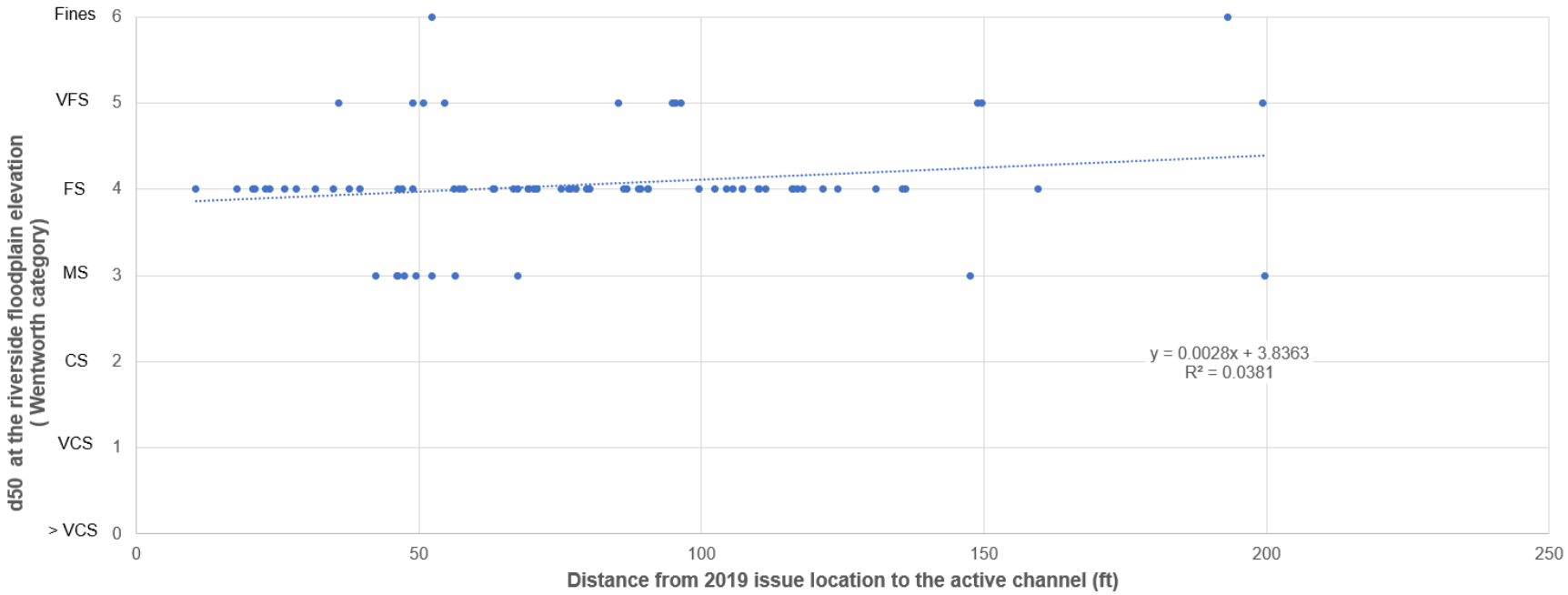

Figure 117. Linear regression of 1935 active channel distance to the 2019 points of interest and d_{50} grain size at the current riverside levee toe elevation.

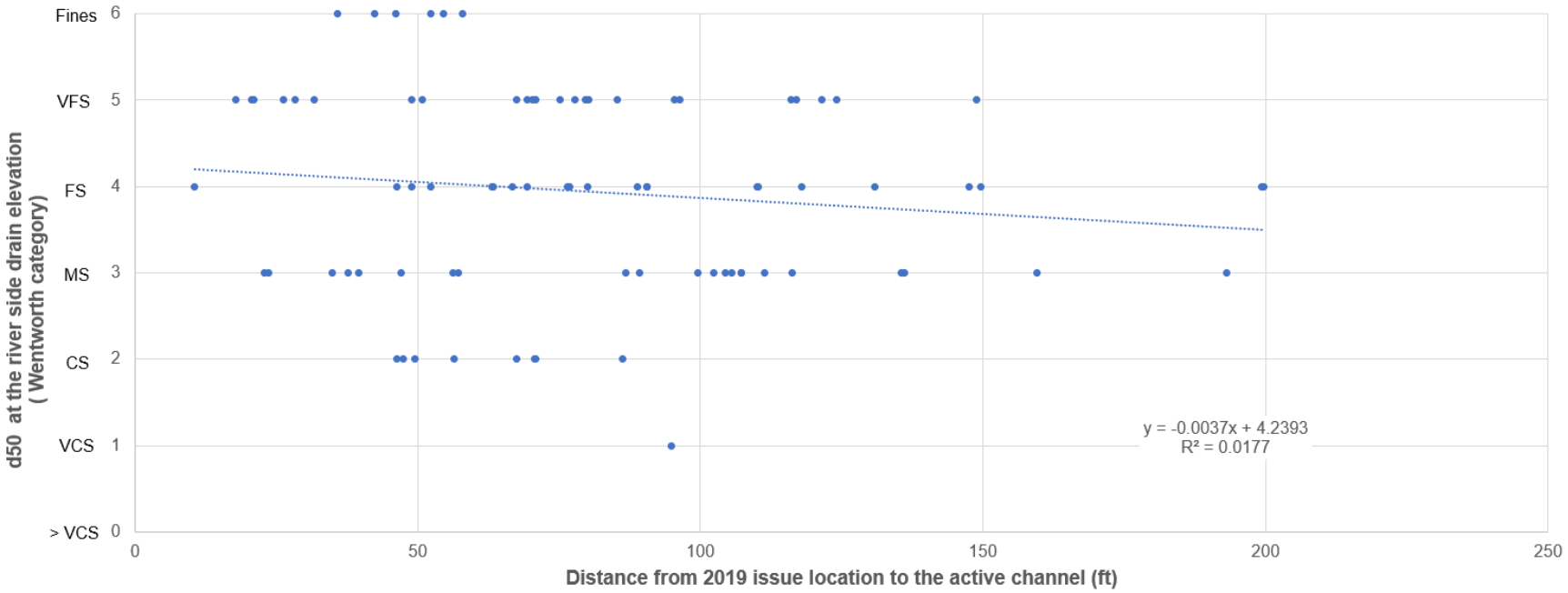

Figure 118. Linear regression of 1935 active channel distance to the 2019 points of interest and d_{50} grain size at the current riverside drain elevation.

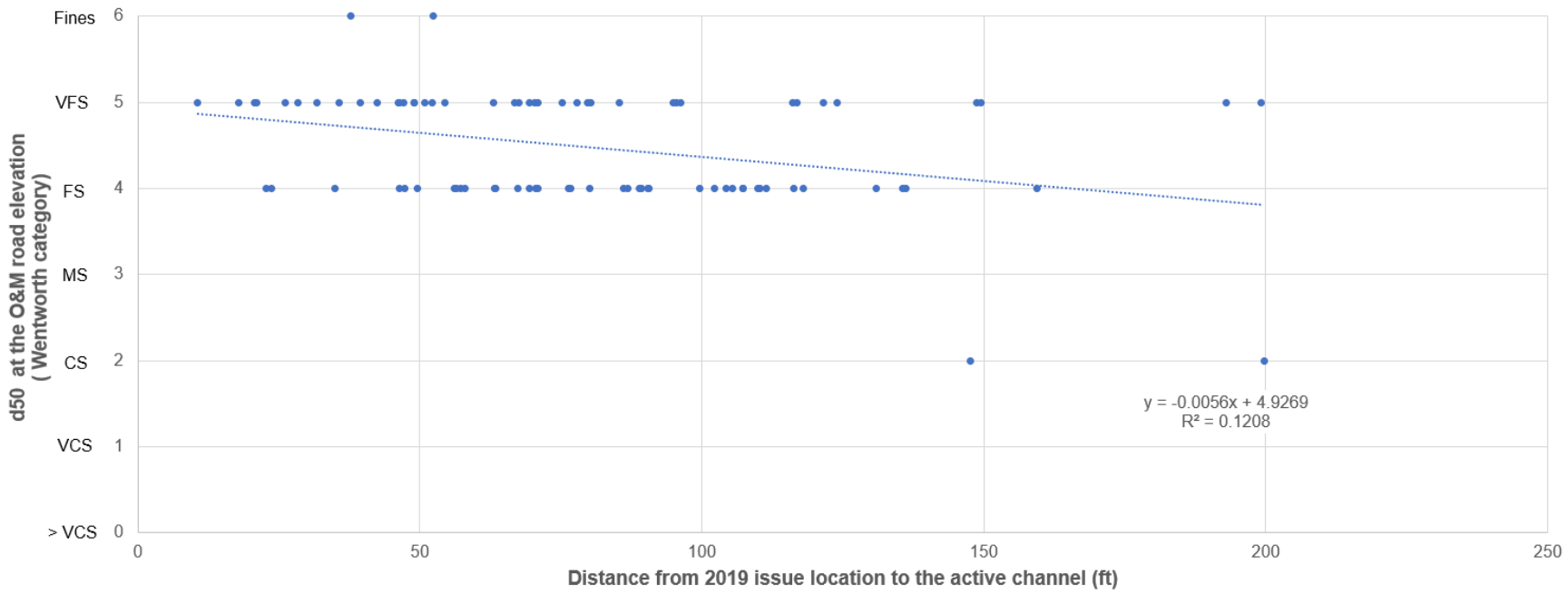

Figure 119. Linear regression of 1935 active channel distance to the 2019 points of interest and d_{50} grain size at the current landside levee toe elevation.

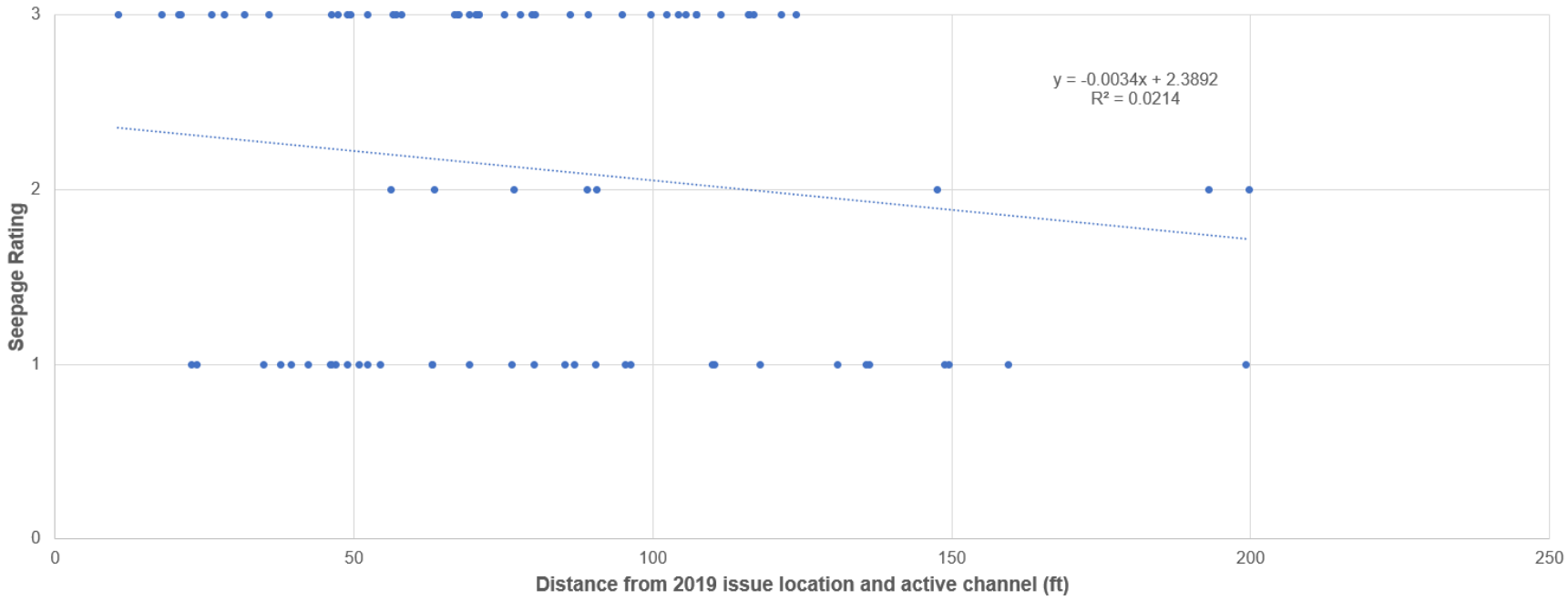

Figure 120. Linear regression of 1935 active channel distance to the 2019 points of interest and the 2006 seepage ratings.

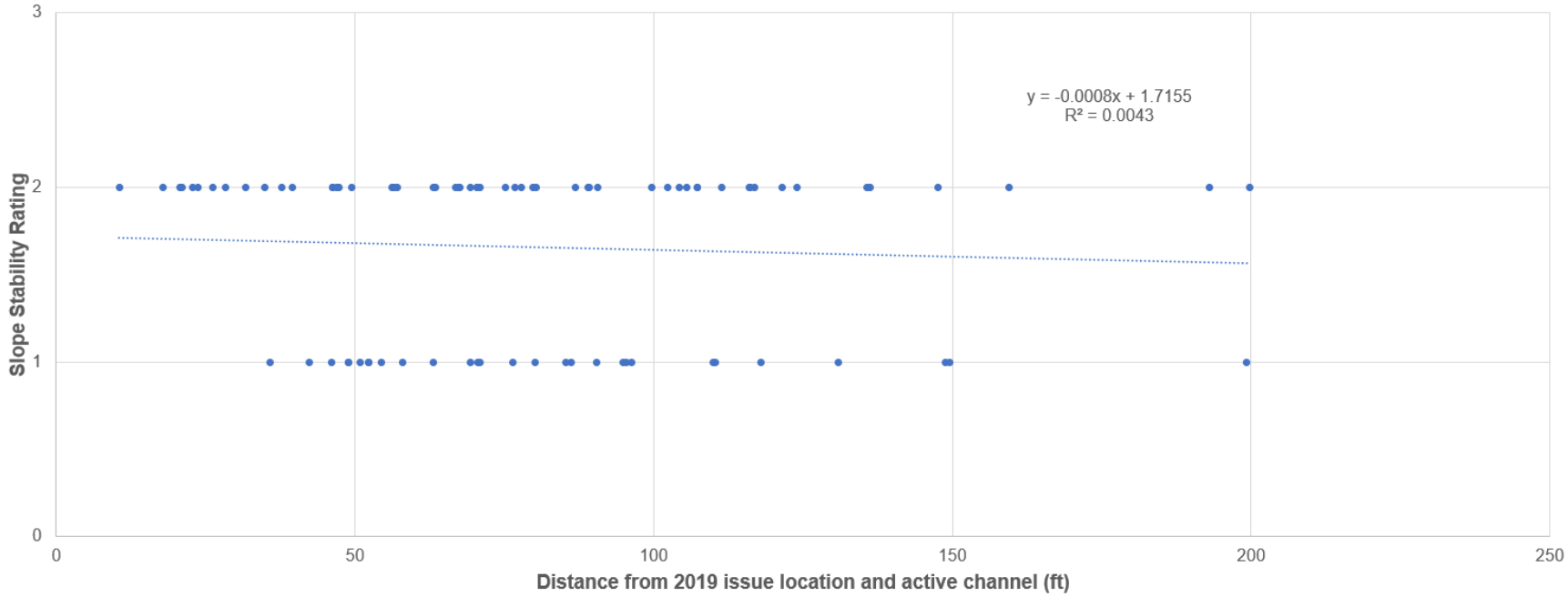

Figure 121. Linear regression of 1935 active channel distance to the 2019 points of interest and the 2006 slope stability ratings.

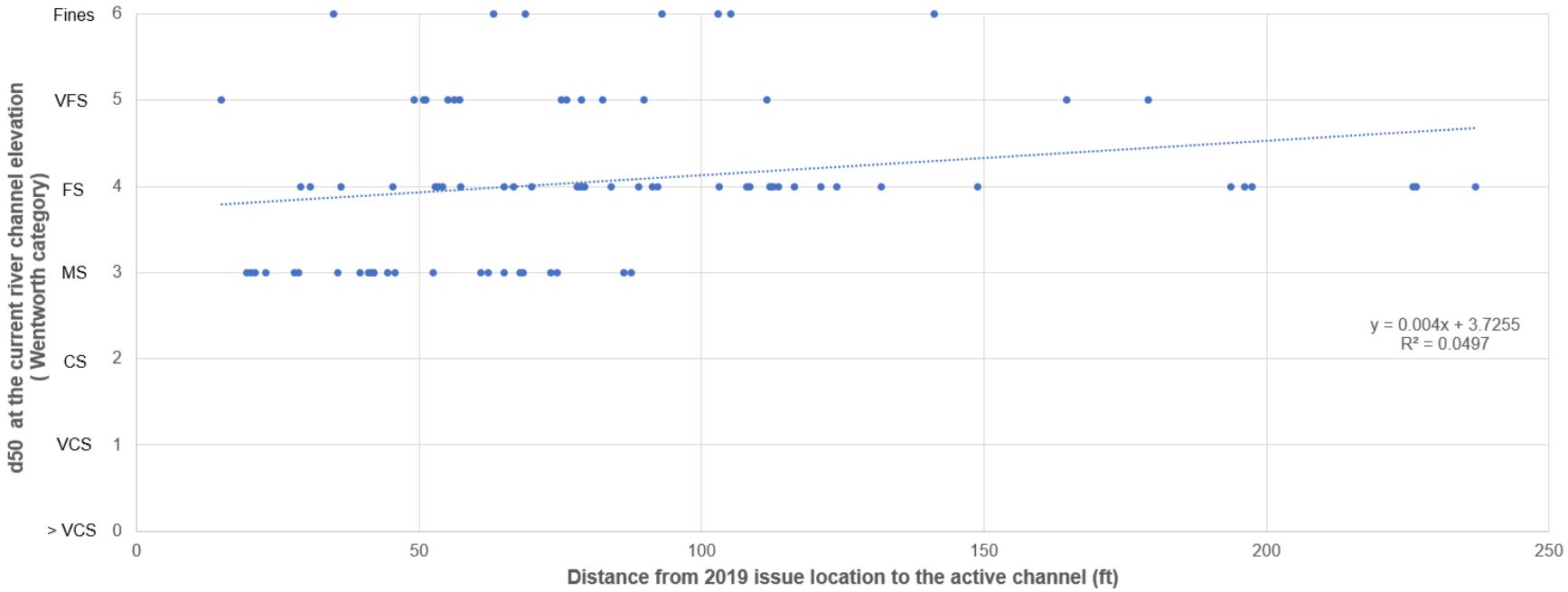

Figure 122. Linear regression of 1949 active channel distance to the 2019 points of interest and d_{50} grain size at the current river channel elevation.

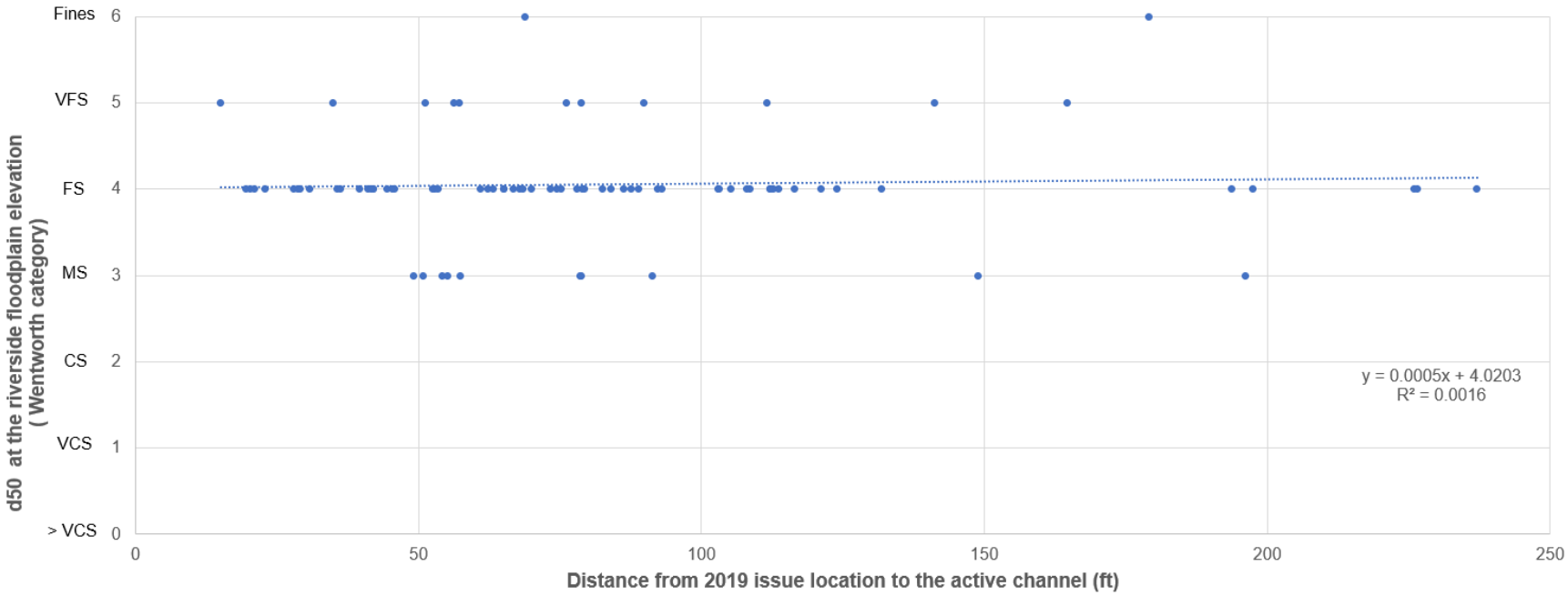

Figure 123. Linear regression of 1949 active channel distance to the 2019 points of interest and d_{50} grain size at the current riverside levee toe elevation.

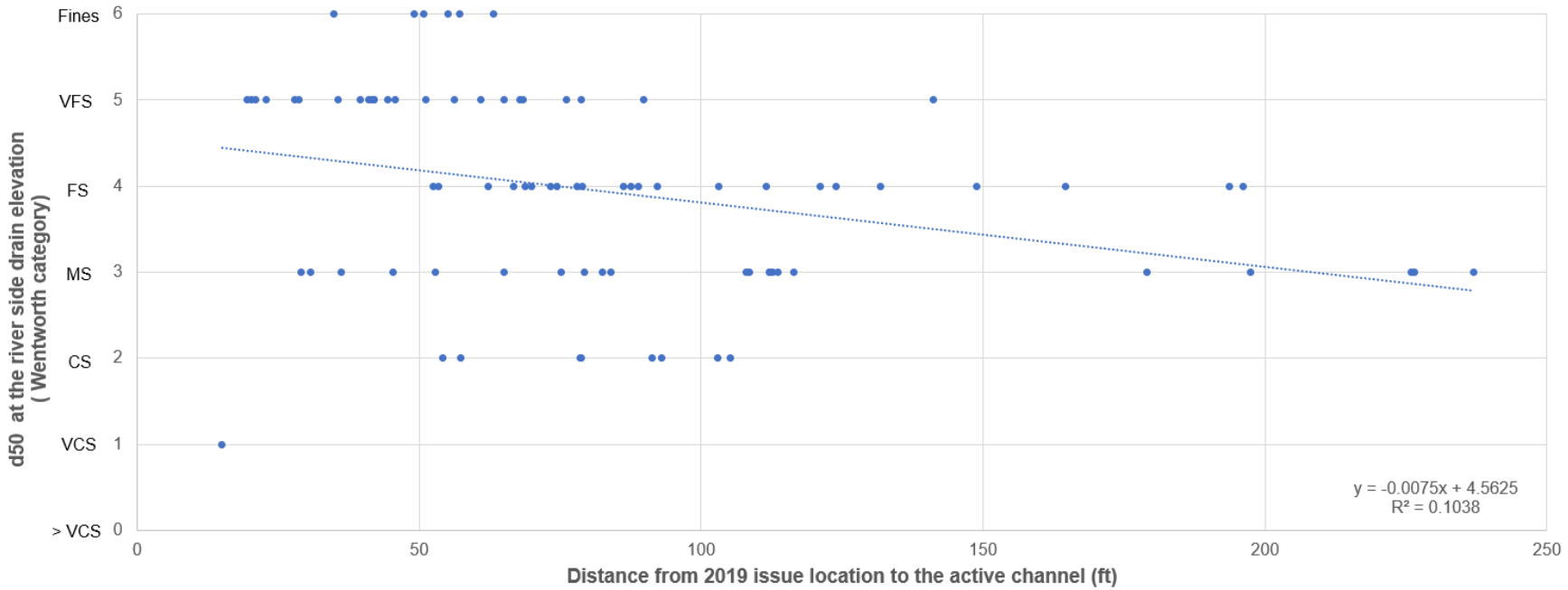

Figure 124. Linear regression of 1949 active channel distance to the 2019 points of interest and d_{50} grain size at the current riverside drain elevation.

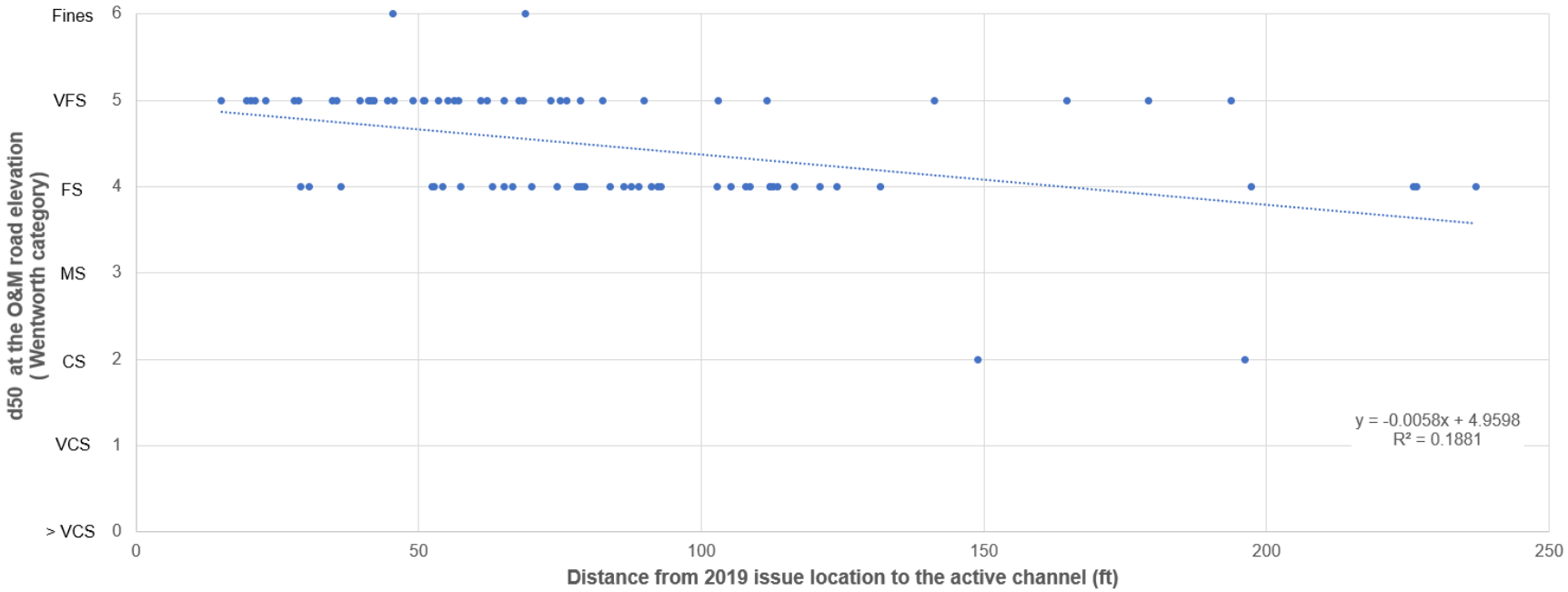

Figure 125. Linear regression of 1949 active channel distance to the 2019 points of interest and d_{50} grain size at the current landside levee toe elevation.

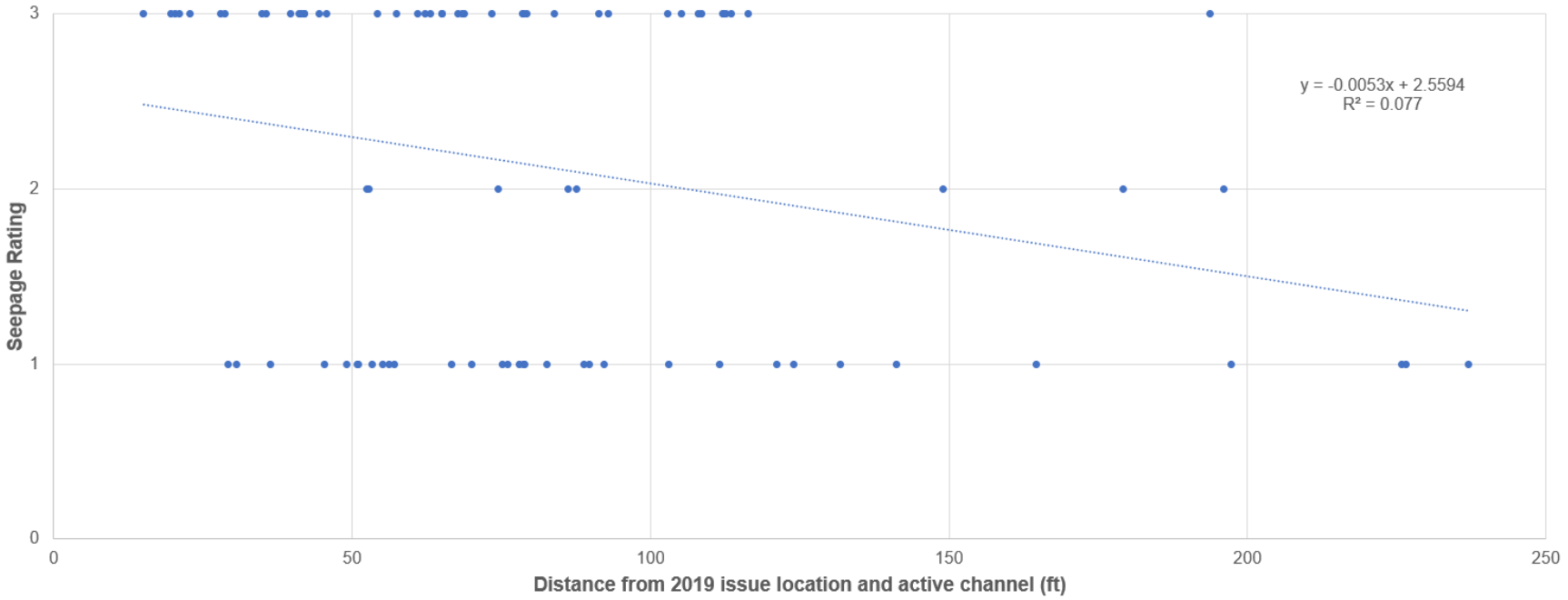

Figure 126. Linear regression of 1949 active channel distance to the 2019 points of interest and the 2006 seepage ratings.

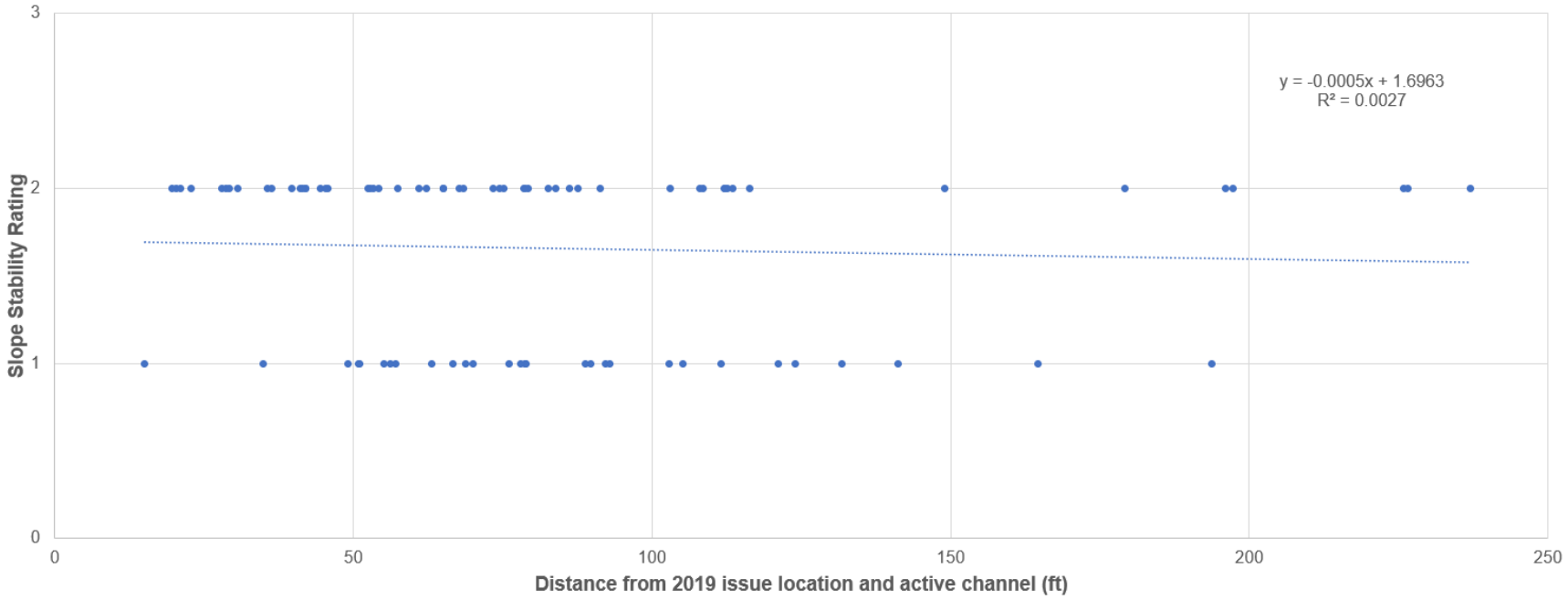

Figure 127. Linear regression of 1949 active channel distance to the 2019 points of interest and the 2006 slope stability ratings.